
JOURNAL OF LIQUID CHROMATOGRAPHY

VOLUME 18 NUMBERS 18 & 19

1995

Editor: DR. JACK CAZES

Associate Editors: DR. HALEEM J. ISSAQ
DR. STEVEN H. WONG

Special Issue on
CAPILLARY ZONE
ELECTROPHORESIS AND
RELATED TECHNIQUES

Edited by HALEEM J. ISSAQ
NCI-Frederick Cancer Research
& Development Center
Frederick, Maryland

Dedicated to
Stellan Hjerten
Uppsala University

JOURNAL OF LIQUID CHROMATOGRAPHY

November 1995

Aims and Scope. The journal publishes papers involving the applications of liquid chromatography to the solution of problems in all areas of science and technology, both analytical and preparative, as well as papers that deal specifically with liquid chromatography as a science within itself. Included will be thin-layer chromatography and all models of liquid chromatography.

Identification Statement. *Journal of Liquid Chromatography* (ISSN: 0148-3919) is published semimonthly except monthly in May, August, October, and December for the institutional rate of \$1,450.00 and the individual rate of \$725.00 by Marcel Dekker, Inc., P.O. Box 5005, Monticello, NY 12701-5185. Second Class postage paid at Monticello, NY. POSTMASTER: Send address changes to *Journal of Liquid Chromatography*, P.O. Box 5005, Monticello, NY 12701-5185.

Volume	Issues	Institutional Rate	Individual Professionals' and Student Rate	Foreign Postage		
				Surface	Airmail to Europe	Airmail to Asia
18	20	\$1,450.00	\$725.00	\$70.00	\$110.00	\$130.00

Individual professionals' and student orders must be prepaid by personal check or may be charged to MasterCard, VISA, or American Express. Please mail payment with your order to: Marcel Dekker Journals, P.O. Box 5017, Monticello, New York 12701-5176.

CODEN: JLCHD8 18(18&19) i-xx, 3557-3944 (1995)

ISSN: 0148-3919

Printed in the U.S.A.

Subscribe Today!

Use the cards below to subscribe to the *Journal of Liquid Chromatography* or to recommend the journal to your library for acquisition.

Order Form

Journal of Liquid Chromatography

Please enter my subscription to Vol. 18, 20 Numbers, 1995 at the institutional rate of \$1450.00; individual rate of \$725.00. *Individual subscriptions must be prepaid in American currency by personal check or credit card. Please add \$3.50 per issue (number) for shipping outside the U.S. For airmail to Europe, add \$5.50 per issue; to Asia, add \$6.50 per issue. Canadian customers please add 7% GST.*

Please send me a proforma invoice.

Check enclosed made payable to Marcel Dekker, Inc.

Charge my: MasterCard Visa American Express

Card No. _____ Exp. Date _____

Signature _____

Name _____

Address _____

City/State/Zip _____

Does your library subscribe to the *Journal of Liquid Chromatography*? Just complete this card and submit it to your librarian or department head.

Attention: Librarian/Department Head: I have examined the *Journal of Liquid Chromatography* and would like to recommend the journal for acquisition.

Signature _____ Date _____

Name _____ Department _____

Journal of Liquid Chromatography
Volume 18, 20 Numbers, 1995: \$1450.00
ISSN: 0148-3919 CODEN: JLCHD8

Sample copy and proforma invoice available upon request.

Please contact the Promotion Department at:

Marcel Dekker, Inc.
270 Madison Avenue
New York, NY 10016
(212) 696-9000 phone
(212) 685-4540 fax

Subscribe Today!

Use the cards below to subscribe to the *Journal of Liquid Chromatography* or to recommend the journal to your library for acquisition.



NO POSTAGE
NECESSARY
IF MAILED
IN THE
UNITED STATES

BUSINESS REPLY MAIL

FIRST CLASS PERMIT NO. 2863 NEW YORK, NY

POSTAGE WILL BE PAID BY ADDRESSEE

Promotion Department
MARCEL DEKKER, INC.
270 Madison Avenue
New York, NY 10016-0601



Journal of Liquid Chromatography

Editor: **JACK CAZES**
Cherry Hill, New Jersey

The *Journal of Liquid Chromatography* contains an outstanding selection of critical, analytical, and preparative papers involving the application of liquid chromatography to the solution of problems in all areas of science and technology, as well as papers that deal specifically with liquid chromatography as a science within itself. The coverage spans such areas as paper and thin layer chromatography and all modes of liquid column chromatography, including classical and HPLC. On a regular basis, entire issues are devoted to special topics in liquid chromatography, including an annual directory of LC manufacturers, suppliers, and services. In addition, each issue offers book reviews, liquid chromatography news, and a calendar of meetings and exhibitions.

JOURNAL OF LIQUID CHROMATOGRAPHY

Editor:
DR. JACK CAZES

Editorial Secretary:
ELEANOR CAZES

*P.O. Box 2180
Cherry Hill, New Jersey 08034*

Associate Editors:

DR. HALEEM J. ISSAQ
*NCI-Frederick Cancer Research
& Development Center
Frederick, Maryland*

DR. STEVEN H. WONG
*Medical College of Wisconsin
Department of Pathology
8700 West Wisconsin Ave.
Milwaukee, WI 53226*

Editorial Board

H.Y. ABOUL-ENEIN, *King Faisal Specialist Hospital & Research Centre,
Riyadh, Saudi Arabia*

V.K. AGARWAL, *Bayer Corporation, West Haven, Connecticut*

J.G. ALVAREZ, *Harvard University, Boston, Massachusetts*

D.W. ARMSTRONG, *University of Missouri, Rolla, Missouri*

A. BERTHOD, *Université Claude Bernard-Lyon 1, Villeurbanne, France*

U.A.TH. BRINKMAN, *The Free University, Amsterdam, The Netherlands*

P.R. BROWN, *University of Rhode Island, Kingston, Rhode Island*

W.B. CALDWELL, *Princeton Chromatography, Inc., Cranbury, New Jersey*

R. DEMURO, *Shimadzu Scientific Instruments, Inc., Columbia, Maryland*

J.G. DORSEY, *Florida State University, Tallahassee, Florida*

Z. EL RASSI, *Oklahoma State University, Stillwater, Oklahoma*

J.C. GIDDINGS, *University of Utah, Salt Lake City, Utah*

E. GRUSHKA, *The Hebrew University, Jerusalem, Israel*

G. GUIOCHON, *University of Tennessee, Knoxville, Tennessee*

N.A. GUZMAN, *R.W. Johnson Pharm. Res. Inst., Raritan, New Jersey*

S. HARA, *Tokyo College of Pharmacy, Tokyo, Japan*

G.L. HAWK, *The Cardinal Instrument Co., Inc., Bristol, Pennsylvania*

W.L. HINZE, *Wake Forest University, Winston-Salem, North Carolina*

(continued)

JOURNAL OF LIQUID CHROMATOGRAPHY

Editorial Board (*continued*)

- C. HORVATH, *Yale University, New Haven, Connecticut*
W.J. HURST, *Hershey Foods Technical Center, Hershey, Pennsylvania*
J. JANCA, *Université de la Rochelle, La Rochelle, France*
G.M. JANINI, *NCI-Frederick Cancer R&D Center, Frederick, Maryland*
M. JARONIEC, *Kent State University, Kent, Ohio*
K. JINNO, *Toyohashi University of Technology, Toyohashi, Japan*
P.T. KISSINGER, *Purdue University, West Lafayette, Indiana*
J. LESEC, *Ecole Supérieure de Physique et de Chimie, Paris, France*
F. LYABAYA, *Shimadzu Scientific Instruments, Inc., Columbia, Maryland*
H.M. MC NAIR, *Virginia Polytechnic Institute, Blacksburg, Virginia*
R.B. MILLER, *Fujisawa USA, Inc., Melrose Park, Illinois*
S. MORI, *Mie University, Tsu, Mie, Japan*
M. MOSKOVITZ, *Consultant, Atlanta, Georgia*
I.N. PAPADOYANNIS, *Aristotelian University of Thessaloniki, Thessaloniki, Greece*
L.A. PAPA ZIAN, *Consultant, Cranbury, New Jersey*
W.H. PIRKLE, *University of Illinois, Urbana, Illinois*
F.M. RABEL, *E-M Separations, Inc., Gibbstown, New Jersey*
D.A. ROSTON, *Searle Research & Development, Skokie, Illinois*
C.G. SCOTT, *Retired, East Stroudsburg, Pennsylvania*
R.P.W. SCOTT, *Consultant, Avon, Connecticut*
Z.K. SHIHABI, *Bowman Gray School of Medicine, Winston, Salem, North Carolina*
J.H.M. van den BERG, *Solvay Duphar BV, Weesp, The Netherlands*
R. WEINBERGER, *CE Technologies, Chappaqua, New York*

JOURNAL OF LIQUID CHROMATOGRAPHY

Indexing and Abstracting Services. Articles published in *Journal of Liquid Chromatography* are selectively indexed or abstracted in:

■ Abstracts Journal of the Institute of Scientific and Technical Information of the Russian Academy of Sciences ■ Alerts ■ Aluminium Industry Abstracts ■ Analytical Abstracts ■ ASCA ■ Berichte Pathologie ■ CAB Abstracts ■ Cambridge Scientific Abstracts ■ Chemical Abstracts ■ Chemical Reactions Documentation Service ■ Current Awareness in Biological Sciences ■ Current Contents/Life Sciences ■ Current Contents/Physical and Chemical Sciences ■ Current Opinion ■ Engineered Materials Abstracts ■ Engineering Index ■ Excerpta Medica ■ Metals Abstracts ■ Reference Update ■ Saltykov-Shchedrin State Public Library ■ Science Citation Index ■ Tobacco Abstracts

Manuscript Preparation and Submission. See end of issue.

Copyright © 1995 by Marcel Dekker, Inc. All rights reserved. Neither this work nor any part may be reproduced or transmitted in any form or by any means, electronic or mechanical, microfilming and recording, or by any information storage and retrieval systems without permission in writing from the publisher.

This journal is also available on CD-ROM through ADONIS™ beginning with the 1991 volume year. For information contact: ADONIS, Marketing Services, P.O. Box 17005, 1001 JA Amsterdam, The Netherlands, Tel: +31-20-626-2629, Fax: +31-20-626-1437.

The journals of Marcel Dekker, Inc. are available in microform from: University Microfilms, Inc., 300 North Zeeb Road, Ann Arbor, Michigan 48106-1346, Telephone: 800-521-0600; Fax: (313) 761-1203.

Authorization to photocopy items for internal or personal use, or the internal or personal use of specific clients, is granted by Marcel Dekker, Inc., for users registered with the Copyright Clearance Center (CCC) Transactional Reporting Service, provided that the fee of \$10.00 per article is paid directly to CCC, 222 Rosewood Drive, Danvers, MA 01923. For those organizations that have been granted a photocopy license by CCC, a separate system of payment has been arranged.

Contributions to this journal are published free of charge.

Effective with Volume 6, Number 11, this journal is printed on acid-free paper.

CAPILLARY ZONE ELECTROPHORESIS AND RELATED TECHNIQUES

Edited by

Haleem J. Issaq
NCI-Frederick Cancer Research & Development Center
Frederick, Maryland

Dedicated to
Stellan Hjerten
Uppsala University

This is a special issue of *Journal of Liquid Chromatography*,
Volume 18, Numbers 18 & 19, 1995.

MARCEL DEKKER, INC. New York, Basel, Hong Kong

JOURNAL OF LIQUID CHROMATOGRAPHY

Volume 18, Numbers 18 & 19, 1995

*Special Issue on
Capillary Zone Electrophoresis
and Related Techniques*

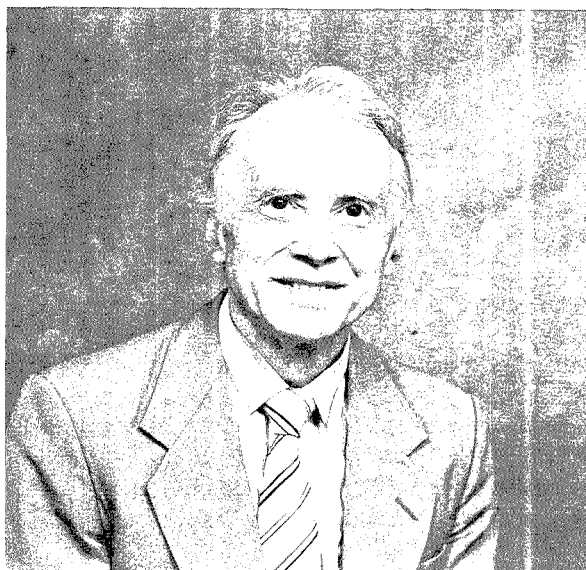
CONTENTS

Dedication	xi
Preface	xv
On-Column and Post-Column Derivatization for Capillary Electrophoresis with Laser-Induced Fluorescence for the Analysis of Single Cells	3557
<i>P. Beyer Hietpas and A. G. Ewing</i>	
Identification of Nucleic Acids and Oligonucleotides by Capillary Zone Electrophoresis with the Four Marker Technique	3577
<i>H. Sirén, J. H. Jumppanen, K. Peltonen, and M.-L. Riekkola</i>	
A Strategy for Sequencing Peptides from Dilute Mixtures at the Low Femtomole Level Using Membrane Preconcentra- tion-Capillary Electrophoresis-Tandem Mass Spectrometry (mPC-CE-MS/MS)	3591
<i>A. J. Tomlinson and S. Naylor</i>	
Application of Capillary Zone Electrophoresis for the Analysis of Proteins, Protein-Small Molecules, and Protein-DNA Interactions	3617
<i>G. M. Janini, R. J. Fisher, L. E. Henderson, and H. J. Issaq</i>	
The Effect of Operating Parameters on the Analysis of a Human Alpha-Interferon by Capillary Zone Electrophoresis	3629
<i>S. J. Craig, D. S. Ashton, C. Beddell, and K. Valko</i>	

Methods Development in Capillary Electrophoresis with Automated Peak Tracking by Chemometric Analysis of Diode Array Detection Data	3643
<i>T. E. Wheat, F. M. Chiklis, and K. A. Lilley</i>	
CE Resolution of Neutral and Anionic Racemates with Glycopeptide Antibiotics and Micelles	3659
<i>D. W. Armstrong and K. L. Rundlett</i>	
Considerations on the Enantiomeric Separation by MEKC of N-Bz-Amino Acids with N-Dodecoxycarbonylvaline as Chiral Selector	3675
<i>E. Van Hove and P. Sandra</i>	
Protein-Based Capillary Affinity Gel Electrophoresis for Chiral Separation of β-Adrenergic Blockers	3685
<i>H. Ljungberg and S. Nilsson</i>	
A Screening Protocol for the Direct Determination of Low PPB Levels of Uranyl Cation Using Arsenazo III and Capillary Electrophoresis	3699
<i>B. A. Colburn, M. J. Sepaniak, and E. R. Hinton</i>	
Relationships Between Capacity Factors and Hydrophobicity of Polycyclic Aromatic Hydrocarbons in Cyclodextrin-Modified Micellar Electrokinetic Chromatography Using Surface Treated Capillaries	3719
<i>K. Jinno and Y. Sawada</i>	
Simultaneous Measurements of Capillary Electrophoresis Fluorescence Peaks and Their Corresponding Spectra	3729
<i>G. A. M. Dalhoeven, N. V. Joshi, N. Rodriguez, and L. Hernandez</i>	
Biomedical Applications of On-Line Preconcentration-Capillary Electrophoresis Using an Analyte Concentrator: Investigation of Design Options	3751
<i>N. A. Guzman</i>	
Micellar Electrokinetic Capillary Chromatography with <i>In Situ</i> Charged Micelles. VII. Expanding the Utility of Alkylglycoside-Borate Micelles to Acidic and Neutral pH for Capillary Electrophoresis of Dansyl Amino Acids and Herbicides	3769
<i>Y. Mechref, J. T. Smith, and Z. El Rassi</i>	

Photoactivation: A Novel Means to Mediate Electrophoretic Separations	3787
<i>V. L. McGuffin</i>	
The Use of Alkylmethylmorpholine-Based Background Electrolytes in Capillary Electrophoresis	3813
<i>R. L. Williams and G. Vigh</i>	
Analysis of the Contrast Agent <i>Iopamidol</i> in Serum by Capillary Electrophoresis	3825
<i>Z. K. Shihabi, M. V. Rocco, and M. E. Hinsdale</i>	
Determination of Photodestruction Quantum Yields Using Capillary Electrophoresis: Application to <i>o</i>-Phthalaldehyde/β-Mercaptoethanol-Labeled Amino Acids	3833
<i>O. Orwar, H. A. Fishman, M. Sundahl, V. Banthia, R. Dadoo, and R. N. Zare</i>	
Separation of Sulfisoxazole, Phenazopyridine, and Their Related Impurities by Micellar Electrokinetic Chromatography	3847
<i>B. Nickerson, S. Scypinski, H. Sokoloff, and S. Sahota</i>	
Capillary Electrophoresis as an Alternative Method for the Determination of Cefotaxime	3877
<i>H. Fabre and G. Castaneda Penalvo</i>	
An Improvement for the Synthesis of a Styrene-Divinylbenzene, Copolymer Based, 6-Aminoquinoline Carbamate Reagent. Applications for Derivatization of Amino Acids, Peptides, and Proteins	3889
<i>G. Li, J. Yu, I. S. Krull, and S. Cohen</i>	
A Comparative Study on the Effect of Hydrochloric, Phosphoric, and Trifluoroacetic Acid in the Reversed Phase Chromatography of Angiotensins and Related Peptides	3919
<i>D. Corradini and G. Cannarsa</i>	
The Book Corner	3933
Announcement	3937
Liquid Chromatography Calendar	3939

DEDICATION



Dedicated to Professor Stellan Hjertén

Professor Hjertén was born to Vilhelm and Judith Hjertén on April 2, 1928 at Forshem, Sweden. He received his studentexamen (Gymnasium Diploma) in 1948, a Bachelor of Science in mathematics, physics and chemistry in 1954 and a Master of Science in 1958. In 1965, he married Laila

Woxström; they have one daughter, Maria. After receiving his Masters Degree, he joined the group of Professor Arne Tiselius and received his Ph.D. in biochemistry in 1967. The title of his thesis was "Free Zone Electrophoresis." He was appointed Professor of Biochemistry at Uppsala University in 1969.

Characteristic of Hjertén's way to develop new methods is that he often combines experimental investigations with theoretical studies. As a pupil of Professor Tiselius (who received the Nobel Prize in 1948 for his electrophoretic and chromatographic studies) Hjertén was influenced by Tiselius' great interest in the development of new methods for the separation of bipolymers. He realized the great importance of such research for the progress of biochemistry and related disciplines. Among methods which he has introduced and which are widely used are:

Chromatography on Hydroxyapatite. [Arch. Biochem. Biophys., 65 (1956) 132].

Gel Filtration (Size-Exclusion Chromatography) on Cross-linked Polyacrylamide. (Anal. Biochem. 3 (1962) 109).

Hjertén was the first to observe the molecular-sieving properties of crosslinked dextran gels [for a review, see Electrophoresis, 9 (1988) 3]; later they became available commercially as "Sephadex." It is also of interest to note that separations of proteins were accomplished with polyacrylamide gels before they were accomplished with dextran gels [A. Tiselius, *Experientia* 17 (1961) 433] and this was done at a time when many (including Tiselius) had doubts whether the slow diffusion of macromolecules into and out of a gel particle would permit separation of molecules as large as proteins.

Gel Filtration (Size-Exclusion Chromatography) on Agarose. (Arch. Biochem. Biophys. 99 (1962) 466).

Electrophoresis and Immunoelectrophoresis in Agarose Gels. (Biochim. Biophys. Acta 53 (1961) 514; 53 (1961) 518).

Electrophoresis in Polyacrylamide Gels.

Two groups in the USA (Raymond and Weintraub; Ornstein and Davis) and Hjertén in Sweden, studied, independently, the usefulness of polyacrylamide gels for analytical electrophoresis of proteins [for a review, see Electrophoresis 9 (1988) 3]. An apparatus for preparative separations was also designed which

permits fractionation of proteins in the range 1 mg - 1 gram with a resolution comparable to that obtained in analytical polyacrylamide gel electrophoresis.

Hydrophobic-interaction chromatography.

Hjertén introduced this term, which now is generally accepted, in connection with synthesis and studies of beds with noncharged, nonpolar ligands [for a review, see *Methods of Biochemical Analysis* (Ed. D. Glick) John Wiley and Sons, New York 1981, Vol. 27, pp. 89-109].

Capillary Electrophoresis. [Chromatog. Rev. 9 (1967) 122].

In this paper, Hjertén stated that there are two ways to perform electrophoresis in capillaries, one being based on rotation of the horizontal capillary around its long axis, the other on the use of a stationary capillary with a very narrow bore (today, the latter method is called high-performance capillary electrophoresis). Hjertén's work focused on the first method, particularly since, at this time (in 1967), no UV detectors were available which would be sensitive enough to detect zones in a tube with diameters much below 1 mm. In this article Hjertén described the advantages of coated capillaries, the effect of sample solution, the separation of metal ions, nucleotides, nucleosides, purine and pyrimidine bases, proteins, nucleic acids, DNA, viruses, subcellular particles and cells; indirect UV detection and the use of additives to increase the capacity and to create isoelectric spectra. In essence, Hjertén, in his 1967 publication, demonstrated the application of free zone electrophoresis, established its foundation, and predicted the bright future and application of this separation technique.

Hjertén's current main interests are centered around the following projects:

1. Chromatography (HPLC) of macromolecules on compressed beds of beads of agarose and on compressed continuous polymer beds. Both types of beds have the attractive feature that the resolution is independent of, or increases, with an increase in flow rate, which is contradictory to classical chromatographic theory [for a review, see *Nature* 356 (1992) 810].
2. High-performance capillary electrophoresis (HPCE), particularly of macromolecules.
3. Methods for the purification of hydrophobic membrane proteins in the presence of SDS, followed by renaturation of the proteins - an approach which very much facilitates the separation of proteins which are insoluble in water (*Biochim. Biophys. Acta* 939 (1988) 476).

4. The utilization of the knowledge and the experiences gained in methodological electrophoretic and chromatographic studies, also in areas other than electrophoresis and chromatography, for instance, for the development of (a) dressings for traumatic injuries; (b) agents against diarrhea; (c) catheters to suppress bacterial adhesion; (d) tooth pastes and mouth washes to prevent bacteria from adsorbing to the teeth; (e) simple methods for the determination of bacteria in urine.

I met Stellan a few years ago and I enjoyed talking and discussing science with him. I was impressed by his knowledge, not only of science, but of other social and human matters. I cherish those moments. I wish Professor Hierten continued success and a long, healthy and happy life.

Haleem J. Issaq, Ph.D.
NCI-Frederick Cancer Research & Development Center
Frederick, Maryland

PREFACE

A study of the history of electrophoresis shows that the introduction of a new, important electrophoresis method usually requires the introduction of a new approach to minimize or eliminate convection, i.e., hydrodynamic flows caused by differences in density between a zone and the surrounding medium. In Tiselius' classical moving boundary method, the density below any boundary is higher than that above it, which affords stabilization against convection. However, if the run is prolonged in an attempt to achieve zone separation, the zones will become blurred by convection in the form of sedimentation.

This disturbing convection can be prevented by rotating a horizontal electrophoresis tube around its long axis. An alternative is to conduct the experiments in an electrophoresis chamber of very narrow cross-section. This approach is the basis of free flow electrophoresis and capillary electrophoresis. The same principle for stabilization against convection can be used for electrophoresis in columns of larger diameters by inclusion of substances which confer a capillary structure on the electrophoresis medium. Grains of starch or plastic; cellulose (and some derivatives) in the form of powder; filter paper, and films; and gels of agar, agarose, starch and polyacrylamide have been employed for this purpose. It should be emphasized that many gels also have molecular sieving properties, i.e., the separations are based not only on differences in zeta

potentials among the substances to be analyzed, but also on differences in molecular size.

An obvious disadvantage of these anti-convection media is that the solutes of interest can adsorb to them. To avoid this, the runs can be performed, instead, in a density gradient, for instance of sucrose, provided that the density of the sample is low enough to avoid sedimentation.

To master convection is important not only in electrophoresis, but also in other (separation) methods, for instance sedimentation (by ultracentrifugation) and chromatography. However, there are many more analogies between these three methods which one can understand intuitively, since the separations they accomplish can be ascribed to differences in the migration velocities of the solutes. In fact, using just migration velocity (v) as a variable in the equation for mass balance, one arrives at the following expression, which is valid not only for electrophoresis, chromatography and sedimentation, but also for other methods based on differences in migration velocities.

$$M_j^\alpha \cdot v_j^\alpha - M_j^\beta \cdot v_j^\beta = v^{\alpha\beta} (M_j^\alpha - M_j^\beta)$$

In this preface, it is not necessary to define the different variables in the equation. It is only of importance to know of the existence of an expression which is so general that it is applicable for all of the methods mentioned. This means that any phenomenon appearing in, for instance, chromatography, will appear also in electrophoresis and sedimentation in an analogous way. Therefore, if one has found something methodologically interesting in chromatography, it is worth while to investigate whether an analogous electrophoresis experiment also gives an interesting result. The analogy between electrophoresis and chromatography tempts one to give analogous separation methods

analogous names. Thus, as an example, I suggest the use of the terms displacement electrophoresis (often called isotachopheresis) and displacement chromatography. In doing so, we also honor the pioneers in these fields who employed these notations.

There are no (or very few) similarities between electrophoresis and chromatography. I want to stress this since discussions in which these two methods are compared can likewise degenerate and become meaningless. No doubt, we need both of these methods. For some purposes, chromatography is preferable to electrophoresis; for other purposes the opposite is true. The resolution obtained in electrophoresis in free solution (i.e., buffer alone) or in a gel such as agarose or cross-linked polyacrylamide is, however, often higher than that obtained in chromatography. One reason is that a chromatographic medium (bed) is not as homogeneous as these electrophoresis media and, therefore, causes a larger zone broadening.

Free electrophoresis is a milder method than chromatography, since the separations are not based on interactions with a bed as in chromatography. The risk of denaturing labile macromolecules, such as proteins, is therefore lower.

I do hope that capillary electrophoresis will not meet the same fate as polyacrylamide gel electrophoresis, the advantage of which is that the experimental conditions (for instance, gel composition and buffer systems) can be varied easily to give optimum resolution for any particular separation problem. This flexibility, however, is seldom utilized. Unfortunately, certain standard conditions are often employed instead. Learning more theory will help the users of capillary electrophoresis to avoid the same trap! They will also characterize the solutes by their mobilities (not migration times) so that data from different laboratories can be compared in a meaningful way. Furthermore, the more one knows about the theory of electrophoresis, the more

information one gets about the physicochemical properties of the solutes.

The general trend in the analysis of biological material goes toward smaller sample amounts (for instance, the contents of a single cell) and shorter analysis times combined with higher resolution. This is a big challenge, particularly since the latter requirement often is incompatible with classical electrophoresis theory. I believe that the success of capillary electrophoresis will accelerate and promote the development of capillary chromatography, not the least because the preparation of columns with diameters as small as 10 μm presents no problem since the introduction of the so-called continuous beds (the column bed is prepared in the same simple way as a gel is prepared for polyacrylamide gel electrophoresis). For instance, the different minute fractions obtained from a micropreparative capillary electrophoresis can be analyzed sequentially on these micro columns by chromatography based on ion-exchange, hydrophobic interaction, bioaffinity, etc. In doing so, we take advantage of the natural complementarity between electrophoresis and chromatography. The trend toward utilization of mass spectrometry for the analysis of electrophoretic fractions will continue.

Although many different separation techniques are available, there is a great need for novel high-resolving methods for the analysis and fractionation of biological materials. As an illustrative example, it may be mentioned that as much as 90% of the total cost to produce a protein by DNA hybridization refers to the analysis and purification (many biotechnical companies went bankrupt because they were not aware of the difficulties to analyze and fractionate protein mixtures). No doubt, capillary electrophoresis will reduce this cost -- and more generally, increase our knowledge in the field of separation science.

Prepared by
Stellan Hjertén
Department of Biochemistry
University of Uppsala
Biomedical Center
P. O. Box 576
S-751 23 Uppsala, Sweden

This preface has been published, with some modifications, also in Japanese in *Capillary Electrophoresis Fundamentals and Applications*, S. Honda & T. Terabe, eds., Kodansha Publication Co., Tokyo, 1995.

ON-COLUMN AND POST-COLUMN DERIVATIZATION FOR CAPILLARY ELECTROPHORESIS WITH LASER-INDUCED FLUORESCENCE FOR THE ANALYSIS OF SINGLE CELLS

PAULA BEYER HIETPAS AND ANDREW G. EWING

*Department of Chemistry
Penn State University
152 Davey Laboratory
University Park, Pennsylvania 16802*

ABSTRACT

Derivatization methods for analysis of single cell components by capillary electrophoresis with laser-induced fluorescence detection are reviewed. Recent advances have lead to the use of this technique for the identification of amino acids and proteins in many different cell lines ranging in size from 8 to 140 μm . Pre-column, on-column, and post-column methods of derivatization are examined in order to determine which results in the least amount of sample handling and dilution leading to better detection limits for the analytes of interest.

INTRODUCTION

Biological systems are extremely complex. In many parts of the body, the cellular environment is highly heterogeneous. In specific tissues, many different cells coexist each with their own purpose and chemical processes. This is especially true of the brain where

a large number of nerve cell types is present. In these cases analysis at the single cell level is necessary for an understanding of their biological significance.

Analyzing samples on the order of a single cell is very challenging. Not only are the cell volumes small, but also the chemical species present are typically found in femtomole to zeptomole amounts. Techniques such as enzyme activity measurements (1), immunoassay (1,2), microgel electrophoresis (3), fluorescence imaging (4), voltammetric microelectrodes (5-7), microcolumn separations (8-27), optical and electron microscopy (13-15), and secondary ion mass spectrometry (16) have all been used to examine single cells; however, each has limitations. They either require an excess of sample, extensive sample preparation, or lack sensitivity or selectivity.

In the late 1980's, Jorgenson and co-workers used the microcolumn separation technique, open-tubular liquid chromatography (OTLC) to analyze single cells (8-11). The microbore columns were 1 to 3 meters in length and had inner diameters (i.d.) ranging from 15 to 20 μm . This resulted in total column volumes between 180 and 940 nL. These investigators studied the large neurons of *Helix aspersa* (about 120-140 μm in diameter). Neurons were dissected and transferred to a 500 nL vial where they were homogenized. A portion of the supernatant was injected onto the OTLC column. Injection volumes were on the order of 5 nL with total analyte amount on the femtomole to attomole level (9-11). Detection of such low analyte levels requires very sensitive detection methods. One detection method with the sensitivity and selectivity for the analysis of single cells is electrochemical (EC) detection.

OTLC-EC was used to determine the easily oxidizable species tyrosine, tryptophan, dopamine and serotonin at femtomole levels (10). In another study, a cell

homogenate was derivatized with naphthalene-2,3-dicarboxaldehyde (NDA) prior to analysis (11). NDA tags primary amines causing them to become electroactive.

Seventeen different amino acids were identified with attomole detection limits (11).

Smaller mammalian cells have also been examined with microcolumn techniques. Packed LC columns were used to separate components of adrenomedullary cells which are about 16 μm in diameter. This analysis indicated that norepinephrine and epinephrine are often present in the same cell (12).

In this article, we review the recently developed procedures developed to derivatize amine-containing solutes for fluorescence detection following capillary electrophoretic separation of single cell components. Capillary electrophoresis (CE) offers many of the same advantages as microbore OTLC without the need for a bonded or coated phase. CE separations are very fast, on the order of 5 to 30 minutes, due to the high separation potentials used. The capillaries typically range from 10 to 100 cm in length and 2 to 100 μm i.d. The ability of CE to sample and analyze extremely small volumes with good selectivity, high efficiency and resolving power has lead to its use for cells as small as 8 μm in diameter (17-31). Although many detection schemes have been demonstrated, the three with the low mass detection limits necessary to identify the femtomole to zeptomole levels of analytes found in single cells are electrochemical (6, 18-21), immunoassay (29), and laser induced fluorescence (LIF) detection (22-26, 28, 31).

Detection methods for CE analysis of single cells have initially relied on the native properties of analytes. Species which were easily oxidized were detected using electrochemical methods whereby an electrode was positioned at or in the elution end of the capillary. Small easily oxidized species from whole snail cells (21, 27), snail cytoplasm

(18-21, 27), and whole human lymphocytes (30) have been examined with CE-EC.

Analytes which are naturally fluorescent have been identified with laser induced fluorescence (32).

Generally, LIF detection is done on-column through a window in the capillary. A laser is focused on the capillary and analytes are detected as they migrate through this window. CE-LIF has been used for separation and detection of hemoglobin and carbonic anhydrase native fluorescence from single human erythrocytes (red blood cells) (23). In these experiments, the 274-nm line of an Argon ion laser was used to excite these proteins for fluorescent detection without derivatization. In addition, CE-LIF has been used to determine the activities of several lactate dehydrogenase isoenzymes in single erythrocytes by monitoring the enzyme-catalyzed production of NADH (28). Materials which have no easily detected native properties have been examined with indirect detection, which is based on the property of displacement. The background buffer is filled with a fluorescent or electrochemical ion which is continuously detected as it elutes past the detector. If a non-fluorescent molecule is present in a high enough concentration, it will displace the background ions and a negative peak will result. Sodium, potassium, lactate and pyruvate have all been identified in single red blood cells with indirect LIF detection (22, 26).

Unfortunately, most species are not easily identified in their natural state and must be modified to be detected. One such method is to derivatize the analyte and label it with a fluorophore. There are a wide variety of fluorophores available to label amino acids, proteins, peptides, and carbohydrates. Some of the most common derivatizing agents used for CE-LIF are NDA (33, 34), o-phthaldialdehyde (OPA) (33, 35, 36), fluorescein isothiocyanate (FITC) (37, 38), and 3-(4-carboxybenzoyl)-2-quinolinecarboxaldehyde

(CBQCA) (30, 39, 40). These fluorophores are readily excited using the lines from the helium-cadmium or argon ion lasers typically used. The first two also have the advantage of being non-fluorescent until the derivatization adduct is formed causing very little background interference. LIF detection boasts very low detection limits, typically around 10^{-18} - 10^{-21} moles (33, 38, 41, 42). Derivatization of analytes, however, is not always an easy task. Some of the problems with derivatization procedures include extensive sample handling which can cause loss of analyte and/or contamination, dilution of the reaction products which may cause diminished sensitivity, slow reaction kinetics which may cause incomplete reactions and lead to irreproducibility, and multiple labeling of solutes with several functional groups. Methods for pre-column, on-column, and post-column derivatization have been developed to address these problems and to determine the optimum time to perform these derivatization labeling reactions.

PRE-COLUMN DERIVATIZATION

Pre-column derivatization is the most straight-forward method to carry out derivatization as it requires no changes to the capillary electrophoresis system. The derivatization reaction is carried out prior to sample injection and separation and often offers the advantage of complete reaction. Pre-column derivatization of single cells has been demonstrated in several ways. Initial experiments included isolation of large invertebrate cells in 200 nL vials. The cells were homogenized and derivatized with NDA in the presence of cyanide (CN⁻). A portion of this homogenate was then injected into the capillary and analyzed (8, 25). Individual snail neurons (8) and bovine adrenal medullary cells (25) have been handled in this manner, and several amine containing analytes have

been identified (8, 25). However, dilution was extensive and only 20% of the cell contents were analyzed in any one separation. A similar method has been used for the analysis of human cerebrospinal fluid using CBQCA derivatization (30). The reaction time for this analysis was 2 hours, necessitating the use of pre-column techniques. Ten different amino acids have been identified and quantitated in the cerebrospinal fluid samples (30). Using a different approach, red blood cells were incubated with monobromobimane (mBBr) which was transported through the cell membrane where it reacted with thiols, particularly glutathione, directly inside the cell (22). This method is only useful when the cell membrane is permeable to the derivatization agent and not the derivatization product and for derivatization reactions which occur rapidly at physiological pH (22).

A recent development in our laboratory is aimed at solving the sample handling and dilution problem associated with pre-column derivatization. Reducing the volume of the reaction vessels for derivatization while maintaining the ability to manipulate such small volumes of solution is necessary to alleviate these problems. Arrays of square pyramidal reaction vials ranging in size from 10 to 500 pL have been fabricated in silicon or polystyrene using standard photolithographic techniques. These vials are similar to the 118 nL vials created by Janssen et. al (43), but are several orders of magnitude smaller. An SEM of a 50 pL vial is shown in Figure 1. The vials are evenly spaced 1 mm apart to allow for eventual automation of sample transfer. Methods for filling these small volume chambers have been developed. Micropipettes are constructed from 5 to 10 μm i.d. fused silica capillaries etched in hydrofluoric acid to an outer diameter around 50 μm . This tip is then epoxied into a glass capillary and the pipette is filled with solution. An Eppendorf pressure injector is used to reproducibly deliver solutions into the picoliter vials. Evaporation from these vials is controlled using 4 to 15% glycerol in all of the solutions.

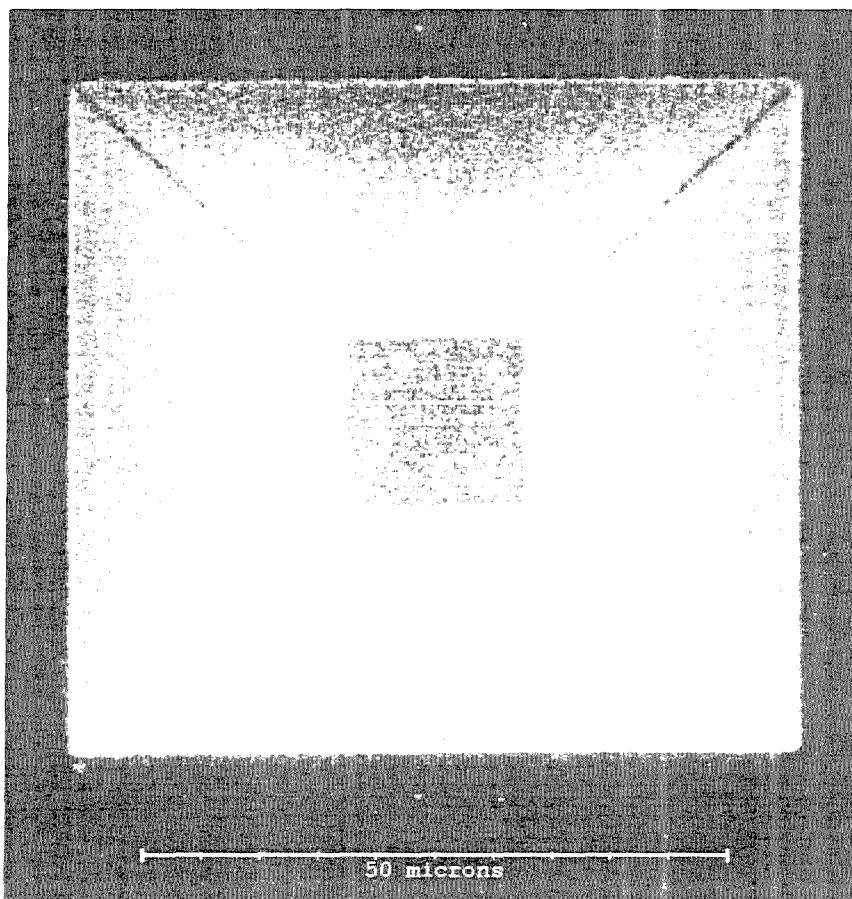


Figure 1 SEM of a 100 pL vial. Dimensions: top, 75 μm ; bottom, 18 μm ; depth 40 μm .

Preliminary experiments have demonstrated the feasibility of performing NDA/CN⁻ derivatization reactions in these vials. Amino acid solutions (10^{-3} M) were injected into 1 nL and 100 pL vials, followed by an equal volume of NDA/CN⁻ solution. The solutions were allowed to react for 10 min. The entire surface of the array of vials has been coated

with a thin metallic layer to serve as an electrophoresis anode for injection. Using this anode, the derivatized amino acid solution was electrokinetically injected into a CE capillary and the peaks for arginine, norepinephrine, dopamine, and glycine are shown in Figure 2. Preliminary detection limits for the vials appear higher than from standard solutions. This may be due in part to adsorption of analytes to the metallic layer in the vials. For this reason, polystyrene vials have been fabricated for future experiments. The next step in these experiments will be to transfer a single cell into a vial followed by derivatization, sampling and separation of cell components.

ON-COLUMN DERIVATIZATION

Another procedure whereby derivatization has been performed prior to separation is known as on-column derivatization. In this type of reaction, the introduction portion of the capillary is used as the reaction chamber (34). For analysis of single cells, the inside of the capillary tip is etched to a cone in HF. This facilitates easier visualization for electrokinetic injection of the cells into the capillary tip. Following cell injection, a derivatization and cell lysing solution is drawn in over the cell. A schematic diagram of this process is shown in Figure 3. As an example of this methodology, individual rat pheochromocytoma (PC12) cells have been analyzed (34).

Individual PC12 cells can be selected and drawn into the capillary at a low potential by electroosmotic flow. Injection times range from 15 to 90 s. In order to determine the amount of cell media and associated solutes injected into the capillary along with the cell, an internal standard of γ -glu-gly is added to the media just prior to injection. After cell injection, the capillary is moved to a solution containing the NDA derivatization

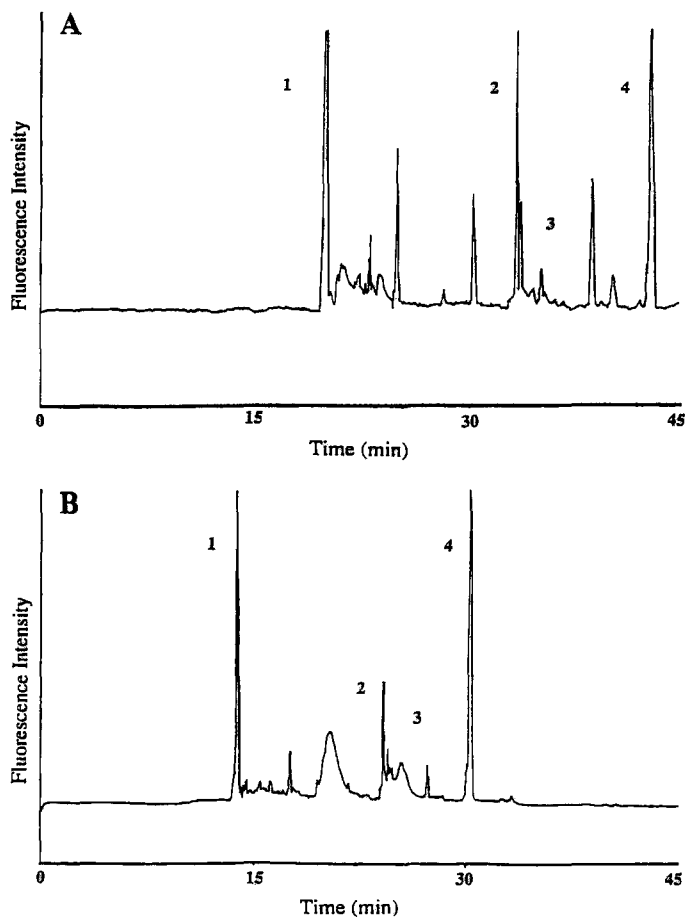


Figure 2 A. Electropherogram of NDA-derivatized solution from a 1 nL vial. Peaks are 1, Arg; 2, Norepinephrine; 3, Dopamine; 4, Gly. Conditions: capillary 50 μm i.d., separation buffer, 100 mM borate, pH 9.5; injection, 10 s at 5 kV; separation potential, 20 kV. B. Electropherogram of NDA-derivatized solution from a 100 pL vial. Peaks identities are the same as in A. Conditions: capillary 22 μm i.d., separation buffer, 100 mM borate, pH 9.5; injection 2 s at 5 kV; separation potential, 30 kV.

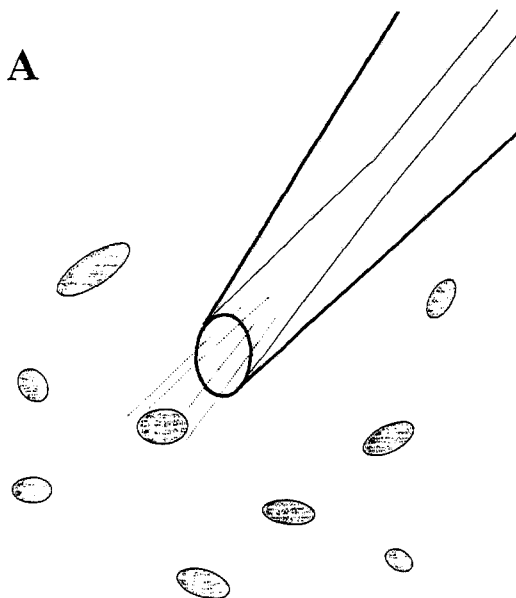


Figure 3 Schematic representation of the on-column derivatization procedure for analysis of single cells. A. A cell is dislodged from the culture dish with the tip of the capillary, and a potential is applied to draw the cell into the front of the capillary by electroosmotic flow. B. The capillary is placed in a reservoir containing derivatizing/lysing buffer, and a potential is applied to draw the reagent over the cell. C. The cell is allowed to lyse in the reagent buffer, and cell contents are derivatized. After sufficient time is allowed for lysing and derivatization, the separation potential is applied, and the NDA-labeled cell contents are detected using LIF after electrophoresis.

(continued)

reagent and a cell lysing agent (digitonin). A second standard (val-tyr-val) is added to determine the extent of derivatization. A 30 s injection of this solution is made, and a 10 min incubation time allowed. After the reaction, the capillary is returned to the separation buffer, and a separation voltage of 30 kV applied (34).

An electropherogram of PC12 cell components and of the cell medium is shown in Figure 4. The analytes have been identified based on electrophoretic mobilities or by

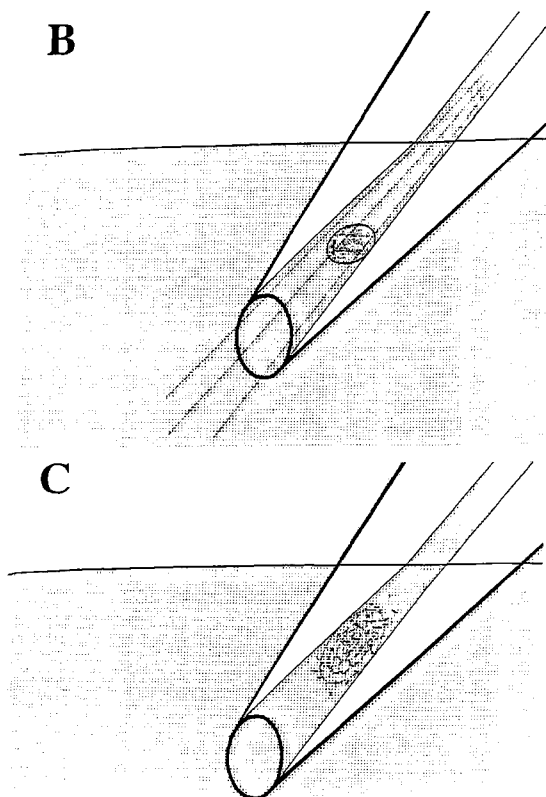


Figure 3 (continued)

spiking the reagent buffer with standard solutions of analytes. Six compounds were quantitatively identified in the PC12 cell experiments. Levels of dopamine, alanine, taurine, glycine, glutamic acid and aspartic acid were in agreement with previous estimates (34).

Dilution in on-column derivatization experiments is limited by the size of the capillary bore and the reaction time. The only source of dilution is diffusion of the

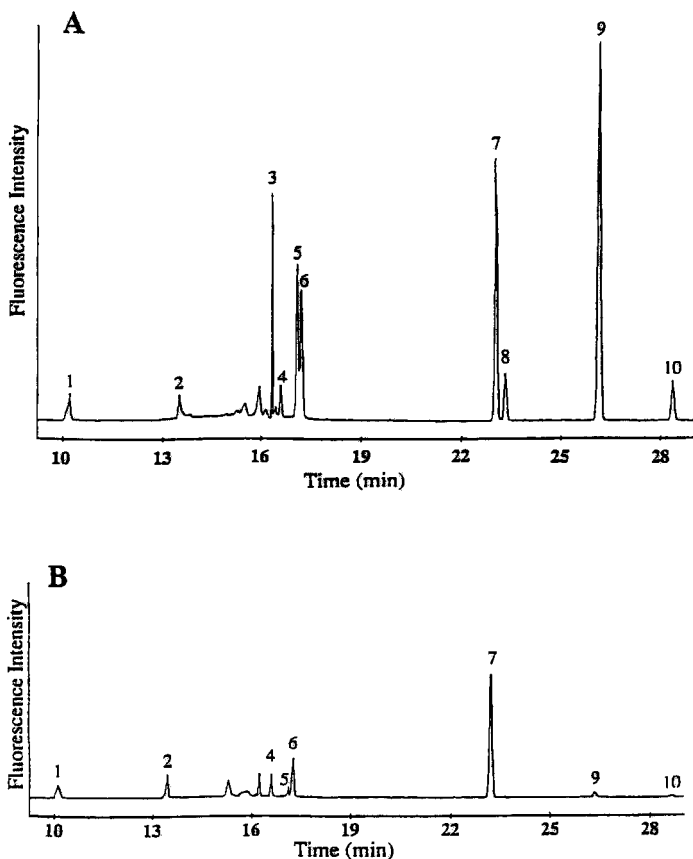


Figure 4 A. Electropherogram of the NDA-derivatized contents from a single PC12 cell. Peaks are 1, neutral peak; 2, Val-Tyr-Val (internal standard); 3, unidentified peak; 4, Ala; 5, taurine; 6, Gly; 7, γ -Glu-Gly (internal standard); 8, unidentified peak; 9, Glu; 10, Asp. B. Electropherogram of a control injection of the medium from the cell culture dish from which the PC12 cell in Figure 4A was injected. The vertical scale is identical to that in Figure 4A, and peak identities are as in A. Reproduced with permission from Ref. 34.

analytes along the capillary bore. The dilution factor in these experiments is around 100, greatly reduced from pre-column derivatization schemes, and sample handling is also reduced (34). There is no need to transfer cells from one vial to another, since the separation capillary acts as the transferring mechanism as well as the reaction chamber.

POST-COLUMN DERIVATIZATION

It is not always optimal to perform derivatization prior to separation. One difficulty with this is multiple labeling of solutes (35). Components such as proteins which may contain more than one amino acid group can result in multiple peaks for the same analyte. In addition, loss of sample can result from the multiple sample handling and transfer steps involved in pre-column derivatization schemes. These difficulties provide the rationale for post-column derivatization work. Three derivatization reagents act rapidly enough to be used in post-column derivation. These are OPA (35, 44-47), fluorescamine (47, 48), and NDA with 3-mercaptoethanol (38). Several post-column reactor designs have also been demonstrated.

In most cases, the separation capillary must be modified to accommodate the introduction of the derivatization reagent. However, one method involves derivatization of the analytes in free solution between the elution end of the capillary and the detector (46). Several post-column designs employ pressure driven introduction of the derivatization agent through coaxially coupled capillaries (35, 44, 48) or cross connectors built directly into the capillary (45). Electroosmotic flow has also been used to introduce reagents and initiate mixing by way of a free-solution reactor (46) or a fluid gap reactor (47). The fluid gap reactor has been designed with the reaction capillary larger than the

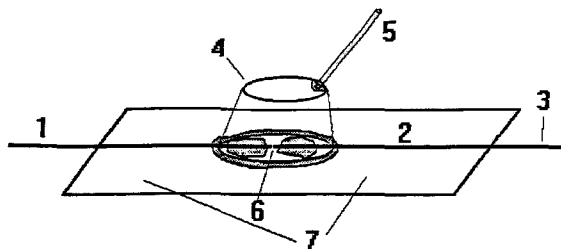


Figure 5 Schematic representation of a gap reactor: 1, separation capillary (applied positive high voltage); 2, reaction capillary (grounded); 3, detection window; 4, plastic gap reservoir (floated); 5, plastic syringe port; 6, capillary gap; 7, glass microscope slide. Lightly shaded areas represent epoxy. Reproduced with permission from Ref. 36.

separation capillary and derivatization agent was pulled into the fluid flow as the analytes traversed the gap. The best detection limits for these post-column reactors has been 41 attomoles with theoretical plates ranging from 175,000 to 600,000 (47). These methods have the capability to detect the levels of material found in single cells, however, they use 25-50 μm i.d. capillaries which are a little too large to conveniently handle single cells.

Another post-column detector based on the fluid gap reactor design uses a break in a single 10 μm i.d. capillary as the introduction port and therefore uses the same i.d. capillary for both the separation and detection ends. This allows for easy alignment of the two ends. A schematic diagram of this detector is shown in Figure 5. Reagent introduction in this system is due to reagent diffusion into the gap and an optimum gap distance of about 4 μm has been determined where peak tailing and band broadening are minimized. A sample electropherogram is shown in figure 6. Reagent introduction through this gap has been demonstrated using amino acid and protein separations with OPA derivatization, and detection limits of 130 amol and 5.2 amol for glycine and transferrin have been determined, respectively (36).

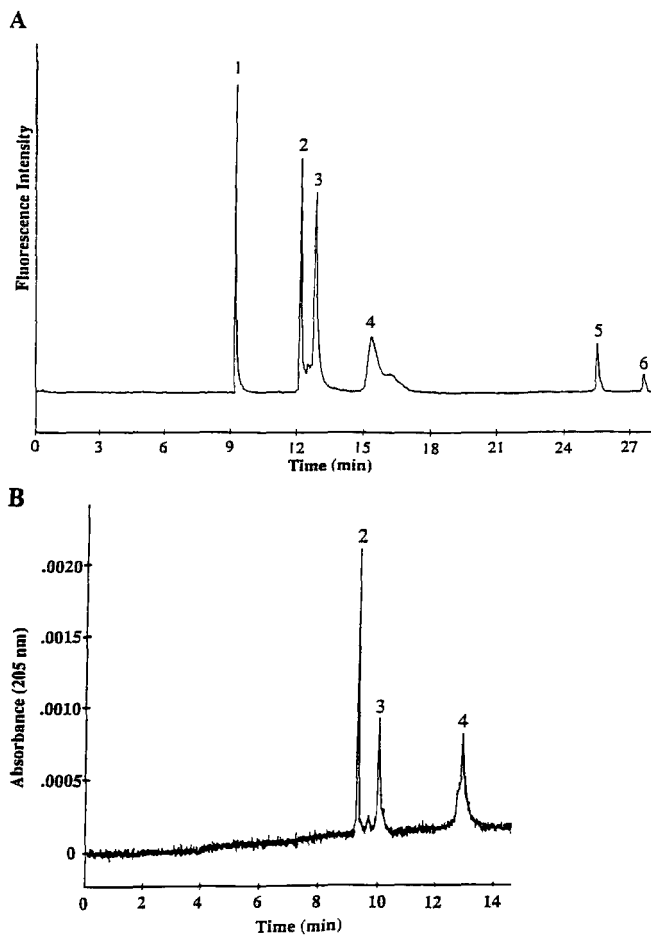


Figure 6 Separation of three proteins and three amino acids using post-column derivatization and LIF detection. Peak identities and sample concentrations are: 1, DL-arginine hydrochloride (5.0×10^{-5} M); 2, horse heart myoglobin (0.5 mg/mL); 3, iron-free human transferrin (0.25 mg/mL); 4, bovine serum albumin (0.5 mg/mL); 5, (L+)-glutamic acid (5.0×10^{-5} M); 6, DL-aspartic acid, (5.0×10^{-5} M). Conditions: capillary, 10 μ m i.d.; 100 cm; 4 μ m gap; injection, 5 s at 10 kV; separation potential, 30 kV; separation buffer, 100 mM borate, pH 9.5. B. Separation of the same protein and amino acid mixture as in Figure 6A with UV absorbance detection at 205 nm. Peak identities, sample concentrations, and separation buffer are the same as in Figure 6A. Conditions: capillary, 25 μ m i.d., 73.3-cm length, 57.6 cm to detector; separation potential, 20 kV; injection, 5 s at 7.0 kV. The three amino acids can not be detected at the concentrations used here. Injection amounts of proteins are: horse heart myoglobin, 25.4 fmol; human transferrin, 2.7 fmol; bovine serum albumin, 5.0 fmol. Reproduced with permission from Ref 36

This same design has also been used with NDA/2-mercaptoethanol derivatization. The use of NDA as a derivatization reagent usually involves reaction with cyanide to form a stable fluorescent product. When reacted with mercaptoethanol the reaction produces a product which is relatively unstable and is not suitable for pre-column techniques; however, the reaction is sufficiently rapid for post-column work. Post-column derivatization with NDA has been used to separate and detect components from homogenates of *Planorbis corneus* neurons and single red blood cells (49).

CONCLUSIONS

CE-LIF is a very sensitive method for the analysis of single cells. It has been used on many different cell lines to examine amino acids and proteins. Pre-column, on-column and post-column methods of derivatization have been examined in order to determine which results in the least amount of sample handling and dilution leading to better detection limits for the analytes of interest. Pre-column derivatization methods have always been limited by dilution. The use of the picoliter reaction vials described here may be a tremendous advance in overcoming that limitation. With these vials it is conceivable that more extensive derivatization procedures which tag otherwise unidentifiable analytes may be used without the dilution problem. On-column derivatization provides an alternative scheme to pre-column work where the sample is confined to the entrance of the capillary as a reaction chamber. This method is highly effective at minimizing sample dilution; however, solutes that can be multiply labeled can still present a problem. In post-column work, multiple labeling of solutes is not problematic as the solutes have already been separated and dilution has been reduced because the volume is limited by the size of

the migrating zone of analyte. However, the derivatization reaction must be complete in a few seconds. Future advances in these analyses will likely focus on new reaction chemistry for rapid and quantitative derivatization as well as instrumental advances to immobilize cells in microvials, and to minimize dilution during derivatization while maintaining the integrity of the separation.

ACKNOWLEDGEMENTS

This research was supported in part by the National Institutes of Health. We would like to thank Dr. Beth Hall and Leann Keim for their assistance with the picoliter vials which were fabricated at the National Nanofabrication Facility at Cornell University, supported by the National Science Foundation.

REFERENCES

1. E. Giacobini, *J. Neurosci. Res.*, **18**, 632-637 (1987).
2. E. Ishikawa, S. Hashida, T. Kohno, K. Hirota, *Clin. Chim. Acta*, **194**, 51-72 (1990).
3. G. T. Matioli and H. B. Niewisch, *Science*, **150**, 1824-1826 (1965).
4. W. Tank, M. Sugimori, J. A. Conner, R. R. Llinas, *Science*, **242**, 773-776 (1988).
5. J. A. Jankowski, T. J. Schroeder, R. W. Holz, R. M. Wightman, *J. Biol. Chem.*, **267**, 18329-18335 (1992).
6. A. G. Ewing, T. G. Strein, Y. Y. Lau, *Accts. Chem. Res.*, **25**, 440-447 (1992).
7. D. J. Leszczyszyn, J. A. Jankowski, O. H. Viverso, E. J. Diliberto, J. A. Near, R. M. Wightman, *J. Neurochem.*, **56**, 1855-1863 (1991).
8. R. T. Kennedy, M. D. Oates, B. R. Cooper, B. Nickerson, J. W. Jorgenson, *Science*, **246**, 57-63 (1989).

9. R. T. Kennedy, R. L. St. Claire III, J. G. White, J. W. Jorgenson, *Mikrochim. Acta*, II, 37-45 (1987).
10. R. T. Kennedy, and J. W. Jorgenson, *Anal. Chem.*, 61, 436-441 (1989).
11. M. D. Oates, B. R. Cooper, and J. W. Jorgenson, *Anal. Chem.*, 62, 1573-1577 (1990).
12. B. R. Cooper, J. A. Jankowski, D. J. Leszczyszyn, R. M. Wightman, J. W. Jorgenson, *Anal. Chem.*, 64, 691-694 (1992).
13. W. S. Sossin and R. H. Scheller, *Brain Res.*, 494, 205-214 (1989).
14. E. Betzig, J. K. Trautman, T. D. Harris, J. S. Weiner, R. L. Kostelak, *Science*, 251, 1468-1470 (1991).
15. W. Tan, Z.-Y. Shi, S. Smith, D. Birnbaum, R. Kopelman, *Science*, 258, 778-781 (1992).
16. D. S. Mantus, G. A. Valaskovic, G. H. Morrison, *Anal. Chem.*, 63, 788-792 (1991).
17. R. A. Wallingford and A. G. Ewing, *Anal. Chem.*, 61, 98-100 (1989).
18. J. B. Chien, R. A. Wallingford, A. G. Ewing, *J. Neurochem.*, 54, 633-638 (1990).
19. T. M. Olefirowicz and A. G. Ewing, *Anal. Chem.*, 69, 1872-1876 (1990).
20. T. M. Olefirowicz and A. G. Ewing, *J. Neurosci. Methods*, 34, 11-15 (1990).
21. T. M. Olefirowicz and A. G. Ewing, *Chimia*, 45, 106-108 (1991).
22. B. L. Hogan and E. S. Yeung, *Anal. Chem.*, 64, 2841-2845 (1992).
23. T. T. Lee and E. S. Yeung, *Anal. Chem.*, 64, 3045-3051 (1992).
24. A. G. Ewing, *J. Neurosci. Methods*, 48, 215-224 (1993).
25. A. M. Hoyt, Jr., S. C. Beale, J. P. Larmann, Jr., J. W. Jorgenson, *J. Microcolumn Sepn.*, 5, 325-330 (1993).
26. Q. Xue and E. S. Yeung, *J. Chromatogr. A*, 661, 287-295 (1994).
27. H. K. Kristensen, Y. Y. Lau, A. G. Ewing, *J. Neurosci. Methods*, 51, 183-188 (1994).

28. Q. Xue and E. S. Yeung, *Anal. Chem.*, 66, 1175-1178 (1994).
29. Z. Rosenzweig, E. S. Yeung, *Anal. Chem.*, 66, 1771-1776 (1994).
30. J. Bergquist, S. D. Gilman, A. G. Ewing, R. Ekman, *Anal. Chem.*, 66, 632 (1994).
31. H. T. Chang and E. S. Yeung, *Anal. Chem.*, 67, 1079-1083 (1995).
32. B. L. Hogan and E. S. Yeung, *Trends Anal. Chem.*, 12(1), 4-9 (1993).
33. B. Nickerson and J. W. Jorgenson, *J. High Resolut. Chromatogr./Chromatogr. Commun.*, 11, 533-881 (1988).
34. S. D. Gilman and A. G. Ewing, *Anal. Chem.*, 34, 58-64 (1995).
35. D. J. Rose, Jr., and J. W. Jorgenson, *J. Chromatogr.*, 447, 117-131 (1988).
36. S. D. Gilman, J. J. Pietron, A. G. Ewing, *J. Microcol. Sep.*, 6, 373-384 (1994).
37. S. Wu and N. J. Dovichi, *Talanta*, 39, 173-178 (1992).
38. J. V. Sweedler, J. B. Shear, H. A. Fishman, R. N. Zare, R. H. Scheller, *Anal. Chem.*, 63, 496-502 (1991).
39. J. Liu, Y. Hsieh, D. Wiesler, M. Novotny, *Anal. Chem.*, 63, 408-412 (1991).
40. J. Liu, O. Shiota, M. Novotny, *Anal. Chem.*, 63, 413-417 (1991).
41. L. Hernandez, J. Escalona, N. Joshi, N. Guzman, *J. Chromatogr.*, 559, 183-196 (1991).
42. L. N. Amankwa, M. Albin, W. G. Kuhr, *Trends Anal. Chem.*, 11, 114-120 (1992).
43. M. Jansson, A. Emmer, J. Roeraade, U. Lindberg, B. Hök, *J. Chromatogr.*, 626, 310-314 (1992).
44. B. Nickerson and J. W. Jorgenson, *J. Chromatogr.*, 480, 157-168 (1989).
45. S. L. Pentoney, Jr., X. Huang, D. S. Burgi, R. N. Zare, *Anal. Chem.*, 60, 2625-2629 (1988).
46. D. J. Rose, Jr., *J. Chromatogr.*, 540, 343-353 (1991).
47. M. Albin, R. Weinberger, E. Sapp, S. Moring, *Anal. Chem.*, 63, 417-422 (1991).

48. T. Tsuda, Y. Kobayashi, A. Hori, T. Matsumoto, O. Suzuki, *J. Chromatogr.*, **456**, 475-481 (1988).
49. S. D. Gilman and A. G. Ewing, *Anal. Methods Instrumentation.*, in press (1995).

Received: July 17, 1995

Accepted: August 6, 1995

IDENTIFICATION OF NUCLEIC ACIDS AND OLIGONUCLEOTIDES BY CAPILLARY ZONE ELECTROPHORESIS WITH THE FOUR MARKER TECHNIQUE

HELI SIRÉN¹, JUHO H. JUMPPANEN^{1,2},
KIMMO PELTONEN³, AND MARJA-LIISA RIEKKOLA^{1*}

¹*Department of Chemistry
Laboratory of Analytical Chemistry
University of Helsinki*

*P.O. Box 55 (A.I. Virtasen aukio 1)
FIN-00014 Helsinki, Finland*

²*Cultor Ltd.*

*Finnsugar Development
FIN-02460 Kantvik, Finland*

³*The Institute of Occupational Health
Topeliuksenkatu 41 aA
FIN-00180 Helsinki, Finland*

ABSTRACT

The paper describes the improvement brought by the four marker technique to the repeatability of the separation of macromolecules [nicotinamide nucleotides (NADPH and NADH), one adenine compound (ATP), two oligonucleotides (135-oligomer and 84-primer containing 135 and 20 bases, respectively) and N2-5'-deoxyquanosine-benzo[a]pyrene-diolepoxide (dG5'BaDE)] by capillary zone electrophoresis with UV detection at the wavelength of 220 nm. Optimized conditions [3-(cyclohexylamino)-1-propanesulphonic acid as the organic electrolyte solution with pH of 11.2, and concentration of 50 mM] were used for the separation. The counter-ion in the system was sodium. The macromolecules could be separated within 20 minutes. The four marker

compounds were (-)-mandelic acid, *meso*-2,3-diphenylsuccinic acid, 1,2-phenylenediacetic acid and *o*-phthalic acid, which were used for the calculations of the mobilities for the analytes. The identification of the macromolecules was confirmed with the coefficients of identification. The reliability of the identification was increased up to 75-fold relative to the use of the absolute migration times.

INTRODUCTION

Living cells produce an impressive variety of macromolecules, chiefly proteins, nucleic acids and polysaccharides, which serve as structural components, biocatalysts, hormones and repositories of energy. Nucleic acids are the fundamental genetic material of all living organisms. Normally they are long-chained polymers consisting of several different components, including phosphoric acid, sugar, and purine and pyrimidine bases. Nucleic acids, including single-stranded DNA, are widely varied in structures.

In general, the procedures for separating nucleic acids and synthetic oligonucleotides are complex processes that differ according to the type of material to be separated. The use of CE for the separation of nucleic acids has been reviewed in a few papers [1,2]. Many recent investigations have been devoted to the development of CE methods for the isolation, purification and sequencing of nucleic acids and their constituents [2]. Dolnik et al. [3] have separated oligonucleotides in CZE and also discovered that spermine added to the electrolyte solution enhances the separation. Yamamoto et al. [4] have suggested that mononucleotides of calf thymus DNA could be separated under similar conditions to those used in isotachophoretic separations of proteins by adding ampholine to the background buffer solution. Later on, Heiger et al. [5] suggested that use of gels would provide better separations of the proteins than in CZE. One example of the excellent efficiency of CZE is the separation of 19- to 60-mers of DNA within 30 min [6]. Senda et al. [7] have described MEKC-separations with fluorescence detection for nicotinamide nucleotides and adenine compounds.

Poor repeatability of absolute migration times of analytes has been a major drawback of capillary electrophoretic techniques, in both qualitative and quantitative analyses. Numerous attempts have been made to improve quantitation by applying internal standards [8-16]. Also, the use of retention indices [17] and attention to the concept of pseudo-effective mobility [18] have been reported to improve the level of quantitation in MEKC. Although the fluctuation of electroosmosis (v_{eo}) is well known to be the major source of variation in analyte absolute migration times, little effort has been made to study the time dependence more closely. Lee et al. [19] and Jumppanen et al. [20] have recently proposed that the problem could be solved by taking the effect of v_{eo} into account by determining its time dependency rather than by trying to suppress it. Our approach relies on marker compounds of known electrophoretic mobilities. Another important factor is the effective electric field strength, which is the net force affecting an ion and depends on the composition of the electrolyte solution as well as on the applied voltage [21,22].

The basic requirement for the use of marker techniques in CZE and MEKC is that the marker compounds do not undergo changes in mobility if small changes occur in the composition of the electrolyte solution [20,23]. In practice, this means that the marker compounds must have pK_a values far from the pH of the buffer, they must not undergo thermal degradation or conformational changes, and, in the case of MEKC, they must not partition strongly into micelles. When these requirements are met, the marker techniques should work well. If they are not, the repeatability will suffer.

Difficulties have been encountered in CZE separations of macromolecules, especially proteins and peptides. Many proteins possess positive, multiply charged domains that may cause proteins to adsorb onto silica capillary walls [24]. Furthermore, proteins and other macromolecules may undergo chemically induced or temperature induced conformational changes that alter their electrophoretic mobilities [25]. Such behaviour also limits the ability of CE to separate compounds in a repeatable way.

Many methods, such as the Randerath ^{13}P -postlabelling assay, are used for the screening of DNA adducts in biological systems [26, 27]. Although the method is very sensitive, however, the assay is not structure-specific, which means that the procedures are unreliable.

The marker techniques developed in our laboratory have worked well for small, rigid molecules. However, the applicability of the technique to enhance the repeatability of the separation of larger molecules by capillary electrophoresis has not yet been tested. Accordingly, the purpose of this work was to compare the reliability of the identification of selected macromolecules by CZE when using the four marker technique and when using absolute migration times.

EXPERIMENTAL

Chemicals

Nicotinamide-adenine dinucleotide phosphate (NADPH, MW 663 g/mol) was from Boeringer Mannheim (Germany). 3-(Cyclohexylamino)-1-propanesulfonic acid (CAPS), adenosine triphosphate (ATP, MW 507 g/mol) and nicotinamide-adenine dinucleotide (NADH, MW 743 g/mol) reduced from β -DPNH and containing β -NADH were purchased from Sigma (Dorset, UK). HPLC-grade methanol, KOH (Titrisol), 1,2-phenylenediacetic acid and *o*-phthalic acid were from Merck (Darmstadt, Germany), *meso*-2,3-diphenylsuccinic acid from Trade TCL (Japan), and (-)-mandelic acid from EGA-CHEMIE (Steinheim, Germany). The racemic mixture of dG5-BaDE (N2-5'-deoxyquanosine-benzo[a]pyrenediolepoxide, MW about 571 g/mol) adduct, the 135-oligomer (MW about 43880 g/mol) and the 84-primer (MW about 6349 g/mol) of oligonucleotides were synthesised, extracted and purified at the laboratory of the Institute of Occupational Health (Helsinki, Finland). The 84-primer products were synthesised by using a conventional nucleic acid synthesiser and the oligonucleotides were cloned by using PCR. N2-5'-

deoxyquanosine-benzo[a]pyrenediolepoxide adduct was synthesised as described in the literature [27]. The structures of the analytes are presented in Figure 1.

Apparatus

CE was performed in a 87.0-cm uncoated fused silica capillaries (80.0 cm to the detector) with 50 μm i.d. and 360 μm o.d. (Composite Metal Services Ltd., The Chase, Hallow, Worcs., UK). The capillary electrophoresis apparatus was a Beckman 2050 P/ACE capillary electrophoresis system with a UV/visible detector (wavelength 220 nm) and a liquid cooling system for the capillary (Beckman Instruments, Fullerton, CA, USA). The data were printed and analysed with an HP 3396A integrator (Hewlett-Packard, Avondale, PA, USA). All experiments were carried out at +23 °C. The samples were injected hydrostatically by pressure (0.500 psi) for 10 s. The running voltage was 22 kV.

Treatment of the capillary

Before starting the analysis a new capillary was successively purged with 0.1 M NaOH for 2 min, followed by water for 2 min and then with the running buffer for 5 min. Before each injection the capillary was flushed for 5.0 min with the running buffer.

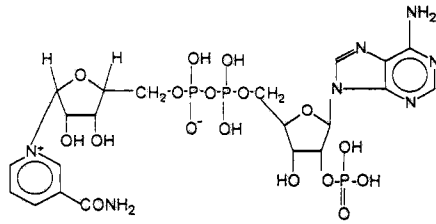
Preparation of electrolytes

The pHs of the solutions were adjusted with a Jenway 3030 pH meter connected to a Jenway electrode (Jenway Ltd., Felsted, England) containing 3

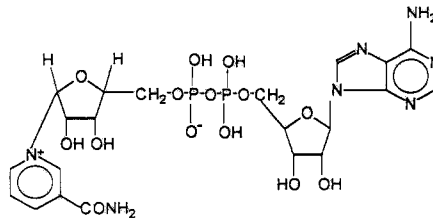
Preparation of electrolytes

The pHs of the solutions were adjusted with a Jenway 3030 pH meter connected to a Jenway electrode (Jenway Ltd., Felsted, England) containing 3 M KCl in saturated AgCl solution. The electrode system was calibrated with Convol BDH buffer solutions (BDH Chemicals Ltd., Poole, UK) and FIXANAL solutions (Riedel-deHaën AG, Seelze, Germany) of pHs 10.00 and

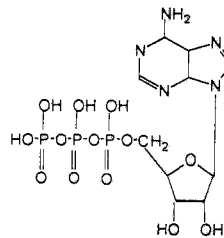
NADPH



NADH



ATP



BASE SEQ TO 20 MER
(84-PRIMER)

5'- gca gca ttt acc tct atc gt

BASE SEQ TO 135 OLIGOMER

ag gcctgctgaa aatgactgag tataaacctg₅ tggtagttgg agctggtggc
gtaggcaaga gtccttgac gatacagcta attcagaatc actttgtgga tgaatatgat
cctacgatag aggtaaatgc tgc

dGS-BaDE

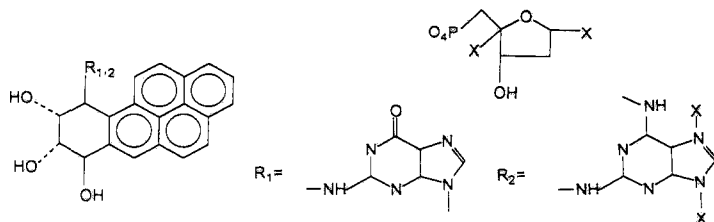


Figure 1. Structures of the macromolecules studied.

11.00. The electrolyte solutions were filtered through 0.45 μm membrane filters (Millipore, Molsheim, France) and degassed before use in an ultrasonic bath.

Determination of viscosity

The absolute viscosity of the electrolyte solutions in CZE separations was determined with an S.I.L.-type viscometer and a pycnometer. The average kinematic viscosity of the 50 mM CAPS solution (pH 11.2) was 0.9273 ± 0.0001 cSt ($n=6$, 23 °C) and the average density was 1.00155 ± 0.00002 g/cm³ ($n=6$, 23 °C). The average absolute viscosity was 0.9288 ± 0.0001 cP. All calculations were carried out with "in-house" designed programs operating in MATLAB (Mathworks Inc.) [20-23].

Preparation of the electrolyte solutions

0.050 M CAPS solution was prepared by weighing 11.2656 g of CAPS powder into 1000 ml total volume of deionized distilled water. The pH was adjusted with 35 ml of 1.000 M NaOH solution to 11.2. After filling the volumetric flask to the one-mark level, the solution was homogenized and kept for 10 min in an ultrasonic bath before filtering it with a Millipore system with 0.45 μm filters. The ionic strength of the solution was 0.085 M.

Preparation of the samples

1000 ppm stock solutions of each nucleic acid and oligonucleotides were prepared to distilled, deionized and filtered water. The 1000 ppm stock solutions of the marker compounds were prepared to HPLC-grade methanol. The final sample was prepared from the stock solutions by pipetting 40 μl of each analyte solution into the sample vial and adding 40 μl of each marker compound and purified, filtered water up to a total volume of 350 μl .

Electrophoretic separations

The final sample solution was analysed nine times by introducing fresh electrolyte solutions after every three injections.

Marker techniques

During one analysis the matrix operation can be expressed as

$$\mathbf{X} = \mathbf{A}^{-1} \mathbf{B}, \quad (1)$$

where the matrices are

$$\mathbf{A} = \begin{matrix} 1/3t_1^3 & 1/2t_1^2 & t_1 & \mu_1 t_1 \\ 1/3t_2^3 & 1/2t_2^2 & t_2 & \mu_2 t_2 \\ 1/3t_3^3 & 1/2t_3^2 & t_3 & \mu_3 t_3 \\ 1/3t_4^3 & 1/2t_4^2 & t_4 & \mu_4 t_4 \end{matrix} \quad \mathbf{B} = \begin{matrix} L_{det} \\ L_{det} \\ L_{det} \\ L_{det} \end{matrix} \quad \mathbf{X} = \begin{matrix} c \\ b \\ a \\ E_{eff} \end{matrix}, \quad (2)$$

where t_1 - t_4 are the the migration times and μ_1 - μ_4 are the electrophoretic mobilities of the four markers, respectively. L_{det} can be calculated from Eq. 3. Constants a , b and c are values for electroosmotic flow velocity (v_{eo}), linear acceleration of v_{eo} and non-linear acceleration of v_{eo} , respectively. E_{eff} is the effective electric field strength.

However, when four markers were used, v_{eo} were approximated to accelerate non-linearly. The mobilities were calculated with Eqs. 2-4. The basic equation is

$$L_{det} = ct_x^3/3 + bt_x^2/2 + at_x + E_{eff} \mu_{ep(x)} t_x, \quad (3)$$

where $\mu_{ep(x)}$ is the electrophoretic mobility of the unknown (x) analyte.

After solving for X in Eq. 1, the electrophoretic mobilities of the macromolecules can be calculated from

$$\mu_{ep(x)} = (L_{det}/t_x - ct_x^2/3 - bt_x/2 - a)/E_{eff} \quad (4)$$

Reliability of the identification

The reliability of the identification can be expressed by the coefficient Q_{id} .

$$Q_{id} = (x_2 - x_1)/(\sigma_1 + \sigma_2), \quad (5)$$

where x_1 and x_2 are the responses of interest (e.g. migration times), and σ_1 and σ_2 are their standard deviations. If the Q_{id} value exceeds 2, the differentiation between two analytes can be considered reliable [21].

RESULTS AND DISCUSSION

We studied the use of marker compounds to improve the reliability of CZE analysis of NADH, NADPH, ATP and three oligonucleotides. The calculations were based on the data obtained from the separations of the mixture containing the analytes and the four aromatic mono- and dicarboxylic acids, (-)-mandelic acid, *meso*-2,3-diphenylsuccinic acid, 1,2-phenylenediacetic acid and *o*-phthalic acid under basic conditions (50 mM CAPS, pH 11.2, 23 °C, Na as the counter-ion, Fig.2). With the four marker technique (4m), it was possible to approximate the electro-osmotic flow velocity (v_{eo}) to be non-linearly accelerating, while the effective electric field strength (E_{eff}) was approximated to stay constant during each run. The marker compounds were selected so that their mobilities were more or less evenly distributed, ($-3.1 \cdot 10^{-8} \text{ m}^2\text{V}^{-1}\text{s}^{-1}$ to $-5.2 \cdot 10^{-8} \text{ m}^2\text{V}^{-1}\text{s}^{-1}$, Table 1) to calibrate for electrophoretic mobilities of the analytes ranging from $2.0 \cdot 10^{-8} \text{ m}^2\text{V}^{-1}\text{s}^{-1}$ to $5.5 \cdot 10^{-8} \text{ m}^2\text{V}^{-1}\text{s}^{-1}$ (Table 2).

In addition, in applying the marker techniques it has proven to be important not to use marker compounds that have electrophoretic mobilities very close to each other in any particular system.

The analytes studied in this work were very different from the marker compounds of relatively small molecular size. The analytes, in turn, were large compounds (MW 500-43880 g/mol), of less rigid structure, and their pKa-values were far closer to the pH of the electrolyte solution than those of the marker compounds. Figure 2 shows that the nucleic acid, adenoside triphosphate and the oligonucleotides migrated in the order of increasing molecular mass in CZE technique.

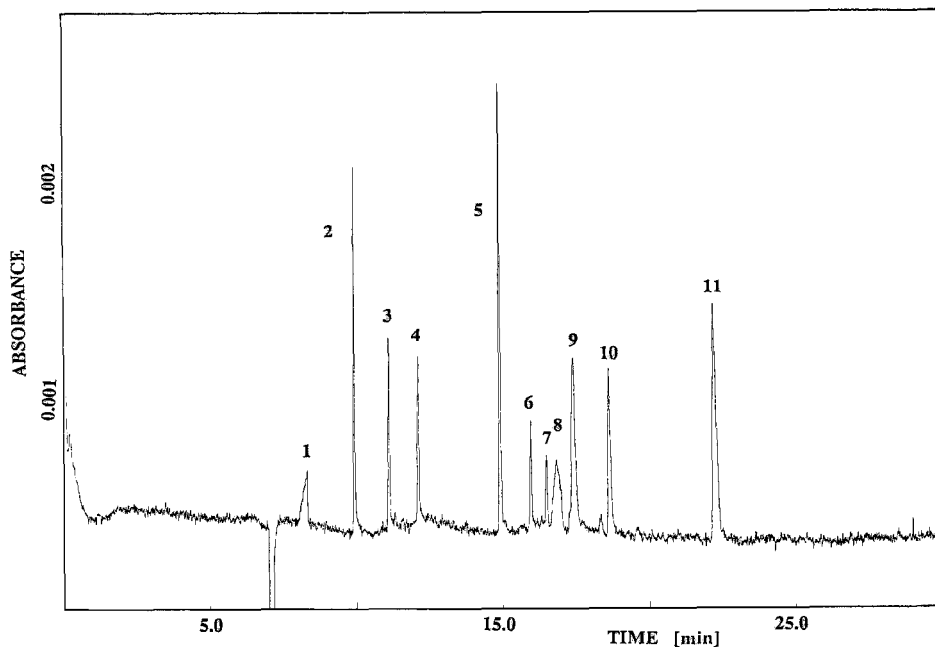


Figure 2. Electropherogram of 35 $\mu\text{g}/\text{ml}$ of 1 = system peak, 2 = 135-oligomer, 3 = NADPH, 4 = (-)-mandelic acid, 5 = *meso*-2,3-diphenylsuccinic acid, 6 = NADH, 7 = 84-primer, 8 = ATP, 9 = dG5'BaDE, 10 = 1,2-phenylenediacetic acid, 11 = *o*-phthalic acid. Migration conditions as described in the Experimental section.

TABLE 1.

Marker compounds and their mobility values in 50 mM CAPS (pH 11.2).

Marker compound	Mobilities $\mu_{\text{app}} \cdot 10^{-8} \text{ m}^2 \text{ V}^{-1} \text{ s}^{-1}$
(-)-mandelic acid	-3.1249
<i>meso</i> -2,3-diphenylsuccinic acid	-3.9799
1,2-phenylenediacetic acid	-4.7544
<i>o</i> -phthalic acid	-5.1964

TABLE 2.

Average values and standard deviations for absolute migration times and for electrophoretic mobilities determined by four marker technique.

$$E_{\text{eff}} = 2.3 \times 10^4 \text{ Vm}^{-1}$$

Analytes	Migration time [min]			Mobilities [$10^{-8} \text{ m}^2\text{V}^{-1}\text{s}^{-1}$]		
	$t_{\text{a,ave}}$ RSD%	SD		$\mu_{\text{ep}}(\text{ave})$	SD	RSD%
135-oligomer	10.12	0.19	1.9	-2.2111	0.0037	0.166
NADPH	11.35	0.24	2.1	-2.7401	0.0018	0.067
NADH	16.47	0.53	3.2	-4.2397	0.0010	0.024
84-primer	17.07	0.59	3.5	-4.4236	0.0125	0.284
ATP	17.38	0.56	3.2	-4.5206	0.0020	0.044
dG5'BaDE	17.95	0.55	3.1	-4.6966	0.0248	0.527

To the macromolecules in this study, the four marker technique enhanced the reliability of the analysis dramatically. The average absolute migration times and electrophoretic mobilities and their relative standard deviations for all the analytes are presented in Table 2. It can be seen, that the repeatabilities of the mobilities of the analytes were very reliable and at promille level.

However, the relative standard deviations of the oligonucleotides are higher than those of nucleic acids and ATP, most presumably because their pK_a -values are too close to the pH of the electrolyte solution. It has been shown elsewhere, [20] that the repeatability of analysis can be increased by a factor up to 350 for aromatic carboxylic acids at pH 10.6. The same research revealed that such excellent repeatabilities are more difficult to achieve for compounds that undergo changes when small changes are induced in the carrier electrolyte. For such compounds there are some practical limits on the use of marker compounds.

TABLE 3.
Values of coefficients for identification of the macromolecules.

Pair of analytes	Coefficient of identification Q_{id}	
	Migration times	Mobilities
135-oligomer - NADPH	2.87	96.1
NADPH - NADH	6.69	525
NADH - 84-primer	0.533	21.8
84-primer - ATP	0.271	3.21
ATP - dG5'BaDE	0.511	7.34

Even though, in this study it can clearly be seen, that the electrophoretic mobilities determined by the four marker technique are clearly more reliable than the absolute migration times themselves, the reliability is more accurately studied by using the coefficient for identification Q_{id} (Eq. 5). The Q_{id} value can be determined from the analyte absolute migration times compared with the Q_{id} value from the electrophoretic mobilities, for each pair of successively eluting analytes. The results are presented in Table 3. For each analyte pair Q_{id} value is much greater when calculated from the electrophoretic mobilities of the analytes by 4m than when calculated from the absolute migration times. All the values obtained on the basis of the mobilities of the marker compounds show that the analyses are very reliable. However, when the values are calculated from the absolute migration times, only few of the results are above 2.

As a conclusion, our results demonstrate the effectiveness of the 4m technique to improve the reliability of CZE analysis, even for analytes of large molecular weights lacking rigid structures. Good repeatabilities (0.04-0.52%) were obtained for the macromolecules studied. The coefficient for identification of the analyte pairs, Q_{id} , was clearly better, when identification was based on electrophoretic mobilities rather than absolute migration times.

REFERENCES

1. Z. Deyl, R. Struzinsky, *J. Chromatogr.*, **569**: 63-122 (1991)
2. W. Kuhr, *Anal. Chem.*, **62**: 403R-414R (1990)
3. V. Dolnik, J.-P. Liu, J.F. Banks, M.V. Novotny, P. Bocek, *J. Chromatogr.*, **480**: 321-330 (1989)
4. H. Yamamoto, T. Manabe, T. Okuyama, *J. Chromatogr.*, **480**: 277-283 (1989)
5. D.N. Heiger, A.S. Cohen, B.L. Karger, *J. Chromatogr.*, **516**: 33-48 (1990)
6. A.M. Chin, J.C. Colburn, The 2nd Int. Symp. on HPCE, 1990, San Francisco, CA, Abstract, TL 106.
7. M. Senda, T. Sasaki, T. Hiyama in Proceedings of the 14th Symposium on Capillary Chromatography, Eds. P. Sandra, M.L. Lee, F. David and G. Devos, Baltimore, Maryland, USA, pp. 545-551.
8. S. Fujiwara, S. Honda, *Anal. Chem.*, **58**: 1811-1814 (1986)
9. S. Honda, S. Iwase, S. Fujiwara, *J. Chromatogr.*, **404**: 313-320 (1987)
10. X. Huang, J.A. Luckey, M.J. Gordon, R.N. Zare, *Anal. Chem.*, **61**: 766-776 (1989)
11. E.V. Dose, G.A. Guiochon, *Anal. Chem.*, **63**: 1154-1158 (1991)
12. T. Lee, E.S. Yeung, *Anal. Chem.*, **63**: 2842-2848 (1991)
13. J.L. Beckers, F.M. Everaerts, M.J. Ackermans, *J. Chromatogr.*, **537**: 407-428 (1991)
14. R. Vespalec, P. Gebauer, P. Bocék, *Electrophoresis* **13**: 677-682 (1992)
15. S. Fujiwara, S. Honda, *Anal. Chem.* **59**: 2773-2776 (1987)
16. K. Otsuka, S. Terabe, T. Ando, *J. Chromatogr.*, **396**: 350-354 (1987)
17. P.G.H.M. Muijselaar, H.A. Claessens, C.A. Cramers, *Anal. Chem.*, **66**: 635-644 (1994)
18. M.T. Ackermans, F.M. Everaerts, J.L. Beckers, *J. Chromatogr.* **585**: 123-131 (1991)
19. T.T. Lee, R. Dadoo, R.N. Zare, *Anal. Chem.*, **66**: 2694-2700 (1994)
20. J.H. Jumppanen, M.-L. Riekkola, *Anal. Chem.*, **67**: 1060-1066 (1995)
21. J.H. Jumppanen, H. Sirén, M.-L. Riekkola, O. Söderman, *J. Microcol. Sep.*, **5**: 451-457 (1993)
22. J.H. Jumppanen, M.-L. Riekkola, *Electrophoresis* (1995), in press.
23. H. Sirén, J.H. Jumppanen, K. Manninen, M.-L. Riekkola, *Electrophoresis*, **15**: 779-784 (1994)
24. J.W. Jorgenson, K.D. Lukacs, *Science*, **222**: 266-273 (1983)
25. R.S. Rush, A.S. Cohen, B.L. Karger, *Anal. Chem.*, **63**: 1346-1350 (1991)
26. M.V. Reddy, K. Randerath, *Carcinogenesis*, **7**: 1543-1551 (1986)
27. K.A. Canella, K. Peltonen, A. Dipple, *Carcinogenesis*, **12**: 1109-1114 (1991)

Received: July 10, 1995

Accepted: August 6, 1995

**A STRATEGY FOR SEQUENCING PEPTIDES
FROM DILUTE MIXTURES AT THE LOW
FEMTOMOLE LEVEL USING MEMBRANE
PRECONCENTRATION-CAPILLARY ELECTRO-
PHORESIS-TANDEM MASS SPECTROMETRY
(mPC-CE-MS/MS)**

ANDY J. TOMLINSON¹ AND STEPHEN NAYLOR^{1,2}

¹Biomedical Mass Spectrometry Facility and

Department of Biochemistry and Molecular Biology

²Department of Pharmacology and Clinical Pharmacology Unit

Mayo Clinic

Rochester, Minnesota 55905

ABSTRACT

A unique method using membrane preconcentration capillary electrophoresis (mPC-CE) on-line with tandem mass spectrometry (mPC-CE-MS/MS) for sequencing <100 fmols of a series of MHC class I synthetic peptides is described. We show how this methodology in conjunction with transient isotachopheresis (tITP) after analyte elution from the membrane improves conventional CE-MS strategies by permitting the analysis of large sample volumes (>100 μ L) while maintaining high analyte resolution and separation efficiencies that are typically afforded by CE. Instrumental parameters, including the internal dimensions of the mPC-CE capillary, collision gas pressure, collision gas type, and collision energy, are all shown to have substantial effect on the abundance of product ions produced in tandem MS/MS spectra when attempting to sequence peptides at the sub 100 femtomole level. Furthermore, we demonstrate that the physico-chemical properties of these analytes can also affect the MS/MS product ion abundance. In

particular, the presence of acidic residue tends to reduce mPC-tITP-CE-MS/MS sensitivity and direct fragmentation processes resulting in incomplete sequence information. This can be overcome by a simple esterification of the carboxylic acid functional group. Ultimately, we present an optimized mPC-tITP-CE-MS/MS approach that permits peptide sequence determination by consumption of ~40 femtomole of peptide analyte.

INTRODUCTION

Peptide sequence determination by tandem mass spectrometry (MS/MS) is a well established technique (1,2). However, many biologically active peptides that require sequencing by MS/MS present two major challenges. First, these analytes are usually components of exceedingly complex mixtures and are not readily isolated in pure form by standard chromatographic procedures. Second, such peptides are invariably present at extremely low concentrations (often attomoles/ μL). These problems are particularly pronounced in the analysis of immunologically important peptides that bind to major histocompatibility complex (MHC) proteins, for presentation at the cell surface to cytolytic T-lymphocytes (3). For example, MHC class I peptides are reported to be extracted in low femtomole-low picomole amounts from $\sim 5 \times 10^{10}$ cells (4). Furthermore, it has been suggested that there are in excess of 10,000 different peptides that can be presented at the cell surface by the MHC protein (5).

We have reported the potential of on-line capillary electrophoresis-mass spectrometry (CE-MS) to effect the separation of complex mixtures of MHC class I peptides (6,7) given the recognized, high resolving capability of CE. However, it was noted that this approach proved to be problematical due to the limited loading capacity of conventional CE

capillaries for CZE separation (8). This is predominantly due to the low volumes (typically 1-2% of total capillary volume) that can normally be injected onto the capillary (9).

Subsequently we evaluated the use of a variety of commonly used sample injection techniques to increase sample loading onto the CE capillary and found transient isotachopheresis (tITP) to be of some limited success (10). Numerous other workers have also investigated the use of analyte stacking (11-15), field amplification (16) and tITP (17-23) to overcome the poor concentration limits of detection (CLOD) of CE and CE-MS in the analysis of a wide variety of compounds. However, since all of these approaches are electrophoretic and are performed within the CE capillary, they are also limited by the total volume of the CE capillary. Therefore, even in the most favorable cases, analyte resolution can only be effected by the introduction of up to 90% of the total capillary volume. This still only represents the analysis of <1 μ L of sample solution. Hence these electrophoretic sample introduction techniques are often of limited use in the analysis of biologically derived peptide mixtures such as MHC class I peptides.

Following the limited success with tITP, we explored the use of on-line preconcentration-CE-MS using an adsorptive phase at the capillary inlet as a potential method to achieve our goal of analyzing and sequencing MHC class I peptides (8). On-line analyte concentration (microreactor) capillaries for use with CE were pioneered by Guzman (24-26) and subsequently developed by us (27-36) and others (37-44). Furthermore, we have, to our knowledge, demonstrated the first use and compatibility of this approach on-line with a mass spectrometer as the

detector (27,30,32,33,35,36,45). Most groups have tended to use a solid phase packing at the inlet of the CE capillary (38-41,44). However, we and others have shown compromised CE performance when using solid phase (28,33,34,38) since it necessitates from a practical perspective the use of a relatively large bed volume. This has also, in part, been attributed to an increased back pressure that reduces hydrodynamic flow within the CE capillary (34,38). In addition, ion flow may be impaired by the solid phase, resulting in reduced or anomalous electroosmotic flow (EOF). We have also previously reported that large volumes of organic solvent required to remove analytes from the solid phase within the CE capillary can also lead to reduced EOF (46,47). These factors can result in the broadening of analyte zones, compromised resolution, and loss of separation efficiency.

To reduce and ensure a consistent bed volume of adsorptive phase, we have developed and demonstrated the use of a preconcentration cartridge that contains a membrane impregnated with a suitable stationary phase (33,34), as shown in Figure 1. The cartridge fits at the inlet of the conventional CE capillary and we have termed this approach membrane preconcentration-CE (mPC-CE). We have also demonstrated the applicability of this technique on-line with mass spectrometry (mPC-CE-MS) (33,35,36). Using this approach sample contaminants (e.g., biological matrix components or chemical reagents) can be pre-eluted from the phase and washed through the CE capillary prior to analyte elution and analysis. Such on-line sample cleanup reduces sample handling and improves analyte recovery.

In the present study, we further demonstrate the applicability of mPC-CE-MS for the analysis of dilute peptide mixtures. In particular we

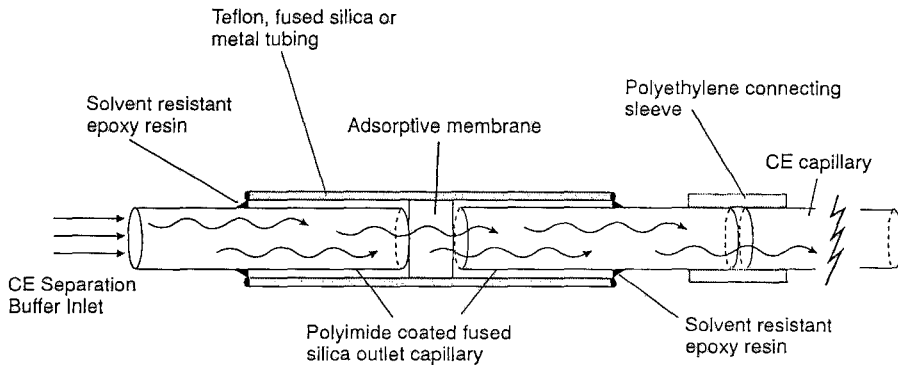


Figure 1 Schematic of a membrane preconcentration-capillary electrophoresis (mPC-CE) cartridge - (not to scale).

discuss the systematic development of mPC-CE-MS/MS for peptide sequence determination of synthetic MHC class I peptides at the low femtomole level. In this regard, it is noted that small changes in the type of collision gas, collision gas pressure, and collision energy can dramatically alter the appearance and quality of MS/MS spectra. We also discuss the improvement in spectral quality that occurs on using a smaller internal diameter CE capillary, as well as the use of chemical modification of peptides to enhance the abundance of product ions produced when glutamate and aspartate residues are present.

MATERIALS AND METHODS

Chemicals and Materials

Acetic acid (99.9%+ grade) was obtained from Aldrich Chemical Company (Milwaukee, WI). Ammonium acetate (99.9%+ grade),

ammonium hydroxide and potassium hydroxide were purchased from Sigma Chemical Company (St. Louis, MO). HPLC grade methanol, isopropanol, and water were obtained from Baxter (Minneapolis, MN). The synthetic MHC class I peptides SGINFEKL, SIINFEKL, and SIINFEKLT were synthesized by the Protein Core Facility at Mayo Clinic. The peptide mixture containing angiotensin II, bombesin, bradykinin, luteinizing hormone releasing hormone [LHRH], α -melanocyte stimulating hormone [α -MSH], leucine enkephalin, methionine enkephalin, oxytocin, and thyrotropin releasing hormone [TRH] was obtained from Biorad (Richmond, CA). Polymeric styrene-divinyl benzene copolymer (SDB) Empore™ membranes (3M, St. Paul, MN) were obtained from Varian (Harbor City, CA). Polyimide-coated fused silica capillary tubing was purchased from Polymicro Technologies (Phoenix, AZ). Teflon tubing was obtained from Chromtech (Apple Valley, MN).

mPC-CE-MS/MS

The CE capillary used in these experiments was prepared from uncoated fused silica tubing pretreated with sodium methoxide (0.5 M), methanol, and CE separation buffer. Membrane PC-CE-MS/MS studies were conducted using a cartridge system containing a SDB membrane as described previously (34) at the inlet of the CE capillary. The final dimensions of the capillary were 25 or 50 μm i.d. x 67 cm in length. After assembly, the entire PC capillary was conditioned under high pressure (20 psi) for ten minutes each with methanol and separation buffer. All subsequent capillary treatments and sample loading, washing, and elution were also carried out under high pressure (20 psi). It is noted that while the use of a mPC-cartridge reduces the rigidity of a CE capillary, this has caused no practical CE instrumentation problems in our hands.

The method of analysis included a cleaning regime of methanol (0.2 min) and separation buffer (5 min), followed by a high pressure injection of the peptide mixture (0.5-2 min injections). The capillary was then washed with separation buffer for 5 minutes and analytes were eluted from the hydrophobic membrane with a solution of methanol:water (80:20, v/v). The transient isotachopheresis (tITP) conditions were developed using a leading stacking buffer (LSB) of 0.1% ammonium hydroxide that was injected into the mPC-CE capillary prior to analyte elution. This was followed by a small volume of separation buffer (2 mM ammonium acetate:1% acetic acid in water) as a trailing stacking buffer (TSB).

Membrane PC-CE-MS/MS analyses were performed using a Beckman P/ACE 2100 instrument (Fullerton, CA, USA) modified with a Beckman-MS adapter kit for use with a mass spectrometer and coupled to a Reason Technology 486 personal computer (Rochester, MN, USA) with system control by System Gold software (Beckman). All analyses were performed on a Finnigan MAT 95Q (Bremen, Germany) of EBQ₁Q₂ configuration (where Q₁ is an rf-only octapole collision cell and Q₂ is a quadrupole mass filter). A Finnigan MAT electrospray ion source was used in positive ion mode. This source employs a spray needle that is floated to voltage (typically 3-5 kV) referenced to the accelerating voltage and a heated metal capillary (225°C) as the first stage of separation of the atmospheric pressure spray region from the vacuum of the mass spectrometer. Neither auxiliary nor sheath gas were used during these studies. The mPC-CE-MS studies were conducted at a resolution of ~1000 and a scan range of 300-1300 Da at a speed of 2 seconds/decade. Membrane PC-CE-MS/MS studies were conducted at a resolution of ~300

at MS_1 and 2-3 amu at MS_2 . The scan range of MS_2 was 60-1100 Da at a speed of 0.4 s/100 amu. Parameters of collision gas and energy are discussed in the figure legends.

RESULTS AND DISCUSSION

mPC-CE-MS

The overall goal in developing mPC-CE was to ensure that the on-line preconcentration cartridge did not adversely effect CE and CE-MS performance. Hence, we found that minimizing the volume of the adsorptive phase by using an appropriately impregnated membrane made it possible to reduce the volume of elution solvent required for efficient removal of analytes from the phase (33,36). Therefore, adverse effects due to the presence of large volumes of organic solvent on CE performance could be overcome. For convenience, the membrane was installed in a cartridge system, e.g., Teflon, fused silica, or metal (stainless steel or titanium) (33), as shown in Figure 1. This facilitates the ready removal of the cartridge to allow CE capillary cleaning/conditioning and activation of the adsorptive membrane. The high loading capacity of such membranes makes it possible to load large volumes (~60-100 μ L) prior to CE or CE-MS analysis (48). However, the small bed volume greatly enhances analyte recoveries using a reduced volume of organic elution solvent. Furthermore, on-line sample cleanup prior to CE-MS analysis is possible. This is particularly important for many samples derived from body fluids such as urine, where the presence of high salt concentrations can dramatically effect CE analyte separations by degrading the efficiency of contemporary CE stacking and focusing

procedures. One final advantage of mPC-CE is that a higher flow rate through the capillary is possible since impedance to flow is minimized, and this leads to faster analysis times and analyte migration is more reproducible.

mPC-tITP-CE-MS

We have previously reported that efficient recovery of peptides from the membrane requires the use of an adequate volume (>50 nL) of organic solvent (36). Hence even with mPC-CE, some peak broadening and degradation of analyte resolution may occur due to the volume of organic solvent present in order to maximize peptide recovery. Therefore we evaluated the use of tITP in conjunction with mPC-CE-MS after the peptides had been eluted from the adsorptive membrane. A nine peptide mixture consisting of angiotensin II, bombesin, bradykinin, LHRH, α -MSH, leucine-enkephalin, methionine-enkephalin, oxytocin, and TRH was loaded onto the mPC-CE cartridge. Transient ITP was effected by elution of the peptides from the membrane between zones of LSB (0.1% NH_4OH) and TSB (1% acetic acid). This method afforded baseline resolution of all of the peptides detected with theoretic plate values of 1.5×10^5 (leucine enkephalin) to 2.6×10^6 for α -MSH (see Figure 2). This example serves to demonstrate the minimal effect that mPC-CE has on CE-MS performance. The very hydrophilic peptide TRH was not detected, and we believe this is due to its poor retention on the SDB impregnated membrane.

We have also shown that variation of the LSB and TSB volumes allows manipulation of both migration time, peak width and resolution (36). More recently we have determined that the ratio of LSB to elution

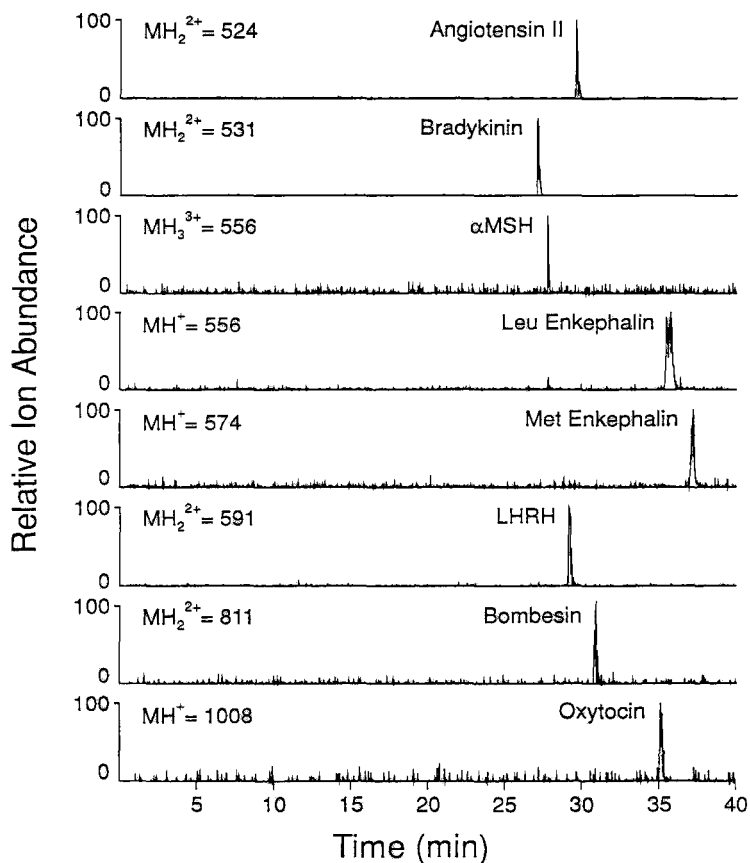


Figure 2 Ion electropherogram of a mPC-tITP-CE-MS analysis of a nine peptide mixture using a Beckman P/ACE 2100 CE connected to a MAT 95Q mass spectrometer. Separation buffer was 2 mM NH_4OAc :1% AcOH, on a 50 μm i.d. x 67 cm uncoated fused silica capillary, CE run at 30 kV. LSB was 0.1% NH_4OH (280 nL), elution solvent was 80:20 MeOH:H₂O (70 nL) and TSB was 1% AcOH (70 nL).

solvent volume is critical for optimal separation performance, and this will be reported elsewhere (48).

Conditions for mPC-CE-MS Analysis of Synthetic MHC Class I Peptides

As discussed, MHC peptides are usually present in low femto-picomole amounts. Therefore, any sample losses can easily result in a peptide concentration that is below the limits of detection. In this study, an uncoated mPC-CE capillary was used, since we have found that many of the coated CE capillaries commercially available are often not suitable for analysis of biologically derived peptides (49). In part, we believe this is due to the ubiquitous presence of trace amounts of surfactant, often used in cell lysis. The surfactants are carried through all the peptide purification steps that are undertaken prior to CE-MS analysis. Hence, while peptide-capillary wall interactions are minimized in coated CE capillaries, the hydrophobic interaction of the surfactant with the coated capillary wall, as well as the peptide with surfactant ultimately leads to peptide loss within the CE capillary. Therefore to minimize losses of biologically derived peptides, we have used the strategy of employing a carrier peptide when using an uncoated CE capillary. The carrier peptide, in this case angiotensin II, is added to the analyte peptide(s) in ~5-fold excess. The hydrophobic angiotensin II preferentially interacts with the active sites of the mPC-CE capillary minimizing analyte peptide losses. This strategy was employed in the mPC-CE-MS analysis of a mixture of three structurally similar, synthetic MHC class I peptides, namely SGINFEKL, SIINFEKL, and SIINFEKLT. The mPC-CE-MS ion abundance for all three peptides was ~30% lower when the carrier

peptide angiotensin II was not present, reflecting sizable losses to the capillary wall and possibly to the mPC-CE cartridge.

Using this approach, variable amounts of a solution containing ~200 attomoles/nL of the three MHC class I peptides were loaded onto the mPC-CE cartridge. Sample amounts of ~60 femtomoles, ~500 femtomoles and ~1.5 picomoles of the peptide mixture were subsequently analyzed by mPC-tITP-CE-MS. The mPC-tITP-CE-MS ion electropherogram for the 60 femtomole peptide mixture is shown in Figure 3. The ion electropherograms for the larger amounts of peptide loaded and analyzed by mPC-tITP-CE-MS also showed no appreciable loss of analyte resolution and quality of peak width and shape (results not shown), demonstrating the excellent dynamic range properties of mPC-CE-MS.

mPC-CE-MS/MS

The ultimate goal of peptide analysis is primary sequence determination. In this regard MS/MS affords both high sensitivity, and the most appropriate method for structural characterization of subpicomole amounts of peptide on-line with chromatographic separation techniques. Therefore, we have investigated the use of mPC-tITP-CE-MS/MS for sequencing synthetic MHC class I peptides present in a mixture at the low femtomole (<100 fmol) amounts.

Initial studies indicated that subtle changes in collision cell parameters led to substantial changes in product ion spectra. These changes appeared to be much greater for the analysis of low femtomole amounts of peptide than is normally observed at higher picomole amounts. This prompted us to systematically investigate the effects of all

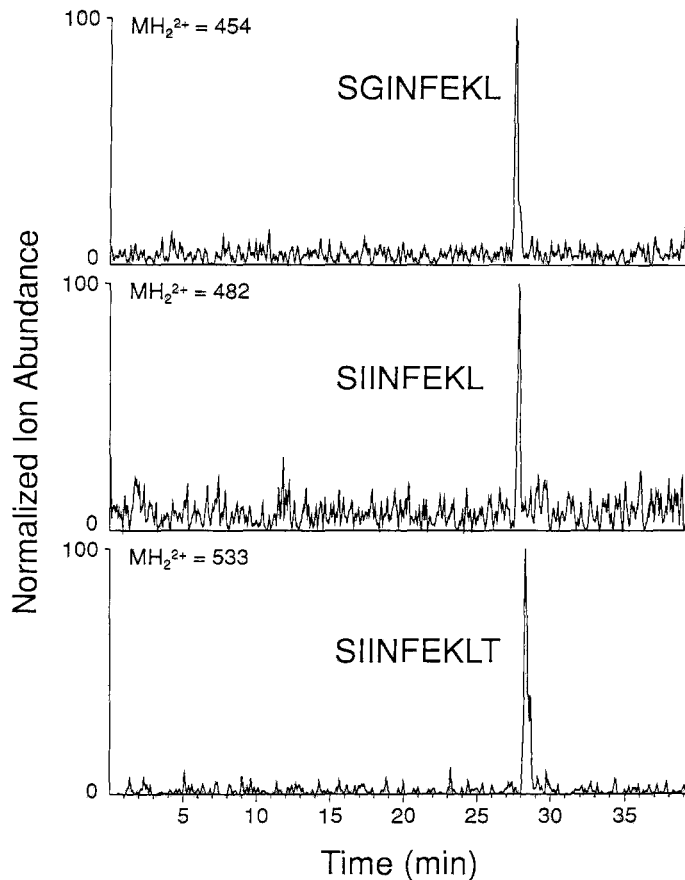


Figure 3 Ion electropherogram of a mPC-tITP-CE-MS analysis of a ~60 femtomole synthetic MHC class I peptide mixture. Conditions as described in Figure 2 except CE capillary was 25 μm i.d. x 67 cm at 20 kV, LSB was 80 nL, elution solvent was 80 nL and TSB was 30 nL.

collision cell parameters on product ion spectra obtained on less than 100 femtomoles of peptide.

Initially we optimized the pressure of the collision gas in order to minimize product ion scatter but maximize product ion formation and transmission (50). We investigated both argon and xenon as candidate target gases and found optimal gas pressures for each gas to be 2×10^{-5} mbar and 1.2×10^{-5} mbar, respectively. The differences observed in the product ion spectra after mPC-tITP-CE-MS/MS analysis of ~60 femtomoles of SIINFEKLT were substantial and are shown Figure 4. As expected from center of mass collision calculations, the larger atomic diameter of xenon gas dramatically increased the attenuation of the doubly charged precursor ion (MH_2^{2+}) (Figure 4B). This results in a substantial increase in yield of product ions detected at MS_2 . From these results xenon appears to be the most appropriate gas for generating abundant sequence-related product ions.

We have also found that small variations in collision energy (5-10 eV) can result in substantial differences of the type and abundance of product ions formed in the MS/MS analysis of low femtomole amounts of peptide. This is demonstrated in Figure 5 where the product ion spectrum of SIINFEKL was obtained using xenon at a gas pressure of 1.2×10^{-5} mbar with three different collision energies of 18, 22, and 26 eV. Clearly even a collision energy of 18 eV (Figure 5A) yields a series of y and b ions that readily allows determination of the peptide sequence. However, the product ion spectrum obtained at 26 eV (Figure 5C) not only contains a more abundant y and b series of ions but also a number of new product ions that were not readily discernible at 18 eV. Since our data

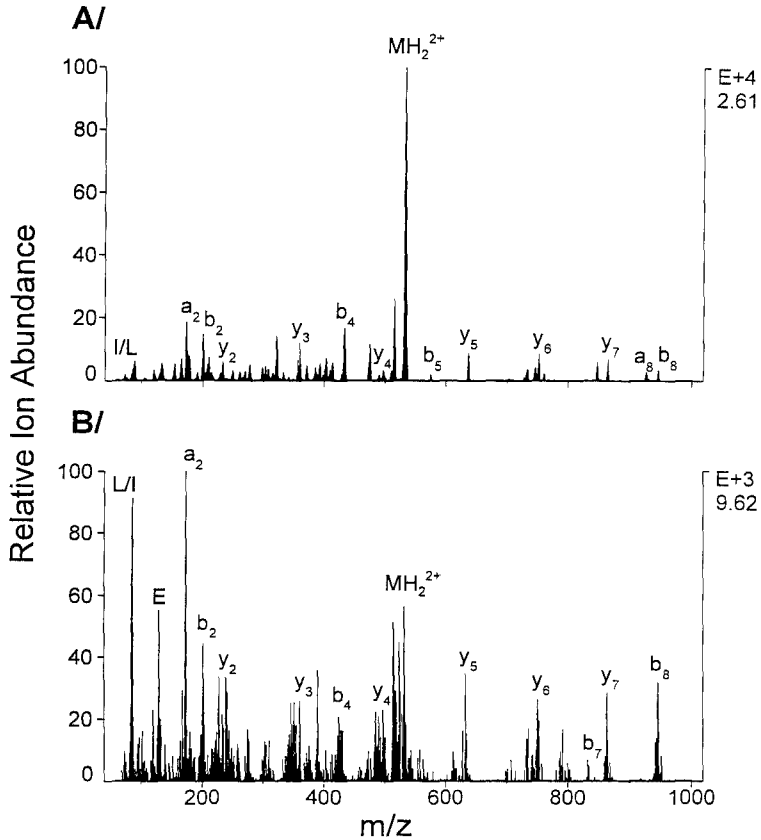


Figure 4 Product ion spectrum after mPC-tITP-CE-MS/MS analysis of ~60 femtomoles of SIINFEKLT, precursor ion selected $MH_2^{2+} = 533$. Conditions as for Figure 2 except separation voltage was 25 kV (plus low pressure infusion - 0.5 psi). LSB was 110 nL, elution solvent volume was 80 nL and TSB was 65 nL. For MS/MS conditions, the collision energy was 22 eV and A) argon was collision gas at a gas pressure of 2×10^{-5} mbar and B) xenon was collision gas at a gas pressure of 1.2×10^{-5} mbar.

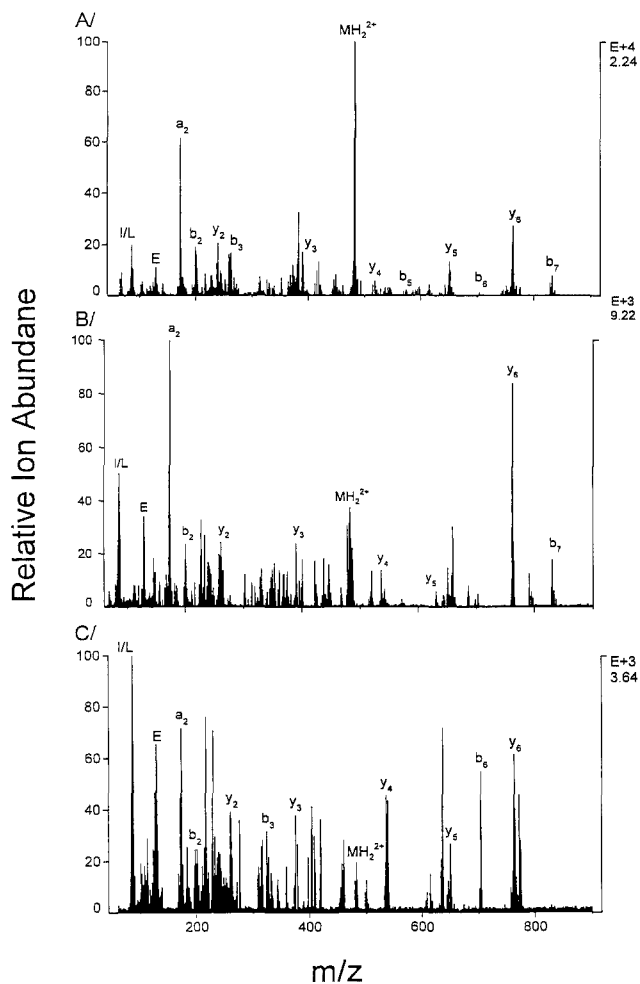


Figure 5 Effect of collision energy on the product ion spectrum of ~60 femtomoles of SIINFEKL precursor ion selected MH_2^{2+} 482, after mPC-tITP-CE-MS/MS analysis. Conditions as for Figure 4 except xenon was used as collision gas at a gas pressure of 1.2×10^{-5} mbar. Collision energies used were: A) 18 eV, B) 22 eV, and C) 26 eV.

base is limited, it is difficult 'a priori' to predict an optimal collision energy for a biologically derived peptide of unknown sequence. Therefore, we suggest and are currently investigating the use of an automatic ramp of the collision energy for each MS₂ scan.

Parameters, other than those associated with the collision cell, that effect both sensitivity and quality of the peptide sequence data obtained by mPC-tITP-CE-MS/MS include the internal diameter of the mPC-CE capillary (51) and the physico-chemical properties of the analyzed peptide (52). It has been previously shown that smaller internal diameter capillaries tend to improve electrospray-MS (ESI-MS) sensitivity by the formation of smaller droplets during spray processes. Therefore, we compared the performance of mPC-CE capillaries of both 25 and 50 μm internal diameter. As expected, from the work of Smith *et al* (51), a mPC-CE capillary of reduced internal diameter greatly improved the signal:noise ratio of MS/MS product ion spectra. This is demonstrated by the analysis of ~70 fmol of the synthetic peptide SIINFEKL using mPC-tITP-CE-MS/MS (Figure 6). These results show a dramatic improvement in signal:noise ratio in the data obtained using a mPC-CE capillary of 25 μm i.d. (Figure 6B). The yield of sequence specific product ions was also enhanced in the latter spectrum, improving the completeness of the sequence information that can be derived by mPC-tITP-CE-MS/MS analysis of such small amounts of peptides.

As discussed, the ultimate sensitivity of a MS/MS method for peptide sequencing is also dependent upon the physico-chemical properties of such analytes. In particular, it is well known that both aspartic and glutamic acid amino acid residues tend to decrease ESI

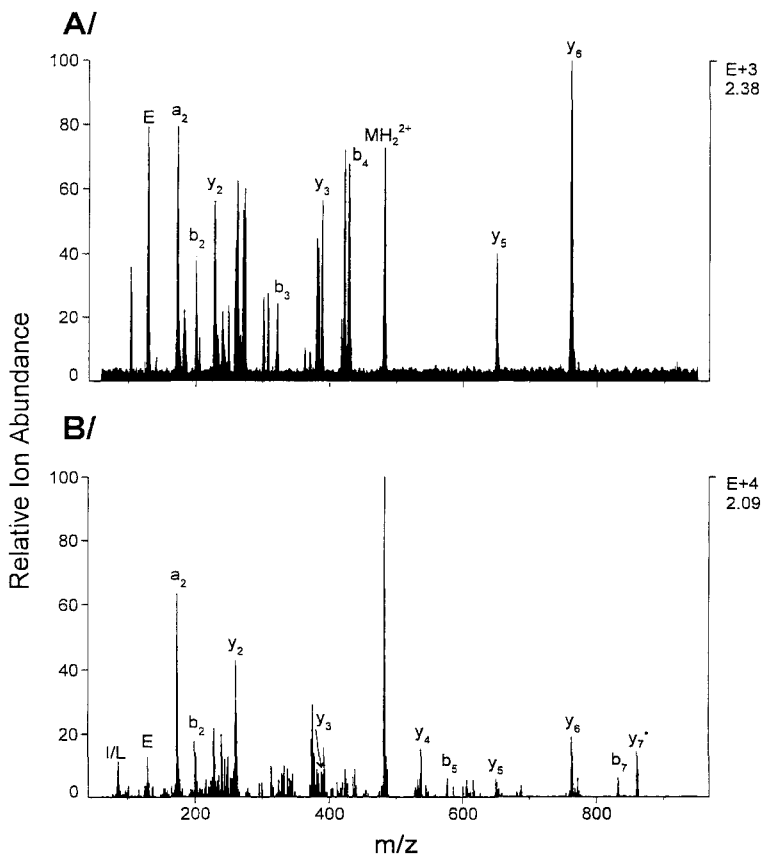


Figure 6 Effect of a change in the internal diameter of CE capillary on the product ion spectrum of ~60 femtomoles of SIINFEKL ($MH_2^{2+} = 482$) after mPC-tITP-CE-MS/MS analysis using 22 eV collision energy. A) Conditions as for Figure 4A using a 50 μm i.d. CE capillary. B) Conditions as for Figure 4A using a 25 μm i.d. CE capillary. LSB was 80 nL, elution solvent volume was 80 nL and TSB was 15 nL.

sensitivity in positive ion mode and also direct fragmentation processes within the collision cell. Reducing the acidic nature of these residues by esterification can minimize such effects on the MS/MS spectra (53). In this regard, since the model peptides used during these studies possessed a glutamic acid residue at position 6, we expected that methylation of both this residue and the C-terminus to improve the sensitivity of our mPC-tITP-CE-MS/MS methodology. Figure 7 shows a comparative analysis of native and methylated analogs of SIINFEKL while these data yielded only partial sequence by consumption of ~80 fmol of the native peptide (Figure 7A) an almost complete sequence was derived from ~40 fmol of its methylated analog (Figure 7B).

In summary, we have shown in this report that careful consideration of good chromatographic practices can lead to an efficient method of on-line preconcentration for CE and CE-MS methodology. Hence, minimizing the bed volume of a suitably impregnated adsorptive membrane can overcome the many limitations experienced by solid phase preconcentration-CE methods. In particular, while mPC-CE methods yield the advantages of large sample (>60 μ L) analysis, it has almost no effect on the CE separation processes when used in conjunction with tITP conditions. Furthermore, the combination of mPC-tITP-CE on-line with a mass spectrometer as the detector leads to a much higher mass sensitivity when compared to conventional UV detectors. In addition, the mass spectrometer is currently the only convenient method of choice for the structural characterization with on-line chromatographic separation. However, we have also shown here and previously (27) that ultimate MS and MS/MS sensitivity is only achieved

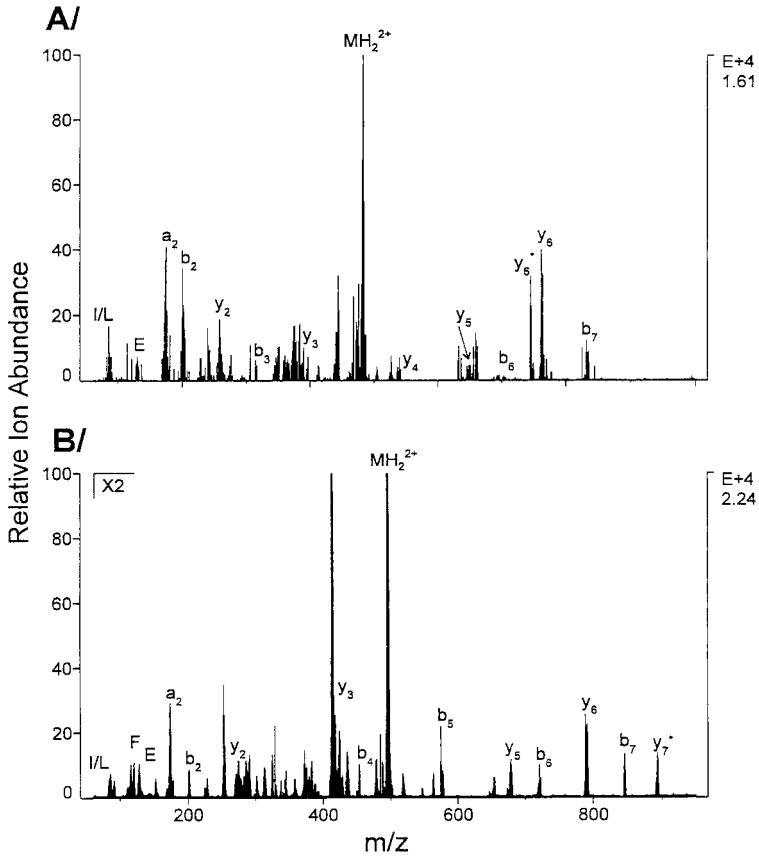


Figure 7 Effect of methylation on the product ion spectrum of SIINFEKL. Conditions as for Figure 4A except:

A) ~80 femtomoles of native peptide - precursor ion $MH_2^{2+} = 482$. B) ~40 femtomoles of methylated peptide - precursor ion $MH_2^{2+} = 510$.

when the chromatographic system and mass spectrometer are considered as one. In this regard, as ESI-MS sensitivity is increased when the internal diameter of the spray needle is reduced, and it was subsequently demonstrated that a smaller bore mPC-CE capillary leads to enhance mPC-CE-MS/MS performance. While this tends to increase analysis times due to a slower hydrodynamic flow resulting in longer on-line sample injection and cleanup times, this potential limitation of mPC-CE may be overcome by off-line preparation of the mPC-CE cartridge. The mPC-CE cartridge being installed into the CE capillary only when ready for analyte elution.

Finally, in this report we have demonstrated ultimate mPC-tITP-CE-MS/MS performance was obtained when the physicochemical properties of the synthetic MHC class I peptides were considered. Hence, in this example, esterification of the C-terminus and glutamic acid residue at position 6 of these peptides yielded more complete sequence data while consuming less peptide. Thus while we continue to refine this strategy to enable sequence determination of smaller amounts of peptide, we have demonstrated the potential of on-line mPC-tITP-CE-MS/MS for sequencing low concentrations (~40 fmol) of a series of synthetic MHC class I peptides.

ACKNOWLEDGMENTS

We thank Mr. Ken Johnson for his assistance with the mass spectrometry and Mrs. Diana Ayerhart for her help in preparing this manuscript. We are also grateful for the funding of this research by Mayo Foundation and, in part, NIH Contract Grant #N01-AI-45197 and the support given by Finnigan MAT and Beckman Instruments.

References

- (1) Biemann, K., Sequencing of Peptides by Tandem Mass Spectrometry and High Energy Collision Induced Dissociation, in *Methods in enzymology: Mass Spectrometry Vol. 193*, McCloskey, J.A. ed. Academic Press, San Diego, 1990, p.455.
- (2) Biemann, K., Primary Structures of Peptides and Proteins, in *Biological Mass Spectrometry: Present and Future*, Matsuo, T., Caprioli, R.M., Gross, M.L. and Seyama, Y. eds. Wiley & Sons, Chichester, 1994, p.275.
- (3) Janeway, Jr., C.A., *Sci. Am.*, 269, 72, 1993.
- (4) Hunt, D. F., Henderson, R. A., Shabanowitz, J., Sakaguchi, K., Michel, H., Sevilir, N., Cox, A. L., Appella, E. and Engelhard, V. H., *Science*, 255, 1261, 1992.
- (5) Cox, A. L., Skipper, J., Chen, Y., Henderson, R. A., Darrow, T. L., Shabanowitz, J., Engelhard, V. H., Hunt, D. F. and Slingluff, C. L., Jr., *Science*, 264, 716, 1994.
- (6) Tomlinson, A. J., Nevala, W. K., Wettstein, P. J. and Naylor, S., *Converted no journal*, 181, 1994.(Abstract)
- (7) Tomlinson, A.J., Nevala, W.K., Braddock, W.D., Strausbauch, M.A., Wettstein, P.J. and Naylor, S., A strategy for isolating and sequencing MHC class I peptides by CE-ESI-MS, in *Proceedings: The 42nd ASMS Conference on Mass Spectrometry and Allied Topics*, 1994, p.23.
- (8) Naylor, S., Braddock, W.D., Oda, R.P., Nevala, W.K., Strausbauch, M.A., Wettstein, P.J. and Tomlinson, A.J., A strategy for isolating and sequencing MHC class I peptides by preconcentration-capillary electrophoresis-ESI-MS, in *Third International Symposium on Mass Spectrometry in the Health and Life Sciences*, 1994, p.108.
- (9) Cai, J. and El Rassi, Z., *J. Liq. Chromatogr.*, 15(6&7), 1179, 1992.
- (10) Benson, L. M., Tomlinson, A. J., Reid, J. M., Walker, D. L., Ames, M. M. and Naylor, S., *J. High Resol. Chromatogr.*, 16, 324, 1993.
- (11) Mikkers, F. E. P., Everaerts, F. M. and Verheggen, Th. P. E. M., *J. Chromatogr.*, 169, 1, 1979.

- (12) Abersold, R. and Morrison, H. D., *J. Chromatogr.*, 516, 79, 1990.
- (13) Gebauer, P., Thormann, W. and Bocek, P., *J. Chromatogr.*, 608, 47, 1992.
- (14) Schwer, C. and Lottspeich, F., *J. Chromatogr.*, 623, 345, 1992.
- (15) Beckers, J. L. and Ackermans, M. T., *J. Chromatogr.*, 629, 371, 1993.
- (16) Chien, R. L. and Burgi, D. S., *Anal. Chem.*, 64, 489A, 1992.
- (17) Foret, F., Sustacek, V. and Bocek, P., *J. Microcol. Sep.*, 2, 229, 1990.
- (18) Smith, R. D., Fields, S. M., Loo, J. A., Barinaga, C. J., Udseth, H. R. and Edmonds, C. G., *Electrophoresis*, 11, 709, 1990.
- (19) Beckers, J. L. and Everaerts, F. M., *J. Chromatogr.*, 508, 19, 1990.
- (20) Stegehuis, D. S., Irth, H., Tjaden, U. R. and vanderGreef, J., *J. Chromatogr.*, 538, 393, 1991.
- (21) Tinke, A. P., Reinhoud, N. J., Niessen, W. M. A., Tjaden, U. R. and Van der Greef, J., *Rapid Commun. Mass Spectrom.*, 6, 560, 1992.
- (22) Foret, F., Szoko, E. and Karger, B. L., *J. Chromatogr.*, 608, 3, 1992.
- (23) Lamoree, M. H., Reinhold, N. J., Tjaden, U. R., Niessen, W. M. A. and Van der Greef, J., *Biol. Mass Spectrom.*, 23(6), 339, 1994.
- (24) Guzman, N. A., Trebilcock, M. A. and Advis, J. P., *J. Liq. Chromatogr.*, 14, 997, 1991.
- (25) Guzman, N.A., Gonzalez, C.L., Trebilcock, M.A., Hernandez, L., Berck, C.M. and Advis, J.P., The use of capillary electrophoresis in clinical diagnosis, in *Capillary Electrophoresis Technology*, Guzman, N.A. ed. Marcel Dekker Inc., New York, 1993, p.643.
- (26) Guzman, N. A., World Patent WO 93/05390, March 18, 1993.
- (27) Tomlinson, A. J., Benson, L. M. and Naylor, S., *J. Cap. Elec.*, 1, 127, 1994.

- (28) Tomlinson, A. J., Benson, L. M., Oda, R. P., Braddock, W. D., Strausbauch, M. A., Wettstein, P. J. and Naylor, S., *J. High Resol. Chromatogr.*, 17, 669, 1994.
- (29) Benson, L. M., Tomlinson, A. J. and Naylor, S., *J. High Resol. Chromatogr.*, 17, 671, 1994.
- (30) Tomlinson, A. J., Benson, L. M., Braddock, W. D., Oda, R. P. and Naylor, S., *J. High Resol. Chromatogr.*, 17, 729, 1994.
- (31) Naylor, S., Benson, L. M. and Tomlinson, A. J., *J. Cap. Elec.*, 1, 181, 1994.
- (32) Tomlinson, A. J., Braddock, W. D., Benson, L. M., Oda, R. P. and Naylor, S., *J. Chromatogr.*, submitted, 1995.
- (33) Tomlinson, A. J., Benson, L. M., Oda, R. P., Braddock, W. D., Riggs, B. L., Katzmann, J. A. and Naylor, S., *J. Cap. Elec.*, 2, 97, 1995.
- (34) Tomlinson, A. J., Benson, L. M., Braddock, W. D., Oda, R. P. and Naylor, S., *J. High Resol. Chromatogr.*, In Press, 1995.
- (35) Tomlinson, A. J. and Naylor, S., *J. High Resol. Chromatogr.*, In Press, 1995.
- (36) Tomlinson, A.J. and Naylor, S., *J. Cap. Elec.*, Submitted, 1995.
- (37) Kasicka, V. and Prusík, Z., *J. Chromatogr.*, 273, 117, 1983.
- (38) Debets, A. J. J., Mazereeuw, M., Voogt, W. H., van Iperen, D. J., Lingeman, H., Hupe, K. -P. and Brinkman, U. A. Th., *J. Chromatogr.*, 608, 151, 1992.
- (39) Swartz, M. E. and Merion, M., *J. Chromatogr.*, 632, 209, 1993.
- (40) Morita, I. and Sawada, J., *J. Chromatogr.*, 641, 375, 1993.
- (41) Hoyt, A. M., Jr., Beale, S. C., Larmann, J. P., Jr. and Jorgenson, J. W., *J. Microcol. Sep.*, 5, 325, 1993.
- (42) Fishman, H. A., Shear, J. B., Colon, L. A., Zave, R. N. and Sweedler, J. V., U.S. Patent 5,318,680, June 7, 1994.
- (43) Pálmarsdóttir, S. and Edholm, L. -E., *J. Chromatogr. A.*, 693, 131, 1995.

- (44) Beattie, J. H., Self, R. and Richards, M. P., *Electrophoresis*, 16, 322, 1995.
- (45) Naylor, S., Tomlinson, A. J., Benson, L. M., Braddock, W. D. and Oda, R. P., U.S. Patent Application, 1995.
- (46) Tomlinson, A. J., Benson, L. M. and Naylor, S., *LC-GC*, 12, 122, 1994.
- (47) Tomlinson, A. J., Benson, L. M. and Naylor, S., *Am. Lab.*, 26, 29, 1994.
- (48) Tomlinson, A. J. and Naylor, S., *J. Cap. Elec.*, Submitted, 1995.
- (49) Tomlinson, A. J. and Naylor, S., manuscript preparation, 1995.
- (50) Tomlinson, A. J., Braddock, W. D., Pesch, R. and Naylor, S., *Rapid Commun. Mass Spectrom.*, Submitted, 1995.
- (51) Wahl, J. H., Gale, D. C. and Smith, R. D., *J. Chromatogr.*, 659, 217, 1994.
- (52) Kebarle, P. and Tang, L., *Anal. Chem.*, 65, 972A, 1993.
- (53) Hunt, D. F., Yates, J. R., Shabanowitz, J., Winston, S. and Haver, C. R., *Proc. Natl. Acad. Sci.*, 83, 6233, 1986.

Received: July 20, 1995

Accepted: August 6, 1995

APPLICATION OF CAPILLARY ZONE ELECTROPHORESIS FOR THE ANALYSIS OF PROTEINS, PROTEIN-SMALL MOLECULES, AND PROTEIN-DNA INTERACTIONS

**GEORGE M. JANINI, ROBERT J. FISHER,
LOUIS E. HENDERSON, AND HALEEM J. ISSAQ**
*SAIC Frederick
NCI-Frederick Cancer Research and Development Center
P.O. Box B
Frederick, Maryland 21702*

ABSTRACT

Capillary electrophoresis with a polyacrylamide-coated capillary was used for the separation of proteins, and the study of protein-small molecule and protein-DNA interactions. The coating (10% T polyacrylamide) is of sufficient thickness and hydrophilicity to reduce protein adsorption and eliminate electroosmotic flow. Data on the effect of sample solvent constituents on the peak shape and position of protein solutes was investigated. The results show that CE is a relevant and fast technique for the study of protein-DNA and protein-drug interaction. Also, the addition of TRIS-buffer to the sample solution resulted in the CE focusing of some basic proteins, while others were not affected.

INTRODUCTION

Capillary Zone Electrophoresis (CZE) is being increasingly recognized as a viable substitute for conventional electrophoresis protocols in molecular biology (1). This is mainly due to its high resolution small sample requirements and automated instrumentation. Recently, several reports appeared that describe CZE studies of protein-small molecule (2-4) and protein -DNA interactions (5,6). An area of unique challenge in the CZE analysis of proteins has been the control and

elimination of adsorption on the capillary inner surface. Adsorption often gives rise to distorted peaks, poor resolution and non-reproducible migration times.

Several strategies, that involve work at extreme pH and the use of buffer additives, were explored to minimize the adsorption of proteins on untreated columns (7-10). A different strategy, that is less restrictive in allowing the separation conditions to be adapted to the requirements of the analytical problem, involves the chemical modification of the fused-silica column surface by a permanent non-adsorptive coating (11-13).

Another area of concern in the CZE analysis of proteins is the effect of sample constituents, other than the protein of interest on peak shape and position. It has been demonstrated by Karger and co-workers (14,15) and others (16,17) that if the sample contains co-ions of the ion of interest with high electrophoretic mobility and if at the same time the mobility of the co-ion of the background electrolyte is lower than the mobility of the ion of interest, a transient isotachophoretic (ITP) migration of the sample ion takes place at the beginning of the migration. This gradually changes to a zone electrophoretic mode. How far does ITP migration proceed before shifting to zone migration depends on the relative mobility and concentration of the sample ion and its co-ions. The transient ITP phenomenon has advantages as well as disadvantages. We have previously shown that the presence of chloride in biological fluids is beneficial for the analysis of nitrate (18). The ITP step created when chloride acts as a leading ion focuses the nitrate peak (over one million theoretical plates) and improves the detection limit. On the negative side, solute migration time and peak shape are largely dependent on the relative concentration of the solute ion and its counter ions, and when the counter ion concentration is too high solute zones migrate close together and eventually co-migrate (18).

We report here on the utility of a polyacrylamide-coated capillary for the analysis of proteins, protein-small molecule and protein-DNA interactions. The coating (10% T polyacrylamide) is of sufficient thickness and hydrophilicity to reduce protein adsorption and eliminate electroosmotic flow.

Data on the effect of sample solvent constituents on the peak shape and position of protein solutes will be presented and discussed.

EXPERIMENTAL

Reagents

Protein samples were purchased from Sigma Chemical Company (St. Louis, MO) as well as Ellman's reagent, EDTA, dithiothreitol and vinyl pyridine. All buffer reagents were purchased from Fisher Scientific (Fair Lawn, NJ). Human immunodeficiency virus type 1 nucleocapsid protein with (NCp7) and without (apo) two coordinated zinc ions and reagents attacking the Cysteine thiolates in the metal ion coordination complex were provided by the Viral Protein Laboratory (SAIC AVP, NCI-FCRDC, Frederick, MD). ETS1-P42 (19) and a specific oligonucleotide DNA were provided by the Laboratory of Cellular Biochemistry (SAIC Frederick, NCI-FCRDC, Frederick, MD).

Buffers were prepared using water purified by a Barnstead NANOpure Ultrapure Water System (Dubuque, IA).

Apparatus and method

A CZE P/ACE System 5500 equipped with a P/ACE diode array detector (DAD), an automatic injector, a fluid-cooled column cartridge, and a System Gold data station (all from Beckman Instruments, Inc., Fullerton, CA) was used in this study. All runs were carried out at 25 °C. The buffers were passed through 0.2- μm nylon filters and degassed prior to use. The capillary inlet and outlet vials were replenished after every tenth run. Injections were made using the pressure mode. The DAD was scanned in the wavelength range of 190-380 nm, and the electropherograms were monitored at 214 nm and 260 nm. Specific experimental parameters are given in the figure captions.

Columns were coated with a thick layer of linear polyacrylamide. The details of the column preparation procedure are given elsewhere (18). Columns coated according to this procedure are

routinely used in our laboratory for the analysis of nitrate and nitrite in biological fluids and in the analysis of proteins and DNA samples. The columns are stable at and below pH 9.0, and could be used over a period of several weeks without any signs of deterioration. Electroosmotic flow (EOF) is negligible, although not completely eliminated. The electroosmotic mobility, μ_{eo} is estimated by measuring the migration time of NO_3^- (18). μ_{eo} values for several columns prepared in our laboratories ranged from $0.03\text{--}0.5 \times 10^{-4} \text{cm}^2 \text{v}^{-1} \text{sec}^{-1}$. μ_{eo} of CZE columns typically ranges from $0\text{--}10 \times 10^{-4} \text{cm}^2 \text{v}^{-1} \text{sec}^{-1}$ depending on column surface chemistry, pH, and buffer additives (18).

RESULTS AND DISCUSSION

Separation of Proteins

The separation of proteins with bare-silica columns is possible only under: (a) very low buffer pH; (b) very high buffer pH; (c) using relatively high salt concentration in the running buffer; and (d) using special additives in the running buffer that associate with either the analyte or the bare-silica surface. All these strategies are inappropriate for the study of protein-DNA complexes, because of the potential interference of extreme pH and additives with the binding activity. The study of protein-DNA complexes would ultimately require more inert non-adsorptive and hydrophilic surfaces than bare-silica in order to accommodate the polyionic nature of these biopolymers. The linear polyacrylamide coated surface used in this study is particularly suited for the study of protein-DNA interaction because: (a) it is hydrophilic; (b) it effectively shields the biopolymers from direct contact with surface silanol groups; (c) it does not interact with the biopolymers; (d) it is chemically stable and resists hydrolytic degradation when in contact with aqueous solutions customarily used in CZE; and (e) the coating procedure yields reproducible capillaries with consistent run-to-run and day-to-day migration times.

Basic proteins are customarily used as probes of the quality of the capillary surface coating because their positive net charge tend to adsorb on the negative charge of the wall on uncoated or poorly shielded surfaces (11-13). The separation of a test mixture of four basic proteins at pH 3 is

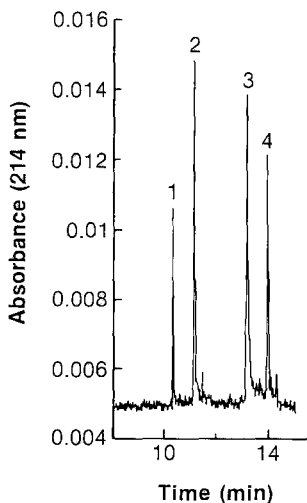


Figure 1. Electropherogram showing the separation of four basic proteins: (1) cytochrome C, (2) lysozyme, (3) ribonuclease A, and (4) α -chymotrypsinogen A. Buffer: 10 mM sodium phosphate, containing 0.1% BRIJ 35; pH: 3.1; Voltage: 15 kV; Instrument: Beckman model P/ACE System 5500; Detection: 214 nm; Injection: 5 seconds at 0.5 psi; Column: 10% T. polyacrylamide-coated fused-silica; Column dimensions: $L_{\text{total}} = 57$ cm, $L_{\text{detector}} = 50$ cm; i.d. = 75 μm ; Solute concentration: 0.2-0.5 mg/mL in 10 mM phosphate buffer.

shown in Figure 1. High efficiencies were obtained indicating optimal coverage of the surface active sites. The protein samples were routinely run over time to confirm the stability of the coating. No loss of column efficiency was observed over several weeks of operation. The proteins were dissolved in the running buffer in order to avoid possible complication from transient on-column ITP. When TRIS was added to the sample solvent it acted as a leading ion and resulted in ITP focusing. Cytochrome C and lysozyme were extremely focused, i.e. gave sharper peak than those in fig. 1, while ribonuclease A and α -chymotrypsinogen A were hardly affected (data not shown). Lysozyme was chosen as an example to illustrate the ITP effect. A 50 μl sample of 250 $\mu\text{g/mL}$ lysozyme in 10 mM phosphate buffer was divided equally into two vials. One vial was diluted to 125 $\mu\text{g/mL}$ with water and the other vial was similarly diluted with 20 mM TRIS. The addition of TRIS to the sample

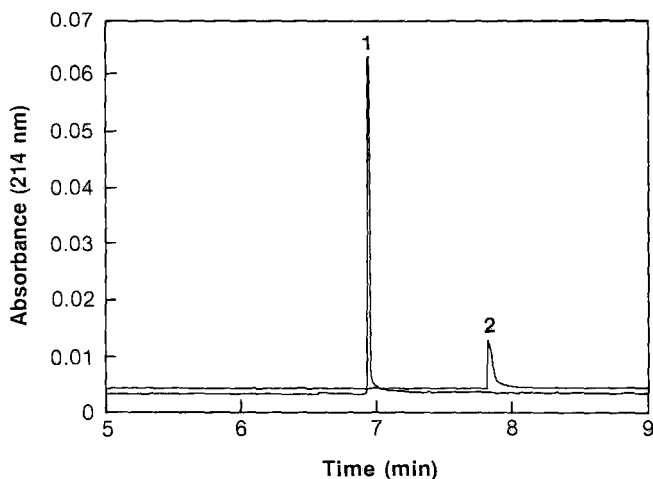


Figure 2. Demonstration of transient on-column ITP focusing. Peak shape of lysozyme with (trace 2) and without (trace 1) TRIS in the sample buffer. Experimental conditions: As in Figure 1, except for column length of 47 cm.

resulted in extreme focusing of the lysozyme peak as illustrated in Figure 2. The number of theoretical plates per meter increased from about 200,000 (Trace 2) to over two million (Trace 1). While this improvement in column efficiency is impressive, it must be cautioned that when the protein peak is focused to such an extent it coelutes with other proteins that are of closely-related charge-to-size ratio (14). Moreover, other complications may arise depending on the relative concentration of the focusing ion (TRIS in this example) and protein. For example, two peaks (one focused and one broad) may appear for a single protein that gives a single peak with no TRIS in the sample solvent (data not shown). The proportions of the areas of the two peaks vary depending on the relative concentration of TRIS in the sample solvent. It may be concluded from the above that the CZE separation of proteins is complicated by the presence of other ions in the sample matrix. Caution must be exercised in interpretation of the electropherogram as a single focused peak might not necessarily indicate a single component and a double peak does not necessarily indicate sample decomposition.

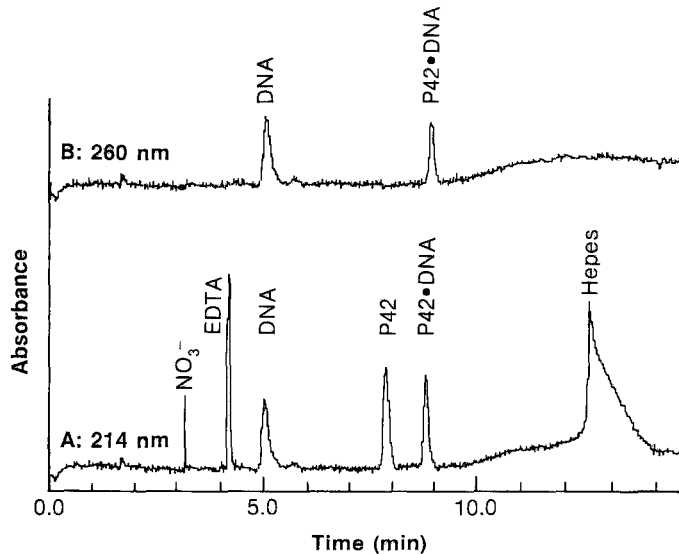


Figure 3. Demonstration of the utility of CZE with coated columns for the study of protein-DNA complexes. Applied voltages: -15 kV; Current: 28 μA ; Buffer: 10 mM phosphate; pH 8.8; Other Experimental Conditions: As in Figure 1.

Study of protein-DNA interactions

The linear polyacrylamide coated column used in this study is particularly suited for the study of protein-DNA interactions because it provides a hydrophilic, non-adsorptive surface that does not interfere with the binding activity. Figure 3 gives an electropherogram that was run about 15 minutes after the initial mixing of 30 μl of 0.6 pmole/ μl of P42 (Mol. Wt. = 40,780) with 3 μl of 20.8 pmole/ μl of a specific oligonucleotide DNA (Mol. Wt. = 12,000). The electropherogram was run at pH 8.8 where all species of interest, P42, DNA and the P42.DNA complex are negatively charged. In a negligible electroosmotic flow environment, and with the detector at the anode end of the column, only negatively-charged components of the injected material will migrate through the length of the column and get detected. The figure demonstrates the unique advantage of CZE over other analytical techniques, instrumental or otherwise. Partial selectivity is obtained when positively-

charged and neutral solutes are separated from the negatively charged solutes of interest. More importantly, only CZE could give peaks for small ions (NO_3^-), complexing agents (EDTA), proteins, DNA and protein-DNA complex in a single run, with real-time on-column detection. Selectivity is also achieved by judicious selection of detector wavelength. For example, Trace B of fig. 3, which was monitored at 260 nm, only shows the peaks of DNA containing species.

Screening of the effect of drugs on proteins

CZE could conveniently be used for the screening of drug-protein interactions. The nucleocapsid protein (NCp7) of human immunodeficiency virus type 1 (HIV-1) (20) was selected to illustrate this application. The protein contains two zinc finger domains which play an important role in the viral replication cycle (21,22). It has been suggested that viral replication depends on the integrity of the Zn finger domains which are preserved in all studied mutant forms of the protein. It is hoped that drugs which disrupt the Zn finger domain may interfere with the virus replication cycle. The protein is positively charged at neutral pH, but migrates very slow towards the negative electrode. In order to shorten the analysis time, the CZE analysis of NCp7 was attempted at pH 3. Figure 4 gives sufficient evidence that shows that the Zn fingers in NCp7 are not disrupted by the change of pH from pH 7 in which the sample is dissolved to pH 3 during migration inside the column. Trace A shows the electropherogram of NCp7 and Trace B shows the electropherogram of the apo form of NCp7. The samples were dissolved in phosphate buffer. TRIS, which is commonly used as a protein buffer constituent, was avoided because the same ITP mechanism described earlier is also operative here. Trace C is an electropherogram of the same sample used to generate Trace A, but with the addition of EDTA which is a strong chelating agent for zinc, and dithiothreitol which is added to obstruct the formation of sulfur bridges after the sulfhydryl residues are freed. The trace clearly shows the gradual conversion of NCp7 to its apo form. Trace D is an electropherogram of the same sample used to generate Trace C but at a later time. In order to test the effect of drugs on NCp7, a 250 $\mu\text{g}/\text{mL}$ solution of the protein was prepared in phosphate buffer and 25 μL was

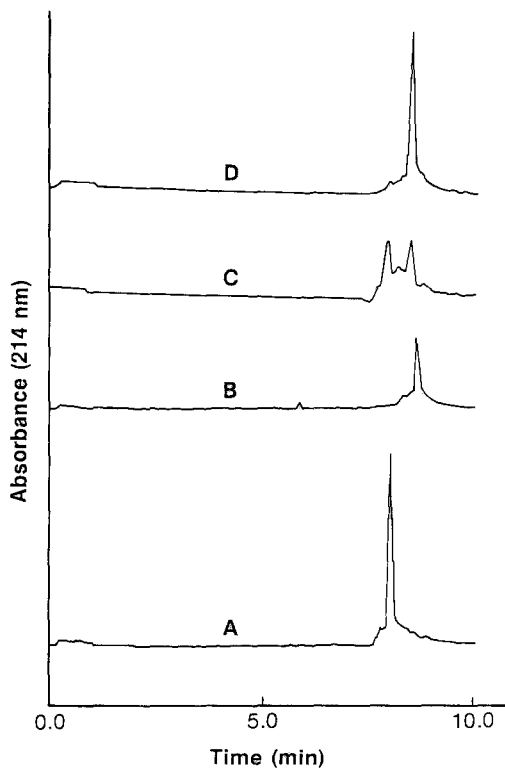


Figure 4. CZE evidence for the transformation of NCp7 to its apo form by the addition of EDTA and dithiothreitol. Trace A: NCp7; B: cpo NCp7; C: NCp7+EDTA+dithiothreitol; and D: Same as C, but at a later time. Experimental Conditions: As in Figure 1.

aliquoted for each determination. The drugs were dissolved in dimethylsulfoxide (DMSO) and less than 1 μl of each drug solution was added to the protein vial to make up a drug-to-protein molar ratio of 6:1. This represents another unique advantage of CZE when only about 6 μg of protein and a few μg of each drug are needed for each screen. Representative examples of NCp7-drug interactions are shown in Figure 5. Trace A shows that NCp7 (second peak) was not disrupted by the addition of vinylpyridine. The reagent modifies free sulfhydryls but does not attack sulfhydryls in the zinc coordination complex of NCp7. Free vinylpyridine is positively charged at pH 3 and is

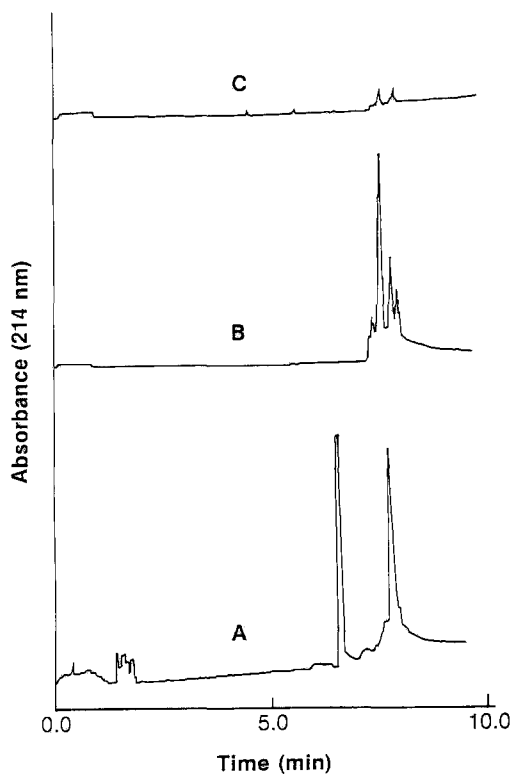


Figure 5. Effect of drugs on NCp7 protein. A: Effect of vinylpyridine; B: Effect of a proprietary drug; and C: Effect of Ellman's reagent. Experimental Conditions: As in Figure 1.

also detected (first peak). Trace B shows an example of a drug that disrupts the Zn fingers, modifies free the sulfhydryl residues and forms several NCp7 derivatives, and trace C gives an example of a drug that disrupts the Zn fingers and causes disulfide cross-links in the protein.

CONCLUSION

The results presented here show that using a polyacrylamide coated capillary can result in excellent separation of basic proteins. Also, the study of protein-drug, protein-DNA interactions by CE is a feasible and efficient method which requires microgram samples.

ACKNOWLEDGEMENT

By acceptance of this article, the publisher or recipient acknowledges the right of the U.S. Government to retain a nonexclusive, royalty-free license and to any copyright covering the article.

The content of this publication does not necessarily reflect the views or policies of the Department of Health and Human Services, nor does mention of trade names, commercial products, or organizations imply endorsement by the U.S. Government.

REFERENCES

1. J.P. Landers, ed., "Handbook of Capillary Electrophoresis", CRC Press, Boca Raton, FL (1993).
2. J.C. Kraak, S. Busch and H. Poppe, *J. Chromatogr.*, **608**, 257 (1992).
3. N.H.H. Heegaard and F.A. Robey, *Anal. Chem.*, **64**, 2479 (1992).
4. Y-H. Chu, L.Z. Avila, H.A. Bieouych and G.M. Whitesides, *J. Med. Chem.*, **35**, 2915 (1992).
5. D.J. Rose, *Anal. Chem.*, **65**, 3545 (1993).
6. N.H.H. Heegaard and F.A. Robey, *J. Liq. Chromatogr.*, **16**, 1923 (1993).
7. R.M. McCormick, *Anal. Chem.*, **60**, 2322 (1988).
8. M.M. Bushey and J.W. Jorgenson, *J. Chromatogr.*, **480**, 301 (1989).
9. M.J. Gordon, K.J. Lee, A.A. Arias and R.N. Zare, *Anal. Chem.*, **63**, 69 (1991).
10. M.A. Strege and A.L. Lagu, *J. Chromatogr.*, **630**, 337 (1993).
11. D. Schmalzing, C.A. Piggee, F. Foret, E. Carrilho and B.L. Karger, *J. Chromatogr.*, **652**, 149 (1993).
12. J.K. Towns and F.E. Regnier, *Anal. Chem.*, **63**, 1126 (1991).
13. K.A. Cobb, V. Dolnik and M. Novotny, *Anal. Chem.*, **62**, 2479 (1990).
14. F. Foret, E. Székely and B.L. Karger, *Electrophoresis*, **14**, 417 (1993).
15. T.J. Thompson, F. Foret, P. Vouros and B.L. Karger, *Anal. Chem.*, **65**, 900 (1993).
16. P. Gebauer, W. Thormann and P. Božek, *J. Chromatogr.*, **608**, 47 (1992).
17. C. Schwer and F. Lottspeich, *J. Chromatogr.*, **623**, 345 (1992).
18. G.M. Janini, G.M. Muschik and H.J. Issaq, *J. Cap. Elec.*, **2**, 116 (1994).

19. R.J. Fisher, S. Koizumi, A. Kondoh, J.M. Mariano, G. Mavrothalassitis, N.K. Bhat and T.S. Papas, *J. Biol. Chem.* 267, 17957-17965 (1992).
20. L.E. Henderson, M.A. Bowers, R.C. Sowder, S.A. Serabyn, D.J. Johnson, J.W. Bess, Jr., L.O. Arthur, D.K. Bryant and C.C. Fenselau, *J. Virol.* 66(4), 1856-1865 (1992).
21. J.W. Bess, Jr., P.J. Powell, H.J. Issaq, L. Schumack, M.K. Grimes, L.E. Henderson and L.O. Arthur, *J. Virol.*, 66, 840-847 (1992).
22. R.J. Gorelick, S.M. Nigida, Jr., J.W. Bess, Jr., L.O. Arthur, L.E. Henderson and A. Rein, *J. Virol.* 64(7), 3207-3211 (1990).

Received: August 3, 1995

Accepted: August 20, 1995

THE EFFECT OF OPERATING PARAMETERS ON THE ANALYSIS OF A HUMAN ALPHA-INTERFERON BY CAPILLARY ZONE ELECTROPHORESIS

S. J. CRAIG, D. S. ASHTON,
C. BEDDELL, AND K. VALKO*
*Department of Physical Sciences
Wellcome Research Laboratories
Langley Court, Beckenham
Kent BR3 3BS, United Kingdom*

ABSTRACT

The influence of the operating parameters in capillary zone electrophoresis (CZE) on the separation of a human alpha-interferon has been investigated. The separation was characterised by the electrophoretic mobility of the first and last observed peaks, and the number of peaks on the electropherogram, whether visible as shoulders or adequately resolved. No peaks could be observed at lower pH values (below pH 4.7) due to capillary wall adsorption. The optimum pH (pH 6.1) for the CZE analysis of human alpha-interferon was close to the isoelectric points of the sample components (pI 5.5 - 6.5). The investigation of the effect of the borate, phosphate and Trizma buffer concentration on the separation showed that increasing buffer concentration generally decreases the electrophoretic mobility with increased resolution, up to a certain optimum. Longer capillary lengths and slightly higher voltages also increased the resolution. The maximum number of peaks (17) was observed by using 200 mM phosphate buffer (pH 6.1) with 50 cm effective length capillary applying 12 kV voltage.

INTRODUCTION

WELLFERON* (interferon alfa-n1 [Ins]) is a highly purified blend of natural human alpha interferons obtained from human (Namalwa) lymphoblastoid cells following induction with Sendai virus [1] and purified by a multistep process [2]. It is used in the treatment of hairy cell leukemia and chronic hepatitis B and non-A, non-B (c) infection. Clinical studies have yielded encouraging results in the treatment of papillomatosis. Preliminary studies are in progress to investigate its effect on delaying the onset or the progress of the acquired immune deficiency syndrome (AIDS), particularly when used in combination with RETROVIR* (zidovudine).

The protein content of alpha interferon has been extensively studied by Zoon et. al. [3-5], and the components have been separated by sequential immunoabsorbent affinity chromatography followed by ultrafiltration and reversed phase high performance liquid chromatography (RP-HPLC). WELLFERON can contain at least twenty-two subtypes, each of which contains 164 -166 amino acids. The apparent molecular weights ranged from 17,500 to 23,000 Da on non-reducing SDS-PAGE and 17,500 to 27,600 Da using reducing SDS-PAGE. The components were sequenced by Edman degradation and compared to those found previously from cDNA or genomic DNA sequences [6, 7]. There was also evidence for glycosylation of one of the subtypes, which contained glucosamine, galactosamine, fucose and/or mannose and galactose [8].

The RP-HPLC analysis of WELLFERON [3] also showed the complexity of the sample, as 11 peaks (many of them only as shoulders) appeared on the chromatogram obtained from a Vydac C-4 column with an acetonitrile gradient and 0.1% TFA in the mobile phase.

High performance capillary zone electrophoresis (CZE) provides a fast, gentle, and non-denaturing separation conditions for the analysis of high molecular weight proteins. It can therefore offer

*This is a Trade Mark of Wellcome group companies. Registered in the U. S. Patent and Trade Mark Office.

an alternative to RP-HPLC for the further analysis of the human alpha-interferon. The resolution in CZE can be increased by changing the pH [9], and the effect of the applied voltage, buffer type and concentration on the resolution has been investigated in several studies [10-12]. A guide for optimisation of resolution in CZE has been given by Atamna et. al. [13].

In this study, the effect of buffer type and concentration, pH, column length and the applied voltage on the separation of the human alpha-interferon components by CZE have been investigated.

EXPERIMENTAL

The WELLFERON sample was obtained "in house". The samples were analysed at concentrations of 0.1 - 0.5 mg/ml diluted with deionised water from a 3 mg/ml sample.

An ISCO Model 3850 capillary electropherograph was used for the CZE analysis (ISCO Inc., Lincoln, Nebraska, U. S. A.). Samples (8µl) were manually injected using a 10 µl syringe, and split 1:1930, so that 4 nl samples were injected onto the column. The separation was monitored using a UV detector at 200 nm. Uncoated fused silica capillaries, with 50 µm internal diameters were obtained from ISCO Inc., and were cut to lengths of 61 cm and 80 cm giving 36 cm and 50 cm effective lengths, respectively. The capillaries were rinsed with deionised water, 0.1M NaOH and deionised water after each buffer change and rinsed with buffer prior to each analysis. The capillaries were stored in 0.1M NaOH overnight.

Analytical grade disodium tetraborate, sodium dihydrogen orthophosphate, disodium hydrogen phosphate, sodium acetate trihydrate, acetic and phosphoric acid were obtained from BDH (Poole, Dorset, U. K.), the Trizma-base and Trizma-HCl from Sigma (Poole, Dorset, U. K.). The deionised water used was obtained from a Millipore Milli Q Plus water purification system. The concentration and pH of the various buffers are summarised in Table 1.

TABLE 1.

The Buffers Used for the CZE Analysis of WELLFERON.

Buffer	Concentration (mM)	pH
1. Borate	20-170	9.02-9.98
2. Phosphate	50-250	6.01-7.29
3. Phosphate	150	3.05
4. Acetate	50-100	4.64-4.72
5. Acetate-phosphate	100-250	4.18-4.37
6. Trizma	50-300	7.40-8.48

The buffers were prepared from the appropriate salt by adjusting the pH with the appropriate acid or base. They were filtered using a 0.4 μm Millipore Millex-HA filter before use.

The conditions optimised were applied voltage, buffer type, concentration and pH. Initially a 36 cm effective length capillary was used with the longer 50 cm effective length being used when the optimum buffer conditions had been found.

The separation was characterised by the mobility of the first and last components which takes into account the variation in applied voltage. The electrophoretic mobility was calculated according to the following formula:

$$\mu = \frac{l \cdot L}{t \cdot V}$$

where μ is the mobility ($\text{cm}^2\text{sec}^{-1}\text{V}^{-1}$), l is the effective capillary length (cm), L is the total length (cm), t is the migration time (sec), V is the applied voltage. The number of peaks, whether visible as shoulders or adequately resolved on the electropherogram were also used for characterising the resolution and the selectivity obtained by varying operating parameters, since the peaks could not be identified and followed from one condition to the other.

RESULTS AND DISCUSSION

Using buffers 3 - 5 (see Table 1) at pH's lower than 4.72, no peaks could be detected on the electropherogram. At the low pH the sample is positively charged, (the isoelectric point of WELLFERON components are in the range of 5.5 to 6.5 [14]) and can adsorb irreversibly onto the negatively charged capillary wall [15]. Therefore, buffers with higher pH than the isoelectric point were used for optimising the separation.

The effect of buffer concentration with three different buffers and pH on the electrophoretic mobility of the first and last peak, together with the number of peaks separated are summarised in Tables 2 - 4.

It can be seen from the data that increasing buffer concentration in general decreased the electrophoretic mobility of the WELLFERON components, which is in agreement with the general theory [10-12]. The resolution also increased as the higher ionic strengths minimise analyte interactions with the silica capillary wall and maintain constant conductivity and pH within the analyte zone, so preventing band broadening. However, high conductivities and currents can produce more heat thus causing band broadening and decreasing resolution [15-16], which results in the decrease in the number of peaks at high buffer concentrations, thus lower mobility does not necessarily result in higher resolution.

The optimum borate buffer concentration was 150 mM pH 9.3 which separated 14 components over an 11 - 15 min period. The electropherogram obtained under these conditions is shown in Fig. 1.

The optimum phosphate buffer concentration was 200 mM with pH 6.1 by which 15 components were separated in 21 - 35 min. The electropherogram can be seen in Fig. 2.

The optimum Trizma buffer concentration was 250 mM, pH 7.9 by which 15 components were separated in 18 - 29 min. The electropherogram obtained under these conditions is shown in Fig. 3. The Trizma buffer contains zwitterions which do not contribute significantly to the overall conductivity, this allows the application of high voltages without the problem of generating excessive heat.

TABLE 2.

The Electrophoretic Mobility of the First and Last Peaks and the Number of Peaks on the Electropherogram of WELLFERON at pH 9.3 ± 0.2 with respect to the Borate Buffer Concentration. Effective Capillary Length 36 cm.

Concentration (mM)	μ , mobility of the		Number of Peaks
	first peak	last peak	
20	4.7	-	1
50	4.1	3.3	6
100	3.4	2.8	8
120	2.8	2.3	9
150	2.2	1.7	14
170	2.0	1.6	14

TABLE 3.

The Electrophoretic Mobility of the First and Last Peaks and the Number of Peaks on the Electropherogram of WELLFERON at pH 6.5 ± 0.2 with respect to the Phosphate Buffer Concentration. Effective Capillary Length 36 cm.

Concentration (mM)	μ , mobility of the		Number of Peaks
	first peak	last peak	
50	4.7	3.6	7
100	3.2	2.1	7
150	2.6	1.8	14
175	2.4	1.6	14
200	2.3	1.7	15
225	2.0	1.6	13
250	2.2	1.8	11

TABLE 4.

The Electrophoretic Mobility of the First and Last Peaks and the Number of Peaks on the Electropherogram of WELLFERON at pH 8.0 ± 0.1 with respect to the Trizma Buffer Concentration. Effective Capillary Length 36 cm.

Concentration (mM)	μ , mobility of the		Number of Peaks
	first peak	last peak	
50	3.8	3.5	4
100	3.1	2.7	6
200	2.3	1.7	12
250	2.0	1.4	15
300	1.9	1.4	14

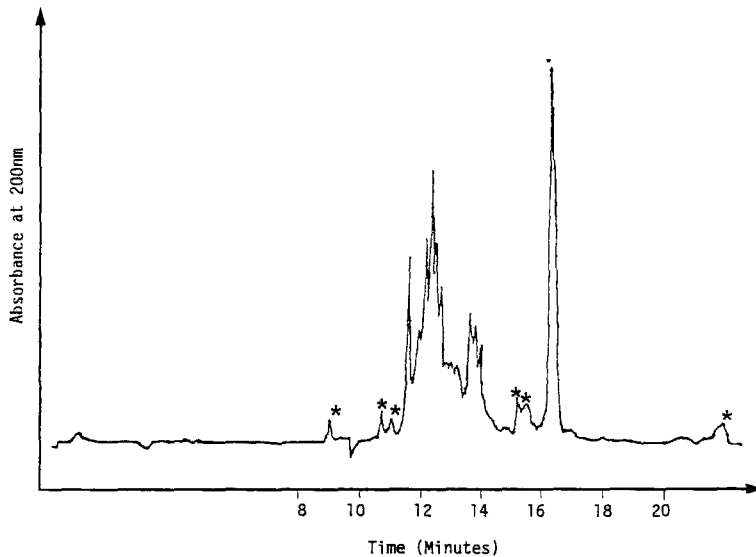


FIGURE 1. Electropherogram of human alpha-interferon. Effective capillary length 36 cm with 150 mM borate buffer pH 9.3. Applied voltage was 15 kV and the current was 93 μ A. The peaks marked with * were found also in the blank sample.

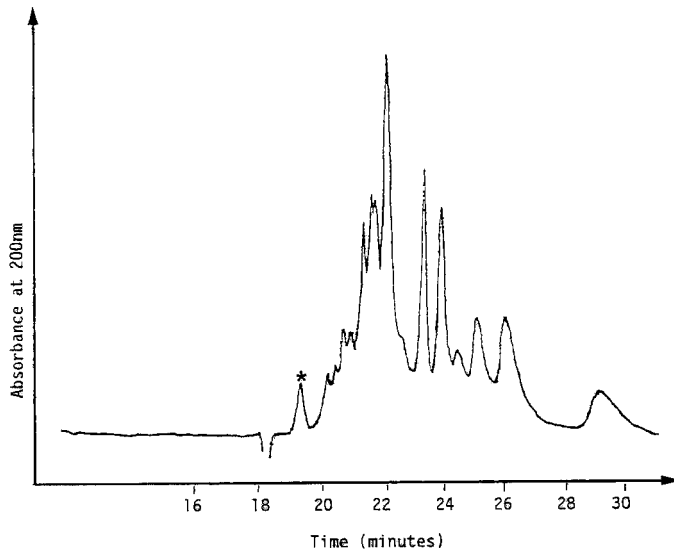


FIGURE 2. Electropherogram of human alpha-interferon. Effective capillary length 36 cm with 200 mM phosphate buffer pH 6.1. Applied voltage was 8 kV and the current was 42 μ A. The peak marked with * was found also in the blank sample.

The overall effect of the buffer concentration, at a given pH, on the number of peaks observed has been summarised in Figure 4.

Table 5 shows the effect of pH and buffer type on the mobility of the first and last peaks and the number of peaks on the electropherogram using 100 mM buffer concentrations.

The mobility of the first peak did not depend significantly on the pH and buffer type. The mobility of the last peak was lowest when phosphate buffer with pH 6.5 was used. This pH is the closest to the isoelectric point of the proteins in the WELLFERON sample. In the range of the isoelectric points some of the components can be in positively charged form, while others are not, thereby differentiating between the sample components with similar shapes and sizes. A pH

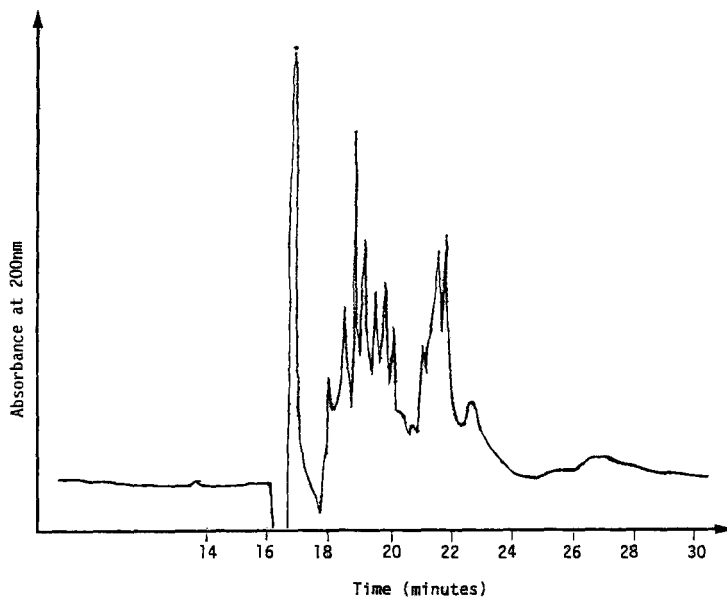


FIGURE 3. Electropherogram of human alpha-interferon. Effective capillary length 36 cm with 250 mM Trizma buffer pH 7.9. Applied voltage was 10 kV and the current was 50 μ A. The peak marked with * was found also in the blank sample.

TABLE 5.

The Electrophoretic Mobility of the First and Last Peaks and the Number of Peaks on the Electropherogram of WELLFERON by Using 100 mM Borate, Phosphate and Trizma Buffers.

Buffer	pH	μ , mobility of the		Number of peaks
		first peak	last peak	
Borate	9.3 \pm 0.2	3.4	2.8	8
Phosphagte	6.5 \pm 0.2	3.2	2.1	7
Trizma	8.0 \pm 0.1	3.1	2.7	6

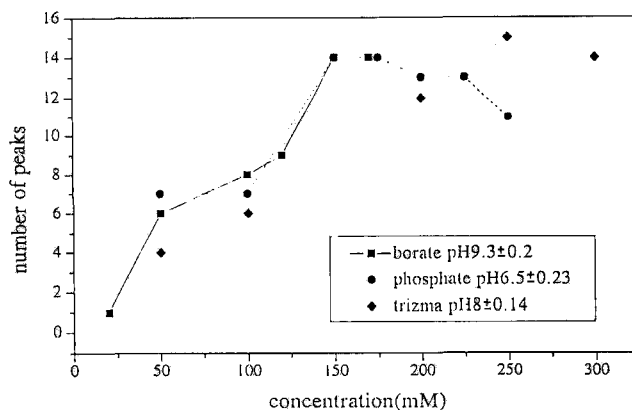


FIGURE 4. The plot of the number of peaks on the electropherogram of human alpha-interferon as a function of buffer concentration.

TABLE 6.

The effect of the capillary length and the applied voltage on the separation of the WELLFERON components with various buffers.

Buffer	Effective Capillary Length					
	No. of Peaks	36cm Voltage (kV)	Current (μA)	No. of Peaks	50cm Voltage (kV)	Current (μA)
150mM Borate pH 9.31	14	15	93	15	15	67
150mM Borate pH 9.5	12	16	100	13	15	68
200mM phosphate pH 6.12	15	9	55	17	12	42
200mM phosphate pH 6.01	15	8	42	16	15	49
250mM Trizma pH 7.9	15	10	50	14	14	50
300mM Trizma pH 7.96	14	8	46	15	15	65

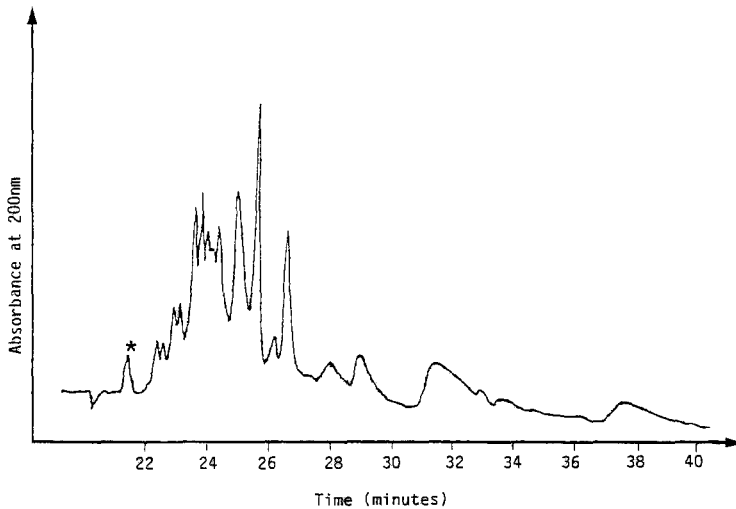


FIGURE 5. Electropherogram of human alpha-interferon obtained by using 50 cm effective capillary length with 200 mM phosphate buffer pH 6.1. Applied voltage was 12 kV and the current was 42 μ A. The peak marked with * was found also in the blank sample.

value near to the midpoint of the isoelectric point range will thus tend to maximise the components net charge differences [17], therefore providing the widest range in their mobilities.

For further optimisation of the separation of the multicomponent WELLFERON sample, the effect of the capillary length and the applied voltage have been investigated by using the three types of buffer at the optimum concentration. As found earlier [13], the resolution can be improved by increasing the voltage up to a certain point, avoiding the heating effect and thus the zone broadening. By increasing the capillary length the migration time and the column efficiency can be increased without changing the selectivity. The separation was characterised by the number of detectable peaks on the electropherogram. Table 6 shows the data

obtained. The greatest number of peaks (17) was obtained by using 200 mM phosphate buffer pH 6.12 with a 50 cm effective length capillary applying 12 kV voltage. The electropherogram obtained is shown in Figure 5.

In conclusion, the protein components of WELLFERON could be best separated at pH 6.1, which is within the isoelectric point range. The increasing buffer concentrations decreased the mobility of the components and increased the peak resolution up to a certain point. The longer effective capillary length with a slightly higher applied voltage also improved the separation of the sample components.

REFERENCES

1. N. B. Finter, K. H. Fantes, *Interferon*, 2: 65 (1980).
2. G. Allen, K. H. Fantes, *Nature*, 287: 408 (1980).
3. K. C. Zoon, D. Miller, J. Bekisz, D. Zur Nedden, J. C. Enterline, N. Y. Nguyen, R. Hu, *J. Biol. Chem.*, 267: 15210 (1992).
4. K. C. Zoon, R. Hu, D. Zur Nedden, T. L. Gerrard, J. C. Enterline, R. A. Boykin, N. Y. Nguyen, *The Biology of the Interferon System 1985*, 55 (1986).
5. K. C. Zoon, R. Q. Hu, D. Zur Nedden, N. Y. Nguyen. *The Biology of the Interferon System*, 1984, 61 (1985).
6. S. Pestka, *Methods Enzymol*, 119: 3 (1986).
7. K. C. Zoon, *Interferon*, 9: 1 (1987).
8. R. Wetzel, *Nature*, 289: 606 (1981).

9. E. C. Richard, M. M. Stroke, R. G. Nielsen, *Anal. Biochem.*, 197: 197 (1991).
10. H. J. Issaq, I. Z. Atamna, C. J. Metral and G. M. Muschik, *J. Liq. Chromatogr.*, 13: 1247 (1990).
11. I. Z. Atamna, C. J. Metral, G. M. Muschik and H. J. Issaq, *J. Liq. Chromatogr.*, 13: 2517 (1990).
12. I. Z. Atamna, C. J. Metral, G. M. Muschik and H. J. Issaq, *J. Liq. Chromatogr.*, 13: 3201 (1990).
13. I. Z. Atamna, H. J. Issaq, G. M. Muschik and G. M. Janini, *J. Chromatogr.*, 588: 315 (1991).
14. P. J. Bridgen, C. B. Anfinsen, L. Corley, S. Bose, K. C. Zoon, *J. Biol. Chem.*, 252: 6585 (1977).
15. J. H. Knox and I. H. Grant, *Chromatographia*, 24: 135 (1987).
16. E. Grishka, R. M. McCormick and J. Kirkland, *Anal. Chem.*, 61: 241 (1989).
17. H. H. Laurel and D. McManigill, *Anal. Chem.*, 58: 166 (1986).

Received: July 10, 1995

Accepted: August 6, 1995

METHODS DEVELOPMENT IN CAPILLARY ELECTROPHORESIS WITH AUTOMATED PEAK TRACKING BY CHEMOMETRIC ANALYSIS OF DIODE ARRAY DETECTION DATA

THOMAS E. WHEAT, FADWAH M. CHIKLIS, AND KIM A. LILLEY

*ATI Separations Group
The Schrafft Center
529 Main Street
Boston, Massachusetts 02129*

ABSTRACT

Developing methods for capillary electrophoresis is complicated by the complex array of interacting variables that affect resolution. Optimizing a separation is, therefore, time-consuming. This process can be minimized and simplified if the individual sample components can be tracked through a minimal structured experimental set. We have adapted an HPLC methods development system, Unicam Diamond Optimization Software, for this purpose. An experimental plane of ten different conditions is executed, and the separations are monitored with a diode array detector. Each three-dimensional data file is subjected to Principal Component Analysis and Iterative Target Transform Factor Analysis to test the spectral homogeneity of each peak and to deconvolute comigrations. The resulting pure spectra are used to track the individual sample components across the experimental plane. In this way, a migration model is calculated for each analyte, and, in turn, a resolution map is constructed. The optimal CE separation is obtained with a minimal number of experiments and without prior knowledge of the sample or the use of standards. This approach is illustrated and tested with over-the-counter pharmaceutical preparations.

INTRODUCTION

The exploitation of the selectivity inherent in electrophoresis as a high resolution technique has been contingent on minimizing dispersion during the separation. Professor

S. Hjertén recognized that this dispersion would be minimized in small diameter tubes and demonstrated this concept in the first capillary electrophoresis system in 1967(1). The extension of this principal to smaller tubes by Virtanen(2) culminated in the use of fused silica capillaries(3) that give extraordinarily high plate counts. This high separation efficiency made it relatively easy to develop separations for a variety of applications, leading to the exponential growth of high performance capillary electrophoresis (HPCE) as an analytical technique. Since high plate counts are so readily achieved, techniques for optimizing chemical selectivity have not been thoroughly explored.

The principles of HPCE separations have been reviewed(4-5). There are many operating parameters that can be manipulated to improve the resolution for a particular sample, including pH, ionic strength, voltage, capillary surface chemistry, etc. The number of variables is even larger when the analytes include both charged and uncharged species that are to be separated by micellar electrokinetic capillary chromatography (MECC)(6-7). The complexities of developing separation methods with so many interacting variables often leads to large numbers of experimental runs. It should be possible to simplify this process by applying some of the principles of automated methods development as applied to HPLC(8).

In both HPLC and HPCE, methods are most commonly developed by either trial-and-error techniques relying on the expertise of the analyst or by a sequential optimization where each result suggests the next experiment. Both approaches are time-consuming and seldom reach true optimum conditions. While the sequential approach can be systematically formalized using Simplex algorithms, it is still sensitive to the conditions selected for the first experiment and prone to identifying local rather than global optima(9). Modeling, or interpretive, methods do not suffer from these disadvantages. In these approaches, a predictive mathematical model of the behavior of each analyte is derived from the observed changes across a limited number of experiments systematically spanning significant variables. These methods, however, are often based on the analysis of standards for each compound so that they can be tracked across the experimental set. The need for standards can be, in part, obviated if spectroscopic data can be used to match peaks among the experiments. Such data can be obtained by monitoring the separations with a diode array detector. For matching, overlapping peaks must be identified and deconvoluted so that pure spectra are available for comparison. A commercially available software package, Unicam Diamond Optimization Software, includes chemometric tools for such spectral analysis. The same system also has algorithms for peak tracking and for calculation of separation models. This software was selected for adaptation to HPCE methods development.

The mathematics underlying this software have been fully documented(10), but they should be briefly described. The migration modeling is based on a triangular, ten experiment plane. The vertices represent any three selected extremes of selectivity variables, e.g., pH, ionic strength, etc., with the seven interstitial points as evenly spaced combinations of these extremes. These ten experiments are monitored with a diode array detector to give the usual three-dimensional data file. Each separation is divided into well-defined peaks or clusters, and the number of analytes in each segment is determined by principal component analysis (PCA) (11,12). All segments are analyzed with Iterative Target Transform Factor Analysis (ITTFA) and overlapping peaks are deconvoluted(13). The result is a set of pure spectra for each experimental separation (14). Each pure spectrum is associated with a time and an amount expressed as the integral volume under the peak across the wavelength range. Each component is then matched across the ten experimental sets based on all three factors (15,16). From the observed time as a function of experimental conditions for each analyte, a model is calculated by a piece-wise quadratic fit (17). The separation models for each analyte are combined into a resolution model and evaluated for quality of resolution(18). In this way, the conditions for optimal resolution are identified in a minimal number of experiments without the use of pure standards or prior knowledge of the sample.

MATERIALS

All separations were performed on an HPCE system including a Crystal 310 Capillary Electrophoresis System, a Crystal 240 Diode Array Detector, Chromascan 3 software, and Diamond Optimization Software(ATI Unicam; Boston, MA).

The capillary was unmodified fused silica, 75 μ x 92cm with the window at 60cm (Polymicro Technologies, Phoenix, AZ). Buffers were prepared from the highest commercially available grade salts and 18m Ω water (Barnstead Nanopure, Dubuque, IA). Buffers were prepared by adjusting the pH of a 50mM Borate stock with either phosphoric acid or tribasic sodium phosphate after adding the required amount of sodium dodecyl sulfate as listed below for each experiment. Samples were prepared by mixing commercially available cough and cold syrups to obtain the desired mix of active ingredients as described below.

METHODS

All sample mixtures were diluted with an equal volume of half-strength running buffer for each run condition. Injections were made by positive pressure at 25mbar for

0.25min. All separations were all performed at 25kV. Spectra were collected at one point per second at full (1.3nm) spectral resolution.

RESULTS

Deconvolution

A sample containing acetaminophen, pseudoephedrine, dextromethorphan, pyrilamine, and various excipients was analyzed in 100mM SDS, pH 9.0, as shown in Figure 1. The last peak, near 22min, is of particular interest. It appears as a single, symmetrical peak with the spectrum as shown. Principal component analysis of a pure, or spectrally homogeneous, peak yields two eigenvalues, one for the baseline and one for the analyte(11-13). However, when this peak is subjected to PCA, it has three eigenvalues. The extra eigenvalue indicates the presence of at least one additional component in this peak. With the application of Iterative Target Transform Factor Analysis, two pure components are reconstructed as overlapping peaks with the spectra as shown(Figure 2). These spectra correspond to dextromethorphan and pyrilamine. This application of PCA and ITTFA can, therefore, deconvolute comigrating peaks in HPCE and reconstruct pure spectra of sufficient quality for peak identification during methods development.

Migration Modeling for Methods Development

For the methods development experiments, a sample was prepared containing dextromethorphan, pseudoephedrine, guaifenesin, phenylpropanolamine, and several unidentified inactive ingredients found in the commercial formulations. Since this mixture includes both charged and uncharged analytes, it is best separated by MECC. Many variables can influence the selectivity of such a separation, including pH, detergent type and concentration, ionic strength, organic modifiers, and so on(4,7). This sample was separated over a range of increasing pH with the SDS concentration held constant at 100mM(Figure 3). Under these conditions, the last three peaks show substantial changes in relative migration, but the first three are largely unaffected. In contrast, increasing the SDS concentration from 20 to 107mM at a constant pH of 7.5 alters the selectivity for the first three peaks, but does not affect the last three(Figure 4). This pattern of interacting variables affecting analytes to different extents is appropriate for the experimental design and migration modeling embodied in Diamond software.

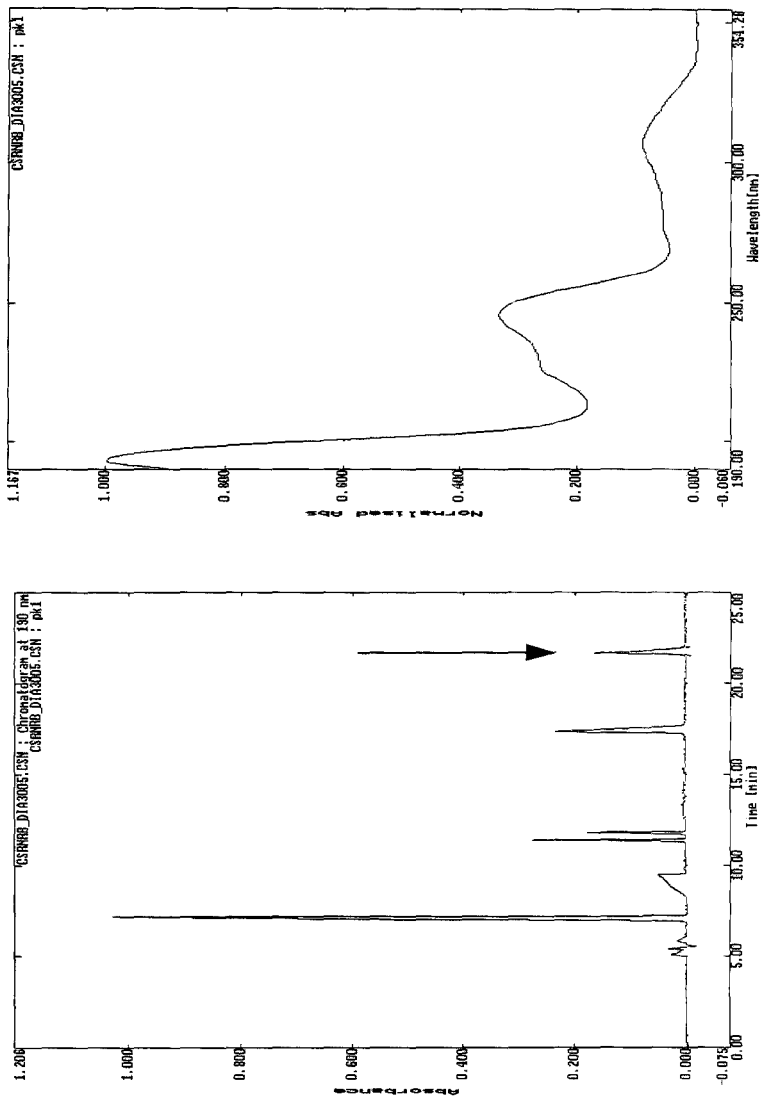


FIGURE 1 Analysis of OTC cough and cold relief formulation by MECC. The left panel shows an electropherogram monitored at 190nm of a sample containing guaifenesin, pseudoephedrine, dextromethorphan, pyrilamine, and excipients. The spectrum of the last peak (arrow) is shown in the right panel. This peak is impure as judged by PCA.

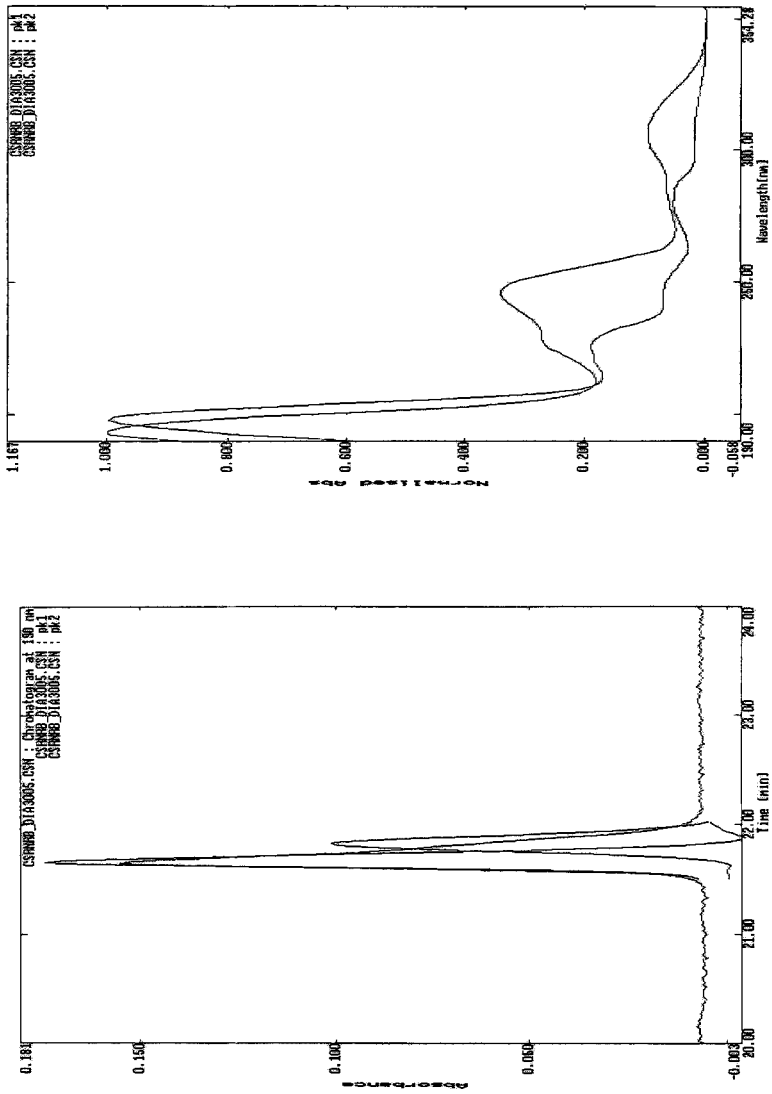


FIGURE 2. Reconstruction with ITTFA. The last peak shown in Figure 1 was deconvoluted with PCA and reconstructed with ITTFA. The two overlapping pure peaks are shown superimposed on the observed single peak in the left panel. The reconstructed pure spectra are shown in the right panel.

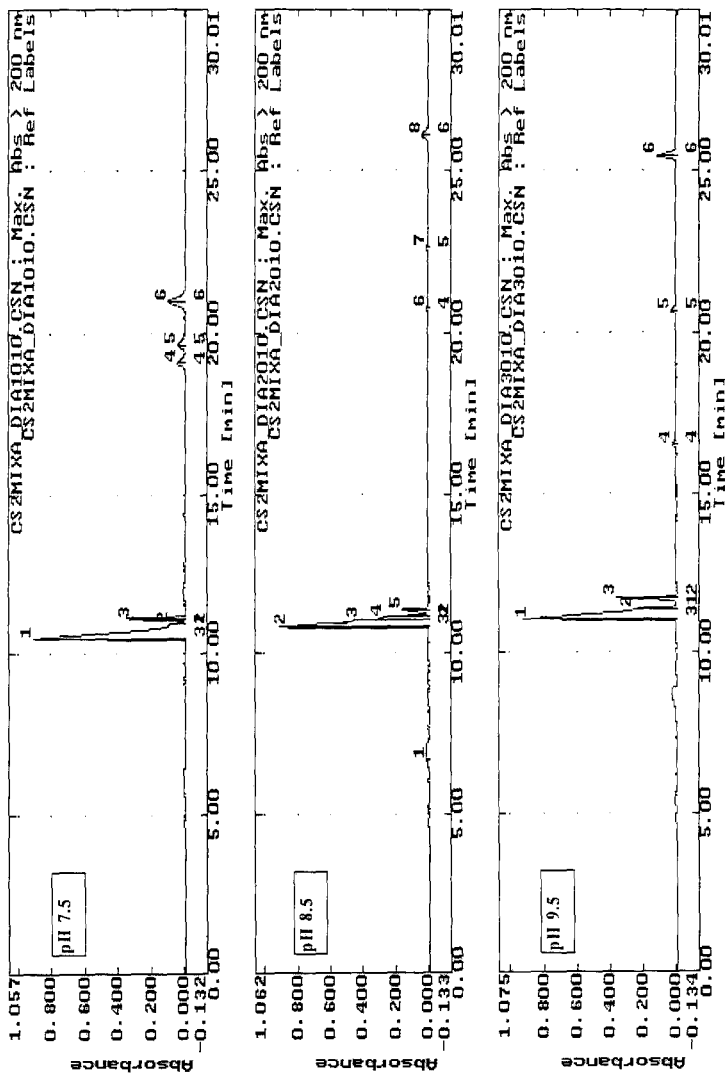


FIGURE 3 Effect of pH on selectivity. A sample containing guaifenesin, pseudoephedrine, phenylpropanolamine, dextromethorphan and excipients was separated in 100mM SDS at pH's of 7.5, 8.5, and 9.5. The peaks in these electropherograms are numbered twice. Numbers above the baseline indicate peaks recognized by the integration algorithm in that particular electropherogram while those below are specific analyte labels common to all three.

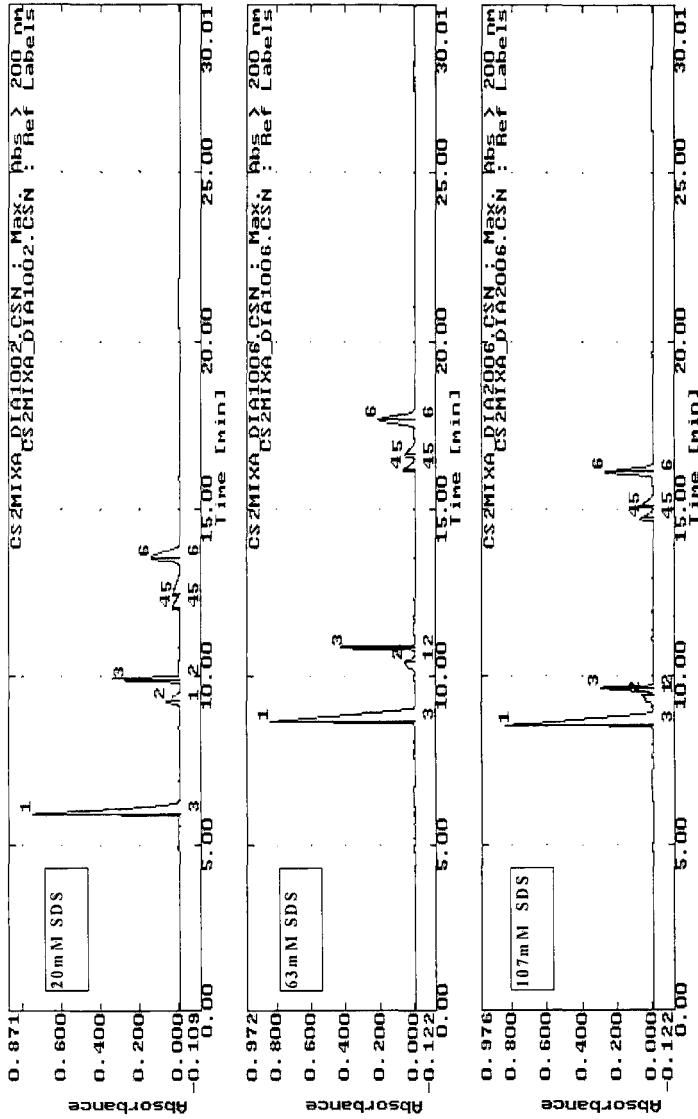


FIGURE 4. Effect of SDS concentration on selectivity. A sample containing guafenesin, pseudoephedrine, phenylpropranolamine, dextromethorphan and excipients was separated in 20, 67, and 107mM SDS at a pH of 7.5. The peaks in these electropherograms are numbered twice. Numbers above the baseline indicate peaks recognized by the integration algorithm in that particular electropherogram while those below are specific analyte labels common to all three.

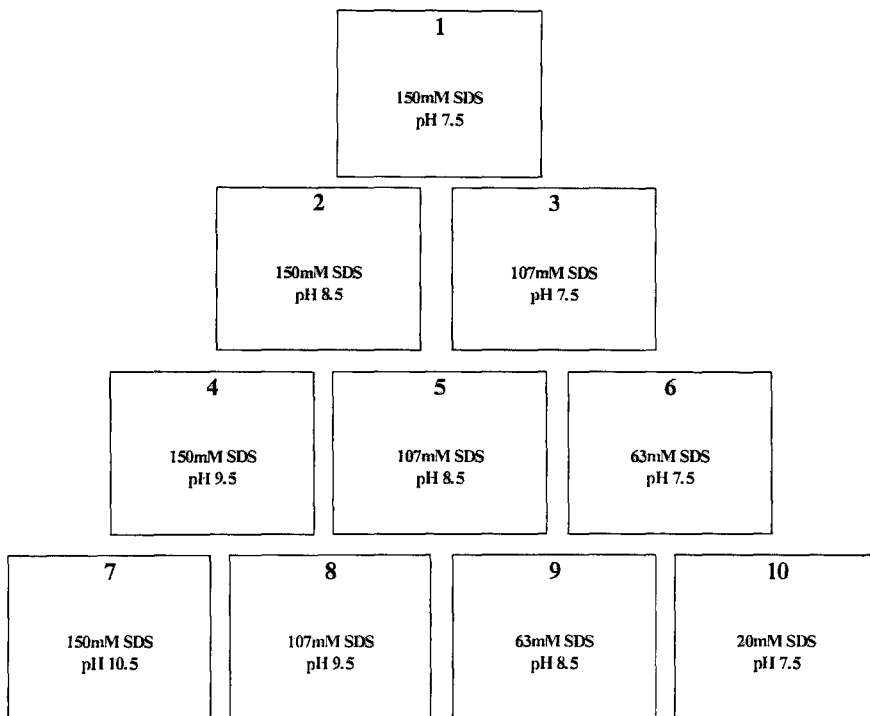


FIGURE 5. Experimental design for methods optimization. The pH and SDS concentrations for the 10 point experimental plane are shown. Each electrolyte was prepared by titrating 50mM borate to the required pH after adjusting the SDS concentration.

An experimental plane was designed to bracket the pH and SDS combinations shown in Figures 3 and 4. The extreme conditions at the vertices define the seven evenly spaced interstitial points (Figure 5). The sample mixture was separated with each electrolyte, and the resulting diode array data files were analyzed with PCA and ITTFA. The result of this process is, for each electropherogram, a table of spectra, migration times, and amounts. These three parameters are used to match the peaks among the several runs of the experimental set(15,16).

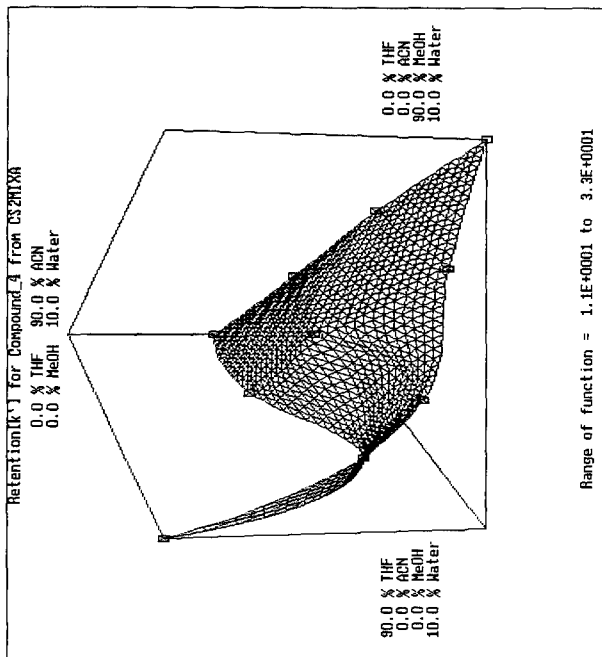
The matching process yields a table showing the migration time of each analyte in each experimental run. It is, therefore, possible to describe the migration behavior of a

given analyte as a function of electrolyte composition. For such a description to be useful, it must accurately predict migration for compositions between the experimental points. First-order linear interpolations are not sufficient so Diamond Software incorporates a piece-wise quadratic fit(17). This function calculates a three-dimensional migration surface for each analyte. Two examples are shown in Figure 6. When examining this figure and those that follow, it must be noted that this software was developed for HPLC, thus the THF, ACN, and MeOH labeling on the printout. In fact, no organic solvents were used. The 90% ACN corner is Experiment 1 in Figure 5. Similarly, 90% THF is Experiment 7 and 90% MeOH is Experiment 10. The plot is designated retention expressed as k' . For these experiments, electrophoretic migration times are equivalent to k' since the calculations are based on a t_0 of 1min. The shapes of these migration surfaces are quite different indicating that substantial changes in separation selectivity are expected over this experimental plane.

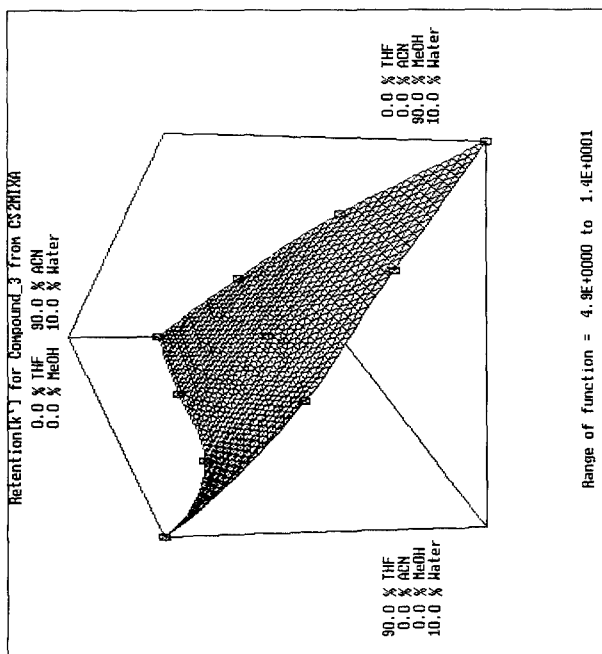
Given that a migration surface has been calculated for each analyte in the mixture, it is straightforward to combine these functions to predict resolution across the experimental plane. This is calculated automatically and expressed as quality of resolution as judged by any of the common evaluation functions(18). The results for this experimental set, judged by the r^* or even spacing function, is shown in Figure 7. A clear optimum is apparent. This three-dimensional plot can also be viewed as a contour plot as shown in Figure 8. Note the cursor placed at the resolution maximum. The composition at this point is shown as well as the predicted electropherogram for these conditions. Although the composition is expressed as percentages of organic solvents, it is straightforward to calculate from Figure 5 that the optimal selectivity for this separation is obtained at 150mM SDS, pH 8.98. Since the cursor on the contour plot can be moved with the mouse, it is possible to examine the experimental plane for other useful separation patterns. For example, as shown in Figure 9, separation at higher pH and slightly lower SDS concentration changes the migration order such that Peak 3 is earlier than Peaks 1 and 2. At the optimum, Peak 3 appeared after Peaks 1 and 2. This predicted behavior matches that observed within the experimental set, confirming the accuracy of this approach to migration modeling.

DISCUSSION

These experiments were designed to test the adaptation of an automated HPLC methods development system for use with capillary electrophoresis. The chemometric



Phenylpropandamine



Guafenesin

FIGURE 6. Migration Models. Two of the six migration models calculated from the methods development experiments are shown. The surface represents migration time as a function of electrolyte composition. The labeling of the corners as organic solvents results from the original development of this software for HPLC. The actual conditions correspond to those in Figure 5. The analytes associated with these models were identified by testing standards after the method was developed. No pure standards were required to calculate the surfaces.

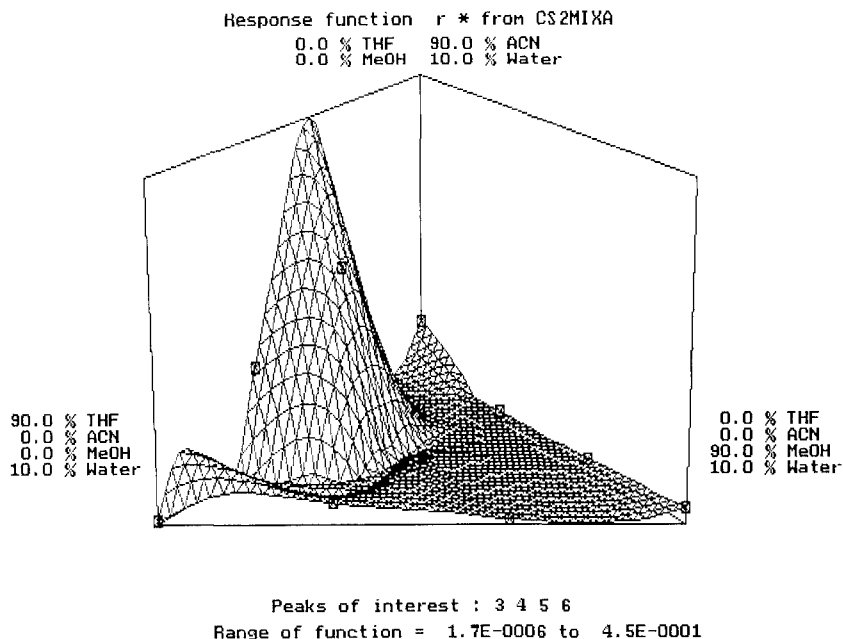


FIGURE 7. Response Function. The response function is a three-dimensional plot reflecting the quality of the separation. Resolution can be calculated in several ways. The function r^* , biased toward equal peak spacing (18), is plotted here as a function of electrolyte composition. The labeling of the corners as organic solvents results from the original development of this software for HPLC. The actual conditions correspond to those in Figure 5.

algorithms proved useful in detecting spectral inhomogeneity in a peak, in deconvoluting the comigration, and in reconstructing the pure spectra contributing to the observed peak. The experimental framework was suitable for minimizing the experiments required to optimize selectivity in MECC. The matching algorithms were successful in tracking the individual analytes across the experimental plane without reference to standards. Migration models were calculated, and an accurate resolution map was constructed. These results confirm that the mathematical tools of Diamond Optimization Software can be applied in HPCE. Further, since these algorithms require high quality spectra, the successful deconvolution and peak tracking results confirm the high spectral sensitivity of this diode array detector.

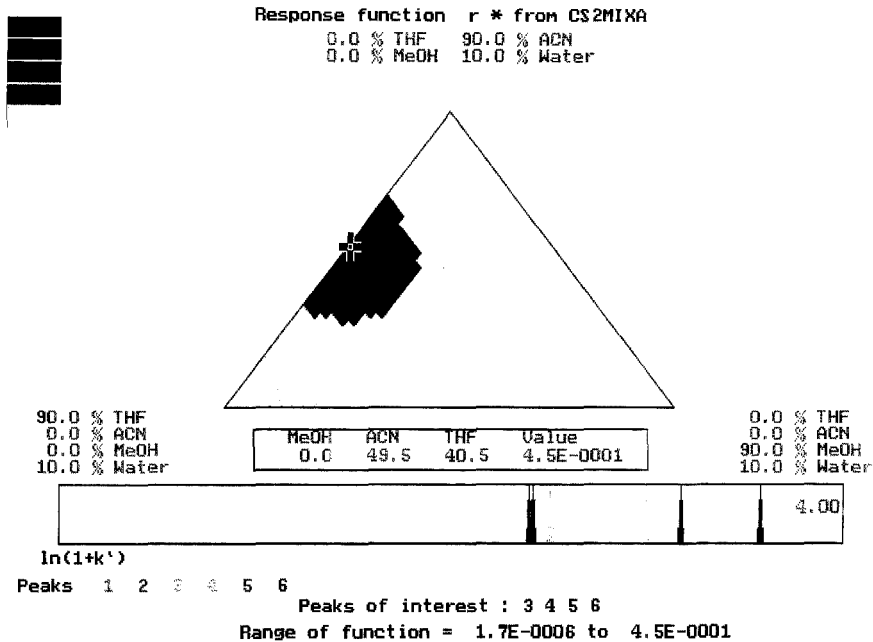


FIGURE 8. Contour plot of response function. The three-dimensional representation of separation quality (Figure 3) is drawn here as a contour plot. The cursor is placed at the point of optimum resolution. The conditions are presented in the frame immediately below the triangle, and the predicted electropherogram is shown in the bottom frame. The labeling of the corners and the optimum conditions as organic solvents results from the original development of this software for HPLC. The actual conditions correspond to those in Figure 5. The actual optimum conditions calculated from the organic percentages are 150mM SDS, pH 8.98.

This software was selected for evaluation for several reasons. It embodies a general approach, interpretive retention modeling, that has proven useful in other separation techniques. It automatically applies PCA and ITTFA to the experimental data to test peak purity and to extract pure spectra. The results are used by peak tracking and migration modeling functions to map resolution without requiring pure standards or prior knowledge of the sample composition. Perhaps most importantly, this process of methods development does not require that the analytes behave in accordance with a well-developed theory of the separation mechanism. It is firmly grounded in an efficient and systematic empirical analysis of raw data.

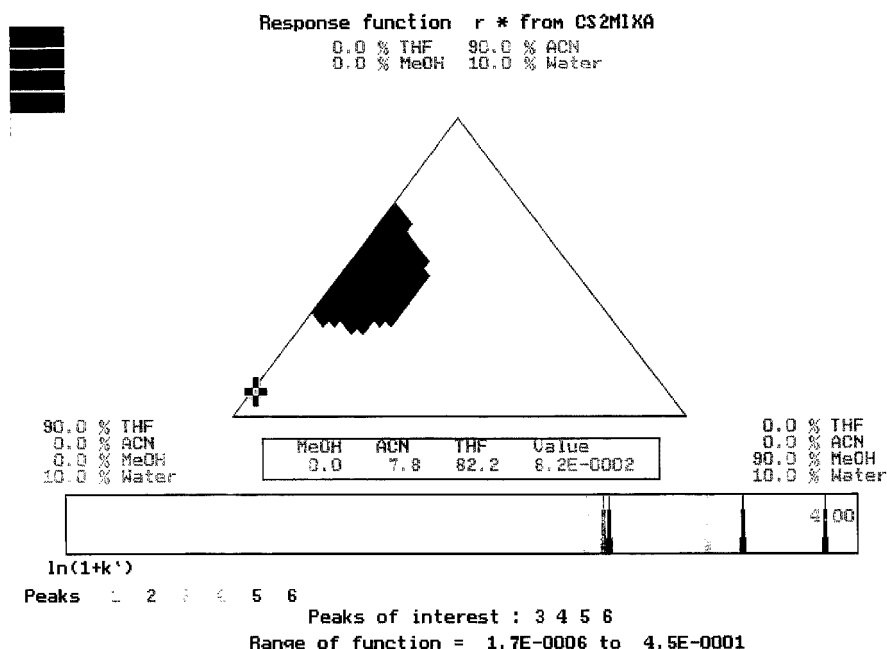


FIGURE 9. Contour plot of response function. The three-dimensional representation of separation quality (Figure 3) is drawn here as a contour plot. The cursor is placed at a point of non-optimum but useful resolution. The conditions are presented in the frame immediately below the triangle, and the predicted electropherogram is shown in the bottom frame. The labeling of the corners and the optimum conditions as organic solvents results from the original development of this software for HPLC. The actual conditions correspond to those in Figure 5. The predicted electropherogram should be compared to that shown for the optimum in Figure 8. Note the change in position of Peak 3 relative to Peaks 1 and 2.

The tools in this software could be used to approach other problems in HPCE. Any variables that affect selectivity can be used as the vertices of the experimental plane. This might include the use of different detergents and mixed micelles in MECC(19) or pH and ionic strength in free-solution capillary electrophoresis(20). The migration and resolution modeling functions should be useful in optimizing chiral separations, although for this application peak tracking cannot be based on spectral discrimination. The chemometric analysis can be used to solve problems outside the realm of methods development. Principal component analysis, iterative target transform factor analysis, and

peak matching can be used to confirm the purity of peaks and their identification in the analysis of complex samples, such as foods and beverages(21) or drugs in biological fluids(20). It may, therefore, be expected that the mathematical approaches embodied in Unicam Diamond Optimization software will be used in a variety of HPCE applications and will serve as a basis for future development of methods development approaches.

REFERENCES

1. S. Hjertén, *Chromatogr. Rev.*, **9**:122-219 (1967)
2. R. Virtanen, *Acta Polytech. Scand. Ch.*, **123**:1-67 (1974)
3. J.W. Jorgenson and K.D. Lukacs, *Science*, **222**:266-272 (1983)
4. R.P. Oda and J.P. Landers, "Introduction to Capillary Electrophoresis," in *Handbook of Capillary Electrophoresis*, J.P. Landers, ed., CRC Press, Boca Raton, 1993, pp.9-42.
5. R. Weinberger, *Practical Capillary Electrophoresis*, Academic Press, Inc, New York, 1993.
6. S. Terabe, K. Otsuka, and T. Ando, *Anal.Chem.*, **56**:111(1984)
7. M.G. Khaledi, "Micellar Electrokinetic Capillary Chromatography," in *Handbook of Capillary Electrophoresis*, J.P. Landers, ed., CRC Press, Boca Raton, 1993, pp.43-93.
8. J.L. Glajch and L.R. Snyder, eds., *Computer-Assisted Method Development for High Performance Liquid Chromatography*, Elsevier, Amsterdam, 1990.
9. J.C. Berridge, "Simplex Optimization of High-Performance Liquid Chromatographic Separations," in *Computer-Assisted Method Development for High Performance Liquid Chromatography*, J.L. Glajch and L.R. Snyder, eds, Elsevier, Amsterdam, 1990, pp3-14.
10. H.A.H. Billiet, and L. deGalan, "Selection of Mobile Phase Parameters and Their Optimization in Reversed-Phase Liquid Chromatography," in *Computer-Assisted Method Development for High Performance Liquid Chromatography*, J.L. Glajch and L.R. Snyder, eds, Elsevier, Amsterdam, 1990, pp27-50.
11. E.R. Malinowsky and D.G. Howery, *Factor Analysis in Chemistry*, Wiley, New York, 1980.
12. J.K. Strasters, H.A.H. Billiet, L. deGalan, and B.G.M. Vandeginste, *J.Chromatogr.*, **499**:499(1990)
13. B.G.M. Vandeginste, W. Derks, and G. Kateman, *Anal.Chim.Acta*, **173**:253(1985)
14. J.K. Strasters, H.A.H. Billiet, L. deGalan, B.G.M. Vandeginste, and G. Kateman, *Anal.Chem.*, **60**:2745 (1988)
15. M.Oto, W. Wegscheider, and E. Lankmayer, *Anal.Chem.*, **60**:517 (1988)
16. B.G.M. Vandeginste, G. Kateman, J.K. Strasters, H.A.H. Billiet, and L. deGalan, *Chromatographia*, **24**:127 (1987)
17. P.J. Naish-Chamberlain and R.J. Lynch, *Chromatographia*, **29**:79-89 (1990)
18. P.J. Schoenmakers, *J. Liq. Chrom.*, **10**:1865-1886 (1987)
19. T.E. Wheat and F.M. Chiklis, The Fifth Annual Frederick Conference on Capillary Electrophoresis, Abstract 29(1994)
20. K.A. Lilley and T.E. Wheat, The Pittsburgh Conference, Abstract 805(1995)
21. F.M. Chiklis and T.E. Wheat, The Pittsburgh Conference, Abstract 703(1995)

Received: July 10, 1995

Accepted: August 6, 1995

**CE RESOLUTION OF NEUTRAL AND ANIONIC
RACEMATES WITH GLYCOPEPTIDE
ANTIBIOTICS AND MICELLES**

DANIEL W. ARMSTRONG* AND KIMBER L. RUNDLETT

*Department of Chemistry
University of Missouri-Rolla
Rolla, Missouri 65401*

ABSTRACT

The glycopeptide antibiotics vancomycin, ristocetin A and teicoplanin have been shown to be effective chiral selectors in capillary electrophoresis (CE). However, most of the resolved enantiomers were anionic or acidic compounds that contained carboxylic acid, phosphate, or sulfonate groups. Conversely, a large number of neutral racemates are resolved using these same chiral selectors attached to the stationary phase in HPLC. The problem in resolving neutral analytes in CE is outlined and discussed. Addition of sodium dodecyl sulfate (SDS) micelles to the run buffer greatly increases the available elution window, thereby facilitating the separation of neutral racemates. Neutral analytes resolved in this CE system include bromacil, bendroflumethiazide and 5-(4-hydroxyphenyl)-5-

phenylhydantion. The separations of coumachlor and warfarin are also demonstrated. In addition, the effect of surfactant concentration and organic co-solvents on elution time and enantioresolution are discussed.

INTRODUCTION

Macrocyclic antibiotics are the newest class of chiral selectors for capillary electrophoresis (CE) and liquid chromatography (1-9). The primary associative interaction between a chiral analyte and the enantioselective antibiotic appears to be electrostatic in nature (2,3,5). For example, rifamycin B (an anionic ansa compound) best resolves compounds containing amine functional groups (2). Conversely, glycopeptide antibiotics are most useful for resolving a variety of acidic or anionic analytes when used below their isoionic point (3,5). The additional secondary interactions needed for chiral recognition (depending on the solvent system used and the nature of the analyte) include one or more of the following: hydrogen bonding, dipolar interactions, hydrophobic interactions, π - π interactions and steric repulsion (1-4).

The use of micelles in CE separations also can be useful (8,10-12). The correct pseudophase model for the use of micelles plus a chiral selector (or any other pseudophase) in CE was elucidated recently (8). Sodium dodecyl sulfate (SDS) micelles tend to enhance the efficiency of many glycopeptide antibiotic CE separations by an order of magnitude (8). Also they change the elution order of all components including enantiomers (8). In this work we extend the use of the antibiotic, vancomycin, as a CE chiral selector to neutral molecules. This is done using an anionic micelle composed of sodium dodecyl sulfate surfactants. The theory and use of micelles in separations has been reviewed previously (12).

EXPERIMENTAL

Materials

Sodium dihydrogen phosphate, sodium hydroxide and potassium hydroxide were purchased from Sigma Chemical Company (St. Louis, MO). Electrophoresis grade sodium dodecyl sulfate was obtained from Bio-Rad (Richmond, CA). Warfarin, coumachlor, bendroflumethiazide and 5-(4-hydroxyphenyl)-5-phenylhydantoin were purchased from Aldrich Chemical Company (Milwaukee, WI). Bromacil was purchased from Chem Service (West Chester, PA). Vancomycin was generously provided by ASTEC (Whippany, NJ). Solvents were purchased from Fisher (St. Louis, MO). Deionized water was used to prepare all buffer solutions.

Methods

Separations were performed using a Beckman P/ACE 2000 capillary electrophoresis unit (Palo Alto, CA) or a Waters Quanta 4000 (Millford, MA). The P/ACE unit was used unless otherwise indicated. The P/ACE was equipped with a 50 mm x 37 cm (30 cm to the detector) fused silica capillary thermostated at 25°C. A 50 mm x 32.5 cm (25 cm to the detector) fused silica capillary at ambient temperature was used with the Quanta 4000. All separations were monitored at 254 nm. Phosphate buffers were prepared by adjusting the pH of sodium dihydrogen phosphate solutions with sodium hydroxide or hydrochloric acid. All phosphate buffers were prepared as 50 mM, pH 7.0 unless otherwise indicated. Samples were prepared at about 0.1 mg/mL in 50/50 methanol/buffer and injected using the pressure mode (0.5 psi) or the hydrostatic mode for 1 second. Capillaries were rinsed daily with 0.5 N potassium hydroxide for 15 minutes followed by water for 10

minutes and run buffer for 15 minutes. Between runs, the capillary was rinsed with 0.1 potassium hydroxide, water and run buffer for 2 minutes each. The run voltage for all separations was +5 kV. Organic solvent/phosphate buffer mixtures were prepared by volume. It should be noted that mixtures of SDS and vancomycin used in this study tend to precipitate in organic solvent/phosphate buffer solutions. These additives can be dissolved initially by sonication but will precipitate from solution within a few hours as evidenced by a deterioration in the electropherogram.

RESULTS AND DISCUSSION

The structure of vancomycin is shown in Figure 1. The properties of this macrocyclic antibiotic which make it a useful chiral selector in LC and CE have been described in detail previously (1,3,4). When used as an HPLC chiral stationary phase, vancomycin resolves a large number of neutral organic racemates as well as negatively charged analytes. However, in CE, only the enantioresolution of negatively charged racemates have been reported thus far.

The isoelectric point of vancomycin is ~ 7.2 (1). Consequently at pH 7.0, it elutes at nearly the same time as a neutral solute carried by the electroosmotic flow. This is illustrated in Figure 2A. Note that a neutral racemate would have to elute and separate in the very small window between the vancomycin peak and eof trough (Fig. 2). This expected elution profile assumes that there is no interaction between the solute-selector complex and the capillary wall. Lowering the pH to 5.0 increases the elution window and therefore the possibility of obtaining a separation to some extent (Fig. 2B). However, this still represents a very limited area in which to achieve a separation. The somewhat greater distance between the vancomycin peak and the eof trough at this pH results from the fact that electrophoretic mobility

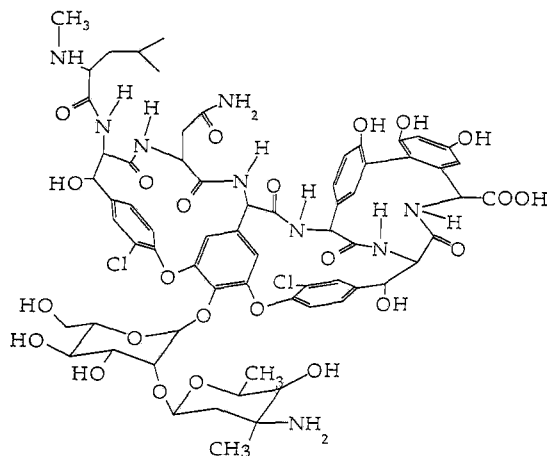


Figure 1. Structure of vancomycin (MW 1449). Note the semirigid aglycone basket composed of 3 fused macrocyclic rings as well as the pendant, freely rotating, disaccharide moiety.

of vancomycin becomes more positive as it acquires a greater positive charge. The addition of sodium dodecyl sulfate (above the CMC) to the run buffer has a more profound effect on the elution window for neutral solutes. This is shown in Figure 2C. Neutral racemates can elute and potentially resolve anywhere between the eof trough and the SDS peak. The elution profile shown in Figure 2C results from the fact that vancomycin binds to the oppositely charged micelle, thereby reversing its electrophoretic mobility. This is illustrated in Figure 3. Previous studies have shown that vancomycin is ~ 90% bound to the micelle under these experimental conditions (8). The analyte can now partition between three pseudophases (i.e., the vancomycin-SDS mixed micelle, the free vancomycin, and the bulk aqueous solution, Figure 3C). A complete theoretical and mathematical treatment of this pseudophase system was published recently (8). The same theory applies to micelle

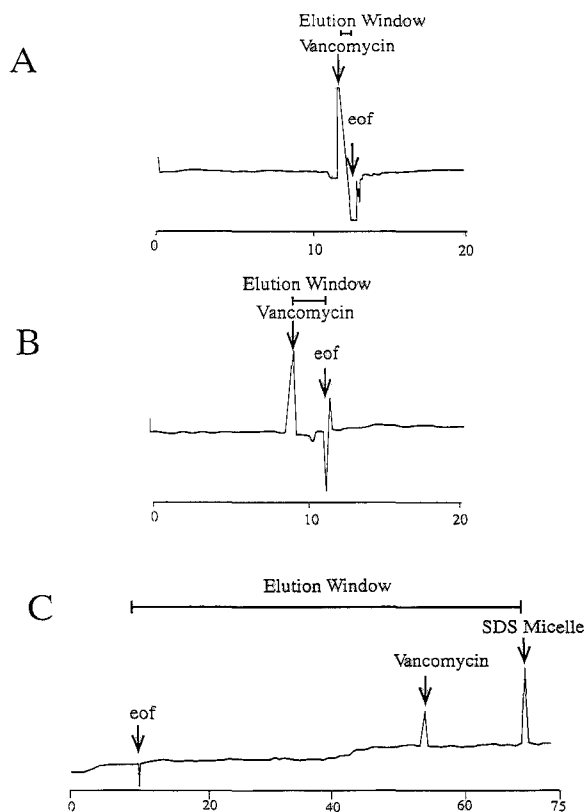


Figure 2. Capillary electropherograms showing the variation in the size of the elution window for neutral solutes in the presence and absence of SDS micelles. These examples do not consider the binding of vancomycin to the capillary wall. Run conditions are as follows: 2 mM vancomycin in phosphate buffer, voltage: +5 kV, capillary: 50 mm x 37 cm (30 cm to detector), detector wavelength: 254 nm.

(A) Demonstration of the small elution window that is available at pH 7.

(B) Example of the slightly extended elution window available for neutral solutes at pH 5.0. The run buffer was prepared from 0.1 M, pH 5.0 phosphate buffer.

(C) Demonstration of the greatly extended elution window brought about by using SDS micelles in the run buffer. The run buffer was prepared from 0.05 M pH 7.0 phosphate buffer containing 100 mM SDS.

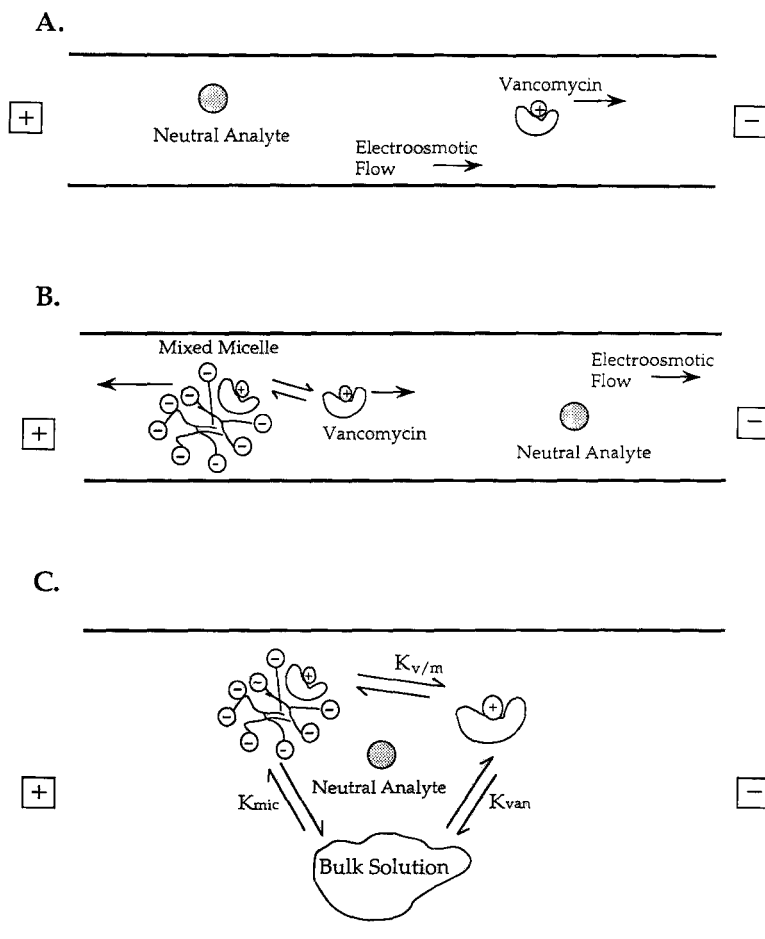


Figure 3. Representation of the electrophoretic mobilities of the neutral analytes, chiral selector and mixed micelles in: (A) buffer containing vancomycin, and (B) buffer containing vancomycin and SDS. Note that the migration time of vancomycin changes from about 8.8 min in phosphate buffer to 33.8 min in 21 mM SDS. (C) shows the pseudophase equilibria of neutral analytes between the bulk solution, the free vancomycin, and the mixed micelle.

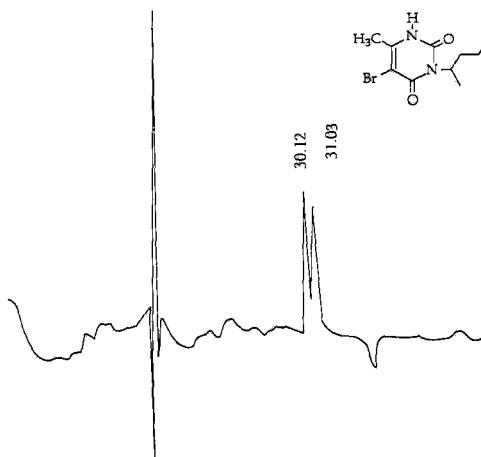


Figure 4. CE separation of the enantiomers of bromacil. Experimental conditions: 2 mM vancomycin, 25 mM SDS, 5% methanol, 95% 50 mM pH 7.0 phosphate buffer. See the experimental section for further details.

cyclodextrin systems, mixed cyclodextrin systems and CE systems that utilize a stationary phase or where wall interactions occur (8). Clearly the micellar association of the chiral selector causes a large change in the electrophoretic mobility of vancomycin. When higher SDS concentrations are used in the run buffer, the vancomycin peak in Fig. 2C elutes even closer to the SDS peak.

Figures 4-8 show the CE resolution of three neutral racemates (bromacil, bendroflumethiazide, 5-(4-hydroxyphenyl)-5-phenylhydantoin) and two anionic racemates (warfarin, and coumachlor) with the vancomycin-SDS system. With the exception of coumachlor, these compounds are not resolved in CE at pH 7.0 without the SDS. Figures 9 and 10 show the effect of SDS concentrations on retention and enantioresolution. In general, higher SDS concentrations increase retention but do not appreciably enhance enantioresolution.

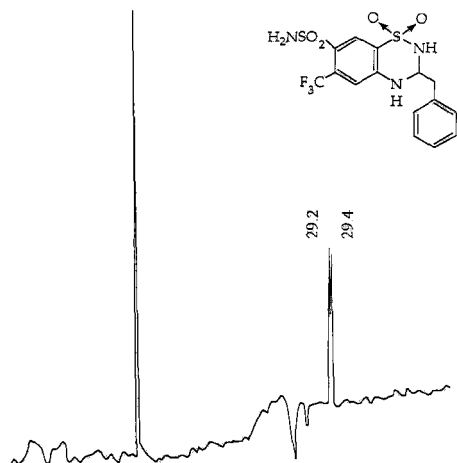


Figure 5. CE separation of the enantiomers of bendroflumethiazide. Experimental conditions: 2 mM vancomycin and 25 mM SDS in 50 mM pH 7.0 phosphate buffer. See the experimental section for further details.

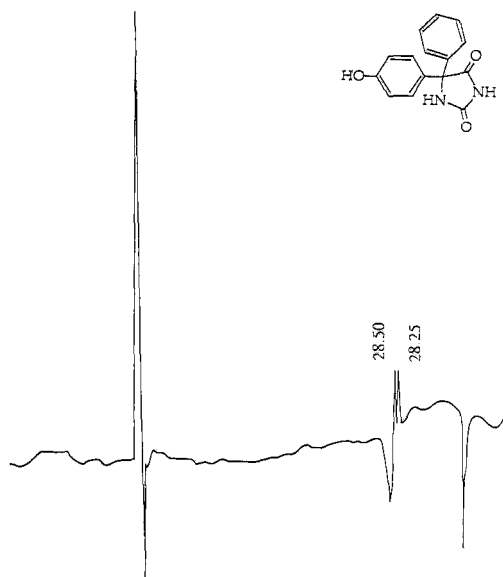


Figure 6. CE separation of the enantiomers of 5-(4-hydroxyphenyl)-5-phenylhydantoin. Experimental conditions: 2 mM vancomycin, 50 mM SDS in 50 mM pH 7.0 phosphate buffer. See the experimental section for further details.

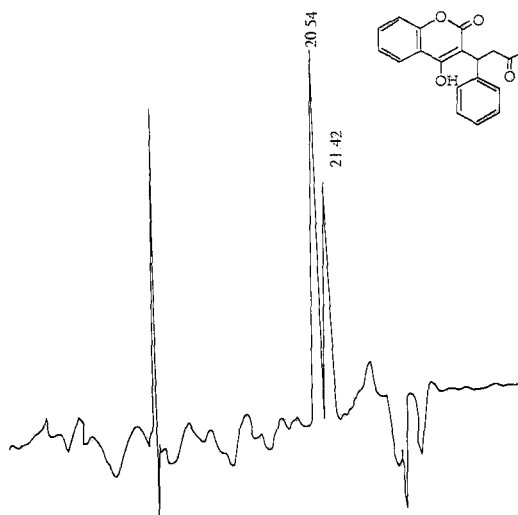


Figure 7. CE separation of the enantiomers of warfarin. Experimental conditions: 2 mM vancomycin, 25 mM SDS in 50 mM pH 7.0 phosphate buffer. See the experimental section for further details.

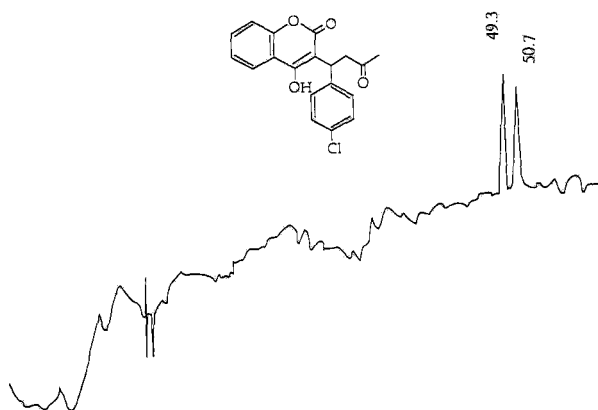


Figure 8. CE separation of the enantiomers of coumachlor. Experimental conditions: 2 mM vancomycin, 50 mM SDS, 10% acetonitrile, 90% 50 mM pH 7.0 phosphate buffer. See the experimental section for further details.

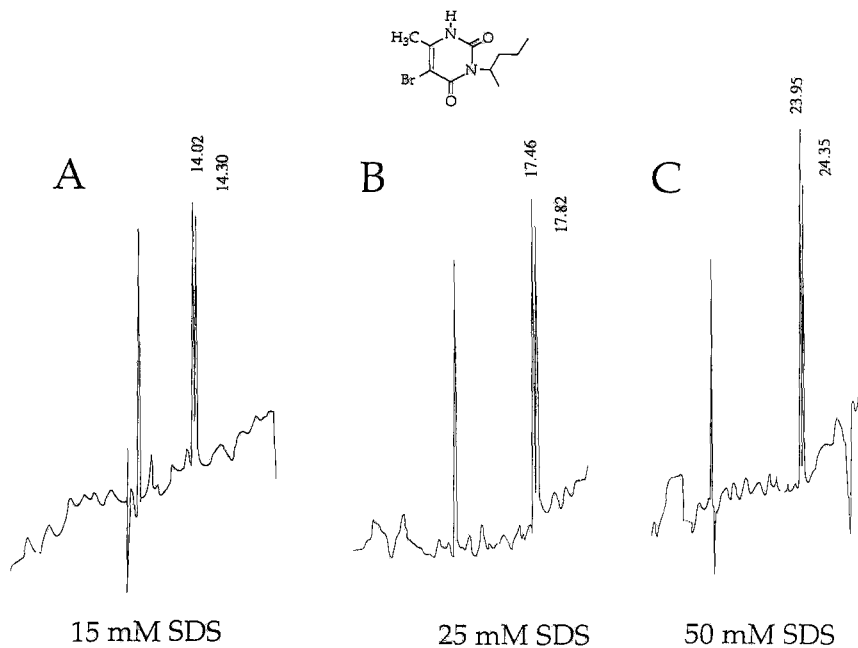


Figure 9. Effect of SDS concentration on the CE separation of the enantiomers of bromacil. Experimental conditions: 2 mM vancomycin with the indicated SDS concentration in 50 mM pH 7.0 phosphate buffer. See the experimental section for further details.

Figure 11 shows the effect of adding miscible organic co-solvents to the run buffer. Previous results have shown that the organic modifiers can sometime enhance enantioresolution in CE systems that utilize certain antibiotic chiral selectors (1,2). As was found previously, organic modifiers increase migration times by decreasing electroosmotic flow velocities. However, in every case with the SDS system, the enantioresolution was either unchanged or significantly impaired when

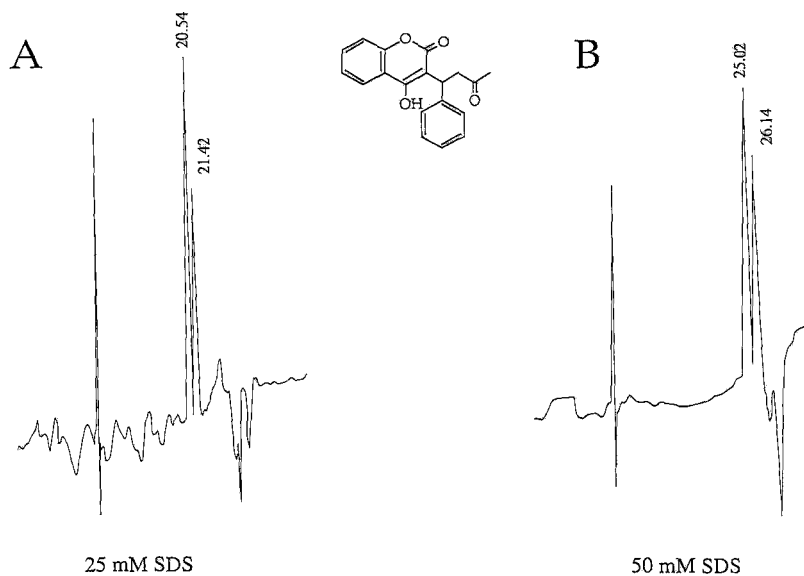


Figure 10. Effect of SDS concentration on the CE separation of the enantiomers of warfarin. Experimental conditions: 2 mM vancomycin with the indicated SDS concentration in 50 mM pH 7.0 phosphate buffer. See the experimental section for further details.

organic solvents were added. Organic solvents inhibit micelle formation by shifting the micellization equilibria to the monomeric form of the surfactant. It also disrupts the solubilization equilibria of the analytes with the micelles.

Figure 12 depicts the enantioresolution of warfarin and coumachlor at pH 4.0 in the absence of SDS. These enol compounds are anionic at pH 4.0. Note that the peaks are broad indicating poor efficiency. This might be explained by the fact that vancomycin, in the absence of SDS, binds to the capillary wall thereby creating a "dynamic stationary phase". Previously it was found that the addition of SDS to

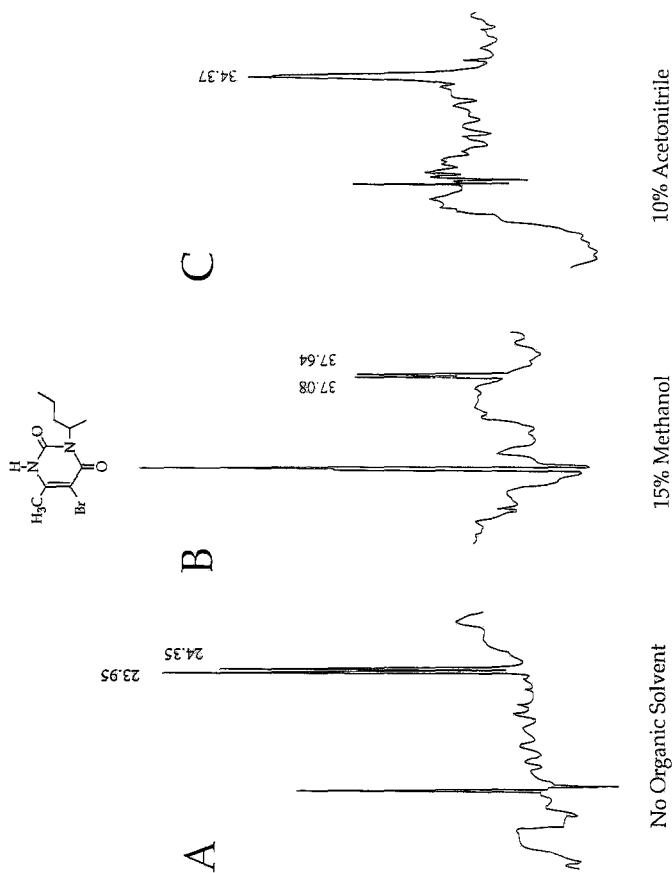


Figure 11. Effect of organic solvent on the CE separation of the enantiomers of bromacil. Experimental conditions: 2 mM vancomycin, 50 mM SDS in 50 mM pH 7.0 phosphate buffer with the indicated volume percent of organic solvent. See the experimental section for further details.

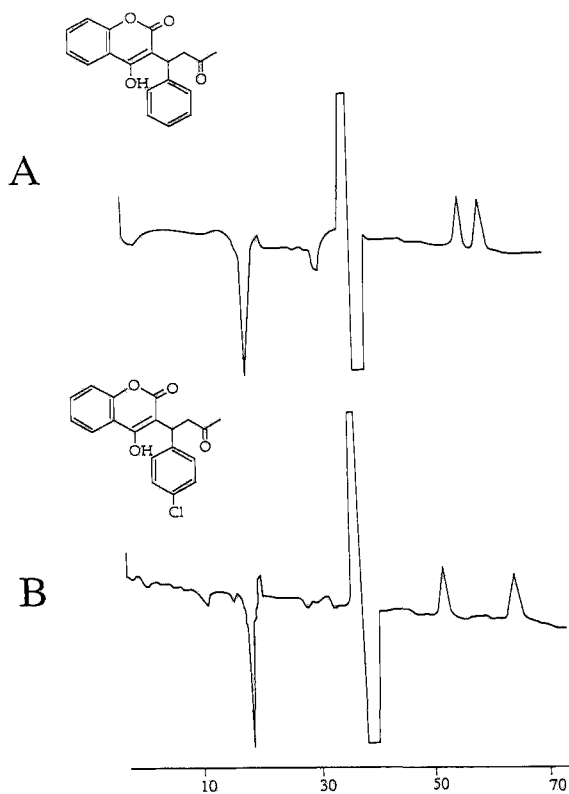


Figure 12 CE separation of the enantiomers of (A) warfarin and (B) coumachlor using vancomycin at pH 4.0 without micelles. The enantiomers elute outside the expected elution window for neutral compounds. This behavior may be due to the binding of the solute-selector complex with the capillary wall. Data was collected using a Waters Quanta 4000 capillary electrophoresis unit using a 50 mm x 32.5 cm (25 cm to the detector) at +5 kV and at ambient temperature.

vancomycin buffers resulted in a decrease in enantioresolution for dansyl-amino acids and nonsteroidal antiinflammatory compounds (8). In the case of the more hydrophobic compound, warfarin, enantioresolution was only observed at pH 7.0 when SDS micelles were added to the system.

CONCLUSION

Previous work demonstrated that the addition of SDS micelles to glycopeptide-mediated CE separations enhanced efficiency by an order of magnitude and reversed the elution order of all components (8). In this work it was further demonstrated that SDS allows the CE separation of neutral enantiomers that may not be resolved with vancomycin alone. Furthermore, the 3-phase model originally proposed for LC (13) and extended to CE (8) can be used to explain the elution behavior of these analytes as well as the expanded elution window that allows their resolution. Unlike many other antibiotic-based enantioseparations, organic modifiers do not improve enantioresolution even though they increase elution times.

ACKNOWLEDGMENT

Support of this work by the Department of Energy, Office of Basic Sciences (grant DE FG02 88ER13819) is gratefully acknowledged.

REFERENCES

1. D. W. Armstrong, Y. Tang, S. Chen, Y. Zhou, C. Bagwill, and J.-R. Chen, *Anal. Chem.*, **66**, 1473 (1994).
2. D. W. Armstrong, K. L. Rundlett and G. R. Reid, III, *Anal. Chem.*, **66**, 1690 (1994).
3. D. W. Armstrong, K. L. Rundlett and J.-R. Chen, *Chirality*, **6**, 496 (1994).

4. D. W. Armstrong and Y. Zhou, *J. Liq. Chromatogr.*, **17**, 1695 (1994).
5. D. W. Armstrong, M. P. Gasper and K. L. Rundlett, *J. Chromatogr.*, **689**, 285 (1995).
6. D. W. Armstrong, E. Y. Zhou, S. Chen, K. Le and Y. Tang, *Anal. Chem.*, **66**, 4278 (1994).
7. S. Chen, Y. Liu, D. W. Armstrong, J. I. Borrell, B. Martinez-Teipel and J. L. Matallana, *J. Liq. Chromatogr.*, **18**, 1495 (1995).
8. Rundlett, K. L., Armstrong, D. W.. *Anal. Chem.* **67**:2088-2095, 1995.
9. D. W. Armstrong, Y. Liu, and H. Ekborg-Ott, *Chirality*, **6** in press (1995).
10. S. Terabe, K. Otsuka, K. Ichikawa, A. Tasuchya, and A. Ando, *Anal. Chem.*, **56**, 111 (1984).
11. S. Terabe, K. Otsuka and T. Ando, *Anal. Chem.*, **57**, 834 (1985).
12. D. W. Armstrong, *Sep. Purif. Methods*, **14**, 213 (1985).
13. D. W. Armstrong, and F. Nome, *Anal. Chem.*, **53**, 1662 (1981).

Received: July 10, 1995

Accepted: August 6, 1995

CONSIDERATIONS ON THE ENANTIOMERIC SEPARATION BY MEKC OF N-Bz-AMINO ACIDS WITH N-DODECOXYCARBONYLVALINE AS CHIRAL SELECTOR

ERIK VAN HOVE AND PAT SANDRA

*Department of Organic Chemistry
Group Separation Sciences
University of Ghent
Krijgslaan 281-S4, B-9000 Ghent, Belgium*

ABSTRACT

N-dodecoxy-carbonyl-(S)-valine was evaluated for the separation of some benzoylated amino acids (alanine, aminobutyric acid and leucine). Successful enantiomeric separation required blocking of the carboxylic function by the formation of the methyl esters in order to avoid repulsion of the charged carboxylate group by the hydrophobic interior of the chiral micelles. A model of chiral recognition is presented. The highest enantioselectivity was obtained for the 3,5-dinitrobenzoyl derivatives ($\alpha > 1.07$). Based on the data, the generally accepted MEKC-resolution equation was experimentally verified and confirmed.

INTRODUCTION

Capillary electrophoresis (CE) is nowadays widely used for the separation of optically active substances. Direct enantioseparation is usually performed by adding chiral selectors to the separation buffer. Zare and coworkers (1,2) were the first to report on electrokinetic enantioseparations applying a ligand-exchange mechanism with Cu^{2+} -L-histidine as chiral selector. Since that initial work, all chiral recognition principles developed for HPLC, have been applied in CE: formation of inclusion complexes utilizing cyclodextrins or crown ethers, chiral micellar

solubilization and chiral polymer-based recognition i.e. with bovine serum albumine (3). Several reviews on this topic have been published (4-6). In MEKC, two approaches to carry out enantiomeric separations have been developed: the use of chiral surfactants or the addition of chiral additives to achiral surfactants. The chiral surfactants can be of natural origin like bile salts, digitonin etc., or synthetic optically active amino acid derivatives. The first reports in MEKC of separations of racemic compounds date from 1989. Yamaguchi et al. (7,8) used a chiral surfactant L-amino acid derivative e.g. sodium N-dodecanoyl-L-valinate to separate N-acylated amino acid isopropyl esters, while Terabe et al. (9,10) utilized bile salts to separate racemic dansylated amino acids. Scientists in Waters, synthesized the chiral surfactants S- and R-N-dodecoxycarbonylvaline, which were successfully applied for the separation of enantiomers of basic drugs (11). The presented work describes the evaluation of the S chiral surfactant for the enantioselective separation of several derivatives of alanine, amino butyric acid and leucine. An interaction model is proposed. Based on the data obtained with the amino acid derivatives the MEKC-resolution equation, developed by Terabe et al. (12), was verified.

MATERIALS AND METHODS

The analyses were performed on a Quanta 4000 (Waters, Milford, MA, USA). The fused silica capillary (Polymicro Technology, Phoenix, AZ, USA) was 75 μm I.D., 375 μm O.D., 59 cm L. with the detection window at 52 cm. The buffer solutions were prepared with deionised water (Milli-Q, Millipore, Bedford, MA, USA) and consisted of 50 mM N-dodecoxycarbonyl-(S)-valine and 25 mM phosphate/25 mM borate, adjusted to pH 7.8. Experiments were also performed with 100, 150 and 200 mM chiral surfactant. The test samples were composed of the N-benzoyl- (Bz), N-p-nitrobenzoyl- (pNBz), N-m-nitrobenzoyl- (mNBz) or N-3,5-dinitrobenzoyl (DNB) derivatives of alanine (ALA), aminobutyric acid (ABA) and, leucine (LEU) and their corresponding methyl esters. Samples were injected hydrodynamically with an elevation of 10 cm during 5 s. Analyses were performed at room temperature with an applied voltage of 15 kV. Detection was at 214 nm. Formamide and dodecanophenone were used as t_0 and t_{MC} markers, respectively. All reported results are average values of three measurements. Between each run, the column was rinsed with the separation buffer for 3 min. A PC workstation with maxima

software (version 3.31, Millipore Corp., Bedford, MA, USA) was used for instrument control and data handling.

RESULTS AND DISCUSSION

The enantiomers of the amino acid N-derivatives with free carboxylate group could not be resolved with N-dodecoxycarbonyl-(S)-valine as chiral selector in the concentration range 50 to 200 mM. This is in accordance with ref. 7, in which N-dodecanoyl-L-valinate was used as chiral surfactant. Enantioselective complexation would require that the charged carboxylate group is oriented towards the hydrophobic interior of the micelle (Figure 1A) which is apparently an unfavorable process.

At a relatively low surfactant concentration of 50 mM, the elution order for similarly substituted species was LEU < ABA < ALA, which is corresponding with a pure electrophoretic movement of the anions. At higher surfactant concentrations, hydrophobic interaction with the micelles occurred, as reflected by the gradually increased retention of leucine, but there was no indication of chiral recognition.

Unlike common polar modifiers, like methanol, acetonitrile and isopropanol, which are aqueous phase modifiers, higher alcohols like butanol are incorporated in the micellar phase and modify the micellar properties (13,14). Because this principle was successfully applied in the MEKC analysis of anionic bitter compounds with SDS (15,16), it was speculated that the addition of butanol to the

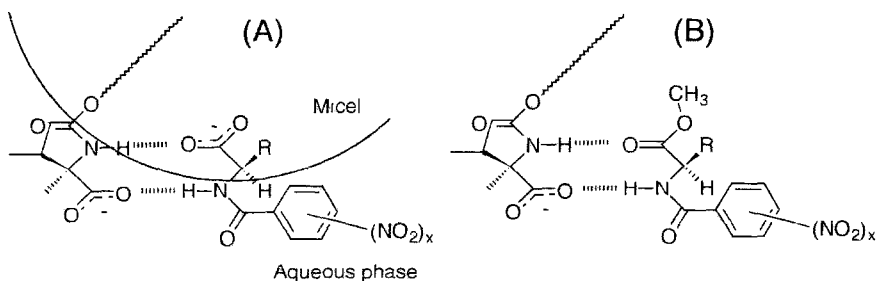


Figure 1. Mechanism of chiral recognition
A. Free carboxylate function; B. Methyl ester.

buffer could facilitate interactions between anionic solutes and micelles, thus creating enantioselectivity. Although some influence on the solute/micelle interaction was noted, no enantioselectivity was observed.

Two other modifications that could increase interactions between similarly charged solutes and micelles are the addition of tetraalkyl ammonium salts (17) or bivalent metal ions (18); and although there is no evidence that they are broadly applicable, they were tried out.

TBAs (tetrabutylammonium salts) have been proposed to improve resolution, but in at least one study dealing with other types of compounds, it was found that TBA had a negative effect on the resolution (19). In this study, the application of TBA modifiers led to buffer systems which gave highly irreproducible and erratic results, serious baseline drift problems and background absorption problems in the case of bromide salts. In those cases where the chlorides were not available, the hydroxydes were applied, followed by pH control with hydrochloric acid. Moreover, addition of 50 mM of these modifiers to 50 mM of surfactant resulted in a strong increase of the current (130 μ A and above, at 15 kV). Given the poor quality of the results, and the complete absence of any enantioselectivity, no further attempts were made to systematically treat the data.

Bivalent metal ions can play a role in the diastereomeric complex formation and thus enantiomer recognition (1,2). Cu^{2+} has been used in combination with a chiral surfactant for the separation of dansylated amino acids (20). The results of our own attempts with N-dodecoxycarbonyl-(S)-valine/ M^{2+} ($\text{M} = \text{Cu}, \text{Zn}$) were all negative.. It must be remarked that this surfactant is not likely to form complexes with the metal cations as illustrated in Figure 2.

The N-benzoylated amino acid methyl esters, on the other hand, could be resolved with N-dodecoxycarbonyl-(S)-valine as chiral selector. Figure 3 shows the separation for the N-3,5-dinitrobenzoyl methyl ester derivatives. The data for the other N-derivatives are summarized in Table 1. At 50 mM surfactant, the elution order of similarly substituted species followed the expectation from the hydrophobicity of their side chains ($\text{ALA} < \text{ABA} < \text{LEU}$).

By analogy to models that have been presented for the chiral recognition in comparable HPLC systems (21), the retention mechanism in Figure 1B is proposed.

With the S-type surfactant, the D-enantiomer elutes before the L-enantiomer in all cases. As L-amino acids have the S-configuration, this means that, according

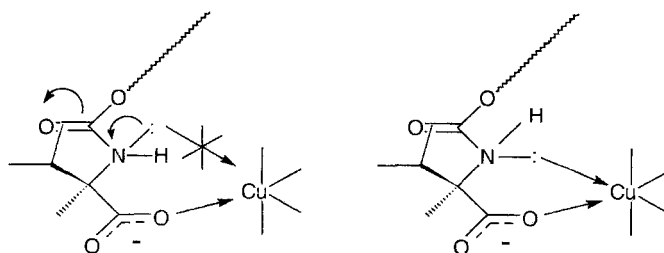


Figure 2. Actual (left) and preferred (right) structure for surfactant/ M^{2+} interaction.

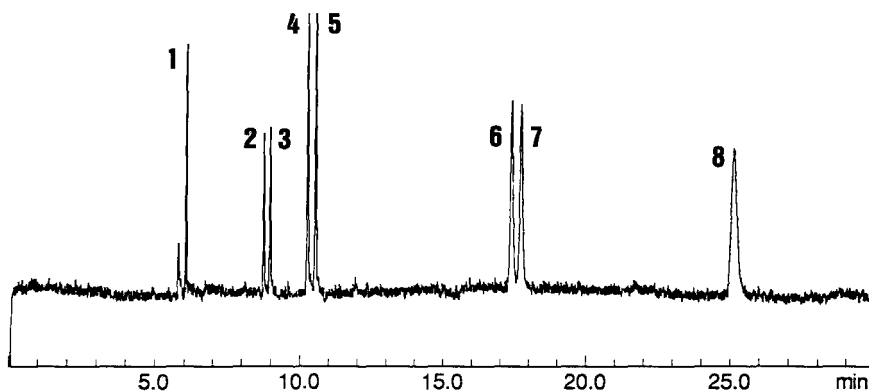


Figure 3. Electropherogram of the N-3,5-dinitrobenzoyl/methyl ester derivatives. Peaks: 1 = formamide (t_0), 2 = D-ALA, 3 = L-ALA, 4 = D-ABA, 5 = L-ABA, 6 = D-LEU, 7 = L-LEU, 8 = dodecanophenone(t_{MC}). Buffer : 50 mM N-dodecoxycarbonyl-(S)-valine, 25 mM borax/50 mM phoshate, pH 7.8. Column : 75 μ m I.D., 52/59 cm L. Applied voltage : 15 kV. Current : 81 μ A. Temperature : ambient. Detection : 214 nm.

Table 1. CE data for the benzoylated amino acid methyl esters.

Bz	t_R (min)	N	R_s	k'	α
t_0	6.06	166839		0	
D-ALA	9.86	193985		1.06	
L-ALA	9.86	193985	0	1.06	1.000
D-ABA	10.2	199440		1.19	
L-ABA	10.2	199440	0	1.19	1.000
D-LEU	13.6	187275		2.86	
L-LEU	13.85	294737	2.21	3.02	1.056
t_{MC}	24.09	101927		inf	
pNBz	t_R (min)	N	R_s	k'	α
t_0	6.16	165490		0	
D-ALA	8.44	231650		0.55	
L-ALA	8.53	235760	1.2	0.57	1.036
D-ABA	9.73	236093		0.92	
L-ABA	9.85	223762	1.52	0.96	1.043
D-LEU	16.24	183701		4.34	
L-LEU	16.47	166294	1.41	4.54	1.046
t_{MC}	26.13	64482		inf	
mNBz	t_R (min)	N	R_s	k'	α
t_0	5.94	163230		0	
D-ALA	8.00	252647		0.53	
L-ALA	8.12	251875	1.82	0.57	1.075
D-ABA	9.29	268078		0.94	
L-ABA	9.45	273299	2.27	1	1.064
D-LEU	15.48	246229		4.83	
L-LEU	15.77	208056	2.22	5.17	1.070
t_{MC}	23.21	105212		inf	
DNBz	t_R (min)	N	R_s	k'	α
t_0	6.05	151000		0	
D-ALA	8.74	248728		0.68	
L-ALA	8.95	249056	3.05	0.75	1.103
D-ABA	10.25	225613		1.17	
L-ABA	10.52	219476	3.12	1.27	1.085
D-LEU	17.37	158440		6.03	
L-LEU	17.71	150212	1.9	6.49	1.076
t_{MC}	25.19	72261		inf	

to the proposed model, the homochiral associations are more stable. This is in accordance with the results of NMR-studies of diastereomeric dimers of N-acetylvaline t-butyl esters (21). Similar elution orders have also been found with the related surfactant (N-dodecanoyl-L-valinate) and comparable amino acid derivatives (2,3).

The data obtained with the amino acid esters (Table 1) have been used to verify experimentally the MEKC-resolution equation (12). In MEKC, the contribution of the capacity factor and the elution range t_0/t_{MC} to resolution can be expressed as:

$$f_k = \frac{\tilde{k}'}{1 + \tilde{k}'} \cdot \frac{1 - \frac{t_0}{t_{MC}}}{1 + \frac{t_0}{t_{MC}} \cdot \tilde{k}'} \quad (\text{Eq.1})$$

For a pair of peaks, the corresponding value is given by:

$$f_k = \frac{\tilde{k}_2}{1 + \tilde{k}_2} \cdot \frac{1 - \frac{t_0}{t_{MC}}}{1 + \frac{t_0}{t_{MC}} \cdot \tilde{k}_1} \quad (\text{Eq.2})$$

The same term can also be evaluated indirectly:

$$f_k = \frac{R_s}{\frac{\sqrt{N_{av}}}{4} \cdot \frac{\alpha - 1}{\alpha}} \quad (\text{Eq.3})$$

The good agreement between the values obtained with Eq.3 and the curve obtained with Eq.1 is surprising (Figure 4). To the best of our knowledge, this is the first experimental and quantitative confirmation of the general MEKC-resolution equation. Although this result is purely academic, the situation as depicted in Figure 4 and representing real-life values, permits a short discussion on the limitations of capacity factor optimization in MEKC.

Ignoring very small and very large values, in the region around the optimal capacity factor, the gain in resolution contribution that can be expected will rarely exceed a factor 3; on the higher side it will even be less. This means that optimizing the separation in a situation where two peaks are just visibly starting to split ($R_s = 0.5$) to a full-baseline separation ($R_s = 1.5$) will be difficult to attain by just varying the surfactant concentration, unless the capacity factors are extremely small or

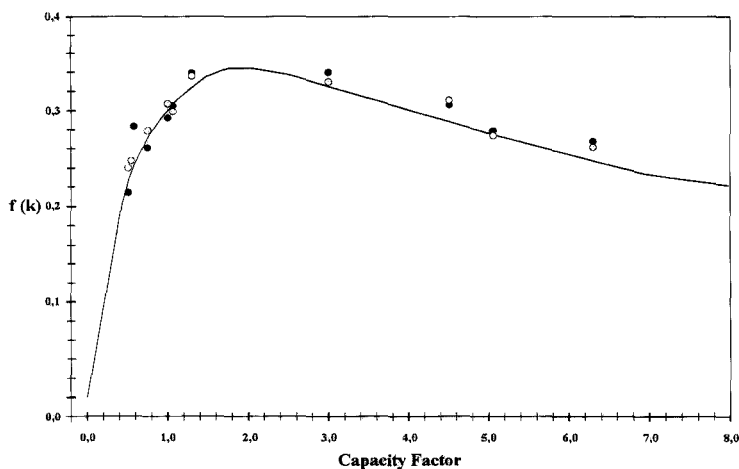


Figure 4. Experimental confirmation of the MEKC resolution equation.
Curve : theoretical values according to Eq. 1 (for $t_0/t_{MC} = 0.246$, this is the average value for all pooled experiments, which ranged from 0.235 to 0.256).
Open Symbols : f_k calculated according to Eq. 2 (these values were obtained by combining capacity factors and their corresponding t_0/t_{MC} and reflect the variability that can be expected around the curve which was calculated with an average t_0/t_{MC}).
Solid Symbols : observed values for f_k , according to Eq. 3.

large. Even in the latter case, it is doubtful whether it will be physically possible to adjust the phase ratio so that the capacity factor changes by more than one order of magnitude. On the lower side there is the limit posed by the CMC value, at the higher side the increase in concentration is limited by the increased current output.

ACKNOWLEDGEMENT

The authors like to thank Dr. J. Vindevogel for his help in the preparation of this manuscript, Waters for the gift of the chiral surfactant and the National Lottery, Belgium for financial support to our CE project. EVH thanks the IWT (Vlaams Instituut voor de bevordering van het Wetenschappelijk-Technologisch onderzoek in de industrie), Vlaanderen, Belgium for a study grant.

REFERENCES

1. E. Gassmann, J.E. Kuo and R.N. Zare, *Science* 230 (1985) 813.
2. P. Gozel, E. Gassmann, H. Michelsen and R.N. Zare, *Anal. Chem.*, 59 (1987) 44.
3. G.E. Barker, P. Russo and R.A. Hartwick, *Anal. Chem.*, 64 (1992) 3024.
4. R. Kuhn and S. Hoffstetter-Kuhn, *Chromatographia*, 34 (1992) 505.
5. I.E. Valko, H.A.H. Billiet, H.A.L. Corstjens and J. Frank, *LC.GC Int.*, 6 (1993) 420.
6. T.H. Bereuter, *LC.GC Int.*, 7 (1994) 78.
7. A. Dobashi, T. Ono, S. Hara and J. Yamaguchi, *J. Chromatogr.*, 480 (1989) 413.
8. A. Dobashi, T. Ono, S. Hara and J. Yamaguchi, *Anal. Chem.*, 61 (1989) 1984.
9. H. Nishi, T. Fukuyama, M. Matsuo and S. Terabe, *J. Microcol. Sep.*, 1 (1989) 234.
10. S. Terabe, M. Shibata and Y. Miyashita, *J. Chromatogr.*, 480 (1989) 403.
11. J.R. Mazzco, E.R. Grover, M.E. Schwartz and J.S. Petersen *J. Chromatogr. A*, 680 (1994) 125.
12. S. Terabe, K. Otsuka, K. Ichikawa, A. Tsuchiya and T. Ando, *Anal. Chem.*, 56 (1984) 111.
13. J.H. Aiken and C.W. Huie, *J. Microcol. Sep.*, 5 (1993) 95.
14. E. Van Hove and P. Sandra, *J. High Resolution Chromatogr.*, in press.
15. R. Szűcs, J. Vindevogel, E. Everaert, L. De Cooman, P. Sandra and D. De Keukeleire, *J. Inst. Brew.*, 100 (1994) 293.
16. R. Szűcs and P. Sandra, *J. High Resolution Chromatogr.*, submitted.
17. H. Nishi, N. Tsumagari and S. Terabe, *Anal. Chem.*, 61 (1989) 2434.
18. A.S. Cohen, S. Terabe, J.A. Smith and B.L. Karger, *Anal. Chem.*, 59 (1987) 1021.
19. Y.K. Yik and S.F.Y. Li, *Chromatographia*, 35 (1993) 560.
20. A.S. Cohen, A. Paulus and B.L. Karger, *Chromatographia*, 24 (1987) 15.
21. A. Dobashi and S. Hara, *J. Chromatogr.*, 349 (1985) 143.

Received: July 10, 1995

Accepted: August 6, 1995

PROTEIN-BASED CAPILLARY AFFINITY GEL ELECTROPHORESIS FOR CHIRAL SEPARATION OF β -ADRENERGIC BLOCKERS

HELÉN LJUNGBERG AND STAFFAN NILSSON*

*Department of Technical Analytical Chemistry
Chemical Center
University of Lund
P.O. Box 124
S-221 00 Lund, Sweden*

ABSTRACT

The proteins cellulase and bovine serum albumin (BSA) have in this study been cross-linked with glutaraldehyde to form a gel which has been used in capillary affinity gel electrophoresis (CAGE) to resolve enantiomeric pairs of β -adrenergic blockers. Both proteins have earlier been used as chiral selectors, especially in HPLC. We have utilized the major quantitatively cellulase, cellobiohydrolase I (CBH I) produced by the fungus *Trichoderma reesei*, in CAGE to separate enantiomers. Since it was difficult to obtain a stable gel with cellulase alone, we copolymerized it with BSA. With this cellulase/BSA gel we could resolve the optical isomers of the β -blocking drugs, *rac*-propranolol, *rac*-metoprolol, *rac*-pindolol and partially *rac*-atenolol. The used capillaries have an inner diameter of 75 μm , a total length of 23,5 cm and an effective length of 15,5 cm filled with gel to the detection window. The buffer used for separation was, 50 mM potassium phosphate buffer at pH 6.8 with 1% 2-propanol added as organic modifier. Samples were electrokinetically introduced and separated at a voltage of 3-3,5 kV. With

this study we want to propose a new model based on copolymerization of proteins, as chiral selectors, to create a gel which has the potential to resolve different types of chiral compounds in capillary affinity gel electrophoresis.

INTRODUCTION

During recent years, the enantiomeric composition of biologically active compounds have become increasingly important due to the different physiological activities/effects that can exist for drug enantiomers. A large interest for different analytical methods within the area of enantiomeric separation techniques has developed. For quite some time researchers have used proteins as chiral selectors for separating optical isomers within the field of chiral chromatography (1, 2). New techniques, such as capillary electrophoresis, have developed into a powerful tool for chiral separations since extremely high efficiency, short separation times, less material and chemicals are consumed. This can be of value in terms of cost and/or when a compound is available in limited amounts (3-7). Another substantial advantage is that only minute amounts of chemical waste is produced.

Two different proteins have been used in this study, cellulase and bovine serum albumin (BSA). Cellobiohydrolase I (CBH I) is the major quantitatively cellulase produced by the fungus *Trichoderma reesei*. The three-dimensional (3D) structure has recently been determined and refined to 1,8 Å resolution by X-ray crystallography. The enzyme contains a 40 Å long tunnel which is thought to be part of the active site (8) where the enantioselection also are thought to take place. Both CBH I, an acidic glycoprotein, and BSA, a globular plasmaprotein, or parts of them, are well known to discriminate between enantiomers. These proteins have earlier been used as chiral stationary phases by bonding (9-11) or adsorbing BSA (12) to silica. In a recent work, CBH I has been used in liquid chromatography (13) and in free solution as an

enantioselective protein in high performance capillary electrophoresis, providing chiral selectivity for some β -blocking drugs (14).

In this study we have used BSA to create a gel which can copolymerize or possibly entrap or hold another protein, CBH I, in a gel-network formed with glutaraldehyde as a crosslinker. BSA has been used earlier, as a model protein for capillary affinity gel electrophoresis (15). However, here we propose a new approach to copolymerize CBH I with another protein, BSA, within a closed network, in order to resolve the enantiomers of the β -adrenergic blockers. The advantages with this mild crosslinking is that the 3D-structure of the selector is kept intact, which is favourable for chiral recognition and separations. Conformational changes seem to be minimized and the chiral selector is more available and stable for interactions with the sample molecules.

MATERIALS AND METHODS

Apparatus.

The experiments were performed with the capillary electrophoretic system from Beckman Instruments Inc., P/ACE 2050 Series, controlled by P/ACE Version 3.0 software and an on-capillary UV-absorbance detector set at 214 nm (Palo Alto, CA, USA). To fill the capillary with the gelation mixture we used a Minipuls peristaltic pump from Gilson (Gilson Medical Electronics, Villiers le Bel, France) with a FloRated, PVC pump tubing 0.015 cc/min Lot. No.:K 1652 6 from Interlab (Westboro, MA, USA).

Material and reagents.

Fused-silica capillary tubing with an internal diameter of 75 μm and an outer diameter of 375 μm was from Polymicro Technologies

(Phoenix, AZ, USA). For the separations we used capillaries with a total length of 23,5 cm and 16,5 cm to the detection window. Bovine serum albumin (BSA), cellulase from *Trichoderma reesei*, (R)-, (S)-, *rac*-propranolol and *rac*-pindolol were obtained from Sigma (St. Louis, MO, USA). *rac*-atenolol (Batch 900232), *rac*-metoprolol (Batch 76029001) from Leiras (Åbo, Finland) and (S)-metoprolol (H 150/65) Batch No H 18 was a kind gift from Astra Hässle (Möln dal, Sweden). 2-propanol, 85% phosphoric acid, sodium citrate and tri-potassium-phosphate-7-hydrate were purchased from Merck (Darmstadt, Germany). Glutaraldehyde, 50%, was bought from Fluka (Buchs, Switzerland). Buffer and sample solutions were prepared from MilliQ water. All solutions were degassed (with helium or ultrasonication) and filtered (0,2 μm DynaGuard ME, Microgon Inc., Laguna Hills, California, USA) before use.

Procedure.

Preparation of cellulase/BSA gel filled capillaries. The on-capillary detection window was prepared 7 cm from outlet end of the capillary, by quickly flaming approximately a 1 cm segment of the polyimide coating, which normally protects the fused silica capillary. The capillary is filled with gelation mixture following the procedure described below (summarized in figure 1). It was first washed with 0,1 ml each of water, 1 M NaOH, water and finally 50 mM sodium-citrate buffer pH 5.0 by flushing it with a syringe. The capillary was then connected to the peristaltic pump. To estimate the capillaries filling time, with the gel mixture up to the the previously made detection window, the capillary was emptied by air injection. Refilling was timed by following the liquid air interface movement. Gelation mixture was prepared of 5 parts 20% (w/v) BSA in water, 21 parts 20 % (w/v) cellulase in 50 mM sodium-citrate buffer pH 5.0 and mixed with 4 parts 50 % glutaraldehyde, in an Eppendorf vial and then the buffer containing capillary was immediately

PREPARATION OF CELLULASE/BSA-GEL FILLED CAPILLARIES

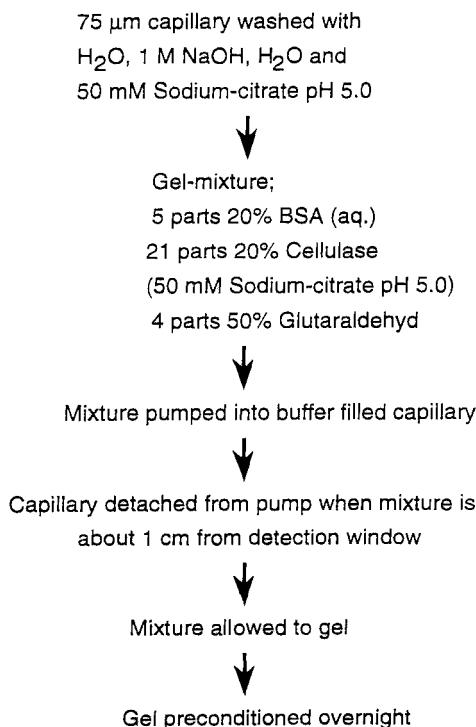


Figure 1. Flow diagram for preparation of gel filled capillaries.

filled. When the mixture had reached approximately 1 cm up to the detection window the filled capillary was disconnected, the pumping tube was snipped with a pair of scissors. Thus, the detection window region of the capillary contained phosphate buffer and not protein gel. After this, the gel filled capillary was placed flat on the bench for gelation. The ends were sealed with (children's) clay preventing the gel to dry out. Before

the capillary was mounted into a Beckman cartridge and preconditioned, it was carefully inspected under a microscope to make absolutely sure that no air bubbles were trapped in it.

Electrophoretic procedure. The gel filled capillary was preconditioned overnight by applying a potential of 2 kV, current limitation was 20 μ A, with the cathode placed at the injection side (reversed polarity). During this time, the buffer was changed to 50 mM phosphate pH 6.8 with 1 % (v/v) 2-propanol. Electrophoresis of the samples were then performed with the anode at the injection side (normal polarity). Samples were electrokinetically introduced, 2 kV, 3 seconds, containing a buffer with half the ionic concentration of the running buffer. The conditions to perform the electrophoresis were, the voltage were varied from 2-7 kV, the gel length was normally 15,5 cm and the total capillary length 23,5 cm, running buffer used was 50 mM potassium phosphate pH 6.8 supplemented with different concentrations of 2-propanol.

RESULTS AND DISCUSSION

Protein-gel preparation.

Various experiments were made to select the proper conditions for making the protein-gel. Initially we simply started by mixing a few drops protein solutions with different concentrations, buffers and glutaraldehyde on open glass ware. With BSA we were able to obtain gelation under several different conditions. It was on the other hand rather difficult to find the proper conditions to obtain a stable gel with cellulase. Instead, a mixture of cellulase and BSA was used and a stable gel could easily be prepared. Conditions were selected to minimize the amount of BSA, in combination with an excess of cellulase. It was found that a stable opaque gel could be formed with 3,3 % (w/v) BSA and 14 % (w/v)

cellulase as final protein concentrations. Gelation was then performed in Eppendorf vials and a stable gel formed in about 3 minutes which gave enough time for filling the capillaries. The capillaries were prepared and filled as described earlier.

Electrophoresis.

Preconditioning. Before use the capillaries were conditioned with reversed polarity. This procedure was established for eliminating dissolved air which often are formed during the capillary filling and/or gelation, if the reversed polarity is used the air bubbles will not be trapped, in the interface between the gel and the buffer. Another reason for reversed polarity, is that non-bound cellulase can be detected as it passes towards the anode during equilibration of the CAGE-capillary, since it carries a net negative charge at pH 6,8. When the UV absorbance was stable the unbound protein has been removed and stable conditions for separation were obtained.

Sample injection. Electrokinetic injection technique was used (2 kV, 3 sec) to introduce the samples. The samples were dissolved in the running buffer, diluted once with water to develop a sharp sample enrichment zone to enhance efficiency (15).

Separation of the enantiomers of β -adrenergic blockers in cellulase/BSA-gel with capillary affinity gel electrophoresis. At pH 6,8 the basic β -adrenergic blockers used in this study all carries a positive charge (pKa above 9) and migrates towards the cathode. We were able to obtain a chiral separation of *rac*-propranolol with CAGE based on cellulase/BSA stationary phase. The electropherogram in figure 2a represent the resolution of 0,5 mM *rac*-propranolol, R- and S-forms were used for verification, (fig 2b,c), although they were not 100 % enantiopure (personal communication with Lars I. Andersson at Astra Pain Control, Sweden). A constant voltage of 3,5 kV was applied giving a stable

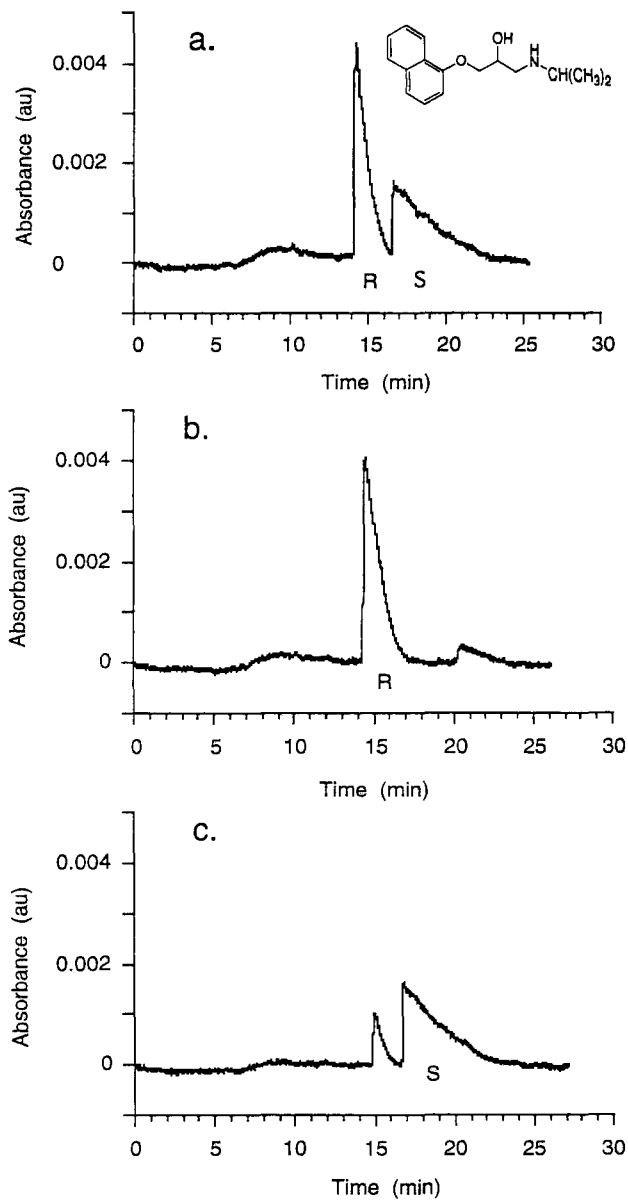


Figure 2. Capillary affinity gel electrophoretic separation of *rac*-propranolol with cellulase/BSA gel. **a.** 1 mM *rac*-propranolol. **b.** 0,5 mM R-propranolol. **c.** 0,5 mM S-propranolol. Conditions: constant applied electric field 3,5 kV (~150 V/cm), 45 μ A; gel length=16.5 cm, total length=23.5 cm; buffer 50 mM potassium phosphate pH 6.8 with 1 % (v/v) 2-propanol; sample injection 2 kV, 3 s.

current of 45 μ A and as a running buffer 50 mM phosphate pH 6.8 with addition of 1% 2-propanol was used. Higher theoretical plate number and some improvement of the separation was achieved if the 2-propanol concentration was raised to 25 % and the constant voltage applied was increased to 7 kV (data not shown). However, under these separation conditions the protein gels were not stable. Therefore, it is preferable if the electrophoresis can be performed under milder conditions. Still the separation is performed within reasonable time. To investigate if it was possible to resolve other β -blocking agents under these milder conditions (3,5 kV), separation of metoprolol, pindolol and atenolol were tested.

The electropherograms in figure 3a represent the resolution of *rac*-metoprolol. The enantiomers has been completely resolved and verified with the (S)-metoprolol (fig 3b). Shorter retention times were achieved, than for *rac*-propranolol, likely according to less hydrophobic interaction with the chiral stationary phase.

In figure 4 *rac*-pindolol has been separated. The loading capacity of the protein-gel capillary was studied by resolving different concentrations of *rac*-pindolol, using UV-detection at 214 nm, 75 μ m inner diameter and 23.5 cm long capillary. The limit of detection (LOD) was estimated to 10 μ M defined as a peak height larger than twice the noise. The upper concentration limit was 1 mM accepting a resolution of, $R=1$ where $R=\Delta V_{RS}/(W_R+W_S)$ and ΔV_{RS} = difference in elution volume of the R- and S-forms, W_R and W_S equals peak width at the inflection points. Thus, the range of sample concentration separated and analyzed was 0.01-1 mM which is a considerable improvement compared to the previous report (15) although seven times higher concentration of the chiral selector was used in this study.

A very promising split in the electropherogram was obtained for *rac*-atenolol as shown in figure 5. The same separation conditions as described earlier, was used. However, no further attempts were tried to resolve this enantiomeric pair, since that was beyond the intention of this study.

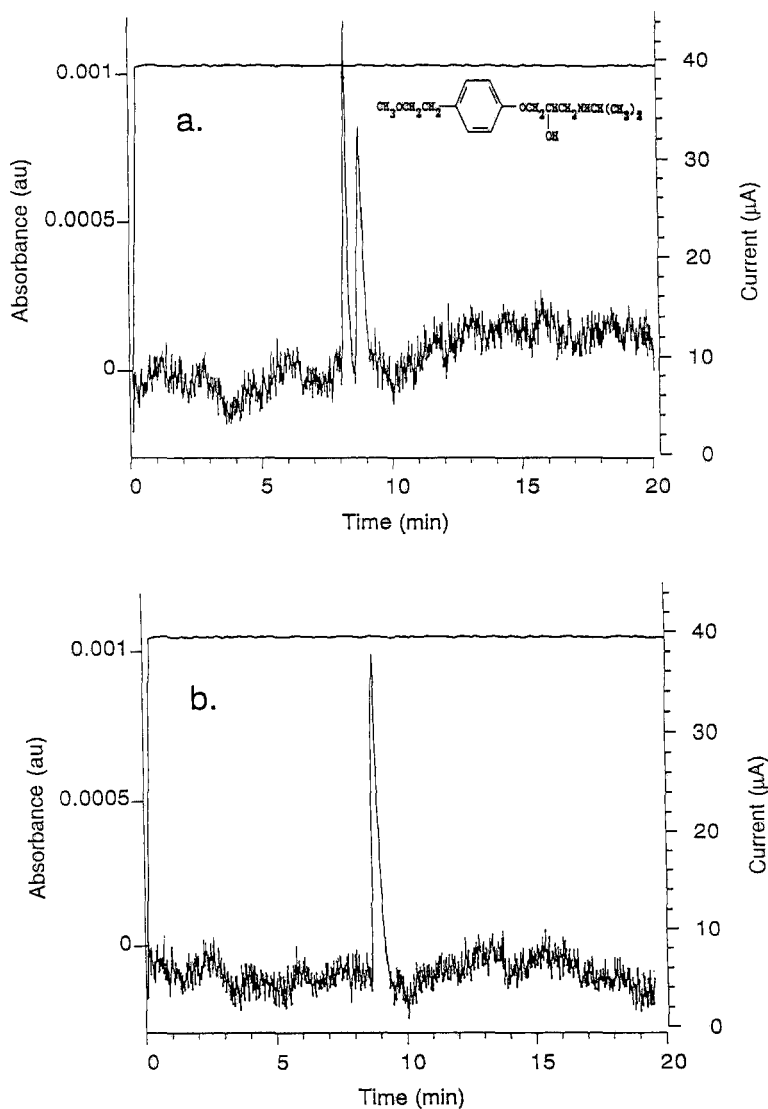


Figure 3 Capillary affinity gel electrophoretic separation of *rac*-metoprolol with cellulase/BSA gel. **a.** 0,15 mM *rac*-metoprolol **b.** 0,075 mM *S*-metoprolol (Identification of racemate.). Conditions: constant applied electric field 3 kV (~ 130 V/cm), 40 μA ; gel length=16.5 cm, total length=23.5 cm; buffer 50 mM potassium phosphate pH 6.8 with 1 % (v/v) 2-propanol; sample injection 2 kV, 3 s.

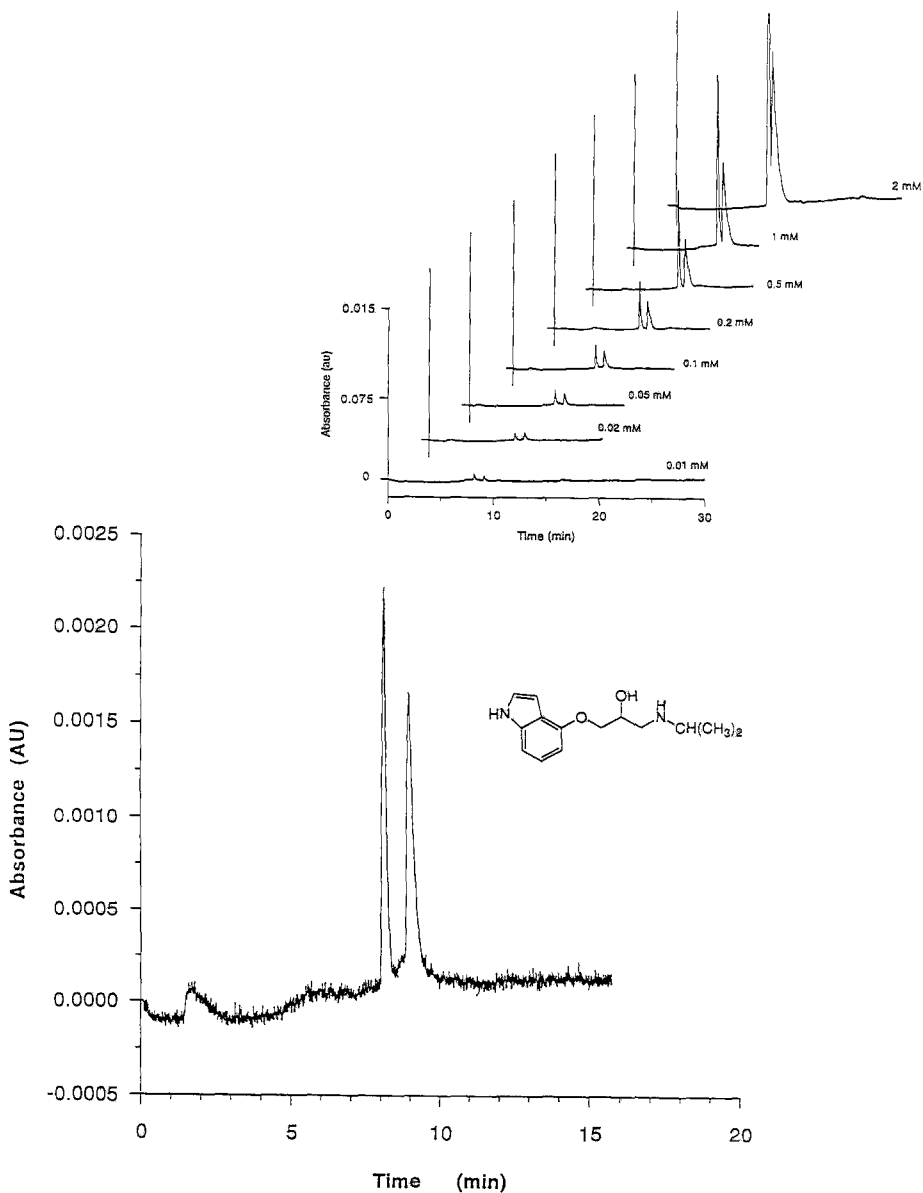


Figure 4. Capillary affinity gel electrophoretic separation of 0,1 mM *rac*-pindolol with cellulase/BSA gel. Insert: Sample loading capacity 0.01-2 mM. Conditions: constant applied electric field 3.5 kV (~150 V/cm), 45 μ A; gel length=16.5 cm, total length=23.5 cm; buffer 50 mM potassium phosphate pH 6.8 with 1 % (v/v) 2-propanol; sample injection 2 kV, 3 s.

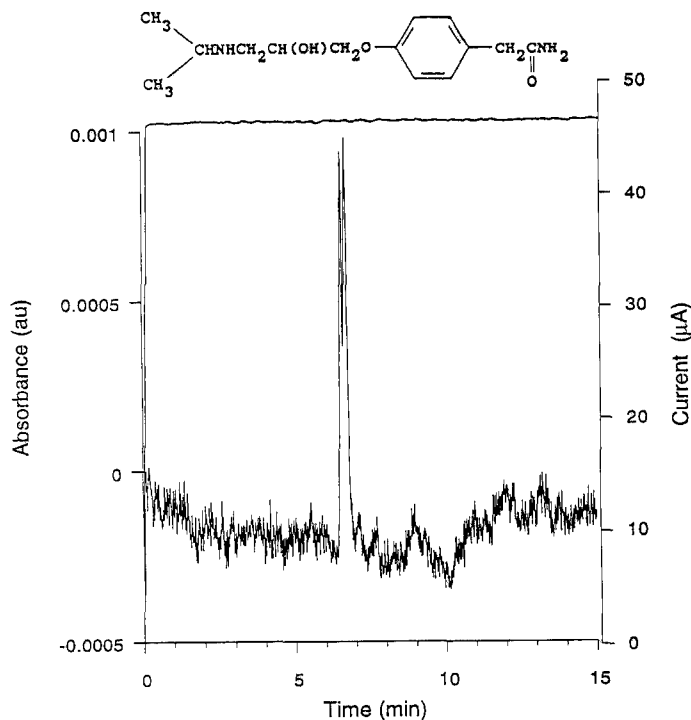


Figure 5. Capillary affinity gel electrophoretic separation of 0,05 mM *rac*-atenolol with cellulase/BSA gel. Conditions: constant applied electric field 3.5 kV (~150 V/cm), 47 μA; gel length=16.5 cm, total length=23.5 cm; buffer 50 mM potassium phosphate pH 6.8 with 1 %(v/v) 2-propanol; sample injection 2 kV, 3 s.

Further improvement of the separations of *rac*-propranolol and *rac*-atenolol as well as resolving other enantiomeric pairs of β-blocking drugs, will be attempted with this selector in a more comprehensive study. Developing studies will also include the addition of other proteins into the gels and by doing so possibly create other chiral phases which can be used for enantiomeric separations of many different kinds of compounds, in the same capillary.

ACKNOWLEDGMENTS

We gratefully acknowledge the financial support from the Crafoord Foundation, Carl Tryggers Foundation, Magnus Bergwall Foundation, the Royal Physiographical Society of Lund and the Swedish National Science Research Council. I thank Maria Petersson for introducing the P/ACE Beckman System (HL).

REFERENCES

1. W. Lindner. *Chromatographia*, 24: 97-107 (1987).
2. S. G. Allenmark, S. Andersson. *J. Chromatogr.* 666: 167-179 (1994).
3. W. G. Kuhr. *Anal. Chem.* 62: 403R-414R (1992).
4. W. G. Kuhr, C. A. Monning. *Anal. Chem.* 64: 389R-407R (1992).
5. C. A. Monning and R. T. Kennedy. *Anal. Chem.* 66: 280R-314R (1994).
6. T. J. Ward. *Anal. Chem.* 66: 633A-640A (1994).
7. J. Yang and D. S. Hage. *Anal. Chem.* 66: 2719-2725 (1994).
8. C. Divne, J. Ståhlberg, T. Reinikainen, L. Ruohonen, G. Pettersson, J.K. Knowles, T.T. Teeri and T.A. Jones. *Science* 265: 524-528 (1994).
9. P. Erlandsson, S. Nilsson. *J. Chromatogr.* 482: 35-51 (1989).
10. S. Andersson, S. Allenmark, P. Erlandsson, S. Nilsson. *J. Chromatogr.* 498: 81-91 (1990).
11. I. Marle. Proteins as chiral selectors in liquid chromatography. PhD Dissertation, University of Uppsala, 1994. ISBN:91-554-3153-4

12. P. Erlandsson, L. Hansson, R. Isaksson. *J. Chromatogr.* 370: 475-483 (1986).
13. J. Mohammad, Y. Li, M.El-Ahmad, K. Nakazato, G.Pettersson S. Hjertén. *Chirality* 5: 464-470 (1993).
14. L. Valtcheva, J. Mohammad, G. Pettersson, S. Hjertén. *J. Chromatogr.* 638: 263-267 (1993).
15. S. Birnbaum, S. Nilsson. *Anal. Chem.* 64: 2872-2874 (1992).

Received: July 10, 1995

Accepted: August 6, 1995

A SCREENING PROTOCOL FOR THE DIRECT DETERMINATION OF LOW PPB LEVELS OF URANYL CATION USING ARSENAZO III AND CAPILLARY ELECTROPHORESIS

B. A. COLBURN¹, M. J. SEPANIAK¹, AND E. R. HINTON²

*¹University of Tennessee
Chemistry Department
Knoxville, Tennessee 37996-1600
²Lockheed-Martin Energy Systems
Analytical Services Organization
Oak Ridge, Tennessee 37831-8189*

ABSTRACT

Capillary electrophoresis is used as a screening protocol for the determination of uranyl ion complexed with Arsenazo III. Long sample plugs are injected and stacked to narrow zones. Capillary column inner diameter, running buffer constituents and concentrations, effective column length and injected sample plug length are optimized and discussed. A limit of detection of 10 ppb is achieved with a linear dynamic range of nearly 3 orders of magnitude in concentration injected. Analytical figures of merit are presented and river water samples are analyzed.

INTRODUCTION

There is interest in the geological, environmental and bioassay fields in a fast and simple analysis tool for uranium due to its presence in water and various mineral samples (1). The toxicity of uranium and its common use in nuclear power stations and nuclear weapons creates the need for a cost effective analysis method (2). Numerous methodologies have been developed for the analysis of uranium including time resolved laser fluorescence (1,3-5), isotope dilution mass spectrometry (6), laser ablation - inductively coupled plasma atomic emission spectrometry (7), and flow injection analysis (8). Most of these are expensive, time consuming and instrumentally complicated. Simpler methods have been effective which depend on spectrophotometry and require the use of masking agents or a separation such as HPLC, ion chromatography or extraction; however, most of these methods use large volumes and are slow (5,9-15).

Capillary electrophoresis (CE), with its high efficiency, speed and small sample and reagent volume requirements, can be more cost effective and time efficient than the aforementioned methodologies. The small capillary diameters are very effective in dissipating Joule heating; thus, large fields can be used to decrease the separation time and the plug-like flow leads to highly efficient separations. Over the past few years, CE has become a very useful separation tool. The high efficiency and speed make it an ideal choice for many applications. However, the diminutive size of the capillary diameter results in poor concentration detectability (9,16-19). Several approaches have been utilized to improve detection limits including sample pre-concentration and non-traditional capillary or detector cell geometry (19,20). Furthermore, sensitive detection methods

such as radiochemistry, fluorescence or electrochemistry have been utilized in an effort to improve CE detection limits (19,20).

Sample stacking is one of the simplest ways to concentrate a sample and improve detectability. In this approach, the analyte is dissolved in either water or low ionic strength buffer and a very large sample volume is injected. The lower ionic strength in the sample region results in a higher field. Thus, the sample ions in the injected volume will migrate at a high velocity. As the sample ions encounter the interface between the sample and relatively high ionic strength running buffer, velocity is reduced due to the presence of a lower field within the running buffer. This causes the analytes to stack into a narrow band. Subsequently, the analytes are separated by free solution CE (16-19). Both anions and cations can be analyzed by this technique. However, field inhomogeneities between the sample plug and the running buffer causes the electroosmotic flow velocity (v_{eo}) to be different between the two regions. This produces a hydrostatic pressure, resulting in a parabolic flow profile which can broaden the solute band and negate the concentrating effect. Longer sample plug lengths or greater disparity between the sample and running buffer ionic strengths will augment the dispersive effects of parabolic flow; thus, an optimum exists between sample stacking and the deleterious effects of band broadening (16-18). Reference 19 is a good general review article concerning stacking and other methods of sensitivity enhancement. Reference 16 provides a mathematical treatise of stacking.

A variety of reagents can be used to form a complex with U(IV) or U(VI) for use in spectrophotometric analyses including PAR, PAN, malachite green and Arsenazo III

(2,14,21-23). Arsenazo III is the most widely used reagent for the determination of uranium. There is a large red shift (about 140 nm) in the lowest energy absorbance band of free Arsenazo III when it forms a metal complex. Thus, excess Arsenazo III present in the system will have a very low background at the complex maximum (2,5,12,13,21-23). Typical spectra appear in Figure 1. Unfortunately, Arsenazo III is not selective and forms complexes with many other metals such as Th, Zr, rare earths, Ba, Sr, S, Pd, Sc, Pb, Fe III, Cu, Ca, Al (12,13,21-23). Solution pH plays an important role in complex formation; the optimum for uranyl ion - Arsenazo III formation is pH 1-4. At these moderately low pH values, some of the aforementioned metals do not form complexes. However, the general lack of selectivity still renders a separation necessary.

The method presented herein uses field amplified CE (18,24) for a fast, simple and sensitive determination of the uranyl cation. A wide variety of experimental parameters are assessed and discussed. These include capillary column inner diameter (i.d.), effective column length (L_{eff}), running buffer composition and concentrations and sample plug lengths. Analytical figures of merit and analyses of local water samples are presented.

EXPERIMENTAL

Concentrated stock solutions of uranyl nitrate hexahydrate (Mallinckrodt, Paris, KY) and 2,2'-(1,8-dihydroxy-3,6-disulfonaphthylene-2,7-bisazo) bisbenzenearsonic acid (Arsenazo III) (Aldrich, Milwaukee, WI) were made in water and diluted to the appropriate concentration as desired. Sodium phosphate, sodium borate,

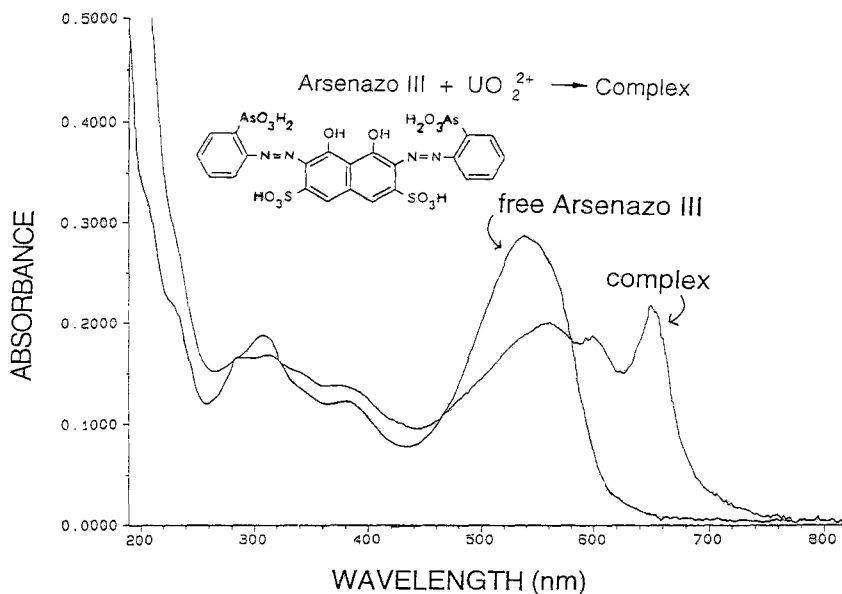


FIGURE 1: Absorbance spectra of (a) free Arsenazo III and (b) Arsenazo III-uranyl complex.

sodium chloride, perchloric acid and methanol were obtained from Sigma (St. Louis, MO) and utilized as needed. Distilled water was purified by a Millipore MilliQ filter (Bedford, MA).

The experimental apparatus has been described in detail elsewhere (25). Briefly, an SSI (Science System Inc., State College, PA) model 504 absorbance detector was used at 650 nm. Fused silica capillaries (50, 75 μm i.d., 360 μm o.d.) were obtained from Polymicro Technologies, Inc. (Phoenix, AZ) and extended light path capillaries (ELP) (25 μm i.d. with 125 μm window, 360 μm o.d.) were purchased from Hewlett Packard (Palo Alto, CA). Running voltages were provided by a Hipotronics (Brewster, NY) high voltage power supply. Electropherograms were recorded using a chart recorder and

a PE Nelson integrator Model 1020 S (Perkin-Elmer Corp, Cupertino, CA).

Prior to initial use, each column was pre-treated by sequentially washing the capillary with 10 mM NaOH, water, 10 mM HCl and water at 20 minutes each. The column was then filled with the running buffer and electrokinetically pumped for 20 minutes to equilibrate the column. Hydrostatic injections were made by elevating the column inlet for a given time. Once an injection was performed, the capillary was returned to the running buffer vial and a negative voltage was applied for the separation (cathodic inlet, anodic outlet). The injected plug length was estimated by determining the linear velocity of the sample during the injection process (v_{inj}). This was accomplished by continuously injecting a Arsenazo III - uranyl complex. Linear velocity is then given by L_{eff}/v_{inj} . The following rinse procedure was utilized between separations: 5 minutes 10 mM NaOH, 3 minutes water, 2 minutes running buffer.

The samples used in this work contained uranyl cation, 0.1 mM Arsenazo III, and 0.1 mM HClO₄ diluted to volume with water. When the running buffer contained methanol, the sample also contained 10% methanol.

RESULTS AND DISCUSSION

Stacking Mechanism

In this method for uranyl ion analysis, relatively long sample plugs (between 1-8 cm) were injected and subsequently stacked in a manner similar to that described by Chien and Burgi (17-19,24). The negatively charged complex has an electrophoretic velocity greater in magnitude

and opposite in direction than the v_{e0} . Thus, the sample buffer is backed out into the running buffer reservoir as the analyte stacks at the moving boundary between the sample and running buffer. This is depicted in Figure 2.

In the experiment depicted in Figure 2, a long sample plug (13 cm) was injected and a negative voltage was applied. A very long sample plug was utilized to elucidate the stacking mechanism. This long sample plug may overload the system and contribute to the triangular shape of the second peak in the electropherogram shown in Figure 2e. The effective column length was only 9 cm; therefore, the sample extended past the detector at the time the voltage was applied (see Figure 2a). Initially, the field and hence the v_{e0} within the sample zone is greater than in the running buffer due to the lower ionic strength in the sample (see Running Buffer Optimization below). However, the net velocity of the complex is greater than the v_{e0} and sample ions begin to migrate towards the anode and stack at the running buffer - sample interface.

The inhomogeneity of the v_{e0} between the two zones causes a hydrostatic pressure to form (see Figure 2b). The velocity due to this hydrostatic pressure makes up the difference between the two v_{e0} s. The analyte stacks at the boundary while the hydrostatic pressure and v_{e0} push the sample plug toward the capillary inlet. The injection plug length decreases and its ionic strength increases causing the field to decrease in the sample zone. Thus, the velocities of both the v_{e0} and complex decrease in the sample zone and increase in the running buffer region. The complex tries to migrate against the v_{e0} but is unable to do so in the running buffer due to the hydrostatic flow. The portion of the sample which extended beyond the detector is swept quickly past the detector as shown by the first peak (at approximately 30

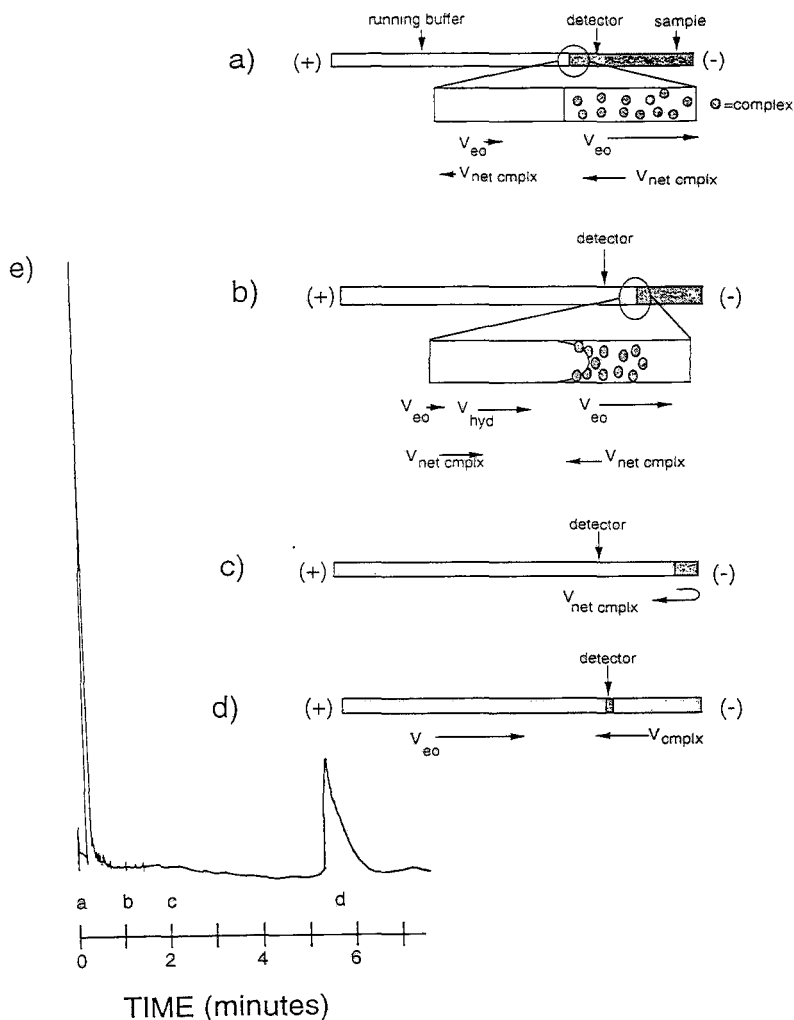


FIGURE 2: Depiction of the stacking mechanism: (a) voltage initially applied, (b) analyte stacking and removal of sample buffer, (c) equilibration of the v_{eo} within the running buffer and sample zones: analyte reverses direction, (d) stacked analyte passes the detector, (e) electropherogram from this experiment. Experimental conditions: $L_{eff} = 9$ cm, i.d. $50 \mu\text{m}$, applied field of 375 V/cm, injected plug length of 13 cm. See Table 1 for running buffer composition.

sec) in the electropherogram resulting from this experiment (Figure 2e).

By the time the sample plug nearly reaches the end of the column (Figure 2c), the hydrostatic pressure has diminished and the v_{e0} s of the sample and running buffer zones have become nearly equal. The analyte is now able to migrate against the v_{e0} (i.e., it reverses direction) and eventually migrates past the detector (Figure 2d). Considering the complexity of these electrophoretic processes, it is not surprising that the analyte band is asymmetric and not particularly efficient (see Figure 2e). In this experiment using a very short effective capillary, the Arsenazo III system peak and the complex show no separation (see below).

System Peak

Typical electrophoretic peak profiles are presented in Figure 3 in which the analyte appears as a shoulder on the system peak. Resolution between the system peak and the shoulder is dependent on the L_{eff} and is discussed below. A capillary with $L_{eff} = 40$ cm is used for this experiment. To assure complete complexation of uranyl ion and any interfering metals present, excess Arsenazo III is added to the sample. Arsenazo III is negatively charged and exhibits a mobility only slightly greater than that of the uranyl ion - Arsenazo III complex. Although the absorbance of free Arsenazo III at 650 nm is minimal (Figure 1), stacking increases the concentration sufficiently to generate the system peak illustrated in Figure 3a. The shoulder on the system peak (uranyl ion - Arsenazo III complex) grew with the concentration of the uranyl cation in the sample until it swamped out the system peak.

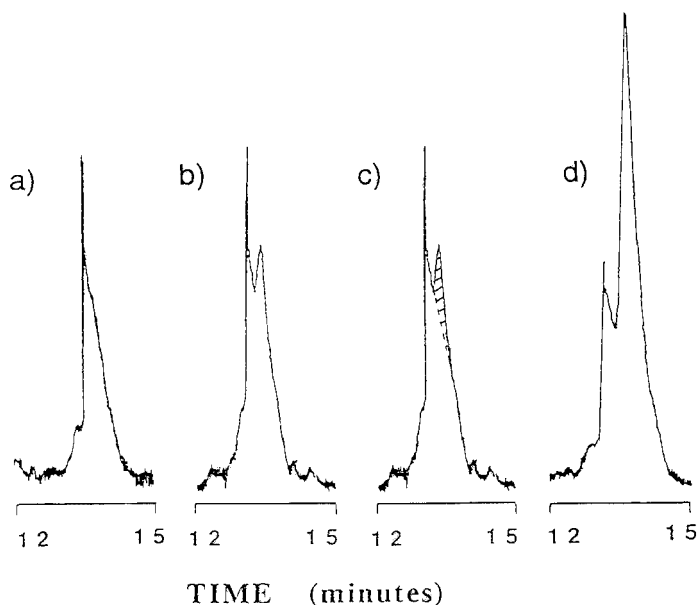


FIGURE 3: Electrophoretic peak profiles: (a) system peak, (b) 25 ppb injected uranyl complex, (c) 25 ppb injected uranyl complex with analyte peak shaded, (d) 200 ppb injected uranyl complex. See Figure 2 for experimental conditions.

Many approaches were attempted to minimize the contribution of the system peak by increasing efficiency, improving the resolution between the system and analyte peaks, or decreasing the magnitude of the system peak. One approach was to improve efficiency by increasing the stacking effect. Increasing the difference in ionic strength between the sample and the running buffer will enhance the stacking phenomenon. Unfortunately, at some point, band broadening from hydrostatic flow became excessive. Moreover, as the running buffer ionic strength was increased, efficiency decreased due to Joule heating. Another approach

was to adjust system retention to increase resolution. Methanol was added to both the sample and the running buffer to decrease Joule heating (increase efficiency) and to slow v_{e0} so that slight differences between the mobilities of the system peak and the analyte peak could be enhanced leading to improved resolution. Unfortunately, this had minimal effect on efficiency and resolution. The concentration of Arsenazo III in the running buffer did not have a noticeable influence on the magnitude of the system peak. Ultimately, it was determined the resolution between the system and analyte peaks appeared to be best when longer columns were used (see "Optimum Column Length and Injection Plug Length" below).

Running Buffer Optimization

Optimum running buffers had to be determined for each column i.d. Each buffer consisted of Arsenazo III, perchloric acid, sodium phosphate, sodium borate and sodium chloride in various concentrations. Methanol was also included on occasion.

A common CE buffer (26,27) of sodium phosphate and sodium borate was included in each running buffer. However, the concentration usually used (10 and 6 mM, respectively) interfered with the complex formation between Arsenazo III and UO_2^{2+} . A tenfold decrease in concentration (i.e., 1 and 0.6 mM, respectively) appeared to cause no interference, as determined by UV/Vis spectrophotometry, and was thus used in all experiments. An acidic medium is required for the formation of the Arsenazo III - uranyl complex and there was little difference in the absorbance of the complex between 10 and 100 mM $HClO_4$. Thus, the 10 mM concentration was included in each running buffer resulting in a pH of 2.7.

Arsenazo III and sodium chloride were doped into the running buffer to prevent complex dissociation and to improve stacking. However, excessive amounts of Arsenazo III resulted in a high optical background while high salt concentrations produced excessive Joule heating. Therefore, an optimum concentration of each component was determined. These optimum concentrations varied with the i.d. of the capillary. Smaller diameter capillaries were able to tolerate higher salt concentrations and dissipate the heat generated better than larger capillaries. Two concentrations of Arsenazo III were tested for each column i.d. - 0.01 mM and 0.1 mM for column i.d.s of 75, 50, and 25 (ELP) μm . For the 75 μm i.d. column, sodium chloride concentrations of 10, 50, and 75 mM were added to each Arsenazo III concentration. For the 50 and 25 (ELP) μm i.d. column, salt concentrations of 50, 75, and 100 mM were tested. Once it was determined that 0.1 mM Arsenazo III was best for the ELP capillary, additional salt concentrations of 125, 150, and 200 mM were also used. Table 1 lists the optimum Arsenazo III and sodium chloride concentrations for each column with approximate limits of detection (LODs) as experimentally determined. It is unknown why the optimum Arsenazo III concentration varied with the capillary employed. The optimum salt concentration varied as expected; that is, smaller i.d. capillaries tolerated higher salt concentrations. In each case, the thermal load is near the limit of causing significant thermal dispersion (28).

By adding methanol to the running buffer, the current could be reduced and higher fields could be employed to reduce separation time. The LODs represent a signal/noise (S/N) of 3 as described below. The LODs follow a trend opposite to that expected; the shortest optical path length has the best LOD and the longest optical path length has the

TABLE 1
Optimized Running Buffers^a

Column (μm)	Arsenazo III (mM)	NaCl (mM)	L_{eff} (cm)	LOD (ppb)	Thermal load (W/m)	Mobility (cm/min)
75	0.01	50	40	33	0.96	1.8
50 ^b	0.01	75	31	25 ^c	1.3	2.3
25 ELP	0.1	150	50	100	1-1.3	4.3

a All running buffers include 10 mM HClO_4 , 1 mM sodium phosphate, and 0.6 mM sodium borate

b Optimum running buffer included 10% MeOH

c Approximate LOD in a $L_{\text{eff}} = 31$ cm column. Can detect 10 ppb in a $L_{\text{eff}} = 50$ cm column.

worst LOD. This is probably an outcome of the complicated stacking process and the presence of the only partially resolved system peak.

Sensitivity and Detectability

Due to the presence of the system peak (Figure 3a), determination of the peak area was complicated. As shown in the figure, the peak shape changes with concentration. At low levels of analyte, the complex peak is a shoulder on the system peak. This is shown for a 25 ppb UO_2^{2+} profile in Figure 3b and the appropriate portion shaded in for Figure 3c. As the analyte concentration increases, the shoulder grows as shown in Figure 3d. From 25 - 100 ppb, the area of the individual peak was determined by manually skimming the tail of the system peak (see Figure 3c). For higher concentrations, the average blank signal was subtracted from

the total peak area to determine the peak area of the complex.

A reproducibility study was conducted by injecting the blank and a 25 ppb UO_2^{2+} solution six times in a $L_{\text{eff}} = 31$ cm, 50 μm i.d. capillary and performing the separation. The average peak area of the blank was 44 arbitrary units with a coefficient of variation (CV) of 8.5%. The average peak area of the 25 ppb UO_2^{2+} peak, skimmed from the system peak as shown in Figure 3c, was 1.9 arbitrary units with a CV of 51%. A CV of 50% corresponds to a S/N of 3 (29). Thus, the LOD for this system is very close to 25 ppb. Lower concentrations can be detected if longer columns are used to improve resolution; however, separation time increases. Although a reproducibility study was not performed by using a longer column ($L_{\text{tot}} = 60$ cm, $L_{\text{eff}} = 50$ cm), 10 ppb could be seen as a shoulder as easily as the 25 ppb peak could be seen in the shorter column. Thus, the LOD in the longer column is approximately 10 ppb.

A calibration curve was constructed from duplicate injections that exhibited a linear dynamic range of 2.8 orders of magnitude in concentration injected (see Figure 4). This linear dynamic range may be extended by increasing the concentration of Arsenazo III in the sample. However, increasing the Arsenazo III concentration in the sample will increase the system peak.

Optimum Column Length and Injection Plug Length

In screening applications, rapid separation times are necessary to increase throughput. In this study, longer column lengths have better resolution and LODs at the

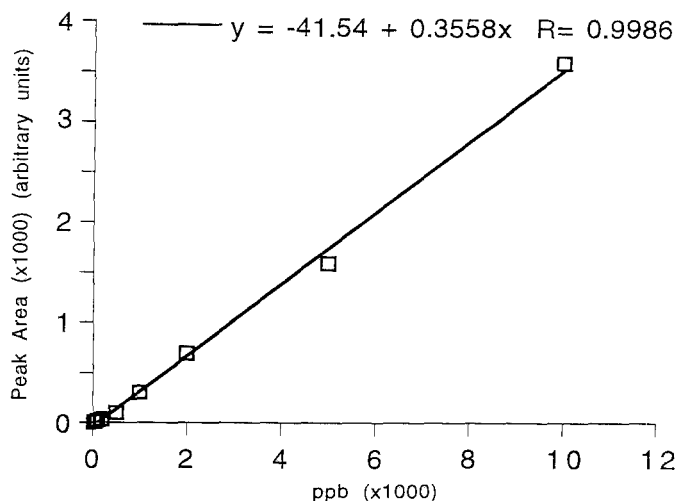


FIGURE 4: Calibration curve for uranyl cation. Injected plug length is 5.8 cm, $L_{\text{eff}} = 31$ cm. See Figure 2 for other experimental conditions.

expense of separation times (see Table 2). Therefore, various column lengths were evaluated using the 50 μm i.d. column to find the optimum between resolution and time. At very short column lengths ($L_{\text{eff}} = 9$ cm), resolution was completely lost. Thus, an effective length of 31 cm was used for most experiments, as it represented a reasonable compromise between resolution and separation time.

The LODs listed in Tables 1 and 2 were determined using optimum injection plug lengths. By injecting more material into the column, LODs should be improved provided efficiency and stacking remain reasonable. The best injection plug lengths were determined for each capillary with its optimum running buffer (see Table 1) by increasing the injection plug length until excessive band broadening occurred. The

TABLE 2
Optimization of Effective Column Length and Injection Plug Length

Column diameter (μm)	Total column length (cm)	Effective column length (cm)	Optimum injection plug ^a (cm)	Approximate LOD (ppb)	Separation time (min)
75	50	40	3.5	33	22
50	60	50	7.8	10	20
	40	31	5.8	25	13
	40	9	3.9	200	6
25 ELP	60	50	1.6	100	12

a Maximum injected plug length before excessive band broadening occurs

optimum plug length (see Table 2) is the best compromise between band broadening and improved LOD.

Interferences and Selectivity

A common limitation in uranyl cation analysis is inadequate selectivity. At a pH of 2.7, Arsenazo III forms complexes with several different metals including Sc, Y, Ln, Bi, Pb, and Fe(III) (12,13,21-23), thus requiring that extractions, pH adjustments, masking agents or some separation be performed. CE proved to be extremely selective in this work. The complex formed between the uranyl ion and Arsenazo III was negatively charged while most other complexes were neutral or positively charged. When the metals expected to be present in real samples (i.e., Hg, Pb, or Ca) were added in excess, no additional peaks were observed, and the uranyl - Arsenazo III peak remained unchanged.

To assess the effects of a "dirty" sample on LOD, water taken from the Pigeon River (Cocke County, TN) was filtered through a 8 μm polycarbonate filter to remove particulate matter and analyzed. Arsenazo III - metal complexes formed at this pH are purple or bluish in color. All samples made with the Pigeon River water were a bright blue color, indicating a high level of complexes of various metals; yet these complexes did not interfere with the uranyl ion determination. A 50 μm i.d., $L_{\text{eff}} = 50$ cm capillary was used for the analysis. A standard addition calibration curve was constructed which was linear with a coefficient of regression of 0.998. No UO_2^{2+} was found in the Pigeon River water. The river water matrix did not interfere with detectability of low concentrations of added uranyl ion (10 ppb).

An additional water sample was taken from Poplar Creek (Oak Ridge, TN) below the Oak Ridge Y-12 Plant and analyzed using the 50 μm i.d., $L_{\text{eff}} = 50$ cm column. Each of the samples made from this water was again blue showing a high concentration of complexed metals. Based on the standard addition method, about 18 ppb UO_2^{2+} was found in the river water. This was the median as reported in the 1995 Y-12 National Pollution Discharge Elimination System Report (30). Collection occurred after a rain shower which has the effect of stirring up the sediment and increasing the uranyl cation concentration.

CONCLUSIONS

This method of uranyl cation analysis is simple, rapid and inexpensive to perform. It has a comparable separation time and LOD with an HPLC method (9) and requires far less

volume of sample and running buffer. However, detectability was limited by the presence of a large system peak. Attempts to increase resolution between the system and analyte peaks were of limited success. Improvements in detectability could be made if the system peak could be removed. Some reduction in the system peak may be accomplished by monitoring the separation at two wavelengths - one at the maximum absorbance of Arsenazo III (about 540 nm), the other at the maximum absorbance of the complex (about 650 nm) - followed by a mathematical manipulation to reduce the effect of the free Arsenazo III background (see Figure 1). Unfortunately, this solution could not be evaluated due to limitations of the equipment. Nevertheless, the method presented herein is a good screening protocol for the uranyl ion at low ppb concentrations that exhibits a high degree of selectivity.

ACKNOWLEDGEMENTS

This work was sponsored by The Division of Chemical Sciences, Office of Basic Energy Sciences, United States Department of Energy, under grant DE-FG05-86ER13613 with the University of Tennessee.

REFERENCES

- (1) R. Brina, A. Miller, *Anal. Chem.*, 64: 1413-1418 (1992).
- (2) A. Bermejo-Barrera, M. Yebra-Biurrun, L. Fraga-Trillo, *Anal. Chim. Acta*, 239: 321-323 (1990).
- (3) T. Matsui, T. Kitamori, H. Fujimori, K. Suzuki, M. Sakagami, *J. Nucl. Sci. Technol.*, 29: 664-670 (1992).

- (4) P. Dolezel, V. Kahle, M. Krejci, *Fresenius J. Anal. Chem.*, 345: 762-766 (1993).
- (5) J. Korkisch, H. Hubner, *Talanta*, 23: 283-288 (1976).
- (6) A. Adriaens, J. Fassett, W. Kelly, D. Simons, F. Adams, *Anal. Chem.*, 64: 2945-2950 (1992).
- (7) D. Zamzow, D. Baldwin, S. Weeks, S. Bajic, A. D'Silva, *Environ. Sci. Technol.*, 28: 352-358 (1994).
- (8) J. Pavon, B. Cordero, E. Garcia, J. Mendez, *Anal. Chim. Acta*, 230: 217-220 (1990).
- (9) A. Kerr, W. Kupferschmidt, M. Attas, *Anal. Chem.*, 60: 2729-2733 (1988).
- (10) H. de Beer, P. Coetzee, *Radiochim. Acta*, 57: 113-117 (1992).
- (11) T. Kiriyaama, R. Kuroda, *Anal. Chim. Acta*, 71: 375-381 (1974).
- (12) J. Perez-Bustamante, F. Delgado, *Analyst*, 96: 407-422 (1971).
- (13) H. Onishi, K. Sekine, *Talanta*, 19: 473-478 (1972).
- (14) S. Dubey, M. Nadkarni, *Talanta*, 24: 266-267 (1976).
- (15) R. Baltisberger, *Anal. Chem.*, 36: 2369-2370 (1964).
- (16) D. Burgi, R. Chien, *Anal. Chem.*, 63: 2042-2047 (1991).
- (17) R. Chien, D. Burgi, *Anal. Chem.*, 64: 1046-1050 (1992).
- (18) R. Chien, D. Burgi, *Anal. Chem.*, 64: 489A - 496A (1992).
- (19) M. Albin, P. D. Grossman, S. E. Moring, *Anal. Chem.*, 65: 489A - 497A (1993).

- (20) Y. Xue, E. Yeung, *Anal. Chem.*, **66**: 3575-3580 (1994).
- (21) S. Savvin, *Talanta*, **8**: 673-685 (1961).
- (22) S. Savvin, *Talanta*, **11**: 1-6 (1964).
- (23) S. Savvin, *Talanta*, **11**: 7-19 (1964).
- (24) D. Burgi, *Anal. Chem.*, **65**: 3726-3729 (1993).
- (25) D. Swaile, M. Sepaniak, *Anal. Chem.*, **63**: 179 (1991).
- (26) C. Copper, T. Staller, M. Sepaniak, *Poly. Arom. Compds.*, **3**: 121-135 (1993).
- (27) C. Copper, J. Davis, R. Cole, M. Sepaniak, *Electrophoresis*, **15**: 785-792 (1994).
- (28) M. J. Sepaniak, R. O. Cole, *Anal. Chem.*, **59**: 472-476 (1987).
- (29) Trace Analysis: Spectroscopic Methods for Elements; J. D. Winefordner, Ed.; J Wiley and Sons: New York, 1976; Vol. 46.
- (30) "Y-12 Oak Ridge Tennessee National Pollution Discharge Elimination System Report," Y-12, 1995.

Received: July 10, 1995

Accepted: August 6, 1995

**RELATIONSHIPS BETWEEN CAPACITY FACTORS
AND HYDROPHOBICITY OF POLYCYCLIC
AROMATIC HYDROCARBONS IN CYCLODEXTRIN-
MODIFIED MICELLAR ELECTROKINETIC
CHROMATOGRAPHY USING SURFACE
TREATED CAPILLARIES**

KIYOKATSU JINNO* AND YOSHIE SAWADA

*School of Materials Science
Toyohashi University of Technology
Toyohashi 441, Japan*

ABSTRACT

The use of cyclodextrins (CDs) as a buffer additive for separation of polycyclic aromatic hydrocarbons (PAHs) in micellar electrokinetic capillary chromatography (CD-MEKC) has been studied in the relationships between the capacity factors ($\log k'$) and their hydrophobicity ($\log P$) using surface coated capillaries as the separation medium. Compared to the case when a surface-untreated capillary was used as the medium C₁ and C₁₈ treated capillaries gave the better linear relationships for the correlation between $\log k'$ and $\log P$ of PAHs, because the electroosmosis flow can be neglected in the latter case and then the hydrophobic interaction between CDs and PAHs is the main function to migration of the solutes in CD-MEKC.

INTRODUCTION

Micellar electrokinetic capillary chromatography (MEKC) has been proven to be a highly efficient separation technique in a great variety of applications.

Especially cyclodextrin (CD) modified-MEKC (CD-MEKC) has been recently developed to be one of the most powerful separation techniques for neutral, hydrophobic compounds such as polycyclic aromatic hydrocarbons (PAHs)[1-4]. Generally it has been found that there is a linear relationship between logarithmic capacity factor ($\log k'$) and their hydrophobicity ($\log P$) in reversed-phase liquid chromatography (RPLC). Therefore, if the similar hydrophobic interaction found in RPLC can be expected in CD-MEKC for PAHs separations, one can obtain a linear relationship between $\log k'$ in CD-MEKC and $\log P$ of PAHs. Some authors have tried to find such relationships in MEKC for several different compound groups [5,6] and the results indicated that the hydrophobic interaction should control the migration time even in MEKC. In our previous work [6], the addition of three CDs such as α -, β - and γ -CDs to the buffer solution in MEKC using an untreated-surface fused-silica tubing was evaluated. Relatively poor correlation coefficients were obtained for the relationship between $\log k'$ and $\log P$. The reason for large deviation from the linear relationship between $\log k'$ and $\log P$ might be due to the capillary surface contribution to electroosmotic flow. As an extension of our previous work, we have evaluated two different types of coated fused-silica capillaries as the separation medium, one is C₁-coated and the other is C₁₈ coated tubings.

EXPERIMENTAL

MEKC system consisted of a 870-CE-UV-VIS detector and 890-CE high voltage power supply (Jasco, Tokyo, Japan). Chromatographic retention data were collected by an 870-IT integrator (Jasco). MEKC was performed by 0.1 mm i.d. x 600 mm long fused-silica capillary tube and the distance from the injection part to the detector was 400 mm. Before use, the capillary was rinsed with 0.1 M

NaOH for 15 minutes to remove any impurities from the surface. Afterwards the NaOH solution in the tube was thoroughly rinsed with deionized water before filling the column with the actual separation buffer. Two other capillaries which have the surfaces treated by C₁ and C₁₈ were purchased from Supelco Japan (now Sigma Japan, Tokyo, Japan) and the total length of these tubings were 400 and 350 mm, respectively. The C₁ capillary has actually 250 mm length and the C₁₈ tube has 120 mm length with 0.05 mm i.d.

Three CDs were obtained from Kishida Chemicals (Tokyo, Japan), sodium dodecyl sulfate (SDS) and urea were purchased from Tokyo Chemical Industry (Tokyo, Japan). Deionized water was produced by a Milli-Q system (Nippon Millipore, Tokyo, Japan). PAHs were also obtained from Tokyo Chemical Industry. The compounds were dissolved in 2 mL of tetrahydrofuran (THF) and diluted by the buffer solution for MEKC analyses. The structures of the PAHs samples are summarized in Figure 1.

The buffer solution was prepared from deionized water and a reagent grade Na₂HPO₄ at pH=9.0. The buffer contains 20 mM of each CDs, 100 mM SDS and 5 M urea. These basic conditions were recommended by Terabe et al. [4]. The migration time of Sudan IV (Aldrich Chemical Co., Milwaukee, WI, USA) was used as the indicator for measuring micelle velocity in MEKC. All solutions were filtered with 0.45 μm HP-0.45 filters from ADVANTEC (Tokyo, Japan) to avoid capillary plugging and were degassed prior to use.

RESULTS and DISCUSSION

In our previous work [6], it has been found that CD-MEKC did not give good linear relationships between log k' and log P for PAHs due to various mechanisms which include inclusion by cyclodextrins, molecular non-planarity of

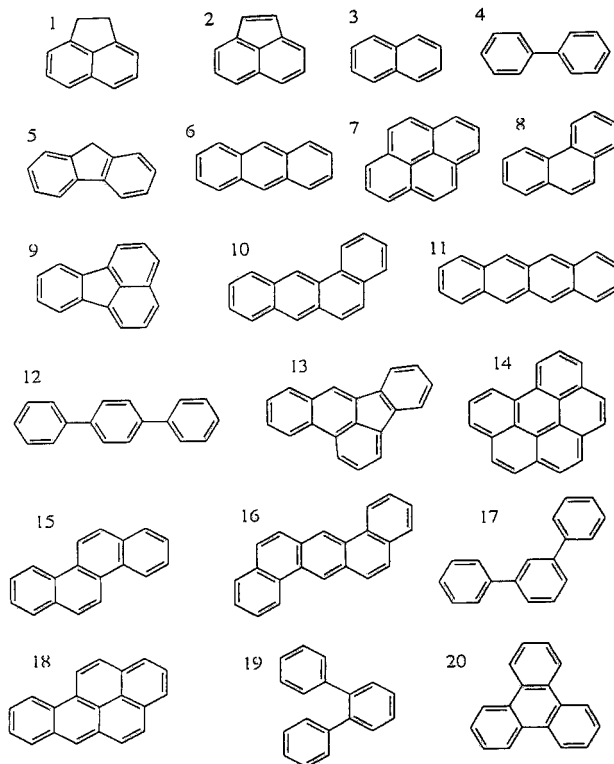


FIGURE 1 Structure of PAHs used in this work. 1=acenaphthene, 2=acenaphthylene, 3=naphthalene, 4=biphenyl, 5=fluorene, 6=anthracene, 7=pyrene, 8=phenanthrene, 9=fluoranthene, 10=benzo[a]anthracene, 11=naphthacene, 12=p-terphenyl, 13=benzo[b]fluoranthene, 14=benzo[ghi]perylene, 15=chrysene, 16=dibenzo[a,h]anthracene, 17=m-terphenyl, 18=benzo[a]pyrene, 19=o-terphenyl, 20=triphenylene

PAHs and unidentified contributions from the untreated capillary inner-surface. Only relatively better correlation has been obtained when γ -CD was added MEKC system. In order to understand the migration mechanism in CD-MEKC system, the surface coated capillaries were evaluated in this work. Two types of capillaries were used, one is C₁ treated and another is C₁₈ treated. If one could get better

correlation between $\log k'$ and $\log P$ with these coated capillaries, the migration mechanism of CD-MEKC can be basically identified as the hydrophobic interaction between CDs and PAHs (except few PAHs which have a possibility to be included in the cavity of each CD).

Although three CDs were selected in this work as an extension of the previous investigation [6], the problem was found when α -CD was used as the additive in the buffer. Several peaks for one solute were observed as shown in Figure 2 where phenanthrene is the test solute. The reason for this phenomenon has not been known yet but the interactions between the C_1 treated capillary inner-surface and the species including CD-analyte complexes caused this phenomenon. For this reason it was impossible to obtain the plots of $\log k'$ against $\log P$ with α -CD added MEKC system. Therefore MEKC with β - and γ -CDs added to the buffer were examined in this work.

Figure 3 shows the plots of $\log k'$ against $\log P$ using the C_1 capillary. The linearity of this relationship using β - and γ -CDs as the additives is better than when compared to the case when the bare untreated capillary was used as found in our previous work [7]. However some solutes gave a relatively large deviation from this linear relationship. With β -CD-MEKC five PAHs are identified as the deviated: 1=acenaphthene, 2=acenaphthylene, 12=p-terphenyl, 17=m-terphenyl and 19=o-terphenyl. Acenaphthene and acenaphthylene are considered to be included into the cavity of β -cyclodextrin and therefore their migration times became shorter than expected. Three terphenyls are non-planar molecules and they should have a little different interaction to β -cyclodextrin from other rather planar PAHs. With γ -CD-MEKC only three solutes deviated: 1=acenaphthene, 2=acenaphthylene and 10=benzo[a]anthracene. The former two are the same as found in the case with β -CD-MEKC and the reason is also considered the same. It is not clear why benzo[a]anthracene did not migrate with γ -CD but migrated with

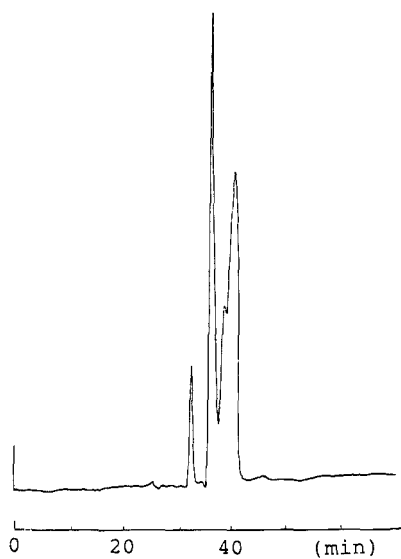


FIGURE 2 Electropherogram of phenanthrene with the addition of α -CD as the modifier in MEKC using C_1 surface-treated capillary.

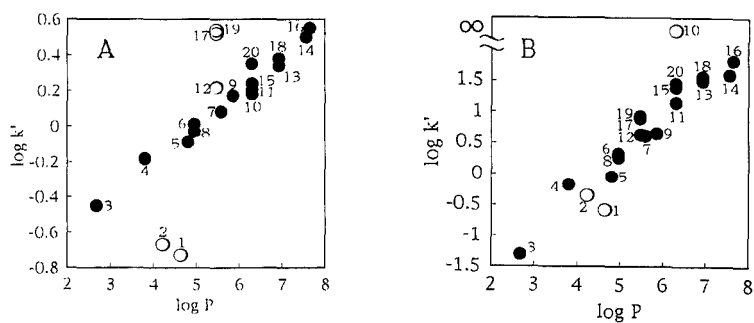


FIGURE 3 Plots of $\log k'$ and $\log P$ of PAHs using C_1 surface-treated capillary. (A) β -CD and (B) γ -CD modified MEKC.

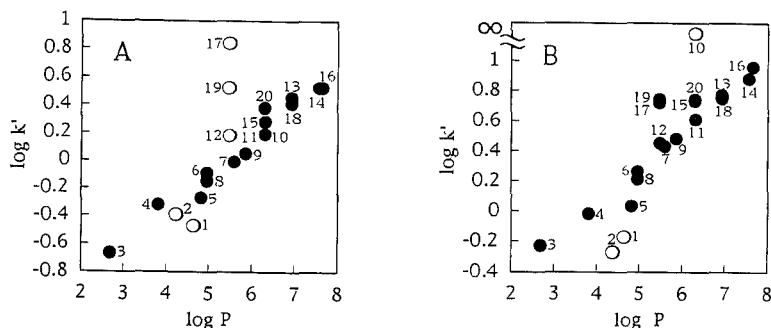


FIGURE 4 Plots of $\log k'$ and $\log P$ of PAHs using C_{18} surface-treated capillary. (A) β -CD and (B) γ -CD modified MEKC.

the micelle, although the same results in γ -CD-MEKC were found with the bare untreated capillary in our previous work [6].

Figure 4 shows the plots of $\log k'$ against $\log P$ with the C_{18} capillary. Very similar trends were seen in this figure to those found in Figure 3. The good linearity can be obtained for the relationships between $\log k'$ and $\log P$ with β - and γ -CD-MEKC systems except few PAHs which are the same as found in Figure 3. The reason for this deviation is considered the same as that discussed previously. The typical electrophoregrams for phenanthrene with three different capillaries are demonstrated in Figure 5. When the bare capillary was used, a characteristic sharp peak which is usually obtained by MEKC was observed. However using C_1 and C_{18} treated capillaries gave some peak tailings. In order to define the difference among those three capillaries the peak width at the peak base (W_b) divided by the peak width at the half height ($W_{1/2}$) was calculated. The values obtained were 1.88, 5.33 and 6.11, for the bare, C_1 and C_{18} capillaries, respectively. It is found that the analytes have some interactions with the inner-surface of the capillary and the alkyl chains on the surface contribute to their migration in the separation

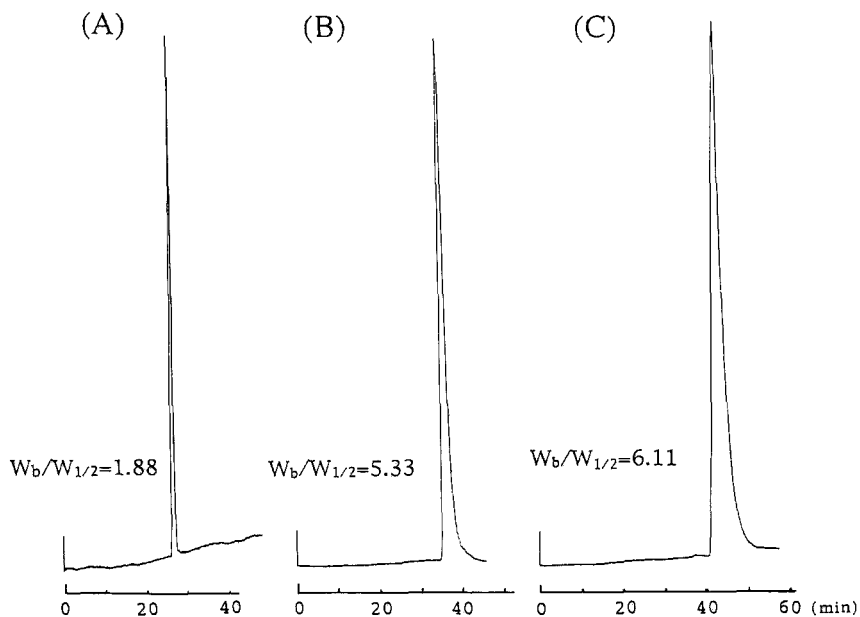


FIGURE 5 Typical electrophoregrams obtained by three different capillaries. (A) bare capillary, (B) C₁ treated capillary, (C) C₁₈ treated capillary for phenanthrene as the solute.

TABLE 1

Correlation coefficients for the relationships between log k' and log P of PAHs with three different capillaries

	bare capillary	C ₁ treated capillary	C ₁₈ treated capillary
α-CD	0.770	-	-
β-CD	0.900	0.986	0.980
γ-CD	0.778	0.964	0.925

For α-CD evaluation the data of three PAHs are excluded: those are 10=benzo[a]anthracene, 13=benzo[b]fluoranthene and 17=m-terphenyl.

For β-CD evaluation the data of five PAHs are excluded: those are 1=acenaphthene, 2=acenaphthylene, 12=p-terphenyl, 17=m-terphenyl and 19=o-terphenyl.

For γ-CD evaluation the data of three PAHs are excluded: those are 1=acenaphthene, 2=acenaphthylene and 10=benzo[a]anthracene.

process. As electroosmosis is prohibited in the latter cases, this fact induces such peak broadening.

Table 1 summarizes the correlation coefficients for log k' and log P relationships with three different types of capillaries. The linearity was apparently improved by using C₁ and C₁₈ treated capillaries as the separation medium. Therefore we can conclude that one can make the separation system in CD-MEK/C using surface coated capillary as the separation medium, where hydrophobic interaction between CD and the solutes can control their migration.

REFERENCES

- [1] Y.F.Yik, C.P.Ong, S.B.Khoo, H.K.Lee and S.F.Y.Li, "Separation of Polycyclic Aromatic Hydrocarbons by Micellar Electrokinetic Chromatography with Cycrodextrins as Modifiers", *J.Chromatogr.*, **598**, 333-338(1992).
- [2] S.Nie, R.Dadoo and R.N.Zare, "Untrasensitive Fluorescence Detection of Polycyclic Aromatic Hydrocarbons in Capillary Electrophoresis", *Anal.Chem.*, **65**, 3571-3575(1992).
- [3] C.L.Cooper and T.D.Staller, "Characterization of Polyaromatic Hydrocarbon Mixtures by Micellar Electrokinetic Capillary Chromatography", *Polycyclic Arom.Comp.*, **3**, 121-135(1993).
- [4] S.Terabe, Y.Miyashita, Y.Ishikawa and O.Shibata, "Cyclodextrin-Modified Micellar Electrokinetic Chromatography: Separation of Hydrophobic and Enantiomeric Compounds", *J.Chromatogr.*, **636**, 47-55(1993).
- [5] B.J.Herbert and J.G.Dorsey, "n-Octanol-Water Partition Coefficient Estimation by Micellar Electrokinetic Capillary Chromatography", *Anal.Chem.*, **67**, 744-749(1995).
- [6] K.Jinno and Y.Sawada, "Relationships between Capacity Factors and Hydrophobicity of Polycyclic Aromatic Hydrocarbons in Cyclodextrin-Modified Micellar Electrokinetic Capillary Chromatography", *J.Cap.Electrophoresis*, **1**(No.2), 106-111(1994).

Received: July 10, 1995

Accepted: August 6, 1995

**SIMULTANEOUS MEASUREMENTS OF
CAPILLARY ELECTROPHORESIS
FLUORESCENCE PEAKS AND THEIR
CORRESPONDING SPECTRA**

**GERHARD A. M. DALHOEVEN¹, NARAHARI V. JOSHI²,
NESTOR RODRIGUEZ², AND LUIS HERNANDEZ^{2*}**

*¹Compulogic Services
St. Janshovenstrasse 121
3572 RB Utrecht, The Netherlands*

*²Department of Physiology
School of Medicine
University of Los Andes
Mérida, Venezeula*

ABSTRACT

Capillary electrophoresis coupled to laser induced fluorescence detection is one of the most sensitive techniques for chemical analysis and its applicability could be remarkably increased if spectral analysis is incorporated to it. With this view we have modified the conventional system by introducing CCD and PMT measurement simultaneously. The data obtained from PMT was processed and the peak position was determined by second derivative to trigger CCD system. With this

method the electropherogram for peak identification by migration time and the spectrum corresponding to each peak were simultaneously recorded. The obtained spectra for various amino acids attached to Fluorescein Isothiocyanate (FITC) are also reported.

INTRODUCTION

Capillary Electrophoresis (CE) with Laser induced fluorescence detection (LIFD) is known to be one of the most sensitive separation and detection techniques [1,2,3]. Using LIFD as low as 10^{-13} molar concentrations of FITC-amino acids has been reported by us [4]. In addition, the method is suitable for detection of very small quantities of analyte enabling useful application in biology, analytical chemistry and medical sciences where the detection of minute traces of some chemicals plays a key role. Laser induced fluorescence detection is normally performed only with a sensitive photomultiplier tube (PMT) to detect fluorescence labeled species. However, the applicability of this technique will be enhanced if it can be used to record the spectrum of each analyte which passes through the capillary window since the spectral analysis can be considered as the fingerprints of the particular substances.

Among the spectral analysis devices, CCD offers a high photoresponse and high dynamic range. Moreover, essential virtue of CCD system for this type of investigation is that the spectral measurements are carried out with a single shot rather than conventional scanning procedure. But a note of caution should be introduced. Being the CCD a charge storing device, its sensitivity increases with exposure. For extremely short collection times (picoseconds) the PMT is more sensitive.

Cheng et al incorporated for the first time a Charge Coupled Device in the snap shot mode to detect amino acids labeled with Fluorescein Isothiocyanate in a CE-LIFD instrument [5]. The CCD was placed as a camera oriented orthogonally to the laser and pictures of the capillary were taken. The fluorescent images were built as peaks by a computer. In this seminal experiment more than 5 seconds were required to transfer the data to the computer and each exposure lasted 0.2 second enhancing the chances of missing bands. In addition, for a typical run massive amount of data were collected.

Using axial illumination and a 2 cm window on the capillary, Sweedler et al at Zare's laboratory analyzed

fluorescence with a CCD in a time delayed integration mode [6]. By synchronizing the movement of the fluorescent band with the clock of the CCD so that the photogenerated charge moved with the band they enhanced the sensitivity of the detection system. Picomolar concentration and zeptomole amounts of Fluorescein and Sulforhodamine were detected. At the same time they were able to obtain the spectra of both dyes. These achievements were due to an elaborated optics and careful considerations in the synchronization procedure. The optics had to expand the laser beam to illuminate the whole 2 cm window and to focus its image on a column of the photosensitive detector array. The clock of the CCD had to be synchronized with a band which moved in nonuniform fashion, a non trivial task and certainly not suitable for routine analytical work.

Taylor and Yeung axially excited an array of capillaries by means of optical fibers [7]. This excitation method simplified cumbersome alignment procedures. The fluorescence was collected with CCD and bands for each capillary were recorded. Since no synchronization of the moving band and the clock of the CCD was used, 0.1 sec snap shot had to be taken and that

diminished the sensitivity. Later on Ueno and Yeung expanded the capillary array to 100 but had to give up to the axial excitation and resorted to a more complicated excitation optics [8]. Although they sacrificed optical simplicity they successfully detected the bands by means of a CCD camera in an array of 100 capillaries.

Nilsson et al followed a different strategy for CCD application in CZE-LIFD [9]. They expanded the laser beam to illuminate a substantial part of the length of the capillary and collected the whole image of the capillary at a given angle with a CCD camera. This allowed to follow all the fluorescent bands in real time on the screen of a computer. By binning the CCD over 50 pixels they obtained a line profile showing the fluorescence intensity versus position along the capillary. Interestingly they found that peak width changes in unpredictable way due to imperfections of the capillary and this should hinder the time delayed integration mode used by Sweedler et al.

Takahashi et al have used the orthogonal arrangement with the sheath flow cuvette method in capillary array electrophoresis [10, 11]. An arrangement of sheath flow

cuvettes was illuminated with a single laser beam that crossed the cuvettes for excitation. A CCD camera was placed perpendicular to the laser beam for simultaneous detection of the bands in the cuvettes.

In most of the above experiments the CCD was used as an imaging facility (i.e. in camera mode) to record the illuminating spot, tube or band. In principle, this does not provide additional information as compared to the conventional PMT detector. In the present work, we are employing a CCD as a detector attached to a spectrometer which permits to record the spectrum of the moving molecules.

In all those CCD experiments the collinear geometry was never employed. Optical simplicity as well as excellent stray radiation rejection are among the main advantages of this geometry. These advantages cooperate for enhanced sensitivity for CE-LIFD applications[12]. In preliminary experiments we have hydrodynamically injected FITC labeled amino acids and analyzed their spectra by means of a liquid nitrogen cooled CCD in a collinear LIF detector. High sensitivity as well as slight but significant differences in the spectra of FITC-amino acids have been observed [13]. However, the

small magnitude of the differences necessarily required a high resolution.

If the CCD system collects in the snap shot mode all the time then, the store devices of the data acquisition system will be quickly saturated. This trouble gets worse when high resolution CCD is employed. Ideally in the snap shot mode the CCD should collect data just for the time that the analyte goes through the detection window of the capillary. This reasoning suggested that the combination of a photomultiplier and a high resolution CCD would allow to record the peak and to trigger the CCD, providing the electropherogram plus the relevant spectral data. Such PMT-CCD combination should not collect data when there is no band in the window.

In the present article we report the successful combination of a PMT and a CCD for the detection of electrophoretically separated FTC-amino acids and their spectral measurements in a narrow bore capillary.

EXPERIMENTAL CONDITIONS

Instrument: Figure 1 shows a diagram of the experimental set up. The CE system is a collinear instrument already described [3,12]. Briefly, a 3 mW Argon ion laser (Ion

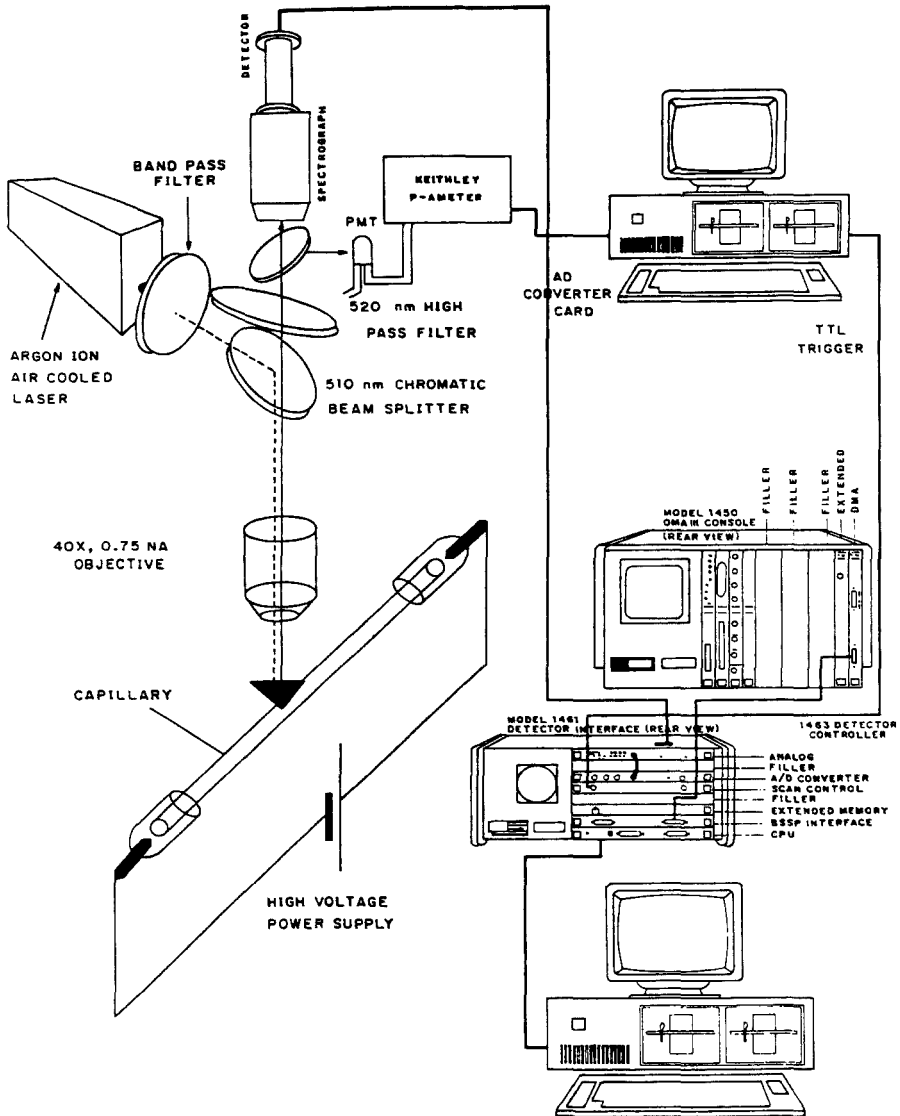


Figure 1.-

Experimental set up to measure CE peaks and corresponding spectra simultaneously.

Laser Technology, Salt Lake City, USA) was tuned to 488 nm and reflected by a dichroic mirror centered at 510 nm (Carl Zeiss, Caracas, Venezuela). The laser was focused by means of a .75 NA objective (Carl Zeiss, Caracas, Venezuela) on the window of the capillary (Polymicro Technologies, Phoenix, AZ, USA). The window was located at 20 cm of the anodic end of a 30 cm long, 20 μ m bore fused silica capillary filled with a 20 mM carbonate buffer at pH 9.4. The fluorescence was collected by the same objective and stray radiation was attenuated by a high pass filter centered at 520 nm (Carl Zeiss, Caracas, Venezuela) and a notch filter centered at 488 nm (Andover, Salem, NH, USA). Then the radiation was split by a beam splitter centered at 530 nm (Andover, Salem, NH, USA). One beam was focused on a R1477 multialkali PMT (Hamamatsu, Bridgewater, NJ, USA) driven by a HC-123 miniaturized high voltage power supply (Hamamatsu, Bridgewater, NJ, USA). The other beam was focused on the entrance slit of the monochromator [13].

The spectrometer had a 0.5 m optical path(EG&G, Princeton, NJ, USA, model 1236) and was employed with a cryogenic cooled CCD detector model 1433-C with a 1433-1 controller and a 1461 detector interface system(EG&G,

Princeton, NJ, USA). The temperature of the detector was maintained at -140°C throughout the experiment. In the present investigation, the scan control board in the detector interface permits TTL level (0-5 Volt) for external triggering. A stand-alone 386 MS-DOS pc runs the Princeton Applied Research OMA-2000 software to collect spectral data via the detector interface.

The PMT anode output is monitored with an Electrometer (Keithley, Cleveland, OH, USA, model 614) which allows us to use the analog preamplifier voltage output between 0 and 5 Volts. The Electrometer signal is sampled with a 5 Volt AD voltage converter card (resolution was 2.4 mV) AIO8G type from ICS (Industrial Computer Source, San Diego, CA, USA) with its corresponding PASCAL software specially prepared for this purpose. It was most convenient to use a second stand-alone 386 microprocessor type MS-DOS PC to process the digitized PMT data. A special program was written to measure the CE recording data and trigger the CCD detector via the scan control board input on the CCD detector interface.

Real-time synchronization of the experiment is performed by using simple build-in PASCAL function

calls. The sampling rate is limited due to computing power to calculate the derivatives. We could sample up to 700 AD conversions and process (including first and second derivatives) per second with the present computer configuration. Averaging a high number of AD conversions is an indispensable tool to reduce the noise. The number of stored data points in memory is limited in our computer configuration to some 4000 time/intensity data points. So averaging about 120 AD conversions permitted us to sample 6-10 data points per second for the required maximum 15 minutes of measuring the electropherogram. The effective sampling rate of 6-10 Hz during 15 minutes turned out to be enough for this purpose.

Recently, Timperman et.al.[14] have demonstrated the feasibility of wavelength resolved fluorescence detection by using a CCD system which was triggered at a certain predetermined time interval independent of whether the analyte was passing through the window or not. This required excessive (and also unnecessary) use of memory of the computer and hence it is not convenient for routine measurements. Moreover duration time used for data collection is limited by triggering

interval. These short comings are overcome by different approach. During the measurements, in the time between each stored data point in memory the program calculates and estimates the first and second derivative which permits us to find the best moment to trigger the CCD detector system to measure a complete luminescence spectrum i.e. somewhere at or just before the CE peak maximum. Triggering on second derivative gave the best result, i.e. near the highest CE peak intensity. The first derivative indicates the beginning of the peak; obviously all the small peaks originated from noise are handled by the software. The triggering due to noise is avoided by setting a certain offset level (see figure 2). The triggering event on the second derivative is typically some 2-3 seconds before the peak maximum. With a typical 3 seconds CCD shutter opening time, it can be covered more or less the whole peak during the CCD exposure. During 1.5 seconds after closure of the CCD shutter (the time needed to read the CCD pixels and transferring the data to the detector interface memory) the CE measurement program does not deliver triggering pulses. This domain is considered as a blind period for which the other spectral measurement cannot be carried out.

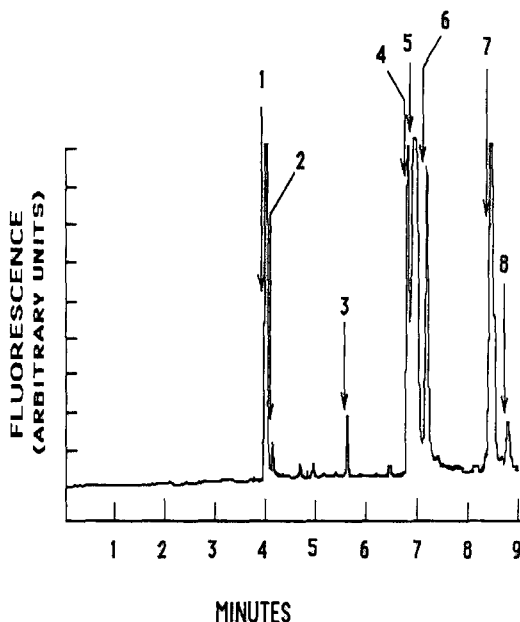


Figure 2.-

Electropherogram of a mixture of 8 amino acids. The arrows indicate the time when the CCD camera was triggered. Notice the absence of arrows on small peaks. 1= FTC-Arginine, 2= FTC-Asparagine, 3= FTC-Glutamine, 4= FTC-Proline, 5= FTC-Threonine, 6= FTC-Glycine, 7) FTC-Tryptophane and 8) FTC-Methionine.

Reagents: Sodium Carbonate, Sodium Bicarbonate, Sodium hydroxide, Arginine, Glutamine, Methionine, Asparagine, Proline, Threonine, Glycine, Tryptophan, Fluorescein Isothiocyanate (Isomer 1) HPLC grade Acetone were obtained from Sigma Chemical Co (Sigma Chemical, ST. Louis, MO, USA).

Derivatization procedure: A 20 mM Carbonate buffer at pH 9.4 was filtered through .22 μm filters (Millipore, Bedford, MA, USA). The amino acids were dissolved in carbonate buffer to obtain a 1 mg/ml solution. A 4×10^{-4} M solution of FITC in acetone was prepared. Then 1 ml of the amino acid solution was combined with 10 μl of FITC solution and allowed to react for 4 hours in the dark. Since FITC was the limiting reactant, the final concentration of FITC-Amino acid was 4×10^{-6} M. This solution was diluted in steps of 10 to measure the limit of detection of the system.

Capillary Electrophoresis: Each amino acid was run individually and also combined with the other amino acids in a single solution. The electrophoretic run consisted in injecting a plug of the test solution by the hydrodynamic method. The anodic end of the capillary was immersed in the sample reservoir and a pulse of -19 psi was applied for 0.3 sec at the cathodic end. The anodic end was withdrawn from the sample reservoir and immersed in a buffer reservoir. Both the cathode and the anode were made of Platinum-Iridium wire. 20 KV from a high voltage power supply (Bertan, Hicksville, NY, USA, model 30R) were applied between the two ends of the

capillary. After each run the capillary was rinsed with 0.1 N sodium hydroxide solution for 2 minutes followed by water for 2 minutes and 20 mM carbonate buffer for 3 minutes.

RESULTS AND DISCUSSION

Figure 2 shows the conventional CE peaks of the mixture of eight amino acids recorded with the PMT detector. The figure also shows the exact time when the trigger was activated. Differences in peak amplitude are due to the reaction time of individual amino acids and different photoluminescence efficiency. Fig 3 and Fig 4 show the spectra corresponding to each peak in CE measurement. Curve number 8 of figure 4 looks like a straight line because of its low intensity as compared with the other curves. We have, therefore, plotted the curves number 1 and 8 with different scales as shown in figure 5. Each peak is identified with the migration time as mentioned in the caption of figures 3, 4 and 5. Intensity of the peak in CE corresponds to the area under the curve of each spectrum and does not show any relation with the peak intensity of the spectrum. It is worth mentioning that with the present experimental set

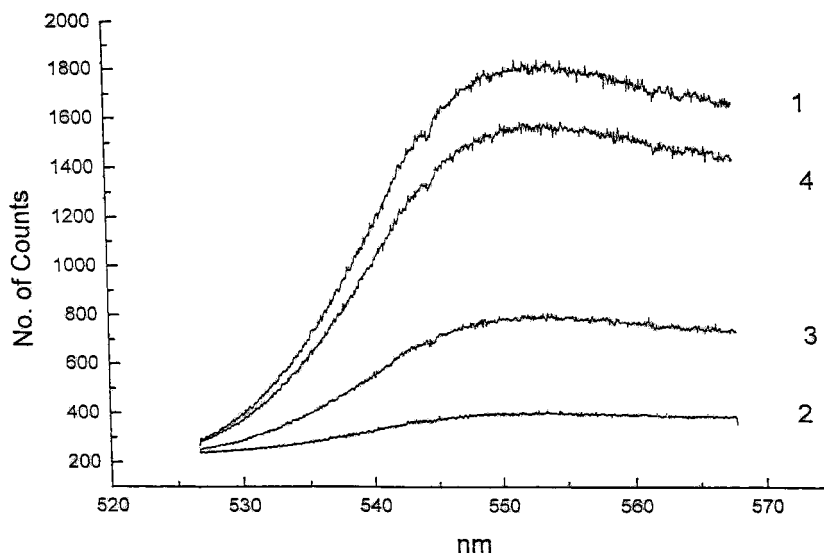


Figure 3.-

Spectra recorded for 1= FTC-Arginine, 2= FTC-Asparagine, 3= FTC-Glutamine and 4= FTC-Proline.

up we could measure photoluminescence spectra down to 10^{-9} molar concentration with a noticeable peak intensity with only 3 seconds exposure. This nanomolar sensitivity is three orders of magnitude lower than the picomolar sensitivity easily reached with the collinear geometry together with a PMT detector. Several factors explain this sensitivity reduction. For instance, compared to the conventional collinear instrument, in the present instrument the optical path to the CCD is

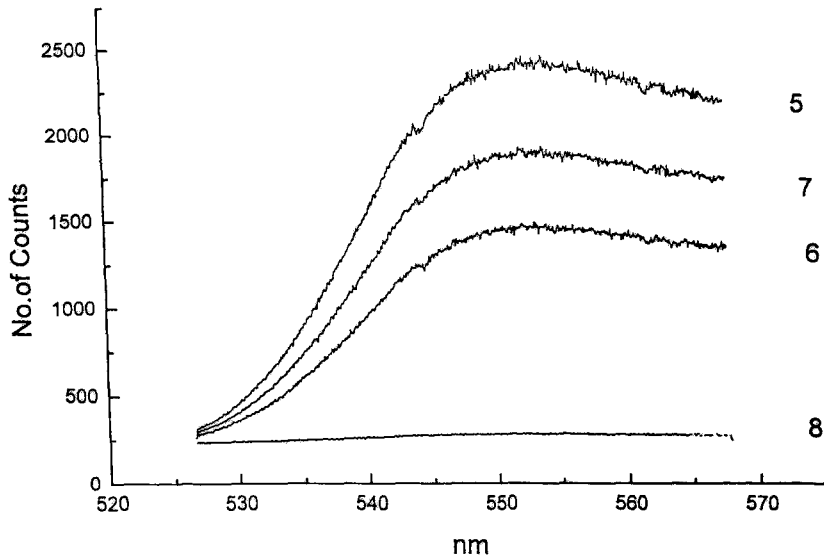


Figure 4.-

Spectra recorded in the same experiment as in figure 3. 5= FTC-Threonine, 6= FTC-Glycine, 7= FTC-Tryptophane and 8= FTC-Methionine. Notice that the spectrum of FTC-Methionine looks flat due to the high scale.

more than 50 cm longer, the fluorescence is split for two photodetectors and the slit of the monochromator limits the amount of fluorescence reaching the CCD. Nevertheless, it is possible to push down the detection limit in the present design by selecting the proper optical component such as a beam splitter with 90 % transmission intensity, using cylindrical mirrors for fluorescence collection (15) and so on. In any event

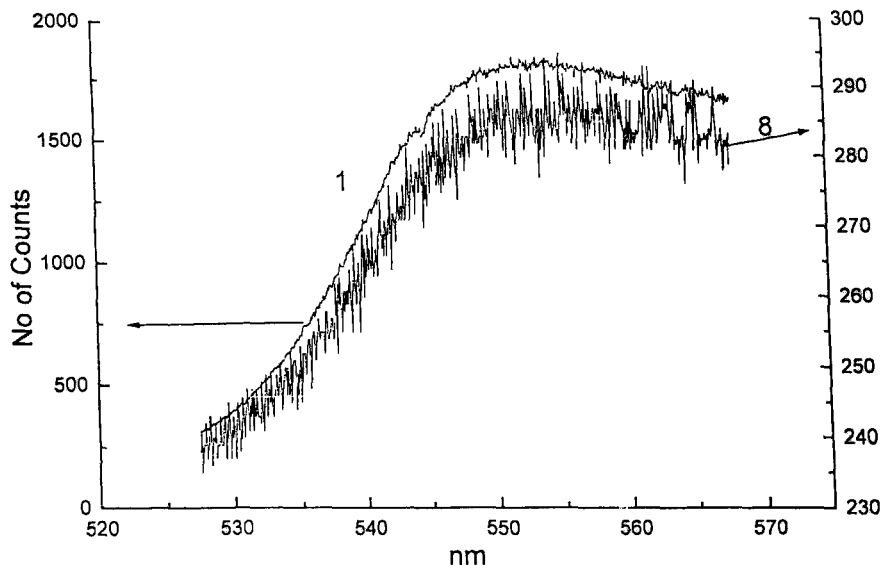


Figure 5.-
Spectra of FTC-Arginine (1) and FTC-Methionine (8).
Notice the different scales for the FTC-Arginine
spectrum (left scale) and for the FTC-Methionine
spectrum (right scale)

this sensitivity is two orders of magnitude higher than the required sensitivity for DNA sequencing applications. In addition, the present design simplifies the discrimination of four different fluorochromes. Other designs have used a complicated combination of filters and until four PMTs to distinguish the four fluorochromes (16). The present design uses a single CCD for the analysis of the four fluorochromes.

In previous experiments we observed slight but consistent spectral differences between the FTC-amino acid spectra. This differences included disparate relative intensity at the peak position and non proportional shape on the high energy side of the FTC-amino acid spectra (13). Similar differences were observed in the present experiments.

In short, the present experimental set up along with the tailored software permit to record simultaneously CE peak and its corresponding photoluminescence spectrum with ease. It is clear that this experimental set up is easy to automate and speed up the measurement capabilities. Reasonable amount of spectral data and their theoretical interpretation will be necessary to explore full possibilities of capillary electrophoresis. Such study will certainly have several applications in ultra sensitive spectroscopy based clinical diagnostic systems. Moreover, in recent investigation on diagnosis of certain diseases, it has been found that spectral information is very useful, particularly in early diagnosis of Cancer [17].

The current approach of analysis is based on the retention time of a particular species. Spectral

analysis will be an additional support for classification and analysis. If properly applied, this methodology can also be useful to improve DNA sequencing techniques based on capillary-array electrophoresis.

ACKNOWLEDGMENTS

The present experimental investigation were carried out under GRANT BID-CONICIT BTS-37. We express our gratitude to Professor Ernesto Palacios for his photographic assistance.

REFERENCES

- 1] E. Gassman, J. E. Kuo and R. N. Zare. *Science*, 230 813-814 (1985)
- 2] S. Wu and N. J. Dovichi. *J. Chromatogr.* 480 141-155 (1989)
- 3] L. Hernandez, J. Escalona, N. Joshi and N. A. Guzman. *J. Chromatogr.* 559 183-196 (1991)
- 4] L. Hernandez, N. Rodríguez, N. Joshi, X. Páez and N. A. Guzman. Pittcon 1995, abstract # 328P, New Orleans, Louisiana, USA.
- 5] Y-Y. Cheng, R. D. Piccard and T. Vo Dinh. *Appl. Spectrosc.* 44 755-765 (1990)
- 6] J. V. Sweedler, J. B. Shear, H. A. Fishman and R. N. Zare. *Anal. Chem.* 63 496-502 (1991)
- 7] J. A. Taylor and E. A. Yeung. *Anal. Chem.* 65 (1993) 956-960

- 8] K. Ueno and E. A. Yeung. Anal. Chem. 66 1421-1431 (1994)
- 9] S. Nilsson, J. Johansson, M. Mecklenburg, S. Birnbaum, S. Svanberg, K-G. Wahlund, K. Mosbach, A. Miyabayashi and P-O. Larsson. J. Cap. Elec. 1 46-52 (1995)
- 10] H. Kambara, and S. Takahashi. Nature, 361 565-566 (1993)
- 11] S. Takahashi, K. Murakami, T. Anasawa and H. Kambara. Anal. Chem. 66 1021-1026 (1994)
- 12] L. Hernandez, N. Joshi, E. Murzi, P. Verdeguer, J. C. Mifsud and N. A. Guzman. J. Chromatogr. 652 399-405 (1993)
- 13] N. V. Joshi, V. O. Joshi, N. Rodriguez and L. Hernandez. Proc. of SPIE. 2386 303 -309 (1995)
- 14] A.T.Timperman, K Khatib & J.V.Sweedler Anal Chem., 67, 139-144 (1995)
- 15] L. Hernandez. French patent #2 649 487, USA patent#5,228,969.
- 16] L. M. Smith. Nature, 349 812-813 (1991)
- 17] T.Vo. Dinh. Proc. of SPIE conference 2387 (1995) In press

Received: July 10, 1995

Accepted: August 6, 1995

BIOMEDICAL APPLICATIONS OF ON-LINE PRECONCENTRATION-CAPILLARY ELECTROPHORESIS USING AN ANALYTE CONCENTRATOR: INVESTIGATION OF DESIGN OPTIONS

NORBERTO A. GUZMAN*

*Protein Research Unit
Princeton Biochemicals, Inc.
Princeton, New Jersey 08543*

ABSTRACT

A method to perform on-line sample preconcentration of serum immunoglobulin E by affinity capture is described. Purified anti-IgE antibodies were covalently bound to an analyte concentrator-reaction chamber or cartridge. The immunoglobulins (IgE) were bound to and eluted from the cartridge by the optimum dissociating buffer system, and the eluent(s) were then subjected to capillary electrophoresis.

The first design used was a 5 mm solid-phase cartridge fabricated by assembling a bundle of multiple microcapillaries in which a monoclonal antibody directed against IgE was covalently bound to the surface of every microcapillary. The whole assembly was connected, through sleeve connectors, to the capillary column for affinity capillary electrophoresis.

The second design used consisted of an analyte concentrator-reaction chamber that was fabricated from a solid rod of glass.

*Present address: The R.W. Johnson Pharmaceutical Research Institute, a Johnson & Johnson company, Raritan, New Jersey 08869, U.S.A.

Several small diameter passages or through holes containing a similar surface area was tested for the same experiments and performance as described above.

A major advantage of these designs, over previously described designs, is the absence of frits and beads. The previously reported designs consisted of derivatized beads confined to the concentrator cartridge by a frit at each end. After limited usage of the cartridge, the beads tends to pack at the outer frit. This lead to restricted flow through the concentrator chamber and ultimately clogging of the system. The designs reported here allows for a constant electroosmotic flow, superior reproducibility of the electropherograms, a reduced possibility of blocking the microcapillaries, and increase number of usages of the cartridge.

The use of this novel analyte concentrator design for the determination of immunoglobulins in biological fluids is demonstrated by capillary electrophoresis of IgE in serum. The general utility of this technique for a variety of biomedical applications is discussed.

INTRODUCTION

Since its discovery in 1967 (1,2) immunoglobulin E and its receptors have been extensively studied to provide a better understanding for their role in host defense against parasites and in the etiology of allergic diseases (3). Biochemical characterization studies were hampered for some time since IgE¹ constitutes a minuscule fraction of the total human immunoglobulin content in serum of non-atopic individuals. Normal levels of IgE in serum of non-atopic individuals range between 50-300 ng/mL versus 7-12 mg/mL of IgG. The discovery of two patients exhibiting a myeloma protein of the Immunoglobulin E class (1,4) and the availability of human myeloma cell line SK007/U266 (5) which secretes human IgE (6) have made possible the purification of this immunoglobulin and its subsequent biochemical and biological characterization. At the present time, a variety of immunoassays are available for the determination of IgE in serum (7,8). In general, enzyme immunoassays offer a number of advantages when compared to radioimmunoassays. Primarily, they eliminate handling of radioactive isotopes and permit the storage of labeled-reagents for prolonged periods. More recently, capillary electrophoresis has been examined as a useful separation method for rapid and efficient immunoassays (9-14).

Capillary electrophoresis has found widespread applications in analytical and biomedical research and can perform analytical sepa-

rations that are often more efficient, faster and with other capabilities far superior to those of traditional separations techniques (15-18). However, the small volume of the capillary limits the amount of sample that can be loaded. This is a major limitation of CE and compromises its use for analysis of very dilute samples. The volume injected into the capillary (without analyte concentrator) normally range between one to twenty nanoliters. In many instances analysis of several microliters of sample solution is often required to enable detection of the analytes of interest. In this regard, several approaches has been developed to preconcentrate samples, including analyte stacking (19-24), field amplification (25-28), and transient isotachopheresis (29-37). However, despite of the unique features of these techniques for preconcentration and separation, they still can only afford the introduction of approximately 1 μL of total volume into the CE capillary, and the presence of high salt concentration affect the efficiency of stacking processes.

In many instances, however, biologically active compounds are present in tissue biopsies, cells, and biological fluids at extremelly low concentrations. In order to detect minute amounts of solutes in these complex matrices, it is necessary to introduce sample volumes that vastly exceed the total volume of the CE capillary ($> 2 \mu\text{L}$). The availability of on-line analyte preconcentration, using the analyte concentrator technique (38-66), is a major advance in overcoming the problem of poor limits of detection for dilute samples. For example, enhancing the loading capacity of CE result in the detection of analytes found in very low concentrations ($< 50 \text{ ng/mL}$) in biological fluids, as is the case of IgE in serum.

An analyte concentrator-reaction chamber (AC-RC) consists of a solid support, inserted near the inlet of the CE capillary. Various chemistries have been covalently bound to the AC-RC in order to concentrate solutes (38-66), or to cleave, on-line, biopolymers into more fundamental components such as peptides or nucleotides (67-75). The dimension of the cartridge normally ranges between 1 and 5 mm in length, and 25 to 400 μm in diameter. The only exceptions to these dimensions, have been the reports in which pieces of entire capillaries of several centimeters have been used to couple enzymes directly to the inner surface (instead of binding to beads or membranes) for macromolecule cleavage (69,73,74).

In this report, we describe an analyte concentrator design made of multiple capillaries associated in bundles, and another having a plurality of small diameter rod passages or through holes. Each with sufficient surface area to covalently link monoclonal antibodies directed against IgE to extract IgE molecules present in serum. IgE molecules were bound to and eluted from the cartridge,

with a very small amount of high salt dissociating buffer, and finally subjected to capillary electrophoresis.

The second design, made of glass and containing several through holes, had several advantages when compared to the cartridges fabricated with the bundle design and those fabricated by other methods (38-66). For example: (a) easier fabrication of the cartridge; (b) better consistency of the electroosmotic flow enabling a high reproducibility of the peak area and migration time; (c) reduced possibility of clogging the system; (d) increased number of uses; (e) greater stability of the chemistries, since no heat was involved in the production of the cartridge; and (f) increased length (up to 5 mm) without changing significantly the electroosmotic flow. The fabrication of a cartridge containing microbeads or membranes, greater than 3 mm in length, can yield a product having consistently low reproducibility of the electroosmotic flow after several uses, an increased tendency for blocking the system, and a short life span. This is due primarily to: (a) use of irregularly-made frits; (b) compacting of the microbeads due to increasing pressure; (c) increase tendency of the membranes to pack yielding an increase back pressure; and (d) difficulty in reproducing the fabrication of the cartridge. Analyte concentrators made longer than 3 mm have a greater tendency to diminish electroosmotic flow and ultimately blocking the system. This is especially true when using several microliters of complex matrices such as serum.

In the present report, we demonstrate the use of both analyte concentrator-reaction chamber designs described above for the determination of the IgE content in serum by capillary electrophoresis. The use of these novel designs enabled a superior affinity capture of IgE. This procedure enhanced the detection of IgE in serum samples where IgE is present as a minute fraction of the total immunoglobulin content. The routine use of this technique for a variety of other biomedical applications is possible. Especially for molecules compatible with affinity interactions and present at concentrations of fg/mL in complex matrices such as tissue biopsies, cells, and biological fluids.

EXPERIMENTAL

Reagents

All chemicals were obtained at the highest purity level available from the manufacturer and were used without additional purification. Sodium hydroxide, Hepes, boric acid, bovine serum albumin,

fetal calf serum, Tween-20, immunoglobulin G, immunoglobulin A, immunoglobulin M, o-phenylenediamine dihydrochloride, horseradish peroxidase, human serum albumin, and ethylene glycol were purchased from Sigma Chemical Co. (St. Louis, MO). IgE was purified by electrophoretic and immunochromatographic procedures (76), and the monoclonal antibodies directed against IgE were generated and purified according to the method described elsewhere (77). All other inorganic chemicals were reagent grade or better and obtained from Mallinckrodt (St. Louis, MO). Reagent solutions and buffers were prepared using triply distilled and deionized water and were routinely degassed and sonicated under vacuum after filtration. Disposable filter units (0.22 μm) were purchased from Scientific Resources, Inc. (Eatontown, NJ), and fused-silica capillary columns were obtained from Polymicro Technologies (Phoenix, AZ).

Fabrication of an analyte concentrator-reaction chamber

Design 1: Bundles of Microcapillaries

Five to 14 polyimide coated capillaries of 25 μm I.D. and 150 μm O.D. were tightly hand-fitted into a rigid plastic tubing of 5 cm in length and about 400-800 μm I.D. as depicted in Figure 1. Portions of approximately 5 mm were cut, first with a stainless steel blade and then with a tip-diamond glass cutter, to produce an analyte concentrator. Monoclonal antibodies directed against IgE were covalently bound to the surface of every microcapillary of the analyte concentrator by a minor modification of a previously described method (43). The whole assembly was connected, through sleeve connectors sealed with epoxy resin, to the capillary column for affinity capillary electrophoresis. (Normally, 5 to 14 microcapillaries can be arranged into bundles with a total length of 2 to 5 mm without significantly affecting performance after a few injections of serum.)

Design 2: Multiple Channels Bored Through a Single Glass Rod

Several small diameter passages or through holes of approximately 25 μm I.D., containing a surface area comparable to design 1, was fabricated from a solid glass rod by laser drilling with a laser beam. Anti-IgE antibodies were covalently bound to the surface of every microcapillary, or through holes, of the analyte concentrator by the same method used above. The whole assembly was also connected, through sleeve connectors sealed with epoxy resin, to the capillary column for affinity capillary electrophoresis.

In order to apply the appropriate chemistry to the inner walls of the microcapillaries, or through holes, the analyte concentrator

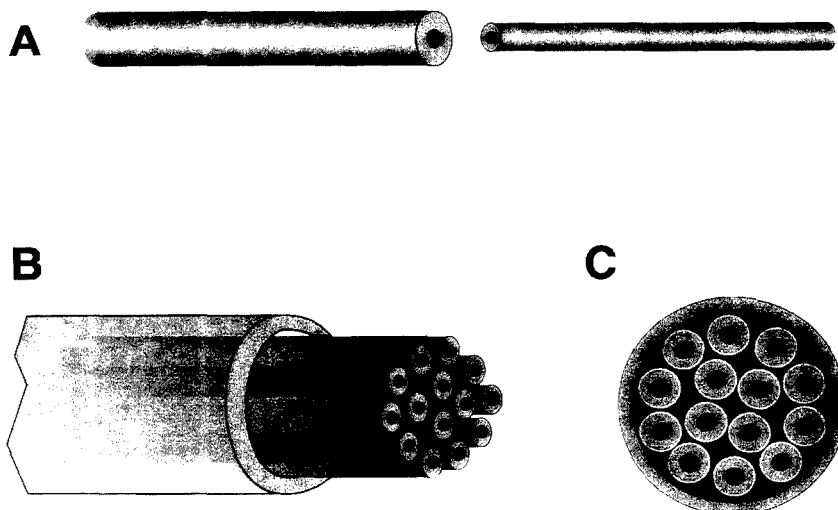


Figure 1. A Schematic Diagram of an Analyte Concentrator Fabricated of Multiple Capillaries. A. Comparison between a 75 μm I.D., 365 μm O.D., and a 25 μm I.D., 150 μm O.D. **B.** A plan view of a portion of the analyte concentrator fabricated with 25 μm I.D., 150 μm O.D. capillaries, and inserted into a sleeve connector for coupling to a separation capillary of 75 μm I.D., 365 μm O.D., 65 cm to the cathode and 7 cm to the anode. **C.** A sectional view of the same analyte concentrator cartridge depicted on B.

cartridge was connected to a syringe, through luer lock-like connector, as described in Figure 2. The various chemistries were sequentially applied slowly at a controllable speed using a syringe pump. The last step of the procedure, was the covalent coupling of the purified monoclonal antibody directed against IgE to form a stable bridge with the column. At this stage, the newly-created multi holes anti-IgE affinity analyte concentrator was removed from the syringe set and connected, and sealed with epoxy resin, to two longer underivatized fused-silica capillary columns (75 μm x 65 cm) for CE analysis. The location of the AC-RC was at 7 cm from the injection side of the capillary.

The entire process of fabrication, coupling and testing of the analyte concentrator was monitored under a stereomicroscope.

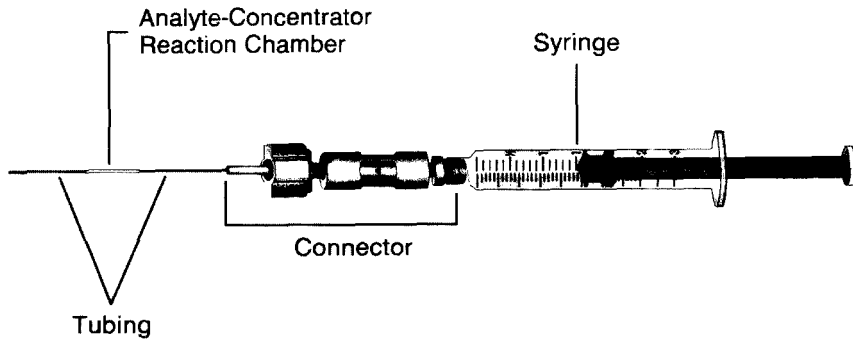


Figure 2. A Schematic Representation of a Syringe Attachment to the Analyte Concentrator. In order to apply the various chemical reagents onto the analyte concentrator, to link IgE to the surface of every microcapillary, it was necessary to fabricate an adaptor system. This system consists of a syringe linked to a commercially available connector to press the capillary in order to avoid any leakage of fluid. The analyte concentrator cartridge was, in turn, connected to two pieces of capillary to enable binding and washing of the AC-RC with appropriate reagents. These capillaries were removed after the AC-RC processing was complete. The 5 cm cartridge-containing bundles of microcapillaries, to which anti-IgE antibody was bound to their inner surfaces, was cut into a working analyte concentrator of a length of approximately 5 mm. This cartridge, was in turn, coupled to the separation capillary. For details see Experimental Section.

Normally, the finished product was allowed to rest for 24 hr at 25°C before use to permit a complete seal of the system. When the AC-RC was not in use, it was stored at 4°C in buffer containing 0.1 M sodium azide.

On-line affinity capillary electrophoresis of IgE

Twenty microliters of serum containing high titers of IgE were injected by pressure into the capillary column followed by a clean-up procedure consisting of a wash buffer to remove salts and other

serum constituents. Once the column was washed with separation buffer, and then equilibrated with 10 column volumes of the same buffer, a plug of 100 nanoliters of an optimized buffer system was applied to elute the antibody. The elution buffer consisted of 75 mM Hepes/NaOH buffer, pH 7.2, containing 3 M MgCl₂, and 25% ethylene glycol (78). After elution of IgE from the AC-RC by the sequential use of elution buffer followed by separation buffer under hydrodynamic pressure, the power was turned on and capillary electrophoresis was performed at 300 Volts/cm. The separation buffer consisted of 50 mM sodium tetraborate buffer, pH 8.3, and the separated component(s) were monitored at 214 nm.

Instrumentation

A laboratory-made apparatus was used similar to the one previously described (77). Briefly, the apparatus contained an on-column UV detection system. Electropherograms were obtained with a strip chart recorder model L-6512 (Linseis Inc., Princeton Junction, NJ) at 20 cm/hr.

Fraction Collection of Samples

Separated samples were fraction collected for further analysis. The fraction collection system used was previously described (79). This system couples two fused-silica capillaries (75 μm I.D. each) together with a third fused-silica capillary of smaller I.D. (10 μm x 10 cm) through a tee assembly system (79). This tee assembly forms a joint that is electrically conductive through the thinner capillary. The location of the tee assembly was after the detection system, five cm before the end tip of the collecting capillary.

Monitoring of the Electroosmotic Flow

The rate of electroosmotic flow was calculated by the method we previously described (80). Using the fraction collection system mentioned above, one measures how long it takes for a drop to form at the tip of the detection capillary. Under a microscope the drop is aspirated by capillarity into a piece of capillary column. Because one can measure with a caliper the distance between the two menisci formed, the total volume that is loaded into the piece of capillary column can be calculated using the formula of a cylinder [$V = \pi (d^2/4)l$]. By knowing the time needed for the drop to form, the volume of the drop, and the size of the detection capillary, one can calculate the rate of electroosmotic flow in nL/mm/sec.

Enzyme-Linked Immunosorbent Assay

Fraction collected samples using capillary electrophoresis were quantitated by ELISA (81,82) as follows: flat bottom 96-well microtiter plates were coated for 16 hr at 25°C with 50 μ L per well of purified anti-IgE monoclonal antibody (at a concentration of 1 μ g/mL in sodium tetraborate buffer, pH 9.6, containing 0.6 M NaCl). After incubation, the microtiter plates were washed three times with phosphate-buffered saline (PBS), pH 7.5, containing 0.05% Tween-20. Nonspecific binding sites were blocked with 2% BSA in PBS and incubated at 90 min at 37°C. Plates were rinsed four times with PBS, pH 7.5. Fifty μ L of fraction collected samples using capillary electrophoresis (or purified IgE, or commercially available IgA, or IgG, or Ig M, or human serum albumin) were added to the wells of the microtiter plate by duplicate, followed by incubation for 1 hr at 37°C. Plates were washed four times with PBS, followed by addition of 50 μ L of purified monoclonal IgE conjugated to horseradish peroxidase (at a concentration of 2 μ g/mL in PBS, pH 7.5, containing 0.05% Tween-20, and 2% fetal calf serum). Plates were incubated for 45 min at 37°C and then were washed again four times with PBS, pH 7.5. The final reaction was visualized by incubation for 30 min at 25°C in the dark with the chromogen substrate o-phenylenediamine (OPD) dihydrochloride. The reaction was stopped with 3N HCl. The resulting absorbance was measured at 492 nm in an ELISA reader.

RESULTS

The efficacy of using on-line preconcentration capillary electrophoresis for determination of IgE in serum is demonstrated. In this study, approximately twenty microliters of serum containing high titers of IgE (900 ng/mL) was analyzed using CE columns containing two kinds of analyte concentrators.

The first design, consisted of a bundle of microcapillaries of 25 μ m I.D., 150 μ m O.D., which were tightly hand-fitted into a rigid plastic tubing of 5 cm in length and about 400-800 μ m of total I.D. The working analyte concentrator consisted of approximately 5 mm in length. As shown in Figure 3A, the eluted material consisted of two main peaks ranging in migration times between 31 to 34 min for the minor peak, and 42 to 54 min for the major peak. Contrary to this observation, the second design of analyte concentrator, made of through holes, shows a single peak ranging in migration times between 42 and 43 min (Figure 3B). The significant variability in mi-

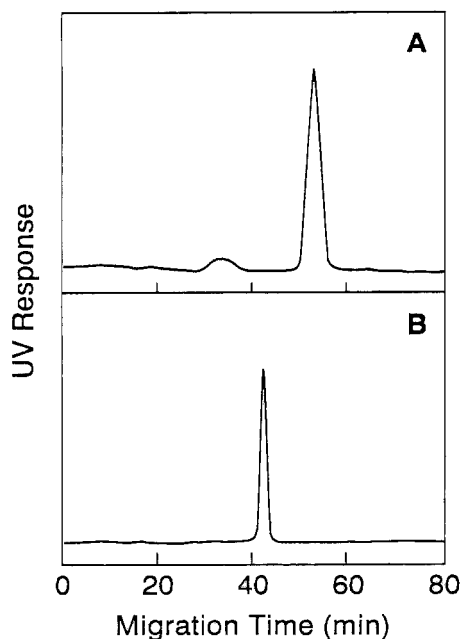


Figure 3. Electropherogram of IgE. Using the analyte concentrator fabricated of multiple capillaries associated in bundles (**panel A**), or using the analyte concentrator fabricated from a solid glass rod having a plurality of small diameter rod passages or through holes (**panel B**). For details see Experimental Section.

gration times (see Table 1), for the analyte concentrator fabricated of multiple capillaries, was due in part to a progressive clogging of the system as reflected by a reduction in the electroosmotic flow (Table 2).

The major peak in Figure 3A, and the single peak in Figure 3B, were collected after several injections by a method described elsewhere (49,79). Further analysis of these collected peaks by ELISA (Table 3) demonstrated that the substances present in the major peaks corresponded to IgE, as indicated by the higher O.D. values for IgE and the major peaks collected versus the near basement O.D. values for the control samples. This observation, strongly suggests

Table 1. IgE Migration Time (in minutes) for Six Consecutive Serum Analyses Using the Same AC-CE Capillary			
Analyte concentrator made of bundles of microcapillaries		Analyte concentrator made of rod passages or through holes	
1	42	1	42
2	44	2	42
3	46	3	42
4	49	4	42
5	51	5	43
6	54	6	43

Table 2. Electroosmotic Flow (nL/mm/sec x 10³) for Six Consecutive Injections of Serum into the Same AC-CE Capillary			
Analyte concentrator made of bundles of microcapillaries		Analyte concentrator made of rod passages or through holes	
1	54	1	56
2	51	2	55
3	48	3	55
4	45	4	54
5	42	5	53
6	39	6	53

minutes and run buffer for 15 minutes. Between runs, the capillary was rinsed with 0.1 potassium hydroxide, water and run buffer for 2 minutes each. The run voltage for all separations was +5 kV. Organic solvent/phosphate buffer mixtures were prepared by volume. It should be noted that mixtures of SDS and vancomycin used in this study tend to precipitate in organic solvent/phosphate buffer solutions. These additives can be dissolved initially by sonication but will precipitate from solution within a few hours as evidenced by a deterioration in the electropherogram.

RESULTS AND DISCUSSION

The structure of vancomycin is shown in Figure 1. The properties of this macrocyclic antibiotic which make it a useful chiral selector in LC and CE have been described in detail previously (1,3,4). When used as an HPLC chiral stationary phase, vancomycin resolves a large number of neutral organic racemates as well as negatively charged analytes. However, in CE, only the enantioresolution of negatively charged racemates have been reported thus far.

The isoelectric point of vancomycin is ~ 7.2 (1). Consequently at pH 7.0, it elutes at nearly the same time as a neutral solute carried by the electroosmotic flow. This is illustrated in Figure 2A. Note that a neutral racemate would have to elute and separate in the very small window between the vancomycin peak and eof trough (Fig. 2). This expected elution profile assumes that there is no interaction between the solute-selector complex and the capillary wall. Lowering the pH to 5.0 increases the elution window and therefore the possibility of obtaining a separation to some extent (Fig. 2B). However, this still represents a very limited area in which to achieve a separation. The somewhat greater distance between the vancomycin peak and the eof trough at this pH results from the fact that electrophoretic mobility

injection sample volume to less than 50 nL, which for low concentration samples can result in no detection of the analyte unless derivatization or concentration of sample is performed.

Since those early reports, considerable progress has been made in reducing the effects of the charged capillary wall. These innovative strategies have been able to minimize the problems of analyte adsorption and lack of reproducibility. However, the remaining of the problem related to the limitation in sample volume that can be injected into the CE column, and still be able to achieve analyte detection sensitivity, has experienced less progress.

In general, components of interest in biological fluids are often found in extremely low concentrations. This fact combined with only being able to sample nanoliters has restricted the use of CE in biomedical applications. Recent reports addressing this issue have focused on derivatization, off-line concentration, as well as low volume on-line preconcentration techniques in order to increase the detection of the material being analyzed (for reviews see ref. 15-18,61,65,75). Derivatization techniques are often difficult to be carried out stoichiometrically for complex molecules. Most preconcentration techniques for CE, although have improved detection limits, still limit the volume sampled to less than 1 μ L.

The present report outlines a major advance in the detection of molecules at ultra-low concentrations (e.g., fg/mL) in biological fluids. It is feasible to increase detectability of samples present in small concentration in biological fluids by affinity concentration using an analyte concentrator-reaction chamber. In this case, it is demonstrated that IgE was bound to and eluted from the analyte concentrator-containing anti-IgE. However, technical problems were encountered with the fabrication of the analyte concentrator made of bundle of microcapillaries. The microcapillaries were hand fitted within another larger tube. This method of fabrication produced empty spaces in between the microcapillaries which made account for the non-specific binding of serum substances, and a progressive reduction in the electroosmotic flow. In turn, the electropherogram of IgE was not reproducible. On the other hand, the multi holes analyte concentrator fabricated without these interspaces, produced a system with a superior performance. The addition of several chemicals to link antibodies directed against IgE to the inner surface of the capillary, may have produced a different kind of chemical reaction(s) in the interspace of the capillaries, since they were coated with polyimide. The resulting chemistries may have cause the accumulation of excess amount of material producing a dysfunctional capillary.

The analyte concentrator-reaction chamber offers the potential of solving some of the problems still unresolved in the CE technology. Especially those problems in which limitations exist in reaching practical concentration limits of detection of biologically active analytes present in tissue biopsies, cells, and biological fluids. Nevertheless, some practical considerations in the fabrication of the AC-RC for routine use is still under investigation. For example, the compactness of beads in the small space within the frits, and the high packing tendency of membranes, normally increases back pressure that reduces hydrodynamic flow within the CE capillary. In fact, it is almost impossible to fabricate a cartridge (containing beads) greater than 3 mm in length without affecting reproducibility of separation and increasing the tendency of blocking the system after limited usage. In the case of commercially available membranes coated/impregnated with an appropriate chemistry, a 1 mm in length solid support is tolerated for an optimum AC-RC, higher capacity preconcentrators-containing membranes using a larger bed volume can produce irreproducible data, the possibility of progressive clogging of the system, and a very short life span. However, it is possible that larger surface areas may be unnecessary when using membranes, since suitably impregnated membranes normally have a high binding capacity for analytes.

In conclusion, a new way to pre-concentrate samples found in minute quantities in biological fluids using a novel design of analyte concentrator is presented. We are currently comparing the efficiency and practicality of fabrication of various kinds of analyte concentrators-reaction chambers described in the literature. We are also improving the methodology of fabrication for massive production, facile of use and performance, and repetitive usages of the cartridges. However, the fabrication of an analyte concentrator-reaction chamber for commercial use faces many improvements in the years to come.

REFERENCES

1. Johansson, S.G.O., and H. Bennich. *Immunol.*, 13: 381-394, 1967.
2. Ishizaka, K., and T. Ishizaka. *J. Immunol.*, 99: 1187-1198, 1967.
3. Sutton, B.J., and H.J. Gould. *Nature*, 366: 421-428, 1993.
4. Ishizaka, K., T. Ishizaka, and E.H. Lee. *Immunochem.*, 7: 687-702, 1970.
5. Ikeyama, S., S. Nakagawa, A. Arakawa, H. Sugino, and A. Kakinuma. *Mol. Immunol.*, 23: 159-167, 1986.
6. Nilsson, K., H. Bennich, S.G.O. Johansson, and J. Pontén. *Clin. Exp. Immunol.*, 7: 477-489, 1970.

7. Hamilton, R.G., R.W. Wilson, T. Spillman, and M. Roebber. *J. Immunoassay*, 9: 275-296, 1988.
8. Hamilton, R.G., and N.F. Adkinson, Jr. In: *Manual of Clinical Immunology* (H.R. Rose, E.C. de Macario, J.L. Fahey, H. Friedman, and G.M. Penn, Eds.). American Society for Microbiology, Washington, D.C., pp. 689-701, 1992.
9. Nielsen, R.G., E.C. Rickard, P.F. Santa, D.A. Sharknas, and G.S.J. Sittampalam. *J. Chromatogr.*, 539: 177-185, 1991.
10. Schultz, N., and R.T. Kennedy. *Anal. Chem.*, 65: 3161-3165, 1993.
11. Shimura, K., and B.L. Karger. *Anal. Chem.*, 66: 9-15, 1994.
12. Rosenzweig, Z., and E.S. Yeung. *Anal. Chem.*, 66: 1771-1776, 1994.
13. Schmaizing, D., W. Nashabeh, X.-W. Yao, R. Mhatre, F.E. Regnier, N.B. Afeyan, and M. Fuchs. *Anal. Chem.*, 67: 606-612, 1995.
14. Regnier, F.E., D.H. Patterson, and B.J. Harmon. *Trends Anal. Chem.*, 14: 177-181, 1995.
15. Guzman, N.A. (Ed.). *Capillary Electrophoresis Technology*. Chromatographic Series, volume 64. Marcel Dekker, Inc., New York, Basel, Hong-Kong, 1993.
16. Camilleri, P. (Ed.). *Capillary Electrophoresis-Theory and Practice*. CRC Press, Boca Raton, 1993.
17. Weinberger, R. *Practical Capillary Electrophoresis*. Academic Press, 1993.
18. Landers, J.P. (Ed.). *Handbook of Capillary Electrophoresis*. CRC Press, Boca Raton, 1994.
19. Mikkers, F.E.P., F.M. Everaerts, Th.P.E.M. Verheggen. *J. Chromatogr.*, 169: 1-10, 1979.
20. Moring, S.E., J.C. Colburn, P.D. Grossman, and H.H. Lauer. *LC-GC*, 8: 34-46, 1989.
21. Abersold, R., and H.D. Morrison. *J. Chromatogr.*, 516: 79-88, 1990.
22. Gebauer, P., W. Thormann, and P. Bocek. *J. Chromatogr.*, 608: 47-57, 1992.
23. Schwer, C., and F. Lottspeich. *J. Chromatogr.*, 623: 345-355, 1992.
24. Beckers, J.L., and M.T. Ackermans. *J. Chromatogr.*, 629: 371-378, 1993.
25. Chien, R-L., and D.S. Burgi. *J. Chromatogr.*, 559: 141-152, 1991.
26. Burgi, D.S., and R-L. Chien. *Anal. Chem.*, 63: 2042-2047, 1991.
27. Chien, R-L., and D.S. Burgi. *Anal. Chem.*, 64: 1046-1050, 1992.
28. Chien, R-L., and D.S. Burgi. *Anal. Chem.*, 64: 489A-496A, 1992.
29. Foret, F., V. Sustacek, and P. Bocek. *J. Microcol. Sep.*, 2: 229-233, 1990.

30. Smith, R.D., S.M. Fields, J.A. Loo, C.J. Barinaga, H.R. Udseth, and C.G. Edmonds. *Electrophoresis*, 11: 709-717, 1990.
31. Beckerts, J.L., and F.M. Everaerts. *J. Chromatogr.*, 508: 19-26, 1990.
32. Stegehuis, D.S., H. Irth, U.R. Tjaden, and J. van der Greef. *J. Chromatogr.*, 538: 393-402, 1991.
33. Tinke, A.P., N.J. Reinhoud, W.M.A. Niessen, U.R. Tjaden, and J. van der Greef. *Rapid Commun. Mass. Spectrom.*, 6: 560-563, 1992.
34. Foret, F., E. Szoko, and B.L. Karger. *J. Chromatogr.*, 608: 3-12, 1992.
35. Benson, L.M., A.J. Tomlinson, J.M. Reid, D.L. Walker, M.M. Ames, and S. Naylor. *J. High Resol. Chromatogr.*, 16: 324-326, 1993.
36. Lamoree, M.H., N.J. Reinhold, U.R. Tjaden, W.M.A. Niessen, and J. van der Greef. *Biol. Mass Spectrom.*, 23: 339-345, 1994.
37. Locke, S.J., and P. Thibault. *Anal. Chem.*, 66: 3436-3446, 1994.
38. Guzman, N.A. PCT Patent WO 89/04966, June 1, 1989.
39. Guzman, N.A. Taiwan Patent 33861, August 21, 1989.
40. Guzman, N.A. South Africa Patent 88/8823, June 27, 1990.
41. Guzman, N.A. U.S. Patent 5,045,172, September 3, 1991.
42. Guzman, N.A., M.A. Trebilcock, and J.P. Advis. The 42nd Pittsburgh Conference & Exposition on Analytical Chemistry and Applied Spectroscopy, Chicago, Illinois, March 4-7, 1991, pp. 160.
43. Guzman, N.A., M.A. Trebilcock, and J.P. Advis. *J. Liq. Chromatogr.*, 14: 997-1015, 1991.
44. Debets, A.J.J., M. Mazereeuw, W.H. Voogt, D.J. van Iperen, H. Lingeman, and K-P. Hupe. *J. Chromatogr.*, 608: 151-158, 1992.
45. Guzman, N.A. U.S. Patent 5,202,010, April 13, 1993.
46. Guzman, N.A. Canada Patent 1,322,221, September 14, 1993.
47. Guzman, N.A. Mexico Patent 169.909, July 30, 1993.
48. Guzman, N.A. PCT Patent WO 93/05390, March 18, 1993.
49. Guzman, N.A., C.L. Gonzalez, M.A. Trebilcock, L. Hernandez, C.M. Berck, and J.P. Advis. In: *Capillary Electrophoresis Technology* (N.A. Guzman, Ed.), Chromatographic Science Series Volume 64, Chapter 22, pp. 643-672. Marcel Dekker, New York-Basel-Hong Kong, 1993.
50. Swartz, M.E., and M. Merion. *J. Chromatogr.*, 632: 209-213, 1993.
51. Hoyt, Jr., A.M., S.C. Beale, J.P. Larmann, Jr., and J.W. Jorgenson. *J. Microcol. Sep.*, 5: 325-330, 1993.
52. Fuchs, M., and M. Merion. U.S. Patent 5,246,577, September 21, 1993.
53. Morita, I., and J. Sawada. *J. Chromatogr.*, 641: 375-381, 1993.
54. Fishman, H.A., J.B. Shear, L.A. Colon, and R.N. Zare. U.S. Patent 5,318,680, June 7, 1994.

55. Tomlinson, A.J., L.M. Benson, R.P. Oda, W. D. Braddock, M.A. Strausbauch, P.J. Wettstein, and S. Naylor. *J. High Res. Chromatogr.*, 17: 669-671, 1994.
56. Benson, L.M., A.J. Tomlinson, and S. Naylor. *J. High Res. Chromatogr.*, 17: 671-673, 1994.
57. Tomlinson, A.J., L.M. Benson, W.D. Braddock, R.P. Oda, and S. Naylor. *J. High Res. Chromatogr.*, 17: 729-732, 1994.
58. Guzman, N.A. Taiwan Patent 68130, October 1, 1994.
59. Tomlinson, A.J., L.M. Benson, and S. Naylor. *J. Cap. Elec.*, 1: 127-135, 1994.
60. Naylor, S., L.M. Benson, and A.J. Tomlinson. *J. Cap. Elec.*, 1: 181-189, 1994.
61. Tomlinson, A.J., L.M. Benson, R.P. Oda, W.D. Braddock, B.L. Riggs, J.A. Katzmann, and S. Naylor. *J. Cap. Elec.*, 2: 97-104, 1995.
62. Pálmarsdóttir, S., and L-E. Edholm. *J. Chromatogr. A*, 693: 131-143, 1995.
63. Beattie, J.H., R. Self, and M.P. Richards. *Electrophoresis*, 16: 322-328, 1995.
64. Strausbauch, M.A., B.J. Madden, P.J. Wettstein, and J.P. Landers. *Electrophoresis*, 16: 541-548, 1995.
65. Tomlinson, A.J., L.M. Benson, W.D. Braddock, and R.P. Oda. *J. High Resol. Chromatogr.*, 18: 381-386, 1995.
66. Brenner, N., and R. Palmieri. U.S. Patent 5,340,452, August 23, 1994.
67. Guzman, N.A. Sixth Annual Symposium of the Protein Society, San Diego, California, July 25-29, 1992, Abstract T-76.
68. Guzman, N.A. The Third Annual Frederick Conference on Capillary Electrophoresis, Frederick, Maryland, October 20-21, 1992, pp. 32.
69. Nashabeh, W., and Z. El Rassi. *J. Chromatogr.*, 596: 251-264, 1992.
70. Guzman, N.A., L. Hernandez, and J.P. Advis. Fifth International Symposium on High Performance Capillary Electrophoresis, Orlando, Florida, January 25-28, 1993, Abstract W-58.
71. Guzman, N.A. Seventh Annual Symposium of the Protein Society, San Diego, California, July 24-28, 1993, Abstract 315-T.
72. Guzman, N.A. Third International Conference on Human Antibodies and Hybridomas, San Antonio, Texas, October 10-13, 1993, Abstract 34.
73. Amankwa, L. N., and W.G. Kuhr. *Anal. Chem.*, 65: 2693-2697, 1993.
74. Licklider, L., and W.G. Kuhr. *Anal. Chem.*, 66: 4400-4407, 1994.
75. Guzman, N.A. In: *Capillary Electrophoresis: An Analytical Tool in Biotechnology* (P.G. Righetti, Ed.), Chapter 4, pp. 101-119, CRC Press, Boca Raton, 1995.

76. Haba, S., and A. Nisonoff. *J. Immunol. Meth.*, 183: 199-209, 1995.
77. Guzman, N.A., and L. Hernandez. In: *Techniques in Protein Chemistry* (T.E. Hugli, Ed.), Chapter 44, pp. 456-467, Academic Press, San Diego, 1989.
78. Tsang, V.C.W., and P.P. Wilkins. *J. Immunol. Meth.*, 138: 291-299, 1991.
79. Guzman, N.A., M.A. Trebilcock, and J.P. Advis. *Anal. Chim. Acta*, 249: 247-255, 1991.
80. Guzman, N.A., B.G. Hoebel, and L. Hernandez. *BioPharm*, 2: 22-37, 1989.
81. Muller, S., G. Guichard, N. Benkirane, F. Brown, M.H.V. Van Regenmortel, and J.-P. Briand. *Peptide Res.*, 8: 138-144, 1995.
82. Greenberger, M.J., R.M. Strieter, S. L. Kunkel, J.M. Danforth, R.E. Goodman, and T.J. Standiford. *J. Immunol.*, 155: 722-729, 1995.

Received: August 18, 1995

Accepted: September 6, 1995

**MICELLAR ELECTROKINETIC CAPILLARY
CHROMATOGRAPHY WITH *IN SITU* CHARGED
MICELLES. VII. EXPANDING THE UTILITY OF
ALKYLGLYCOSIDE-BORATE MICELLES TO ACIDIC
AND NEUTRAL pH FOR CAPILLARY
ELECTROPHORESIS OF DANSYL AMINO
ACIDS AND HERBICIDES¹**

YEHA MECHREF, JOEL T. SMITH², AND ZIAD EL RASSI*

*Department of Chemistry
Oklahoma State University
Stillwater, Oklahoma 74078-0447*

ABSTRACT

Micellar electrokinetic capillary chromatography (MECC) using micelles based on alkylglycoside-borate complexes, i.e., *in situ* charged micelles, was demonstrated over a wide range of pH including acidic media. The surfactants used in this study were of the alkyl-*N*-methylglucamide (MEGA) types that possess a linear sugar moiety as the polar head group. These surfactants showed the ability to complex with borate even at acidic pH, thus expanding the pH range over which *in situ* charged micelles can be used in MECC. The electrokinetic behavior of the MEGA-borate micelle at acidic and neutral pH using relatively high borate concentration was different than that observed at alkaline pH using lower borate concentration. These studies which were performed at high borate concentration suggested the formation of polyborates which increased the ionic strength and viscosity of the running electrolyte without further increasing the surface charge density of the micelle. This led to decreasing the electrophoretic mobility of the micelle and the electroosmotic flow with increasing borate concentration. The net result was an increase in the migration time window at increasing borate concentration. Moreover, the magnitude of the migration time window could be adjusted by varying the pH of the running electrolyte over the pH range from 3.5 to 9.0. The MEGA-borate systems proved useful for the separation of phenoxy acid herbicides and their esters, urea herbicides, dansyl amino acids and aromatics.

¹Presented as a lecture (# 91) at the 33rd Eastern Analytical Symposium, November 13-18, 1994, Somerset, New Jersey, U.S.A.

²Current affiliation: Monsanto Company, 800 North Lindbergh Boulevard, St. Louis, MO 63167, U.S.A.

INTRODUCTION

Several types of *in situ* charged micelles for use in micellar electrokinetic capillary chromatography (MECC) of neutral and charged species have been recently introduced and characterized by our laboratory [1-7]. These new micellar phases are essentially anionic complexes formed between alkyl- [2-7] or steroidal-glycoside [1] surfactants and borate or boronate anions. *In situ* charged micelles possess many unique and attractive features including: (i) an adjustable surface charge density (ii) a weaker hydrophobic character than the traditional alkyl surfactants, and (iii) chiral selectivity. In addition, and as a result of the variable surface charge density, *in situ* charged micelles allow the manipulation of the migration time window and in turn the optimization of analysis time, resolution and peak capacity *via* changing pH and borate or boronate concentration of the running electrolyte.

Thus far, we have demonstrated the usefulness of *in situ* charged micelles in the alkaline pH range in MECC of chiral and achiral polyaromatics, pesticides, amino acids, barbiturates and medicarpins and precursors [1-7]. In this report, we wish to extend the useful pH range of *in situ* charged micelles to the acidic as well as neutral pH.

In earlier reports on *in situ* charged micelles [2, 3], we have demonstrated by ¹¹B NMR studies that alkylglycoside surfactants with acyclic sugar head groups, such as MEGA surfactants, have 3 to 5 fold higher affinity for borate ions than their counterparts with cyclic sugar head groups (e.g., octylglucoside, octylmaltoside). This observation, which corroborates well previous findings [8] in that linear sugars complex stronger with borate than cyclic ones, prompted us to select the MEGA surfactants for our present studies at lower pH range. The principles of *in situ* charged micelles have been discussed in previous contributions from our laboratory [2, 3, 7], and the complexation of borate with polyols have been briefly described recently by El Rassi [9], El Rassi and Nashabeh [10], and Hoffstetter-Kuhn et al. [11]. For simplicity, the term "borate ions" or "borate" is used in this article to refer to all kinds of borate species. But, whenever a specific borate species is involved the exact term is utilized instead.

EXPERIMENTAL

Instrument

The instrument for capillary electrophoresis was assembled in-house from commercially available components [2, 12]. It was comprised of two high-voltage power supplies of positive and negative polarity, Models MJ30P400 and MJ30N400, respectively, from Glassman High Voltage (Whitehouse Station, NJ, USA) and a UV-Vis variable wavelength detector Model 200, equipped with a cell for on-column detection from Linear Instruments (Reno, NV, USA). The detection wavelength was set at 240 nm for the detection of phenoxy acid herbicides and phenoxy ester herbicides as well as urea herbicides, 254 nm for the detection of alkyl phenyl ketones and dansyl amino acids and 340 nm for the detection of Sudan III. Electropherograms were recorded with a Shimadzu computing integrator Model CR4A (Columbia, MD, USA).

Fused-silica capillary columns of 50 μm I.D. and 365 μm O.D. were obtained from Polymicro Technology (Phoenix, AZ, USA). Throughout the present study, the total length of the capillary was 80 cm while the separation length was 50 cm.

Reagents and Materials

Nonanoyl-*N*-methylglucamide (MEGA 9) and decanoyl-*N*-methylglucamide (MEGA 10) were purchased from Calbiochem Corp. (La Jolla, CA, USA). All herbicides were purchased from ChemService (West Chester, PA, USA). Sudan III, which was used as the tracer of the migration time of the micelle, and alkyl phenyl ketones were obtained from Aldrich Chemical Co. (Milwaukee, WI, USA). Dansyl amino acids were purchased from Sigma Chemical Co. (St. Louis, MO, USA). The chemicals used in the preparation of electrolytes as well as the 0.2 μm Uniprep Syringeless filters used in the filtration of the electrolyte were purchased from Fisher Scientific (Pittsburgh, PA, USA). All solutions were prepared with deionized water.

RESULTS AND DISCUSSION

Dependence of the Magnitude of the Migration Time Window on Borate Concentration

As shown in Fig. 1a, the migration time window of the micellar phase under investigation increased with borate concentration, and to a larger extent at borate concentration higher than 500 mM. This increase is primarily due to the decrease in the electroosmotic flow, EOF, (see Fig. 1b) given the fact that the electrophoretic mobility of the MEGA 9-borate micelle decreased slightly in the range 100 to 600 mM borate or remained almost the same at borate concentrations above 600 mM as shown in Fig. 1b. Since by increasing the borate concentration in the running electrolyte, the values of both the electroosmotic velocity, v_{eo} , and electrophoretic velocity of the micelle, $v_{ep(mc)}$, are decreasing and approaching each other (see Fig. 1b), the difference between the two velocities will decrease with increasing borate concentration. Due to the fact that the electroosmotic velocity and electrophoretic velocity of the micelle are of opposite sign, and according to the following equation, which relates the migration time of the micelle, t_{mc} , to v_{eo} , $v_{ep(mc)}$ and the separation distance in the capillary, l ,

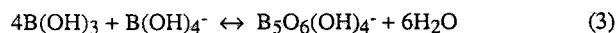
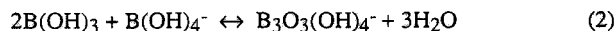
$$t_{mc} = \frac{l}{v_{eo} + v_{ep(mc)}} \quad (I)$$

t_{mc} will increase, and consequently the breadth of the migration time window will enlarge with increasing borate concentration, see Fig. 1a.

Aqueous borate solutions contain tetrahydroxyborate anion, which is formed according to the following equilibrium,



as well as polyborate anions [13-15] such as $B_3O_3(OH)_4^-$, $B_5O_6(OH)_4^-$, $B_3O_3(OH)_5^{2-}$ and $B_4O_5(OH)_4^{2-}$. Singly charged trimer and pentamer borate anions are formed by the following equilibria, respectively [16]:



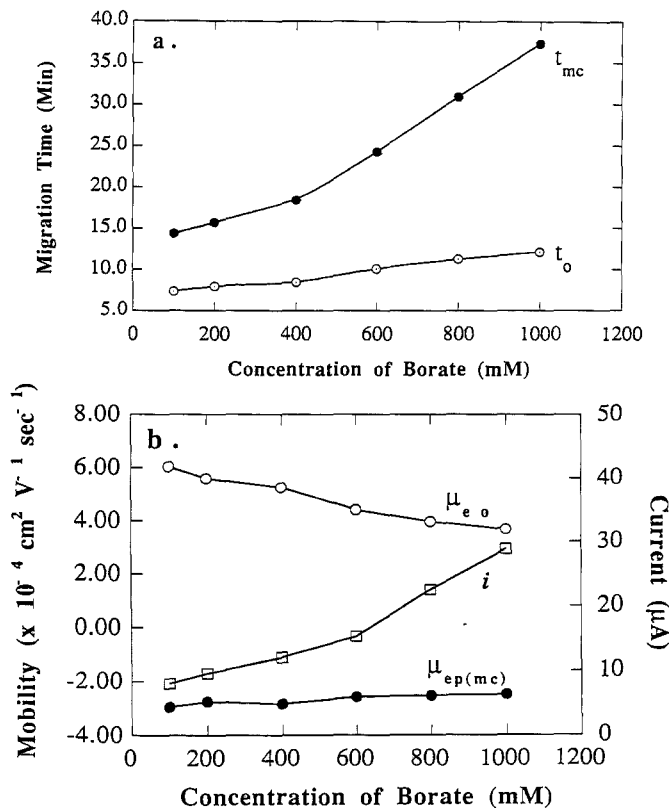
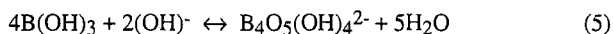
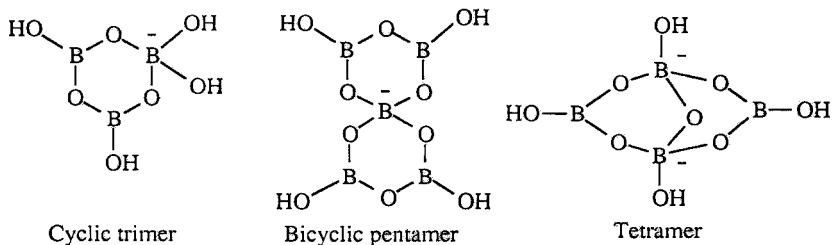


FIGURE 1. Effect of borate concentration on the magnitude of the migration time window in (a) and the electrophoretic mobility of the micelle as well as the electroosmotic mobility and current in (b). Separation capillary, bare fused-silica, 50.0 cm / 80.0 cm x 50 μm i.d.; running electrolyte, 5.0 mM sodium phosphate containing 50.0 mM MEGA 9 and various borate concentration, pH 7.0; running voltage, 15.0 kV; tmc tracer, sudan III; t_o marker, methanol.

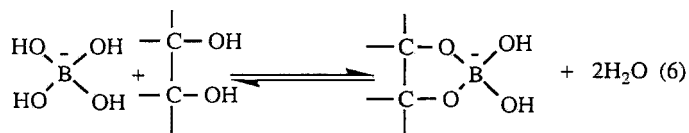
while doubly charged trimer and tetramer anions are produced by the two following equilibria, respectively:



Whereas equilibria 1 and 2 are predominant at low borate concentration (e.g., ≤ 200 mM), the other polyborate anions formed by equilibria 3, 4 and 5 become important species at high borate concentration [15]. For three of these polyborate anions the following structures were suggested [16, 17]:



The complexation of borate with compounds having vicinal hydroxyl groups, such as the MEGA surfactant used in this study, is thought to occur mainly *via* the reaction of the tetrahydroxyborate ion $B(OH)_4^-$ and the polyolic compound according to the following equilibrium:



In fact, equilibrium 6 is favored when the O-O distances for the vicinal diol in the polyol compound and for the hydroxyls in the borate ion are on the order of 2.4 \AA . This distance is that of the O-O in the tetrahedral boron [18]. On this basis, among polyborate anions, only the cyclic trimer will have the probability to complex with the polyol head group of the MEGA surfactant. However, it can be suggested that due to steric hindrance, the cyclic triborate will complex less than the tetrahydroxyborate anion with a given polyolic compound.

Returning to Fig. 1b, the decrease in the EOF and electrophoretic mobility of the micelle can be explained as follows. At 100 mM borate, pH 7.0, the electrophoretic mobility of the micelle ($\mu_{cp(mc)}$) is quite high which is indicative of the formation of complexing borate ions, e.g., tetrahydroxyborate and cyclic trimer. As the amount of

added boric acid was increased between 200 and 1000 mM, $\mu_{ep(mc)}$ decreased. This may indicate that the concentration of polyborate species such as those shown in equilibria 3, 4 and 5 had increased, a phenomenon that would increase the ionic strength of the running electrolyte without further increasing the surface charge density of the micelle. In fact, and as shown in Fig. 1b, the current i , which is an indirect measure of the magnitude of the ionic strength, has increased with borate concentration over the concentration range studied. As discussed above, the polyborate species such as $B_5O_6(OH)_4^-$, $B_3O_3(OH)_5^{2-}$ and $B_4O_5(OH)_4^{2-}$ are unlikely to complex with vicinal diols. Thus, since increasing the ionic strength of the running electrolyte is accompanied by little or no further increase in the surface charge density of the micelle, the net result is a decrease in the electrophoretic mobility of the MEGA-borate micelle. The decrease in EOF is due to increasing the ionic strength of the running electrolyte. Moreover, the decrease in both parameters (i.e., EOF and electrophoretic mobility of the micelle) may be in part attributed to increasing the viscosity of the running electrolyte at high borate concentration.

Figure 2 displays typical electropherograms of alkyl phenyl ketones obtained at various borate concentrations. As can be seen in this figure, increasing the borate concentration of the running electrolyte have resulted in longer analysis time, i.e., wider migration time window. The rationale of being able to change the migration time window is well illustrated in Fig. 2, whereby the solutes can be completely resolved in less than 15 min using a running electrolyte with borate concentration as low as 100 mM at pH 7.0.

Dependence of the Magnitude of the Migration Time Window on pH.

The effect of the pH of the running electrolyte on the magnitude of the migration time window is shown in Fig. 3a. Increasing the pH of the running electrolyte between pH 3.5 and 6.5 is accompanied by an increase in EOF and electrophoretic mobility of the micelle (see Fig. 3b). The increase in the EOF with increasing pH is due to the ionization of the silanol groups on the inner capillary walls, while the increase in the electrophoretic mobility of the micelle is indicative of increasing the charge density of the micelle. At 400

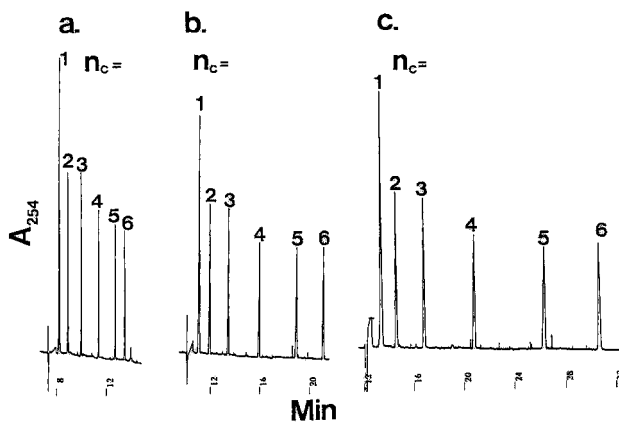


FIGURE 2. Typical electropherograms of alkyl phenyl ketones obtained at different sodium borate concentrations. Running electrolytes, 5.0 mM sodium phosphate containing 50.0 mM MEGA 9, pH 7.0, at various borate concentration: 100 mM (a), 600 mM (b) and 1000 mM (c). Solutes: 1, acetophenone; 2, propiophenone; 3, butyrophenone; 4, valerophenone; 5, hexanophenone; 6, heptanophenone. Other conditions as in Fig. 1.

mM borate in the running electrolyte, increasing the pH between 3.5 and 6.5 may have resulted in yielding higher amounts of complexing borate anions such as tetrahydroxyborate and cyclic trimer anions. This means that equilibria 1 and 2 shifted to the right as the pH was increased (high OH^- concentration).

On the other hand, at $\text{pH} > 6.5$ and using 400 mM boric acid in the running electrolyte, the EOF decreased with increasing pH of the medium. This decrease in the EOF may be attributed to a higher ionic strength at elevated pH as more borate ions are produced. In fact, Fig. 3b shows the sharp increase in the current at $\text{pH} > 6.5$, which is reflective of an increase in the ionic strength of the running electrolyte. Moreover, the electrophoretic mobility of the micelle decreased slightly or stayed the same at pH values greater than 6.5. This may reflect that the magnitude of the increase in the ionic strength is greater than that of the surface charge density of the micelle. It is likely that at 400 mM borate concentration, $\text{pH} > 6.5$, non complexing polyborates start to be produced in a

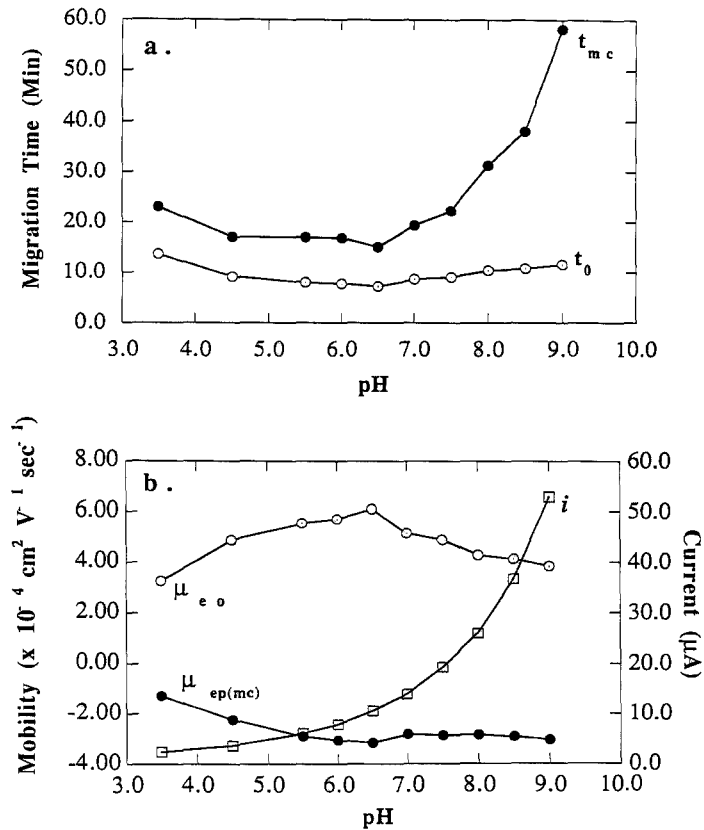


FIGURE 3. Effect of pH on the magnitude of the migration time window in (a) and the electrophoretic mobility of the micelle as well as the electroosmotic mobility and current in (b). Running electrolyte, 5.0 mM sodium phosphate containing 50.0 mM MEGA 9 and 400 mM borate at various pH values. Other conditions as in Fig. 1.

significant amount so that the increase in the ionic strength of the running electrolyte would outweigh the increase in the surface charge density of the micelle.

The increase in the breadth of the migration time window at pH values of 7.0 and above is the result of the decrease in the difference between the electroosmotic velocity and the electrophoretic velocity of the micelle (see eqn I). As can be seen in Fig. 3a, in the pH range 3.5-6.5 the migration time window exhibits almost constant breadth. This can be

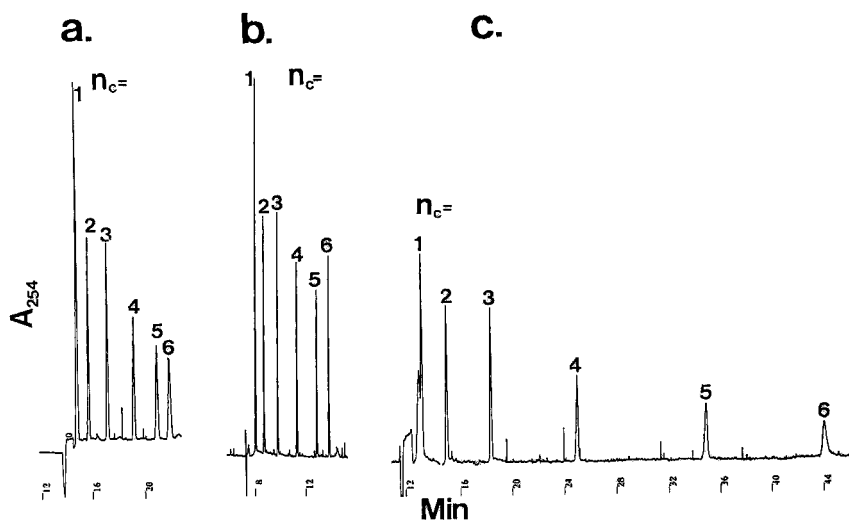


FIGURE 4. Typical electropherograms of alkyl phenyl ketones at various pH. Running electrolyte, 5.0 mM sodium phosphate containing 50.0 mM MEGA 9 and 400 mM borate, at pH 3.5 (a), 6.5 (b) and 9.0 (c). Solutes: 1, acetophenone; 2, propiophenone; 3, butyrophenone; 4, valerophenone; 5, hexanophenone; 6, heptanophenone. Other conditions as in Fig. 1.

attributed to the fact that both the EOF and the electrophoretic mobility of the micelle increased by almost the same factor.

Figure 4 shows representative electropherograms of alkyl phenyl ketones at various pH values. Using 400 mM borate even at a pH as low as 3.5, a negative charge can be introduced into the micelle and the separation of the various solutes can be achieved. As in the case of various borate concentration (see Fig. 2), the results obtained at various pH (see Fig. 4) show the advantage of being able to manipulate the migration time window. Using 400 mM borate at pH 6.5 as the running electrolyte seems to provide the fastest analysis time with excellent resolution among the various homologous solutes.

In summary, using relatively high borate concentration (e.g., 400 mM) in the running electrolyte, the migration time window and the analysis time of the *in situ* charged micellar system can be varied conveniently with changing pH. This represents a definitive

advantage over traditionally used micelles such as sodium dodecyl sulfate (SDS) which are characterized by a fixed surface charge density. In fact, with the MEGA-borate micelles, the EOF remains stronger in magnitude than the electrophoretic mobility of the *in situ* charged micelles, thus allowing the migration of the micelle toward the cathodic end over a wide pH range. This was not the case of the SDS micelle, where it was shown that the direction of the micelle was reversed as the pH was lowered to below pH 5.0 [19]. Under this condition, weakly or non partitioning solutes into the micellar system would be very retarded or would not elute.

Correlation Between Capacity Factor and Carbon Number, n_c , of Homologous Series.

The retention behavior of alkyl phenyl ketones, having alkyl chains with carbon number, n_c , from 1 to 6, was examined using a MEGA 9-borate micellar phase. Plots of the logarithmic capacity factors ($\log k'$) of the alkyl phenyl ketone homologous solutes versus n_c of the homologous series at different pH values and borate concentration yielded straight lines, and the linear regression data are listed in Tables 1 and 2. These data are in accordance with those reported previously with MEGA 9-borate micelle phase at pH ≥ 9 [2], and follow the linear expression

$$\log k' = (\log \alpha) n_c + \log \beta$$

where the slope $\log \alpha$ is a measure of methylene group (CH_2) or hydrophobic selectivity which characterizes nonspecific interactions, while the intercept $\log \beta$ reflects the specific interactions between the residue of the molecule and the aqueous and micellar phases. This equation implies a constant contribution to the free energy of transfer of the solute between the aqueous phase and the micellar phase with each CH_2 increment in the chain length of the homologous series. The data obtained at acidic and neutral pH values were in good agreement with those reported previously at pH ≥ 9 [2] to the extent that the slope and the intercept values are almost identical. This would suggest that the retention behavior of these micellar phases towards uncharged solutes at neutral and acidic pH conditions is similar to that obtained at alkaline conditions.

TABLE 1

Values of Slope, Intercept and R for the Correlation Between Capacity Factor, k' , and Carbon Number in the Alkyl Chain of Alkyl Phenyl Ketones [$\log k' = (\log \alpha) n_c + \log \beta$] at Various pH Values^a.

pH	$\log \beta$	$\log \alpha$	R
3.5	-1.04	0.360	0.999
4.5	-1.03	0.367	0.999
5.5	-0.97	0.340	0.999
6.5	-0.97	0.330	0.999
7.5	-1.03	0.340	0.999
8.5	-1.09	0.350	0.999

^a[MEGA 9] = 50 mM; [Borate] = 400 mM; [Phosphate] = 5 mM; 15.0 kV.

TABLE 2

Values of Slope, Intercept and R for the Correlation Between Capacity Factor, k' , and Carbon Number in the Alkyl Chain of Alkyl Phenyl Ketones [$\log k' = (\log \alpha) n_c + \log \beta$] at Various Borate Concentration^a.

[Borate], mM	$\log \beta$	$\log \alpha$	R
100	-0.92	0.34	0.999
200	-1.10	0.37	0.999
400	-1.02	0.33	0.999
600	-1.12	0.34	0.999
800	-1.10	0.34	0.999
1000	-1.15	0.34	0.999

^a [MEGA 9] = 50 mM; pH 10.0; [Phosphate] = 5 mM; 15.0 kV.

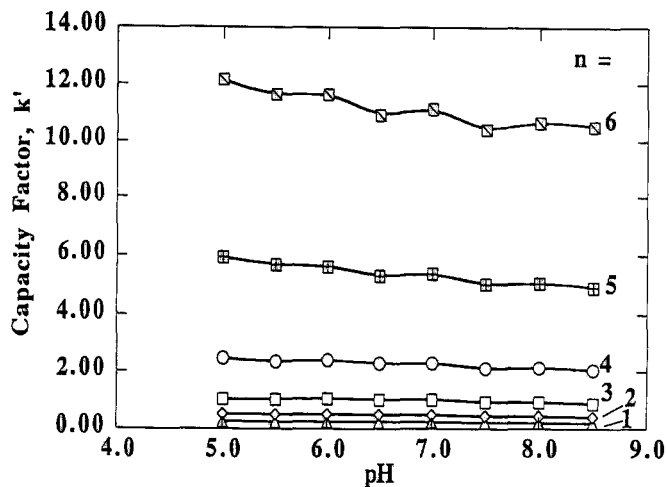


FIGURE 5. Plots of capacity factor k' vs. pH of the running electrolyte. solutes as in Fig. 2. Other conditions as in Fig. 1.

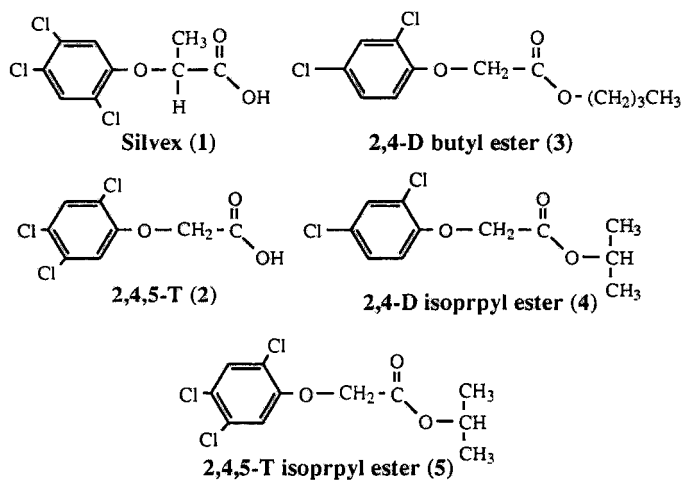
Dependence of Capacity Factor on pH.

Figure 5 shows the dependence of the capacity factor on pH. As expected, the value of the capacity factor remained more or less constant over the pH domain studied. These results agree with those observed at higher pH domain [2]. The capacity factors of the first four solutes of the homologous series were practically unaffected by pH, while the k' of the other two solutes ($n_c = 5$ and 6) showed slight decrease and some fluctuations as the pH was changed. The slight fluctuations are within the range of experimental errors while the decrease in retention may be attributed to increasing Joule heating as a result of increasing the current with pH.

Illustrative Applications

Phenoxy Acid Herbicides and their Esters. An advantage of the MEGA-borate micellar phase at low pH resides in its ability to separate acidic herbicides and their esters. The separation of ester herbicides employing MEGA-borate micellar phases at alkaline pH

values was not successful due to the fact that esters hydrolyze readily in alkaline media (results not shown). Figure 6 illustrates the separation of a mixture of five herbicides (see below for structures) consisting of two acidic herbicides (silvex and 2,4,5-T) and three ester herbicides namely 2,4-D isopropyl ester, 2,4-D butyl ester and 2,4,5-T isopropyl ester.



The separation was carried out using 200 mM sodium borate containing 50 mM MEGA 9 and 5.0 mM sodium phosphate, pH 7.0. Under these separation conditions, silvex and 2,4,5-T are negatively charged and as a result they associate very weakly with the negatively charged MEGA-borate micellar phase, thus migrating mostly by their own electrophoretic mobility faster than the other three analytes. The ester herbicides are neutral and therefore their elution order reflects their relative hydrophobicity. The separation is completed in less than 15 min with an average plate count of 325 000 plates/m.

Urea Herbicides. Fig. 7a and b illustrates the separation of nine urea herbicides (for structures, see below) using MEGA 10-borate micellar phases at pH 5.0 and 7.0, respectively. With the exception of terbacil, the elution order of the components of the standard mixture is the same as that reported in an earlier study [2] using the same micellar phase but at pH 10.0. At pH 5.0 and 7.0, terbacil eluted first while at pH 10.0 it migrated

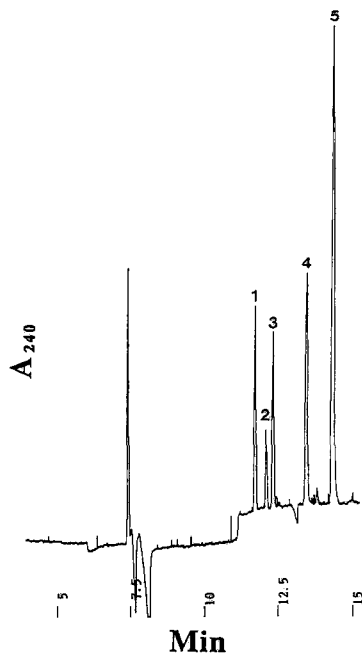
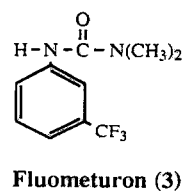
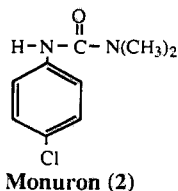
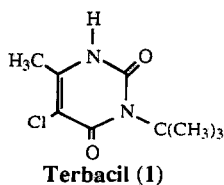


FIGURE 6. Electropherogram of phenoxy acid herbicides and their esters. Running electrolyte, 5.0 mM sodium phosphate containing 50.0 mM MEGA 9 and 400 mM borate, pH 7.0. Solutes: 1, silvex; 2, 2,4,5-T; 3, 2,4-D butyl ester; 4, 2,4-D isopropyl ester; 5, 2,4,5-T isopropyl ester. Other conditions as in Fig. 1.

slower than monuron and fluometuron [2]. This illustrates the advantages of being able to utilize a given *in situ* charged micellar phase over a wide range of pH, as far as changing the selectivity of the MECC system is concerned. The average plate counts per meter were 224 000 and 189 000 at pH 5.0 and 6.0, respectively.



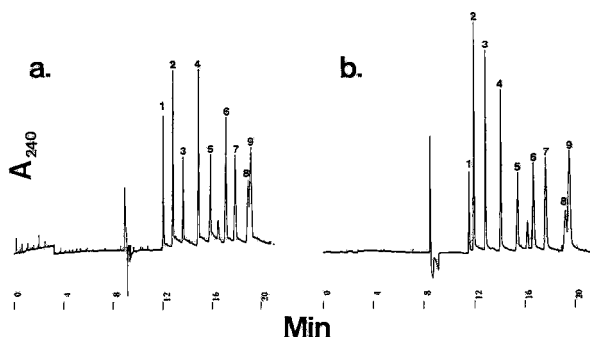
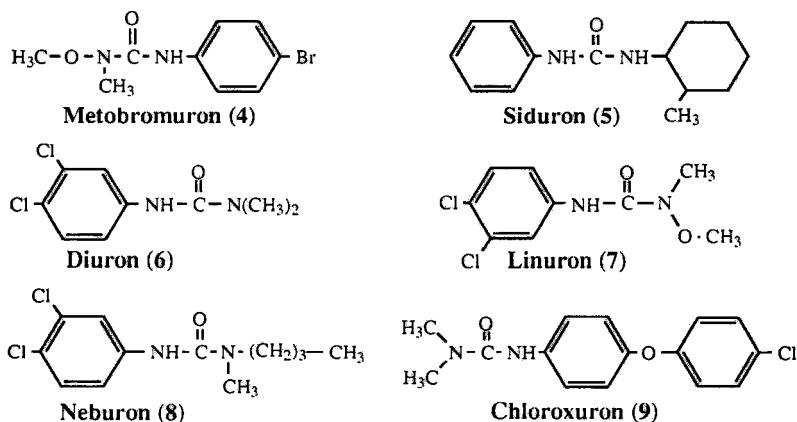


FIGURE 7. Electropherograms of urea herbicides. Running electrolytes, 5.0 mM sodium phosphate containing 50.0 mM MEGA 10 and 400 mM borate, pH 5.0, in (a) or 200 mM borate, pH 7.0 in (b). Solutes: 1, terbacil; 2, monuron; 3, fluometuron; 4, metobromuron; 5, siduron; 6, diuron; 7, linuron; 8, neburon; 9, chloroxuron. Other conditions as in Fig. 1.



Dansyl Amino Acids. Figure 8 illustrates the electropherogram of 15 dansyl amino acids using MEGA 10-borate micellar phase at pH 7.0. As can be seen in this figure, the system provided a baseline separation of 13 dansyl amino acids. The order of migration of the different analytes was the same as that observed in an earlier study using the same

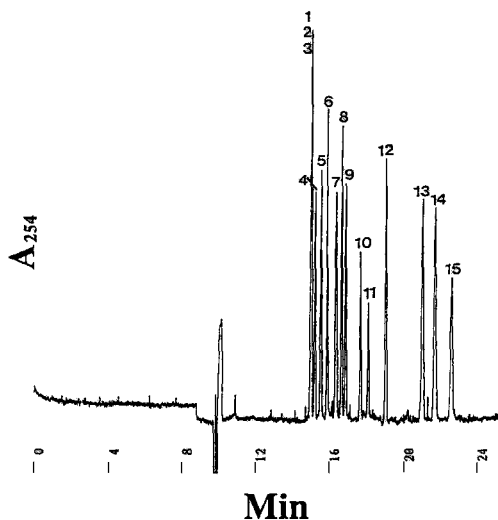


FIGURE 8. Electropherogram of dansyl amino acids. Running electrolyte, 400 mM borate containing 100 mM MEGA 10, pH 7.0. Solutes: 1, glutamine; 2, asparagine; 3, threonine; 4, serine; 5, valine; 6, methionine; 7, glycine; 8, isoleucine; 9, leucine; 10, arginine; 11, phenylalanine; 12, tryptophan; 13, glutamic acid; 14, aspartic acid; 15, cysteic acid. Other conditions as in Fig. 1.

micellar phase but at pH 10.0 [2]. Although, dansylated glutamine, asparagine and threonine co-migrated at pH 7.0, the resolution among the other thirteen dansyl amino acids is much better than that obtained at pH 10.0 [2]. The difference between the two separations may be attributed to differences in the degree of ionization of the solutes at pH 7.0 and 10.0. The separation was achieved in less than 24 minutes with an average plate count of 332 000 plates/meter.

ACKNOWLEDGMENTS

This material is based upon work supported by the Cooperative State Research Service, U.S. Department of Agriculture, under Agreement No. 94-37102-0989. Yehia Mechref is the recipient of the Phillips Petroleum Fellowship in Chemistry.

REFERENCES

- [1] Y. Mechref and Z. El Rassi, *J. Chromatogr. A*, in press (1995)
- [2] J. T. Smith, W. Nashabeh and Z. El Rassi, *Anal. Chem.*, 66: 1119 (1994)
- [3] J. T. Smith and Z. El Rassi, *J. Microsep. Sep.*, 6: 127 (1994)
- [4] J. T. Smith and Z. El Rassi, *Electrophoresis*, 15: 1248 (1994)
- [5] J. T. Smith and Z. El Rassi, *J. Chromatogr. A*, 685: 131 (1994)
- [6] J. T. Smith and Z. El Rassi, *J. Cap. Elec.*, 1: 136 (1994)
- [7] J. Cai and Z. El Rassi, *J. Chromatogr.*, 608: 31 (1992)
- [8] H. B. Davis and C. J. B. Mott, *J. Chem. Soc. Faraday I*, 76: 1991 (1980)
- [9] Z. El Rassi, *Adv. Chromatogr.*, 34: 177 (1994)
- [10] Z. El Rassi and W. Nashabeh, in Z. El Rassi (Z. El Rassis), *Carbohydrate Analysis: High Performance Liquid Chromatography and Capillary Electrophoresis*, Elsevier, Amsterdam, 1995, 267.
- [11] S. Hoffstetter-Kuh, A. Paulus, E. Gassmann and H. M. Widmer, *Anal. Chem.*, 63: 1541 (1991)
- [12] Y. Mechref, G. K. Ostrander and Z. El Rassi, *J. Chromatogr. A*, 695: 83 (1995)
- [13] N. Ingri, *Acta Chem. Scand.*, 16: 439 (1962)
- [14] N. Ingri, *Acta Chem. Scand.*, 17: 581 (1963)
- [15] J. L. Anderson, E. M. Eyring and M. P. Whittaker, *J. Phys. Chem.*, 68: 1128 (1964)
- [16] R. K. Momii and N. H. Nachtrieb, *Inorg. Chem.*, 6: 1189 (1967)
- [17] N. Ingri, *Sv. Kem. Tidskr.*, 75: 199 (1963)
- [18] C. C. Christ, J. R. Clark and H. T. Evans, *Acta Cryst.*, 11: 761 (1958)
- [19] K. Otsuka and S. Terabe, *J. Microcol. Sep.*, 1: 150(1989)

Received: July 10, 1995

Accepted: August 6, 1995

PHOTOACTIVATION: A NOVEL MEANS TO MEDIATE ELECTROPHORETIC SEPARATIONS

VICTORIA L. MCGUFFIN
*Department of Chemistry
Michigan State University
East Lansing, Michigan 48824*

ABSTRACT

By introducing electromagnetic radiation of the appropriate wavelength, polarization, and power, the electronic charge within a solute molecule can be redistributed in ways that affect its electrophoretic mobility. Consequently, photoactivation may be utilized to control and to enhance electrophoretic separations in a selective and predictable manner. The general concept and theory of the photoactivation method are elucidated, and the feasibility is demonstrated for representative photoionization and photodissociation reactions.

INTRODUCTION

In order to enhance resolution in electrophoretic separations, many parameters have been used to manipulate the solute mobility (1-8, and references therein). For example, the properties of the solution may be varied by means of the buffer type, pH, and ionic strength (4,8-15), as well as the type and concentration of an organic solvent (16,17), complexing agent (18-20), or other modifier (21-23). In addition, a secondary phase

with sieving properties such as a gel (24,25) or entangled polymer (26,27) matrix may be added. While these traditional parameters are effective in altering the solute mobility, the strength and selectivity cannot be easily or rapidly changed during the electrophoretic separation. This limitation is especially important for high-speed applications and for two-dimensional electrophoresis–electrophoresis and chromatography–electrophoresis applications (28-30).

In this work, photoactivation is explored as an alternative approach to mediate electrophoretic separations. In this approach, the solute molecules or ions are exposed to radiant energy (photons) rather than a chemical potential or other source of energy. The molecules that absorb this radiation will selectively undergo a transition to the excited state (Figure 1A). If this transition induces a change in either the mass or the charge of the solute molecule, its electrophoretic mobility will be concomitantly altered. There are two simple mechanisms by which a change in mass and/or charge may occur: photoionization and photodissociation. In the former case (Figure 1B), an electron will be ejected from the molecule if the energy of the absorbed photon exceeds the ionization energy. The resulting positively charged ion will have a higher mobility than the unperturbed molecule. In the latter case (Figure 1C), the equilibrium constant for an acid–base, complexation, or other reversible reaction may differ significantly between the ground and excited states. As the molecules associate or dissociate in order to reach equilibrium, their charge and mass will be altered, thereby influencing their mobility.

Unlike other parameters that are used to control electrophoretic separations, the photoactivation method has the advantage that it is

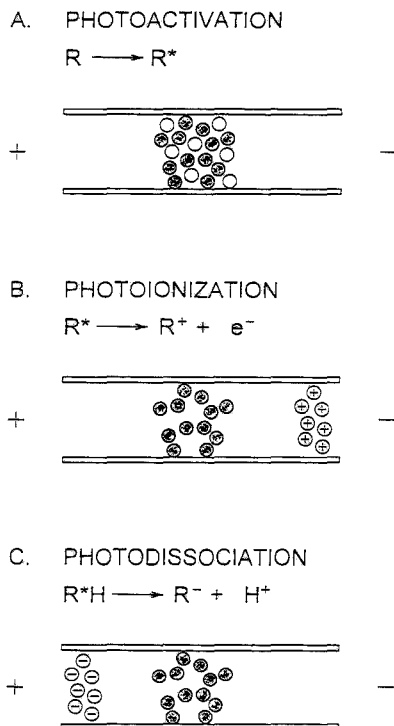


FIGURE 1: Schematic illustration of solute photoactivation (A) with subsequent photoionization (B) and photodissociation (C) reactions.

mediated through an externally applied electromagnetic field that can be rapidly modified in both strength and selectivity. In this paper, the conceptual and theoretical basis of this technique will be described together with preliminary experimental studies that support its feasibility.

THEORETICAL CONCEPTS

Upon interaction with electromagnetic radiation in the UV-visible region, molecules will undergo a transition to an electronically and/or

vibrationally excited state (31). The extent of such transitions can be broadly described by the absorption factor (α_o) at a specified frequency (ν), which is related to the power of the incident (ϕ_o) and transmitted (ϕ) radiation passing through a cell of pathlength (b) containing solute molecules of molar absorptivity ($\epsilon(\nu)$) and molar concentration (C):

$$\alpha_o(\nu) = (\phi_o - \phi) / \phi_o = 1 - 10^{-\epsilon(\nu) b C} \quad [1]$$

This expression can be extended to include optically active molecules (32,33) if linearly polarized light is separated into the individual components, left and right circularly polarized light. Molecules that possess a chiral center exhibit different degrees of absorption for these two components, whereas optically inactive molecules show no preference. For an optically active molecule, the difference in molar absorptivity is represented by

$$\Delta \epsilon(\nu) = \epsilon(\nu)_L - \epsilon(\nu)_R \quad [2]$$

which is known as the circular dichroism. Because each solute has a unique absorption spectrum, it is possible to control selectivity by varying the frequency and polarization. In addition, the strength can be controlled by varying the power of the electromagnetic radiation.

In the simplest case, these transitions lead to the formation of an excited state with a finite lifetime (τ) that decays to the initial ground state *via* radiative or nonradiative relaxation. Alternatively, the molecule may undergo a reversible or irreversible chemical reaction such as ionization, dissociation, isomerization, etc. before relaxation to another, distinctly different ground state. In the former case, the electronic charge distribution within the molecule is temporarily affected during the lifetime of

the excited state, whereas in the latter case, the change is more long-lived and may, in fact, be permanent. These changes in charge distribution may potentially be exploited to alter the solute velocity in electrophoretic separations.

The solute velocity will be altered if the effective electrophoretic mobility differs between the ground and excited states. For a solute that consists of several (n) species in dynamic equilibrium through an acid-base, complexation, or other reversible reaction, the effective mobility (μ_{eff}) is calculated from the following summation (1,8):

$$\mu_{\text{eff}} = \sum_{i=1}^n \alpha_i \mu_i \quad [3]$$

where α_i is the fraction and μ_i is the electrophoretic mobility of each species. The fractions α_i are dependent upon the equilibrium constants of the solute, as well as the concentration of the counter ion (e.g., pH or pM) in the buffer medium (34). Because the equilibrium constants are influenced by the electronic charge distribution within the solute molecule, they may differ substantially between the ground (g) and excited (e) states. Therefore, the fraction of each species and, hence, the effective mobility of the solute may be altered by photoactivation:

$$\mu_{\text{eff}} = (1 - F) \sum_{i=1}^{n(\text{g})} \alpha_{\text{gi}} \mu_{\text{gi}} + (F) \sum_{i=1}^{n(\text{e})} \alpha_{\text{ei}} \mu_{\text{ei}} \quad [4]$$

In order to establish the potential magnitude of this effect, it is necessary to determine the fraction (F) of solute molecules that will undergo a transition to the excited state. If the transition arises from a single-photon absorption that obeys the Beer-Lambert law (31), then the fraction of molecules in the excited state is given by

$$F = [\phi_o \alpha_o(\nu) w] / [h \nu N b C] \quad [5]$$

where ϕ_o and w are the irradiance and pulse width of the laser source at frequency ν , $\alpha_o(\nu)$ is the absorption factor from Equation [1], h is Planck's constant, and N is Avogadro's number. Because of the assumptions inherent in the Beer–Lambert law, this equation is not applicable at high irradiance where saturation may occur. Under these conditions, the absorption factor in Equation [5] must be replaced by

$$\alpha(\nu) = [\alpha_o(\nu) \phi_{\text{sat}}] / [\phi_{\text{sat}} + \phi_o] \quad [6]$$

where ϕ_{sat} is the irradiance at which the absorption factor $\alpha(\nu)$ is decreased to one-half of its initial value $\alpha_o(\nu)$ (35). Although it may be advantageous to operate under saturation conditions, the dependence of the fraction of excited-state molecules on experimental variables will be considered only within the linear region of Equation [5] for the purposes of this discussion.

The dependence of the fraction F on the characteristics of the radiant source is shown in Figure 2. Within the typical operating range of laser systems, the fraction is linearly dependent upon the irradiance ($10^4 - 10^8 \text{ W cm}^{-2}$) and pulse width ($10^{-3} - 10^{-9} \text{ s}$). The dependence of the fraction F on the characteristics of the solute molecule is shown in Figure 3. At low concentration, the fraction remains relatively constant because the concentration-dependent terms in the numerator and denominator of Equation [5] increase proportionately. Under these conditions, the fraction of molecules in the excited state is solely a function of the molar absorptivity. As the concentration increases, however, the absorption factor approaches a limiting value of unity whereas the denominator

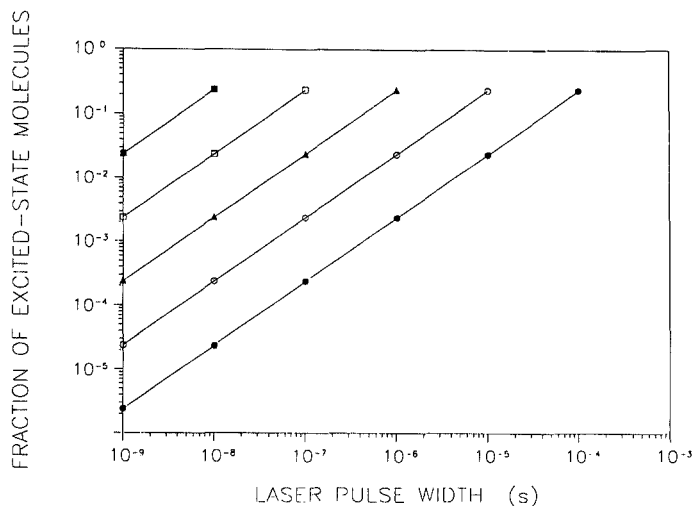


FIGURE 2: Fraction of excited-state molecules (F) versus laser pulse width (w) as a function of laser irradiance (ϕ_0) calculated according to Equation [5]. $\phi_0 = 10^8 \text{ W cm}^{-2}$ (■), 10^7 W cm^{-2} (□), 10^6 W cm^{-2} (▲), 10^5 W cm^{-2} (○), 10^4 W cm^{-2} (●); $\nu = 1.21 \times 10^{15} \text{ s}^{-1}$; $b \equiv [\pi(0.0075/2)^2]^{1/2} \text{ cm}$; $C = 10^{-7} \text{ mole L}^{-1}$; $\epsilon(\nu) = 10^4 \text{ L mole}^{-1} \text{ cm}^{-1}$.

increases unbound. It is not advisable to operate within the nonlinear region of Figure 3, because the fraction of molecules in the excited state and, hence, the resulting effective mobility of the solute will be concentration dependent. It is noteworthy that the concentration range over which the fraction F remains constant decreases by one order of magnitude for each ten-fold increase in molar absorptivity.

To gain an appreciation for the magnitude of the photoactivation effect, it is instructive to calculate the fraction of molecules in the excited state under conditions that are representative of our experimental system ($\phi_0 = 2.17 \times 10^6 \text{ W cm}^{-2}$, $w = 2.3 \times 10^{-8} \text{ s}$, $\nu = 1.21 \times 10^{15} \text{ s}^{-1}$). For a very

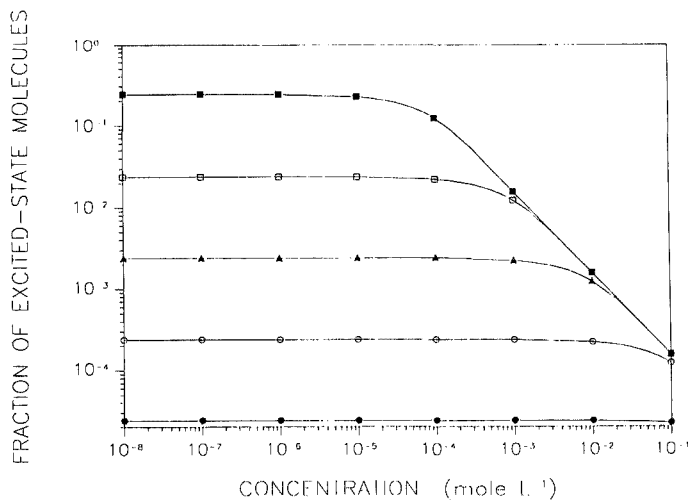


FIGURE 3: Fraction of excited-state molecules (F) versus molar concentration (C) as a function of molar absorptivity ($\epsilon(\nu)$) calculated according to Equation [5]. $\phi_0 = 2.17 \times 10^6 \text{ W cm}^{-2}$; $w = 2.3 \times 10^{-8} \text{ s}$; $\nu = 1.21 \times 10^{15} \text{ s}^{-1}$; $b \equiv [\pi(0.0075/2)^2]^{1/2} \text{ cm}$; $\epsilon(\nu) = 10^6 \text{ L mole}^{-1} \text{ cm}^{-1}$ (■), $10^5 \text{ L mole}^{-1} \text{ cm}^{-1}$ (□), $10^4 \text{ L mole}^{-1} \text{ cm}^{-1}$ (▲), $10^3 \text{ L mole}^{-1} \text{ cm}^{-1}$ (○), $10^2 \text{ L mole}^{-1} \text{ cm}^{-1}$ (●).

favorable solute ($\epsilon(\nu) = 10^6 \text{ L mole}^{-1} \text{ cm}^{-1}$, $C = 10^{-6} \text{ mole L}^{-1}$), a large fraction of molecules will be in the excited state ($F = 24 \%$). For more typical solutes ($\epsilon(\nu) = 10^3 \text{ L mole}^{-1} \text{ cm}^{-1}$, $C = 10^{-3} \text{ mole L}^{-1}$), the fraction is more modest but still effective ($F = 0.024\%$). Consequently, if the equilibrium constant differs between the ground and excited states, the effective mobility of the solute will be significantly altered by photoactivation.

This change in the effective mobility will directly influence the resolution in an electrophoretic separation. The electrophoretic resolution (R_s) in the elution mode is calculated as follows:

$$R_s = [N^{1/2} / 2] [(\mu_1 - \mu_2) / (2 \mu_{osm} + \mu_1 + \mu_2)] \quad [7]$$

where N is the number of theoretical plates and μ_{osm} is the electroosmotic mobility. Depending upon the specific circumstances, either the solute with larger effective mobility (μ_1) or with smaller effective mobility (μ_2) can be selectively photoactivated in order to enhance the electrophoretic resolution.

EXPERIMENTAL METHODS

Reagents

Reagent-grade N,N,N',N' -tetramethyl-1,4-phenylenediamine and phenol (Aldrich, Milwaukee, WI, USA) are purified by vacuum sublimation. Stock solutions of these solutes at 10^{-1} – 10^{-4} M concentration are prepared freshly as needed in the appropriate buffer solution. The sodium salts of phosphoric acid (J.T. Baker, Phillipsburg, NJ, USA) are used to prepare buffer solutions in the range of pH 5.0 – 9.0 with ionic strength of 0.01 M. Water is deionized and doubly distilled in glass (Model MP-3A, Corning Glass Works, Corning, NY, USA).

Capillary Electrophoresis System

The experimental system for these studies is illustrated schematically in Figure 4. A regulated high-voltage DC power supply (Model EH50R0.19XM6, Glassman High Voltage Inc., Whitehouse Station, NJ, USA) may be operated under constant-voltage (0 – 50 kV) or constant-current (0 – 190 μ A) conditions. The power supply is connected to platinum rod electrodes in two small reservoirs that contain the

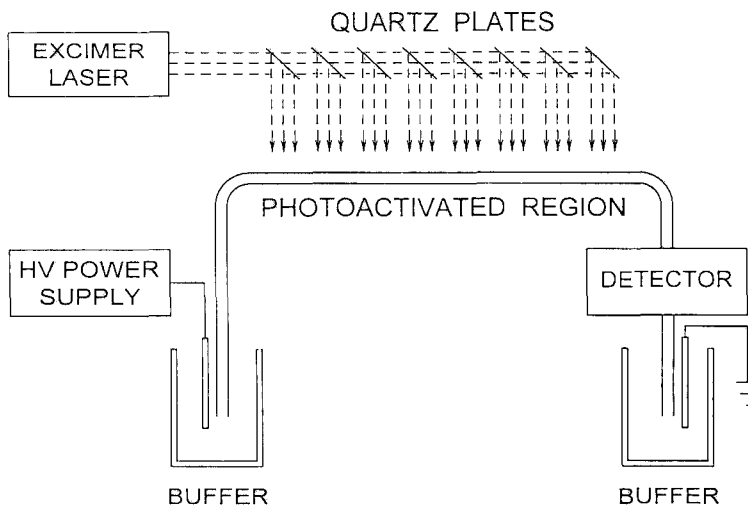


FIGURE 4: Experimental system for capillary electrophoresis with solute photoactivation and detection. Photoactivation is achieved by reflection and transmittance of excimer laser radiation using fused-silica plates. Detection is performed by UV-visible absorbance or fluorescence immediately after the photoactivated region.

phosphate buffer solutions. A straight length of fused-silica capillary tubing (75- μm i.d., 375- μm o.d., 75-cm length, Polymicro Technologies, Phoenix, AZ, USA), which serves as the migration channel, is immersed at each end in the buffer solutions. This tubing is optically transparent, to allow uniform irradiation for the photoactivation studies, and of sufficiently small diameter to dissipate both radiant and Joule heat efficiently.

Photoactivation System

The photoactivation system utilizes an excimer laser (Model EMG 101 MSC, Lambda Physik, Goettingen, Germany) that has beam

dimensions of 1.5 x 3.0 cm at the exit of the laser cavity. Although several wavelengths between 193 and 351 nm are available using different gases, krypton fluoride has been used in the initial studies to provide irradiation at 248 nm with typical pulse energy of 70 – 250 mJ, pulse width of 2.3×10^{-8} s, and repetition rate of 10 s^{-1} . A series of fused-silica plates are situated to reflect and transmit this light in order to provide uniform irradiance along a 10- to 25-cm length of the capillary tube.

Detection Systems

Solute detection is accomplished by using either UV–visible absorbance or fluorescence. A variable-wavelength absorbance detector (Model Uvidec 100-V, Japan Spectroscopic Co., Tokyo, Japan), modified to allow the capillary tube to be used as the flowcell, is capable of detecting solutes at the picomole (10^{-12} mole) level with a linear dynamic range of approximately 10^3 . In contrast, the laser-induced fluorescence system developed in our laboratory can achieve detection limits at the attomole (10^{-18} mole) level with a linear range of 10^8 (36,37). A helium-cadmium laser (Model 3074-40M, Omnicrome, Chino, CA, USA), with approximately 30 mW of continuous-wave power at 325 nm, is used as the excitation source. The laser radiation is focused directly upon the optically transparent fused-silica capillary and solute fluorescence is collected perpendicular and coplanar to the excitation beam. The emission is then isolated by appropriate interference filters (Corion, Holliston, MA, USA) and is focused onto a photomultiplier tube (Model Centronic Q4249B, Bailey Instruments, Saddle Brook, NJ, USA). The resulting photocurrent is amplified by a picoammeter (Model 480, Keithley Instruments, Cleveland,

OH, USA) and is displayed on a chart recorder (Model 585, Linear Instruments, Reno, NV, USA).

RESULTS AND DISCUSSION

Preliminary Studies of Photoactivation

In preliminary studies, it is necessary to establish that any apparent changes in the electrophoretic separation are due to selective photoactivation of the solute, rather than other non-selective processes that may arise from laser irradiation.

The first potential problem to be addressed is that of photoinduced thermal effects. Because the vibration–translation relaxation time for the aqueous buffer medium is much less than the duration of the laser pulse (38), radiant heat is not expected to accumulate within the capillary tube. For the case where the absorption transition is not saturated, the average change in temperature can be calculated as follows (38):

$$\Delta T = \phi_0 \alpha_0(\nu) w \rho / C_p b \quad [8]$$

where ϕ_0 and w are the irradiance and pulse width of the laser source, $\alpha_0(\nu)$ is the absorption factor from Equation [1], b is the optical pathlength, and ρ and C_p are the density and heat capacity of the buffer medium. Based on this equation, the estimated temperature change (ΔT) under the representative experimental conditions described previously is 0.03 °C. In practice, the temperature change is likely to be less than this calculated value because of the low repetition rate of the laser as well as the efficient heat dissipation of the capillary with a high surface-area-to-volume ratio.

Although the temperature change is calculated to be quite small, it is known that temperature has a significant effect on both electroosmotic and electrophoretic velocities (39-42). The effect of increasing temperature on electroosmotic velocity is manifested as a decrease in the viscosity and, hence, an increase in the conductivity of the buffer solution within the irradiated region of the capillary. This effect was examined experimentally by monitoring the current generated under constant-voltage conditions or, conversely, the voltage generated under constant-current conditions as a function of the irradiance. From these measurements, the resistance and the equivalent conductivity were calculated by using the classical equations (43). As shown in Figure 5, the equivalent conductivity of the buffer solution does not vary significantly with irradiance in the range from 0 – $1.4 \times 10^5 \text{ W cm}^{-2}$. Therefore, photothermal heating may be considered negligible with respect to Joule heating under these experimental conditions.

Another potential problem is that the fused-silica capillary may absorb the laser radiation to a small extent. Because the dissociation constant (pK_a) of the weakly acidic silanol groups may differ between the ground and excited states, the fraction of such groups in the ionic form on the surface may be altered by irradiation. This change in surface charge will influence the zeta potential and, hence, the electroosmotic velocity (44,45). This effect was examined by measuring the velocity as a function of pH under constant-voltage and constant-current conditions. As shown in Figure 6, the electroosmotic velocity increases in the normal and customary manner within the range from pH 5.0 – 9.0 (11,12,46). There is no statistically significant difference in the electroosmotic velocity

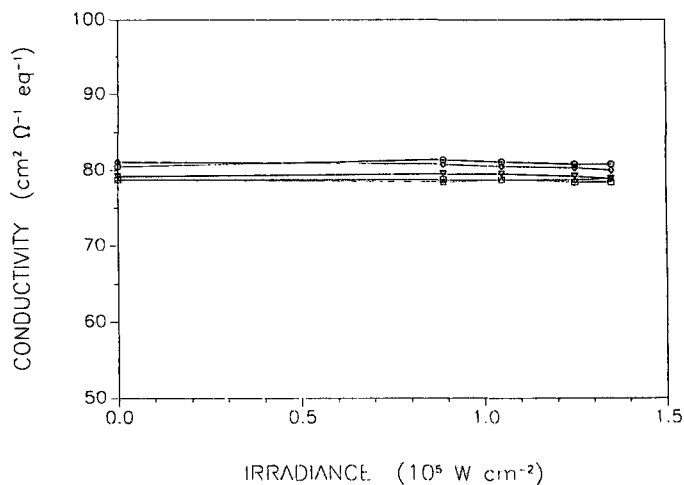


FIGURE 5: Equivalent conductivity *versus* irradiance as a function of the pH of the phosphate buffer solution. pH 5.0 (○), pH 6.0 (□), pH 7.0 (△), pH 8.0 (▽), pH 9.0 (◇).

measured without and with irradiation. Moreover, there is no significant change in the slope of these graphs as the pH approaches the pK_a of the silanol groups (5.2 – 7.7) (45-49). These observations suggest that the charge density of the silica surface is not significantly altered by irradiation.

In order to demonstrate the feasibility of the photoactivation method, it is desirable to employ chemical reactions that are irreversible. Although such reactions do not have analytical utility, they conclusively verify the ability to generate ions in good yield by photoactivation and to separate those ions from the parent neutral solutes. Two validation studies using irreversible photoionization and photodissociation reactions are described in the following sections.

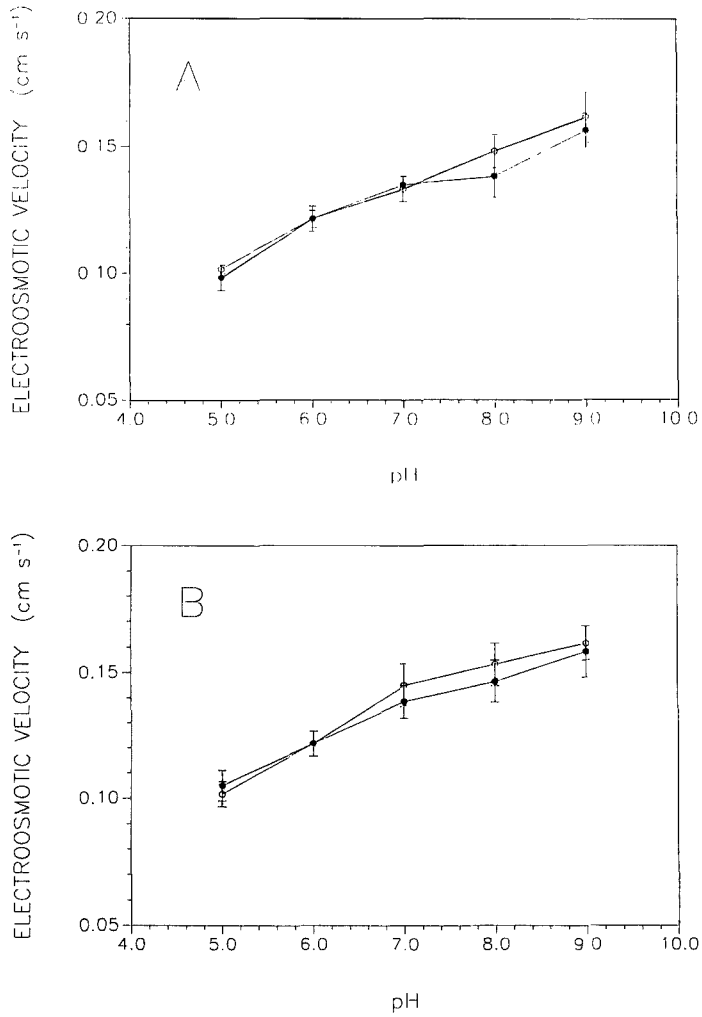
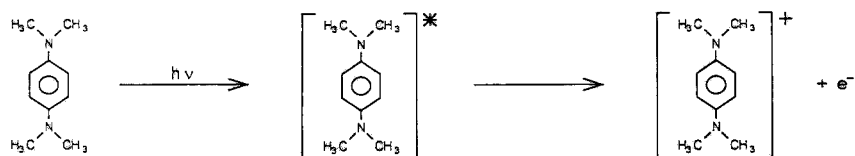


FIGURE 6: Electroosmotic velocity *versus* pH of the phosphate buffer solution (○) without and (●) with photoactivation under (A) constant-voltage conditions (27.5 kV) and (B) constant-current conditions (8.5 μA).

Validation Study with Solute Photoionization

N,N,N',N'-tetramethyl-1,4-phenylenediamine (TMPD) is chosen as the solute for this validation study because it provides visual verification of the photoionization process; the neutral molecule is colorless, whereas the cation has an intense and characteristic blue color. Although ionization can occur by two-photon excitation *via* simultaneous (50) and sequential (51) mechanisms, only one-photon excitation is expected under the experimental conditions employed in this study (52,53).



In the gas phase, the one-photon ionization threshold of TMPD has been reported as 6.2 eV (54). In the liquid phase, the ionization threshold varies from a maximum of 5.0 eV in nonpolar solvents such as hexane (55) to 3.5 eV in polar solvents such as methanol and water (52,56). At the 248 nm (5.0 eV) wavelength of the excimer laser, TMPD has a molar absorptivity of approximately 2800 L mol⁻¹ cm⁻¹ and, thus, should be readily photoionized in aqueous buffer media. Once the geminate cation–electron pair has become solvated to form free ions, the probability of recombination is low and the reaction is essentially irreversible (57).

The electropherograms of TMPD in phosphate buffer solution were recorded using the experimental system shown in Figure 4. In the absence of irradiation (Figure 7A), the single peak observed in the electropherogram is attributable to neutral TMPD, which migrates at the

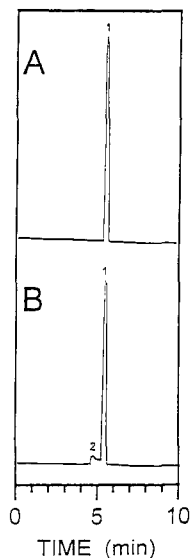


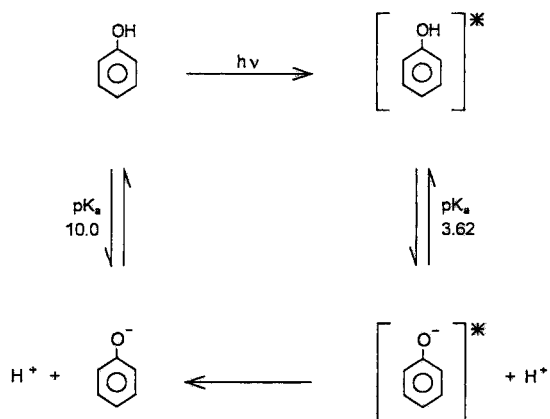
FIGURE 7: Electropherograms of 10^{-3} M N,N,N',N'-tetramethyl-1,4-phenylenediamine (A) without and (B) with photoactivation. Capillary: $75\ \mu\text{m}$ i.d. \times 75 cm fused-silica capillary. Buffer: 0.010 M phosphate buffer at pH 6.7. Electrophoresis: $8.5\ \mu\text{A}$ constant-current conditions. Photoactivation: 115 mJ at 248 nm. Detector: UV-visible absorbance detector, 230 nm, 0.005 AUFS. Solutes: (1) TMPD, (2) TMPD cation.

electroosmotic velocity. Upon irradiation of a 25-cm length of the capillary with 115 mJ at 248 nm (Figure 7B), an additional peak appears with a higher electrophoretic mobility and, hence, a more positive charge. The unusual shape of this peak arises because the photoactivation product is not formed instantaneously but, rather, continuously to some extent along the irradiated length of the capillary. In order to confirm the identity of this product, a solution of TMPD in a cuvette was thoroughly irradiated to form the characteristic blue color of the cation. Upon electrophoretic separation of this independently irradiated solution, two peaks are observed with the

same mobilities as those shown in Figure 7B. Thus, this study demonstrates that photoionization reactions can be used to generate cations *in situ*, which can then be separated by electrophoresis.

Validation Study with Solute Photodissociation

Phenol is chosen as the solute for this validation study because the acid–base equilibrium constants are known to differ substantially between the ground and excited states (58-60):



The molar absorptivity of phenol is approximately $440 \text{ L mol}^{-1} \text{ cm}^{-1}$ at the 248 nm wavelength of the excimer laser. If the phosphate buffer solution is maintained at pH 7.0, phenol is neutral in the ground state ($\text{p}K_a = 10.0$) and anionic in the excited state ($\text{p}K_a = 3.62$). When the excited state anion relaxes to the ground state, recombination by diffusion alone is inefficient because of the low concentration of hydrogen ions and the competition with stronger bases (e.g., PO_4^{3-} and OH^- , with $\text{p}K_a$ of 12.4 and 14.0, respectively (34,61)). Thus, the photodissociation of phenol is not reversible within the time scale of the electrophoretic experiment.

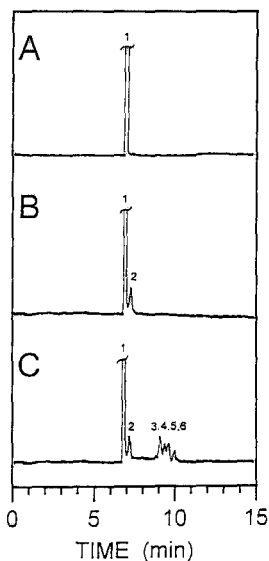


FIGURE 8: Electropherograms of 10^{-2} M phenol (A) without and (B,C) with photoactivation. Photoactivation: (B) 80 mJ at 248 nm, (C) 115 mJ at 248 nm. Solutes: (1) phenol, (2) phenol anion, (3) – (6) photochemical byproducts of phenol or phenol anion. All other experimental conditions as given in Figure 7.

In the absence of irradiation (Figure 8A), the single peak observed in the electropherogram is attributable to neutral phenol, which migrates at the electroosmotic velocity. Upon irradiation of a 25-cm length of the capillary at 80 mJ (Figure 8B), one additional peak appears with a lower electrophoretic mobility and, hence, a more negative charge. This product can be unambiguously identified by comparison of the electrophoretic mobility with that of the phenol anion generated in the absence of irradiation at pH 11.0. Upon irradiation at 115 mJ (Figure 8C), however, several peaks are observed in addition to phenol and the phenol anion.

The number and intensity of the additional peaks appears to be dependent upon the phenol concentration, the pH, and the irradiance. Phenol is known to undergo a wide variety of photochemical reactions in aqueous solution, including oxidation by oxygen, ozone, and peroxide, as well as addition of hydroxyl and phenoxy radicals (60,62-65). A variety of stable photochemical byproducts have been isolated, such as the positional isomers of dihydroxy- and trihydroxybenzene as well as the isomers of phenoxyphenol (60,64,65). It is noteworthy that the additional peaks shown in Figure 8C are also formed when phenol is irradiated separately in a cuvette, followed by electrophoretic separation.

This study clearly demonstrates that photodissociation reactions can be used to generate ions *in situ*, which can then be separated by electrophoresis. However, the electropherogram shown in Figure 8C illustrates one of the potential problems of this method: the photophysics and photochemistry of the solute must be reasonably well understood in order to provide reliable analytical application in complex mixtures. At the same time, this feature can be used to advantage in order to study the photophysics and photochemistry of solutes in their pure form. For example, benzo[a]pyrene and its monohydroxyl and dihydroxyl isomers are known to undergo photochemical reactions similar to those of phenol (60). The toxicity and carcinogenicity of these isomers varies considerably with the position of hydroxyl substitution (66,67). Although these isomers are difficult to separate chromatographically and electrophoretically (68-71), their acid-base equilibrium constants differ substantially between the ground and excited state (72,73), as summarized in Table 1. Thus, the photoactivation method may provide a unique method to study the

TABLE 1

Acid-Base Dissociation Constants for the Ground (pK_a) and Excited (pK_a^*) States of the Monohydroxyl Isomers of Benzo[a]pyrene (72)

Benzo[a]pyrene Isomer	pK_a	pK_a^*	ΔpK_a
10-hydroxy	11.1	0.0	11.1
5-hydroxy	10.8	1.0	9.8
11-hydroxy	10.2	2.3	7.9
8-hydroxy	10.2	1.6	8.6
9-hydroxy	9.5	5.8	3.7
4-hydroxy	9.4	1.6	7.8
2-hydroxy	9.3	3.2	6.1
6-hydroxy	9.2	1.0	8.2
7-hydroxy	9.2	-0.4	9.6
1-hydroxy	9.0	2.0	7.0
12-hydroxy	9.0	1.6	7.4
3-hydroxy	8.6	4.3	4.3

photochemistry of these environmentally and biochemically important solutes.

CONCLUSIONS

The enhancement of electrophoretic separations by photoactivation of the solutes appears to be a novel and promising approach. Unlike other means to control electrophoretic mobility, this method has the advantage that it is mediated through an externally applied electromagnetic field that can be rapidly modified in both strength and selectivity. The strength of photoactivation may be controlled by the laser irradiance and pulse width, whereas the selectivity may be controlled by the wavelength and polarization. Moreover, stepwise and linear gradients in irradiance and wavelength may be implemented using standard spectroscopic

instrumentation. Although this investigation has been limited to the solute as the photoactive species, it is apparent that this general principle can be extended to other species in the separation system. Thus, this approach can potentially be applied to membrane and chromatographic separation systems where a component of the mobile or stationary phases is photoactivated.

ACKNOWLEDGEMENTS

The author is grateful to Dr. Faye K. Ogasawara for technical assistance and to Dr. L. David Rothman (Dow Chemical Company) for many insightful discussions. Preliminary studies were facilitated by an Affirmative-Action Postdoctoral Fellowship and an All-University Research Initiation Grant from Michigan State University. This research was supported by the U.S. Department of Energy, Office of Basic Energy Sciences, Division of Chemical Sciences, under contract number DE-FG02-89ER14056.

REFERENCES

1. F. M. Everaerts, Isotachopheresis: Theory, Instrumentation, and Applications, Elsevier Scientific Publishing, New York, 1976.
2. J. W. Jorgenson, ACS Symp. Ser., 355: 182 (1987).
3. R. A. Wallingford, A. G. Ewing, Adv. Chromatogr., 29: 1 (1989).
4. A. G. Ewing, R. A. Wallingford, T. M. Olefirowicz, Anal. Chem., 61: 292A (1989).
5. W. G. Kuhr, Anal. Chem., 62: 403R (1990).
6. W. G. Kuhr, C. A. Monnig, Anal. Chem., 64: 389R (1992).
7. C. A. Monnig, R. T. Kennedy, Anal. Chem., 66: 280R (1994).

8. P. D. Grossman, J. C. Colburn, Capillary Electrophoresis: Theory and Practice, Academic Press, San Diego, CA, 1992.
9. K. D. Lukacs, J. W. Jorgenson, HRC&CC J. High Res. Chromatogr. Chromatogr. Comm., 8: 407 (1988).
10. P. Bocek, M. Deml, J. Pospichal, J. Sudor, J. Chromatogr., 470: 309 (1989).
11. B. B. Van Orman, G. G. Liversidge, G. L. McIntyre, T. M. Olefirowicz, A. G. Ewing, J. Microcol. Sep., 2: 176 (1990).
12. J. Vindevogel, P. Sandra, J. Chromatogr., 541: 483 (1991).
13. J. S. Green, J. W. Jorgenson, J. Chromatogr., 478: 63 (1989).
14. H. J. Issaq, I. Z. Atamna, C. J. Metral, G. M. Muschik, J. Liq. Chromatogr., 13: 1247 (1990).
15. I. Z. Atamna, C. J. Metral, G. M. Muschik, H. J. Issaq, J. Liq. Chromatogr., 13: 2517 (1990).
16. S. Fujiwara, S. Honda, Anal. Chem., 59: 487 (1987).
17. C. R. Yonker, R. D. Smith, J. Chromatogr., 517: 573 (1990).
18. E. Gassmann, J. Kuo, R. Zare, Science, 230: 813 (1985).
19. Y. Walbroehl, J. W. Jorgenson, Anal. Chem., 58: 479 (1986).
20. D. F. Swaile, M. J. Sepaniak, Anal. Chem., 63: 179 (1991).
21. J. Snopek, I. Jelinek, E. Smolkova-Keulemansova, J. Chromatogr., 452: 571 (1988).
22. S. Terabe, K. Otsuka, K. Ichikawa, A. Tsuchiya, T. Ando, Anal. Chem., 56: 111 (1984).
23. D. Burton, M. Sepaniak, M. Maskarinec, J. Chromatogr. Sci., 25: 514 (1987).
24. A. Cohen, B. Karger, J. Chromatogr., 397: 409 (1987).
25. V. Dolnik, K. A. Cobb, M. Novotny, J. Microcol. Sep., 3: 155 (1991).
26. J. B. Poli, M. R. Schure, Anal. Chem., 64: 896 (1992).
27. K. Ganzler, K. S. Greve, A. S. Cohen, B. L. Karger, A. Guttman, N. C. Cooke, Anal. Chem., 64: 2665 (1992).
28. D. Kaniansky, J. Marak, J. Chromatogr., 498: 191 (1990).

29. M. M. Bushey, J. W. Jorgenson, *Anal. Chem.*, **62**: 978 (1990).
30. A. V. Lemmo, J. W. Jorgenson, *Anal. Chem.*, **65**: 1576 (1993).
31. J. D. Ingle, S. R. Crouch, *Spectrochemical Analysis*, Prentice-Hall, Englewood Cliffs, New Jersey, 1988.
32. N. Purdie, K. A. Swallows, *Anal. Chem.*, **61**: 77A (1989).
33. K. P. Wong, *J. Chem. Ed.*, **51**: A573 (1974).
34. H. A. Laitinen, W. E. Harris, *Chemical Analysis*, 2nd Ed., McGraw-Hill, New York, 1975.
35. J. I. Steinfeld, *An Introduction to Modern Molecular Spectroscopy*, 2nd Ed., MIT Press, Boston, Massachusetts, 1985, pp. 334-335.
36. V. L. McGuffin, R. N. Zare, *Appl. Spectrosc.*, **39**: 847 (1985).
37. S. H. Chen, C. E. Evans, V. L. McGuffin, *Anal. Chim. Acta*, **246**: 65 (1991).
38. D. H. Turner, E. W. Flynn, N. Sutin, J. V. Beitz, *J. Amer. Chem. Soc.*, **94**: 1554 (1972).
39. J. W. Jorgenson, K. W. Lukacs, *Science*, **222**: 266 (1983).
40. T. Tsuda, *J. Liq. Chromatog.*, **12**: 2501 (1989).
41. Y. K. Zhang, N. Chen, L. Wang, *J. Liq. Chromatogr.*, **16**: 3689 (1993).
42. N. Chen, L. Wang, Y. Zhang, *J. Chromatogr.*, **644**: 175 (1993).
43. A. J. Bard, L. R. Faulkner, *Electrochemical Methods: Fundamentals and Applications*, John Wiley and Sons, New York, 1980.
44. P. J. Scales, F. Grieser, T. W. Healy, L. R. White, D. Y. C. Chan, *Langmuir*, **8**: 965 (1992).
45. G. A. Parks, *Chem. Rev.*, **65**: 177 (1965).
46. M. F. M. Tavares, V. L. McGuffin, *Anal. Chem.*, in press.
47. M. L. Hair, W. Hertl, *J. Phys. Chem.*, **74**: 91 (1970).
48. D. N. Strazhesko, V. B. Strelko, V. N. Belyakov, S. C. Rubanik, *J. Chromatogr.*, **102**: 191 (1974).
49. J. Nawrocki, *Chromatographia*, **31**: 177 (1991) and **31**: 193 (1991).

50. S. Takeda, N. Houser, R. Jarnagin, *J. Chem. Phys.*, 54: 3195 (1971).
51. C. Braun, T. Scott, A. Albrecht, *Chem. Phys. Lett.*, 84: 248 (1981).
52. J. W. Judge, V. L. McGuffin, *Anal. Chem.*, 63: 2564 (1990).
53. J. W. Judge, V. L. McGuffin, *Appl. Spectrosc.*, 48: 1102 (1994).
54. Y. Kakato, M. Ozaki, A. Egawa, H. Tsobomura, *Chem. Phys. Lett.*, 9: 615 (1971).
55. R. Holroyd, R. Russell, *J. Phys. Chem.*, 78: 2128 (1974).
56. Y. Hirata, N. Mataga, *Prog. Reaction Kinetics*, 18: 273 (1993).
57. L. Onsager, *Phys. Rev.*, 54: 554 (1938).
58. I. Avigal, J. Feitelson, M. Ottolenghi, *J. Chem. Phys.*, 50: 2614 (1969).
59. J. A. Bartrop, J. D. Coyle, *Excited States in Organic Chemistry*, John Wiley and Sons, New York, 1975, pp. 49-51.
60. J. Malkin, *Photophysical and Photochemical Properties of Aromatic Compounds*, CRC Press, Boca Raton, Florida, 1992.
61. D. A. Skoog, D. M. West, F. J. Holler, *Analytical Chemistry*, 5th Ed., Saunders College Publishing, Philadelphia, Pennsylvania, 1990.
62. R. O. Kan, *Organic Photochemistry*, McGraw-Hill, New York, 1966.
63. M. Ye, R. H. Schuler, *J. Phys. Chem.*, 93: 1898 (1989).
64. M. Y. Ye, *J. Liq. Chromatogr.*, 15: 875 (1992).
65. R. W. Matthews, S. R. McEvoy, *J. Photochem. Photobiol. A*, 64: 231 (1992).
66. H. V. Gelboin, P. O. P. Ts'o, *Polycyclic Hydrocarbons and Cancer*, Vol. 1, Academic Press, New York, 1978.
67. C. E. Seale, *Chemical Carcinogens*, American Chemical Society, Washington, D. C., 1984.
68. M. Mushtaq, Z. Bao, S. K. Yang, *J. Chromatogr.*, 385: 293 (1987).
69. R. G. Croy, J. K. Selkirk, R. G. Harvey, J. F. Engel, H. V. Gelboin, *Biochem. Pharm.*, 25: 227 (1976).
70. S. K. Yang, D. W. McCourt, P. P. Roller, H. V. Gelboin, *Proc. Natl. Acad. Sci. USA*, 25: 227 (1976).

71. D. R. Thakker, H. Yagi, A. Y. H. Lu, W. Levin, A. H. Conney, D. M. Jerina, *Proc. Natl. Acad. Sci. USA*, 73: 3381 (1976).
72. A. C. Capomacchia, J. V. Kumar, C. Brazzel, *Talanta*, 29: 65 (1982).
73. A. C. Capomacchia, J. V. Kumar, R. N. Jennigs, *J. Chem. Soc. Perkin Trans. II*, 1989: 937 (1989).

Received: July 10, 1995

Accepted: August 6, 1995

THE USE OF ALKYL METHYLMORPHOLINE-BASED BACKGROUND ELECTROLYTES IN CAPILLARY ELECTROPHORESIS

ROBERT L. WILLIAMS AND GYULA VIGH*

*Chemistry Department
Texas A&M University
College Station, Texas 77843-3255*

ABSTRACT

A homologous series of alkylmethylmorpholinium hydroxides has been synthesized, characterized and used as the source of cationic co-ions in mobility-matching background electrolytes designed to eliminate the efficiency-degrading effects of electromigration dispersion. The mobilities of the co-ions vary over the $25 \cdot 10^{-5}$ to $45 \cdot 10^{-5}$ cm^2/Vs range in 25 mM mobility-matching background electrolytes, prepared from phosphoric acid and the respective alkylmethylmorpholinium hydroxides. It was demonstrated experimentally that electromigration dispersion-related extra peak broadening could be minimized and difficult electrophoretic separations could be realized when these alkylmethylmorpholinium cations were used as co-ions.

1 INTRODUCTION

Ideally, in capillary electrophoresis (CE), separation efficiency is high because the sole cause of peak dispersion is longitudinal diffusion [1]. In well designed instruments this is indeed the case as long as severe solute — wall interactions are

absent and electromigration dispersion is [2,3] negligible. Electromigration dispersion (ED) is caused by the local distortion of the electric field strength in the sample zone (*vis-a-vis* to the electric field strength in the surrounding pure background electrolyte) that occurs when the conductivities are different in the sample zone and in the pure background electrolyte (BGE). Generally, ED-induced band broadening can be minimized by keeping the transference number of the sample low [2,3]. Unfortunately, this simple approach is not always feasible due to the limited detection sensitivity of the currently used UV detectors. Mikkers et al. [2] suggested that ED is absent when the mobilities of the analyte and the BGE co-ion are equal. Such equality can be established, for example, by dynamically controlling the mobility of a zwitterionic BGE co-ion via multiple secondary chemical equilibria [4], a feasible, though difficult approach. An alternative, much easier approach was suggested by our laboratory when it was discovered that by assigning the buffering functions of the BGE solely to the counter-ion and the mobility matching functions solely to the co-ion, the mobilities of the analyte and the co-ion could be matched without altering the pH of the BGE [5]. For example, for weak base analytes, the BGE can be formed by adjusting the pH of a weak acid solution to the desired value with a strong base, the cation of which has a mobility equal to the effective mobility of the analyte at the given pH and ionic strength. Such BGEs were termed mobility-matching BGEs and the validity of the principle has been demonstrated with tetralkylammonium ions as co-ions [6]. The drawback of the tetralkylammonium cations is that the choice of available mobilities is limited. Therefore, a research program was initiated to synthesize and characterize a homologous series of cationic co-ions which cover the useful mobility range more evenly than the tetralkylammonium ions do. The power of the suggested mobility-matching BGEs is illustrated in Figure 1 by showing the electropherograms of a sample (the reaction mixture of styrene epoxide and N,N,N,N-

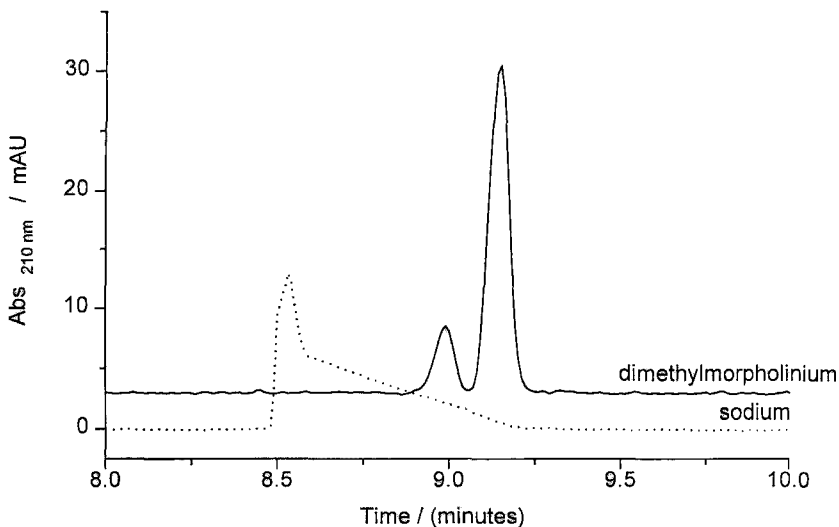


Figure 1.

Electropherograms of the major components (a and b) of the reaction mixture shown in Figure 2 in 0.2% hydroxyethyl cellulose, 35 mM phosphate, pH 1.9 BGEs, (i) co-ion: 35 mM sodium (dotted line), (ii) co-ion: 35 mM N,N-dimethylmorpholinium (solid line). Field strength: 169 V/cm. Other conditions as in Experimental.

tetramethylethylenediamine) in 0.2% hydroxyethylcellulose, 35 mM phosphoric acid, pH 1.9 BGEs, containing 35 mM NaCl and N,N-dimethylmorpholinium chloride, respectively. Except for the two co-ions, all other conditions of the separations were identical (injected amounts, BGE concentrations of all the components, field strengths, etc.). Clearly, the electropherogram obtained with the Na⁺-containing BGE is useless, while symmetrical peaks and complete separation is obtained for the N,N-dimethylmorpholinium-containing BGE. Note, that the tail-end of the skewed second peak (representing infinite dilution) in the Na⁺-containing BGE appears at the same

time as the maximum of the symmetrical second peak in the N,N-dimethylmorpholinium-containing BGE, indicating that the infinite dilution electrophoretic mobilities of the analyte are identical in both BGEs and no selectivity change has taken place.

Naturally, even the alkylmorpholinium-based BGEs are useful only for the analytes whose mobility is within the range covered by the homologous series. The synthesis and characterization of these co-ions, as well as the results of their use will be discussed in this paper.

2 EXPERIMENTAL

A P/ACE 5510 system (Beckman Instruments, Fullerton, CA) was used for the mobility measurements. The injection-side electrode was kept at the high positive potential. 47 cm long (40 cm from injector to detector) uncoated, 25 μm I.D. fused silica capillaries (Polymicro Technologies, Phoenix, AZ), thermostatted at 37 $^{\circ}\text{C}$, were used for the mobility determinations. 50 μm I.D. eCAP Neutral capillaries (Part Number 477441, Beckman) with a neutral internal coating was used for the analysis of the samples shown in Figure 6. Unless otherwise noted, power dissipation was kept between 170 to 300 mW/m, corresponding to field strengths of 80 to 320 V/cm. All samples were injected electrokinetically. The electroosmotic flow velocity was measured by electrokinetically injecting a benzylalcohol solution. The reported mobilities are corrected for the effects of the linear potential ramp at the beginning of the separation [7].

All chemicals used for the synthesis of the mobility markers and the mobility-matching co-ions were reagent grade (phosphoric acid, sodium hydroxide, trimethylamine, triethylamine, tripropylamine and tributylamine, N,N,N,N-tetramethylethylenediamine, N-methyl-morpholine, styrene oxide, and 1,2-epoxy-3-

phenoxy-propane as well as methyl-, ethyl-, propyl-, butyl-, hexyl- and dodecyl iodide, octyl- and nonyl bromide), and were obtained from Aldrich (Milwaukee, WI). The 250 MHR PA hydroxyethylcellulose sample was obtained from Aqualone (Wilmington, DE). Deionized water from a Millipore Q unit (Millipore, Milford, MA) was used to prepare the BGEs.

The quaternary ammonium test solutes were synthesized according to a modified version of the procedure described in [8] and shown by the reaction scheme in Figure 2. The co-ions were synthesized according to a modified version of the procedure described in [9,10] and shown by the reaction scheme in Figure 3. Briefly, 0.1 moles of the starting amine and the respective alkyl halide were added to 200 mL of toluene. The solution was refluxed overnight. (The reaction with N-methylmorpholine and methyl iodide was very exothermic and required cooling in an ice water bath.) The off-white precipitate formed in the reaction was separated from the reaction mixture, washed with toluene, dissolved in deionized water, and extracted with dichloromethane. The aqueous phase was then passed over an anion exchange column in hydroxide form (Dowex 1X8, Fluka, Ronkonkoma, NY). The collected effluent was reduced to 100 mL and assayed by titrating it with a standardized solution of HCl. Overall product yields varied between 10 and 60%. The structures of the newly synthesized compounds were confirmed by ^1H NMR spectroscopy.

3 RESULTS

The mobilities of the newly synthesized alkylmethylmorpholinium BGE co-ions at a constant ionic strength, were determined according to the simple electrophoretic method described in [6]. UV active quaternary ammonium analytes, whose electrophoretic mobilities varied in the $(10-55) \times 10^{-5} \text{ cm}^2/\text{Vs}$ range were analyzed in pH 2.2 BGEs, which were prepared from a 50 mM phosphoric acid solution. The pH of the

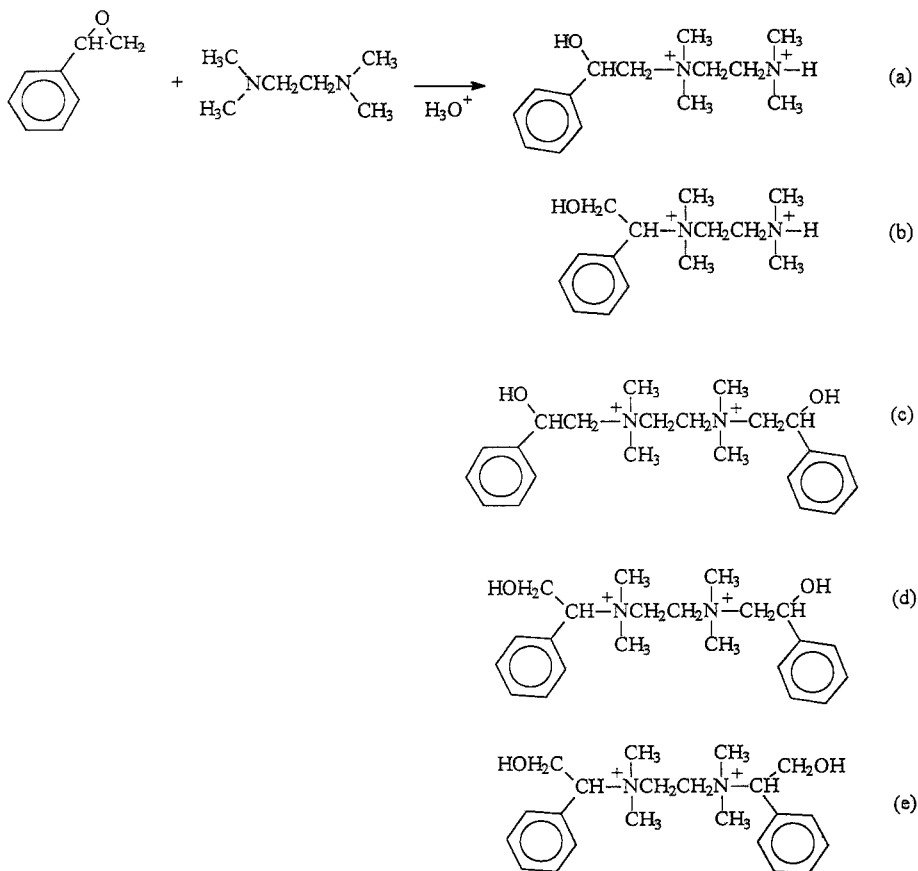


Figure 2.

Reaction scheme used for the synthesis of the cationic mobility markers.

BGEs was adjusted with the respective alkylmethylmorpholinium hydroxide solutions. Since the analyte concentrations were high, fronting (or tailing) analyte peaks were observed when their mobilities were larger (or smaller) than those of the BGE co-ion. By measuring the peak asymmetries (at 10% peak height) and plotting them as a function of the electroosmotic flow corrected effective mobility of the particular peak,

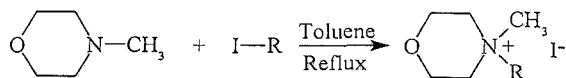


Figure 3.

Reaction scheme used for the synthesis of the N-alkyl-N-methylmorpholinium hydroxides.

plots similar to that shown in Figure 4 for N-methyl-N-propylmorpholinium, were obtained. The mobility where the $\log(\text{peak asymmetry})$ vs. effective mobility curve crosses the zero line is equal to the effective mobility of the BGE co-ion studied at the given ionic strength. The closer the mobilities of the test solutes are to those of the BGE co-ions, the more accurate is the determined value of the mobility of the BGE co-ion.

By repeating these measurements (Figure 4) for all the newly synthesized co-ions, the effective electrophoretic mobilities of the alkylmorpholinium cations could be determined as shown in Figure 5. The effective electrophoretic mobilities of the alkylmorpholinium cations decrease almost linearly with the logarithm of their molecular weight. However, since the solubility of the nonyl and higher derivatives is more limited than desirable for a buffer component, the relationship could not be tested beyond the N-methyl-N-octylmorpholinium co-ion.

Compared to the lower tetraalkylammonium co-ions [6], the effective mobilities of the alkylmorpholinium cations cover the $(25-45) \times 10^{-5} \text{ cm}^2/\text{Vs}$ range more evenly and permit closer mobility matching for the analytes. Together, the two cation series offer 11 different mobilities in the $(20-50) \times 10^{-5} \text{ cm}^2/\text{Vs}$ range.

To demonstrate the value of co-ion-based mobility-matching in difficult CE separations, the electropherograms of a sample that contains the disubstituted geometric isomers (c and d in Figure 2) are shown in Figure 4. To facilitate

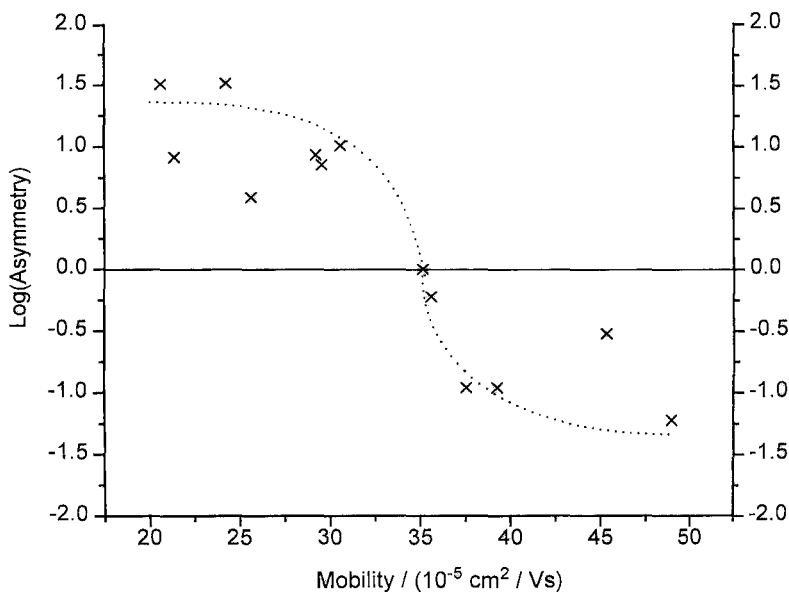


Figure 4.

Determination of the mobility of the N-methyl-N-propyl-morpholinium BGE co-ion. BGE: 50 mM phosphoric acid, pH 2.2, adjusted with N-methyl-N-propyl-morpholinium hydroxide. Field strength: 320 V/cm. Other conditions as in Experimental.

comparison, the electropherograms are plotted in terms of mobilities, rather than migration times. The electropherograms were obtained with 50 mM phosphoric acid BGEs whose pH was adjusted to 2.2 with N-ethyl-N-methyl-morpholinium hydroxide, N-methyl-N-propyl-morpholinium hydroxide and N-hexyl-N-methylmorpholinium hydroxide, respectively. The counter-ion (dihydrogenphosphate), hydronium, and N-methyl-N-alkylmorpholinium ion concentrations are the same in all three BGEs. It can be seen that the mobilities of the tail-ends and the front-ends of the skewed peaks (mobilities at infinite dilutions) and at the peak maxima of the symmetric peaks are

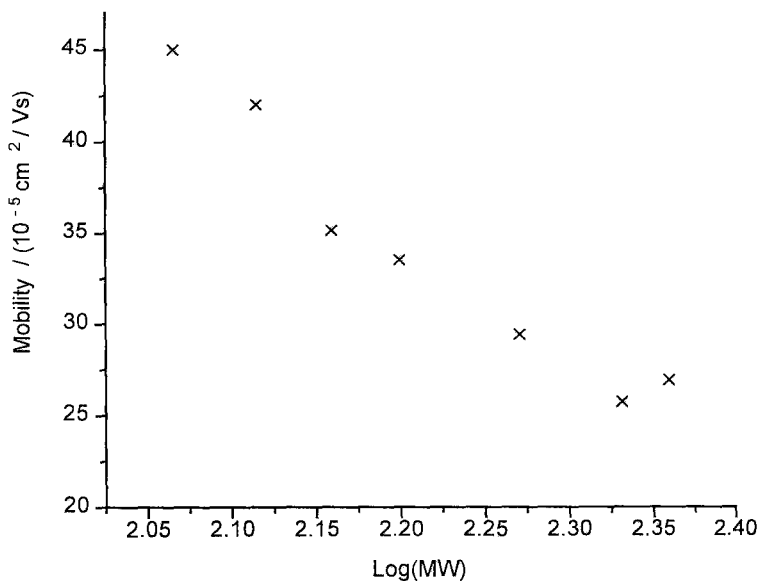


Figure 5.

Effective mobility vs. logarithm of molecular weight plot for the N-alkyl-N-methylmorpholinium cations in 50 mM phosphoric acid BGEs, pH 2.2 adjusted with the respective N-alkyl-N-methylmorpholinium hydroxide. Other conditions as in Figure 4.

identical, consequently the separation selectivities, which are the ratios of the effective mobilities, are also identical. However, the extent of peak distortion is very different and leads to peak resolutions which range from inadequate to almost baseline-baseline. The N-methyl-N-propyl-morpholinium ion ($\mu^{\text{eff}} = 35 \cdot 10^{-5} \text{ cm}^2/\text{Vs}$) results in symmetric solute peaks ($\mu_1^{\text{eff}} = 35.3 \cdot 10^{-5} \text{ cm}^2/\text{Vs}$ and $\mu_2^{\text{eff}} = 34.6 \cdot 10^{-5} \text{ cm}^2/\text{Vs}$), the N-ethyl-N-methyl-morpholinium ion ($\mu^{\text{eff}} = 42 \cdot 10^{-5} \text{ cm}^2/\text{Vs}$), the faster co-ion results in tailing solute peaks, while the N-hexyl-N-methylmorpholinium ion ($\mu^{\text{eff}} = 28 \cdot 10^{-5} \text{ cm}^2/\text{Vs}$), the slower co-ion, results in fronting solute peaks.

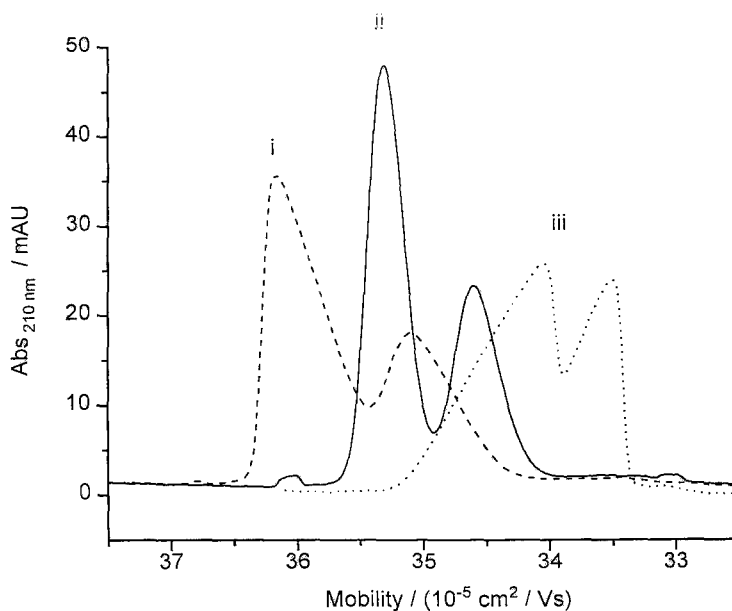


Figure 6.

Electropherograms of the minor components (c and d) of the reaction mixture shown in Figure 2 in 50 mM phosphate, pH 2.2 BGEs, (i) co-ion: 25 mM N-ethyl-N-methyl-morpholinium (dashed line), (ii) co-ion: 25 mM N-methyl-N-propyl-morpholinium (solid line), (iii) co-ion: 25 mM N-hexyl-N-methyl-morpholinium (dotted line). Field strength: 80 V/cm. Other conditions as in Experimental, except the eCap Neutral capillary was used.

4. CONCLUSIONS

A set of new N-alkyl-N-methyl-morpholinium hydroxides were synthesized. The mobilities of the cations were determined in pH 2.2, 50 mM phosphate buffer BGEs and found to span the $(25-45) \cdot 10^{-5} \text{ cm}^2/\text{Vs}$ range, permitting their use in weak acid-derived mobility matching background electrolytes. Together with the

tetraalkylammonium cations, these new reagents offer 11 distinct co-ions which can be used in the $(20-50) \cdot 10^{-5} \text{ cm}^2/\text{Vs}$ effective mobility range to eliminate much of the electromigration dispersion that plagues most CE separations. By utilizing the concept of mobility matching BGEs, co-ion mobility-independent pH-control (as required by separation selectivity) can be achieved by the counter-ion, while pH-independent mobility matching can be achieved by the appropriate co-ion. These BGEs facilitate difficult separations that could not be achieved otherwise, even if the concentration of the analytes was kept very low. The utility of the approach is limited only by the lack of strong electrolytes with appropriately low mobilities. Therefore, further work is under way in our laboratory to synthesize cations which have mobilities below $20 \cdot 10^{-5} \text{ cm}^2/\text{Vs}$.

ACKNOWLEDGEMENTS

Partial financial support of this project by the Advanced Research Program of the Texas Coordinating Board of Higher Education (Grant No. 010366-016), Beckman Instruments Co. (Fullerton, CA) and the R.W. Johnson Pharmaceutical Research Institute (Spring House, PA) is gratefully acknowledged.

REFERENCES

- 1 J. W. Jorgenson and K. D. Lukacs, *Anal. Chem.* 53 (1981) 1298.
- 2 F.E.P. Mikkers, F.M. Everaerts and Th.P.E.M. Verheggen, *J. Chromatogr.* 169 (1979) 1.
- 3 V. Šustáček, F. Foret and P. Boček, *J. Chromatogr.* 545 (1991) 239.
- 4 Y. Y. Rawjee, R. L. Williams and Gy. Vigh, *Anal. Chem.* 66 (1994) 3777.
- 5 Y. Y. Rawjee, Gy. Vigh and R. L. Williams, US Patent pending, 1994.
- 6 R. L. Williams and Gy. Vigh, *J. Chromatogr. A* (1995) in press

- 7 B. A. Williams and Gy. Vigh, *Anal. Chem.* in press (1995).
- 8 J. N. Kanazawa and N. S. Nishinomiya US. Patent 3,134,788 (1964).
- 9 H. Z. Sommer and L. L. Jackson, *J. Org. Chem.* 35 (1970) 1558.
- 10 H. Z. Sommer, H. I. Lipp and L. L. Jackson, *J. Org. Chem.* 36 (1971) 824.

Received: July 10, 1995

Accepted: August 6, 1995

ANALYSIS OF THE CONTRAST AGENT IOPAMIDOL IN SERUM BY CAPILLARY ELECTROPHORESIS

Z. K. SHIHABI, M. V. ROCCO, AND M. E. HINSDALE

*Pathology Department
Bowman Gray School of Medicine
Wake Forest University
Winston-Salem, North Carolina 27103*

ABSTRACT

A rapid method for the analysis of the contrast agent iopamidol (isovue) in serum by CE is described. The method involves deproteinization with acetonitrile to remove serum proteins followed by direct capillary zone electrophoresis. It is rapid (about 10 min) and sensitive. Other contrast agents and compounds used for renal function tests such as iohexol, iothalamic acid and p-aminohippuric acid can be detected by the same method. The use of acetonitrile in this method to remove serum proteins results in sample stacking allowing the detection of levels less than 1 mg/L.

INTRODUCTION

Iopamidol (Isovue, Squibb Diagnostics, Princeton, NJ) is an iodinated, non-ionic radiographic contrast medium similar to iohexol in chemical structure (1,2).

It is used frequently in cardiology for angiography. Because it is a non-metabolizable compound, does not bind to serum proteins, and is cleared by the kidney; it can also potentially be used as a measure of renal function. It is usually administered in large quantities, therefore it can cause contrast nephropathy (2,3) especially in patients with pre-existing risk factors. These patients exhibit delayed clearance of this compound.

In order to perform such studies and to access its use as a renal function measure a simple and rapid method for the assay of this compound is important. Previously this agent has been analyzed by HPLC (4) Here we show that this compound can be analyzed easily by capillary zone electrophoresis.

MATERIALS AND METHODS

Instrument

A Model 2000 capillary electrophoresis instrument (Beckman Instruments, Palo Alto, CA) was set at 8 KV, 24 C and 254 nm. The capillary was 42 cm X 50 um (i.d.). The electrophoresis buffer was boric acid (175 mmol/L) adjusted to pH 9.4 with sodium hydroxide (2 mol/L). Samples were introduced by pressure injection for 8 s (2.5% of the capillary).

Method

Serum, or standard, 50 uL was deproteinized by mixing for 15 s with 100 uL acetonitrile containing an internal standard 80 mg/L of 3-isobutyl-1-methyl-

xanthine The mixture was centrifuged for 30 s at 15,000 rpm and the supernatant was injected on the capillary.

Chemicals

Iopamidol, was obtained from Squibb Diagnostics, Princeton, NJ; iohexol, from Winthrop Pharmaceuticals, New York, NY; iothalamic acid, from Malinckrodt, St. Louis, MO; p-aminohippuric acid from Sigma Chemicals, St. Louis, MO ; and 3-isobutyl-1- methyl-xanthine from Aldrich Chemical Co., Milwaukee, WI).

Stock Standard

Iopamidol 3000 mg/L of water containing 9 g/L sodium chloride.

Working Standard

Dilute the stock standard in serum.

Calculation

Peak height was used for calculation.

RESULTS AND DISCUSSIONS

Iopamidol has a maximum light absorbency at about 240 nm and a strong signal at 254 nm. Iopamidol, iohexol, iothalamic acid, and p-aminohippuric acid are common compounds which can be used in angiography, or as a measure of renal function. All of these compounds have a strong absorption at 254 nm and can be separated at the same time by CE, Fig 1. Although we optimized the separation for iopamidol these compounds can also

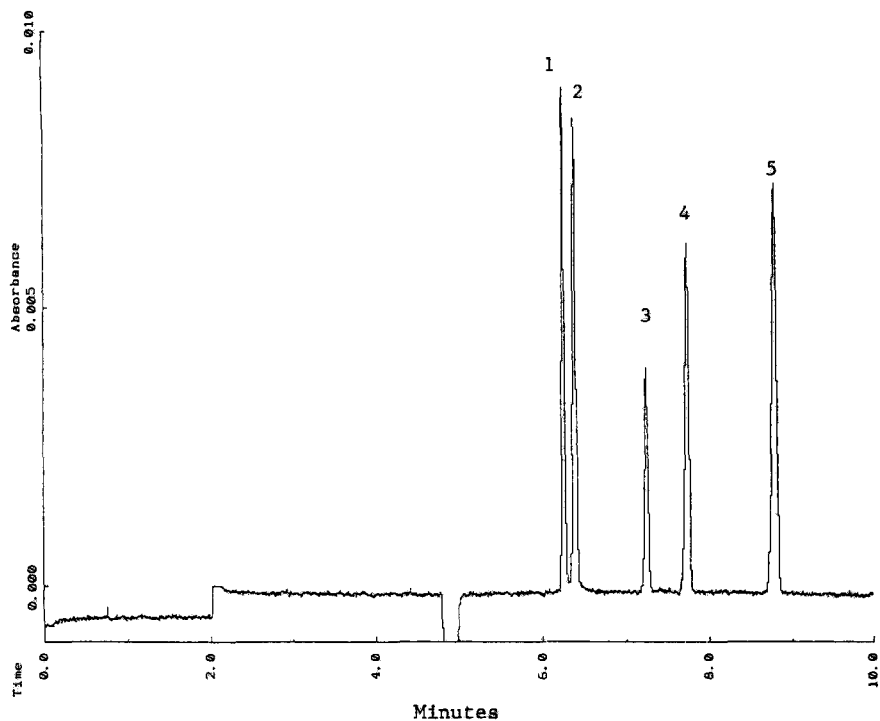
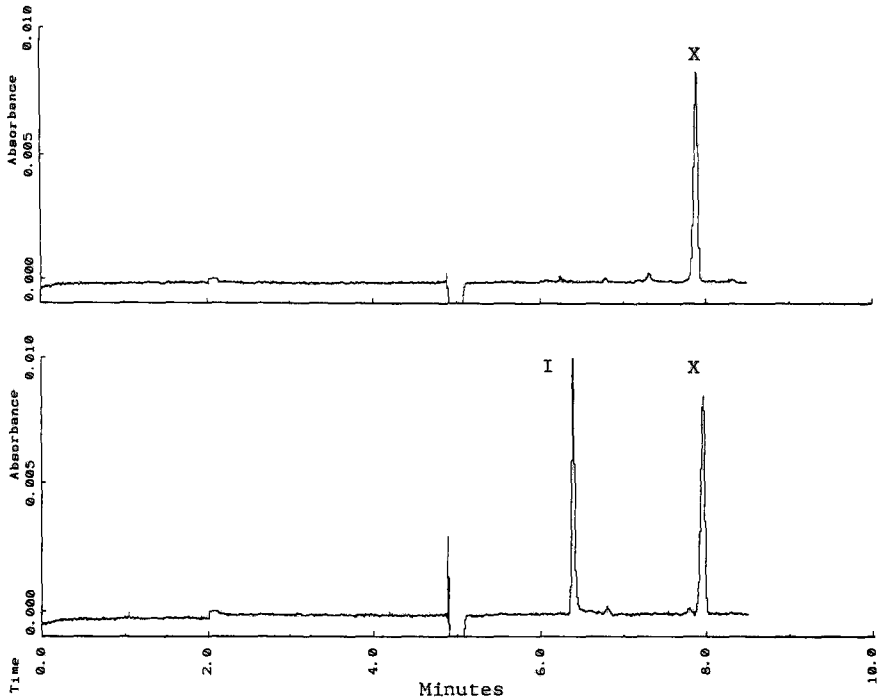


Fig 1. Separation of iopamidol and a few other related compounds in 1% sodium chloride. (1 =iopamidol 110 mg/L, 2 = iohexol 80 mg/L, 3= iothalamic acid 40 mg/L, 4 =internal standard, 5= p-aminohippuric acid 90 mg/L).

be analyzed by this method. Figure 2 illustrates the detector response to a sample from a patient receiving this drug. The electropherograms are relatively clean. Acetonitrile treatment eliminates proteins and allows for a larger sample volume to be injected on the capillary. The separation is fast and can be completed in less than 10 min.

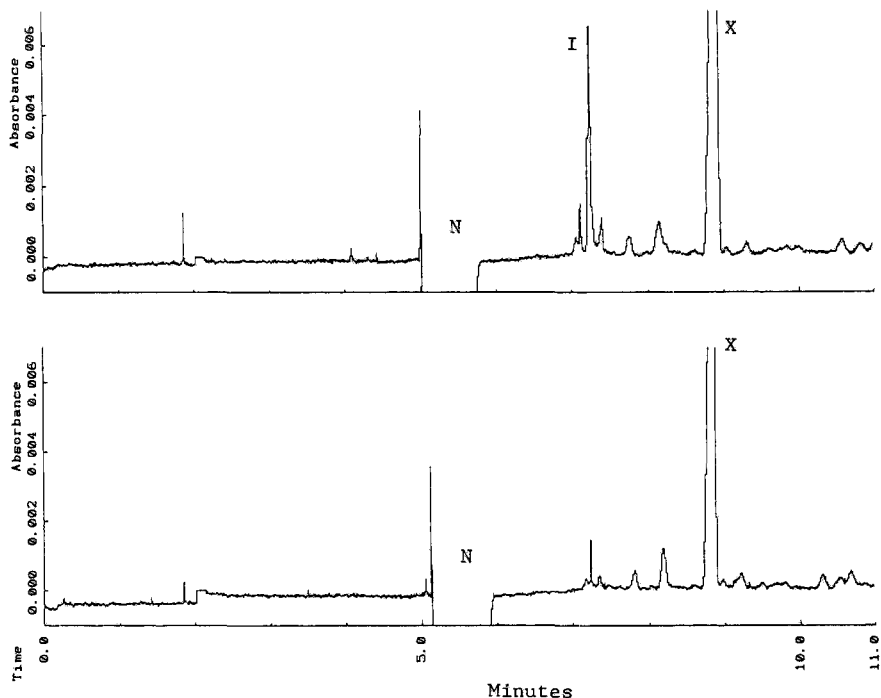
The analysis, by peak height is linear between 5 and 450 mg/L (Conc. mg/L= mA x 0.54+ 0.4, r=0.99). The



2-Electropherogram of (top) a patient free from iopamidol; and (bottom) a patient administered with the contrast agent (135 mg/L, I = iopamidol, X = Internal standard).

average recovery of 150 mg/L added to serum was 91 % relative to standards (n=4). To avoid the difference due to matrix the standards were prepared in serum free of this compound(6).

The lowest detection limit is 5 mg/L. Previously we have shown that samples deproteinized with acetonitrile can be concentrated by stacking(5) due to the low conductivity of the acetonitrile. Under such conditions, half of the capillary can be loaded with



3- Top) Serum sample spiked with 5 mg/L iopamidol; and bottom) same sample before spiking (I = iopamidol, X= Internal standard, N= neutral compounds).

sample(7). Prolonging the injection time to 40 s (12.5% of the capillary) increased the sensitivity of detection such that levels < 1 mg /L can be detected, Fig 3. However, at this high volume of sample the effective length of the capillary decreases. Some compounds which are present normally in trace amounts in serum concentrate too. Without better separations (e.g. longer capillary) they may interfere, Fig 3. We did not see any need for analyzing at the present time such low levels; however, this illustrates the

potential of this method to concentrate and detect low levels of samples in general by CE. We checked about 20 samples from normal individuals for possible interference. Hemolysis (1 g/L), bilirubin (100 mg/L) and none of the common drugs which we tested, such as salycilate, acetaminophen, and phenobarbital interfered with the test.

Several investigations(1-4) have established that iohexol is a reliable and convenient compound for GFR measurements(1-4,8). It is also possible to use iopamidol as another compound for GFR measurement. We analyzed 32 serum samples from patients received this agent as part of cardiac catheterization . The serum values had a wide range, depending on the time of sample collection and the dose, ranging from <5- 5100 mg/L, with a mean of 667 and SD of 1266 mg/L.

REFERENCES

1. Shihabi Z.K., Constantinescu M.S., Clin. Chem., 38, 2117, 1992.
2. Spinler S.A., Ann. Pharmacotherapy, 26: 56-64,1992.
3. Katholi R.E., Taylor G.J., Woods W.T., Womack K.A., McCann W.P., Moses H.W., Dove J.T., Mikell F.L, Woodruff R.C, Miller B.D., Schnieder J.A., Radiology, 186: 183-187, 1993.
4. Harapanhalli R.S, Yaghami V., Patel Y.D., Baker S.R., Rao D.V., Anal. Chem., 65: 606-612, 1993.
5. Shihabi Z.K., *J. Chromatogr.*, 680:471,1993
6. Shihabi Z.K, Garcia L.L., in: Landers, J.P., (ed.), Handbook of electrophoresis. Boca Raton, FL:CRC Press,1994, 537-548.
7. Shihabi Z.K., (*manuscript in preparation*).
8. Rocco M. Buckalew V., Shihabi Z., Am. J. Nephrol., (in Press).

Received: July 10, 1995

Accepted: August 6, 1995

**DETERMINATION OF PHOTODESTRUCTION
QUANTUM YIELDS USING CAPILLARY ELECTRO-
PHORESIS: APPLICATION TO *o*-PHTHALALDE-
HYDE/ β -MERCAPTOETHANOL-LABELED
AMINO ACIDS**

OWE ORWAR¹, HARVEY A. FISHMAN¹, MIKAEL SUNDAHL²,
VISHAL BANTHIA¹, RAJEEV DADOO¹, AND RICHARD N. ZARE^{1*}

¹*Department of Chemistry
Stanford University
Stanford, California 94305-5080*
²*Department of Organic Chemistry
Chalmers University of Technology
Göteborg, Sweden*

ABSTRACT

Photodestruction quantum yields, Φ_D , were determined for *o*-phthalaldehyde/ β -mercaptoethanol-labeled protein amino acids in aqueous alkaline solution using *trans*-azobenzene actinometry. The Φ_D values ranged from 0.020 to 0.062; the highest were obtained for amide-containing amino acid derivatives (Gln and Asn; $\Phi_D = 0.062$ and 0.054, respectively). The average maximal number of fluorescent photons obtained from the chromophores ranged from 6.4 to 19.0 per molecule. We show that Φ_D values can be determined with the help of an internal standard using capillary electrophoresis with laser-induced fluorescence detection. Generally, good agreement between the Φ_D values obtained in this way and Φ_D values obtained using *trans*-azobenzene actinometry was found. Furthermore, we show that knowledge of the analyte's photochemical properties assists identification of components separated by capillary electrophoresis.

INTRODUCTION

Hjertén (1) was one of the first to demonstrate what he termed "high-performance electrophoresis" by analogy with high-performance liquid chromatography in which

electrophoretic separations were carried out in thin-walled glass tubes of small inner diameter (0.05 to 0.3 mm). Such small glass tubes allowed for efficient heat dissipation so that thermal distortion of the zones was small even at high field strengths. In a classical paper, Jorgenson and Lukacs (2) demonstrated separation efficiencies in excess of 400,000 theoretical plates by performing electrophoresis in capillaries with inner diameters of 75 μm . This methodology is commonly referred to as capillary electrophoresis (CE). Taking full advantage of the high separation efficiencies achieved with CE requires a sensitive and selective detection scheme that does not contribute to any extraneous band broadening. One such scheme is on-line laser-induced fluorescence (LIF) detection (3), but the CE-LIF detection process can be optimized only if several key photophysical and photochemical properties of the analytes are known (4,5). Unfortunately, all the required photophysical and photochemical parameters are not generally known even for derivatives obtained with commonly employed reagents. Another complication of this scheme that has to be taken into account is that separated analytes migrate at different velocities within the CE column and are therefore excited by the laser light for different periods of time (5,6). In this report, we present photodestruction quantum yields (Φ_D) obtained using *trans*-azobenzene actinometry for ten protein amino acids labeled with *o*-phthalaldehyde/ β -mercaptoethanol (OPA/BME), a reagent used extensively to label protein amino acids for use in liquid chromatography (LC) and CE (7). The fluorescence quantum yields (Φ_f) of these chromophores have been reported (8). It is now feasible to calculate the number of fluorescent photons (n_f) that can be obtained from a single chromophore as described by Hirschfeld (9) and Mathies and coworkers (4) as:

$$n_f = \Phi_f / \Phi_D = k^o_f / k_d \quad (1)$$

where k^o_f (s^{-1}) is the rate of fluorescence and k_d (s^{-1}) is the rate of photodestruction. Knowledge of n_f is important because it determines the detection sensitivity that can be achieved for a given fluorophore.

Furthermore, we present CE-LIF detection at low and high excitation irradiances of separated standard amino acid derivatives that have equal optical densities. The low-excitation irradiance corresponds to excitation of the chromophores with a few quanta of light, and under these conditions fluorescence intensity, I_f , is proportional to $\Phi_f \tau_t$, where τ_t is the time a molecule is interrogated by the laser beam. The high-excitation irradiance produces complete apparent fluorescence saturation of the chromophores, and under these

conditions I_f is proportional to Φ_f/Φ_D . We show that in the limit of high excitation irradiances, it is feasible to obtain Φ_D values using CE-LIF detection provided that an internal standard with known Φ_f/Φ_D ratio is available to characterize the instrumental response.

MATERIALS AND METHODS

Apparatus

The quantum yields of photodestruction were measured in an optical bench arrangement that consisted of a Xe arc lamp and a monochromator (Applied Photophysics, Leatherhead, UK), as described previously (10). *trans*-Azobenzene (11), calibrated against ferrioxalate (12), was used as an actinometer. The CE experiments in 800-mm long x 67- μm i.d. fused silica capillaries (Polymicro, Phoenix, AZ) were performed using a high-voltage power supply (Glassman, Whitehouse Station, NJ) operated at ~ 5 to 25 kV. Injections were performed by raising the inlet end of the capillary ~ 5 cm above the outlet end of the capillary for 30 seconds.

LIF detection in CE experiments was performed using the 325-nm line from a model 4240 NB Liconix He-Cd laser (Santa Clara, CA). An interference filter centered at 325 nm with a 10.5-nm FWHM (Omega Optical, Brattleboro, VT) was used to reject plasma discharge emission and unwanted laser light. The laser beam was focused onto the fused silica capillary using a 50-mm focal-length lens. The beam waist at the focal point ($1/e^2$ intensity) was calculated to be 11 μm . A linear-graded neutral density filter (Melles Griot, Irvine, CA) was used to control excitation laser powers. The detection zone of the capillary, which was produced by stripping off the polyimide layer on a 5-mm length by heating was housed in a parabolic mirror. The fluorescence emission was collected at a right angle with respect to the incident laser beam and focused by a 150-mm focal length plano-convex lens onto the photomultiplier tube (Hamamatsu model R4632, San Jose, CA). The photomultiplier tube was biased at 500 V. The fluorescence emission was filtered to reject Raman and Rayleigh scattered light by a 450-nm notch interference filter (~ 30 nm FWHM) from Omega Optical. The photomultiplier tube current was amplified by a picoammeter, converted to voltage, and digitized using an analog-to-digital board (Chrom-1, Omega Engineering, Stamford, CT). It was displayed using commercial software (Galactic Industries, Salem, NH) run on a personal computer. Absorbance measurements were performed using a UV-VIS spectrophotometer (model 8450, Hewlett Packard, Palo Alto, CA).

Amino Acids, Reagents, and Derivatization Procedures

10-mM solutions of amino acid standards (Sigma, St. Louis, MO) were prepared in distilled deionized water. A borate buffer for use in CE experiments was prepared from disodiumtetraborate (~11 mM, pH 9.1) (Merck, Darmstadt, Germany). Another borate buffer for use with reagents was prepared by dissolving boric acid in distilled deionized water to a final concentration of 0.4 M. The pH was adjusted to 9.5 with 5.0-M NaOH. The OPA/ β ME reagent solutions were prepared by dissolving 100 mg OPA (99%, Sigma) in 1 mL of methanol and adding to this solution 100 μ L of β ME (99%). The borate buffer was added to this solution to create a final volume of 10 mL. Derivatizations were performed in polypropylene vials. Reagent-to-standard-volume ratios of 1 : 2 were typically used. In all CE experiments, concentrations of analytes were corrected to give the same absorbance at 325 nm. Determination of photodestruction quantum yields by *trans*-azobenzene actinometry was performed in a 50-mM borate buffer (pH=9) using stoichiometric amounts of reactants. The completion of the reactions was ascertained by absorption measurements at 336 nm.

RESULTS AND DISCUSSION

Table 1 lists several photophysical and photochemical properties of OPA/ β ME-labeled amino acids. Included are the Φ_D values that we obtained using *trans*-azobenzene actinometry, together with the fluorescence quantum yields (8), and the fluorescence and photodestruction rate constants. The Φ_D values obtained here are similar to previous estimates of the monophotonic photodestruction quantum yields of aromatic amino acids using excitation at 254 nm (Φ_D , Trp = 0.9 %; Φ_D , Tyr = 2.2 %; Φ_D , Phe = 1.9 %) (13). The highest Φ_D values were obtained, however, for the amide-containing chromophores OPA/ β ME-Asn and OPA/ β ME-Gln; their Φ_D values are 5.4% and 6.2%, respectively. Earlier studies of OPA/ β ME-labeled α -peptides correlated high photodestruction quantum yields with the proximity of amide groups to the isoindole moiety (14). Intramolecular electron transfer, in which the isoindole functions as an excited-state electron donor and nearby amide groups function as electron acceptors, may be the mechanism underlying these effects.

Recall that the ratio between the fluorescence quantum yield and the photodestruction quantum yield, Φ_f/Φ_D , determines the average maximum number of fluorescent photons a molecule can yield (4,9). These ratios for the OPA/ β ME-labeled amino acids are listed in Table 1; note that they are several orders of magnitude lower than those of chromophores

TABLE 1

Photophysical and photochemical properties of *o*-phthalaldehyde/ β -mercaptoethanol-labeled amino acids

AMINO ACID	^a Φ_f	^b Φ_D	^c Φ_f/Φ_D	^d k_f/s^{-1}	^e k_f^0/s^{-1}	^f k_d/s^{-1}
Ala	0.40	0.031*	12.9	5.43×10^7	2.17×10^7	1.68×10^6
Arg	0.40	0.021	19.0	5.13×10^7	2.05×10^7	1.08×10^6
Asn	0.40	0.054	7.41	5.75×10^7	2.30×10^7	3.10×10^6
Asp	0.41	0.031	13.2	5.38×10^7	2.20×10^7	1.67×10^6
Gln	0.40	0.062	6.45	5.40×10^7	2.16×10^7	3.53×10^6
Leu	0.41	0.037	11.1	5.00×10^7	2.05×10^7	1.85×10^6
Ser	0.41	0.037	11.1	5.05×10^7	2.07×10^7	1.87×10^6
Thr	0.36	0.043	8.37	5.24×10^7	1.89×10^7	2.25×10^6
Trp	0.33	0.027	12.2	4.98×10^7	1.64×10^7	1.34×10^6
Tyr	0.33	0.020	16.5	5.00×10^7	1.65×10^7	1.00×10^6
Val	0.34	0.035	9.71	5.00×10^7	1.70×10^7	1.75×10^6

^aFluorescence quantum yields (Φ_f) taken from Chen et al. (8).^bPhotodestruction quantum yields (Φ_D) obtained using *trans*-azobenzene actinometry as described in the experimental section.^cThe ratio between the fluorescence quantum yield and the photodestruction quantum yield (Φ_f/Φ_D), which equals the maximum number of fluorescent photons that can be obtained for a single chromophore.^dThe observed rate of fluorescence (k_f) taken from Chen et al. (8).^eThe rate of fluorescence (k_f^0) was calculated as; $k_f^0 = k_f \Phi_f$.^fThe rate of photodestruction (k_d) was calculated as; $k_d = k_f \Phi_D$.

* Data taken from ref. 10

employed as laser dyes and high-sensitivity fluorescence markers, for example, Rhodamine 6G in ethanolic solution ($\Phi_f/\Phi_D = 1.9 \times 10^6$) (15), Texas Red in ethanolic solution ($\Phi_f/\Phi_D = 1.4 \times 10^6$) (15), and fluorescein in water-based solution ($\Phi_f/\Phi_D = 3.7 \times 10^4$) (16).

As stated, the optimization of LIF detection requires knowledge of certain molecular parameters. For cases in which only singlet saturation and photochemistry are important, an equation that describes the fluorophore behavior has been derived by Mathies and co-workers (4):

$$n_f = (\Phi_f/\Phi_D)[1 - \exp\{-k\tau/(k + 1)\}] \quad (2)$$

This function asymptotically approaches Φ_f/Φ_D . For a population of molecules, the fluorescence intensity (I_f) is obtained by multiplying the right side of Eq. 2 by the number

of molecules. The parameters needed to calculate n_f for a given excitation irradiance are: Φ_f , Φ_D , and τ , which the last is the ratio of the transit time τ_t (s) to the photodestruction time τ_D (s); and k , which is the ratio between the rate of absorption k_a (s^{-1}) and the observed rate of fluorescence k_f (s^{-1}). Even though different OPA/ β ME-labeled analytes can be photoionized to different extents in aqueous alkaline solution (10), we assume that analysis using Eq. 2 is sufficient for the chromophores in the present study. This assumption is based on the idea that we are concerned mainly with obtaining a qualitative description of the excitation irradiance dependence for the chromophores. Spectroscopic observations in water-based solutions suggest that triplet absorption is negligible in some OPA/ β ME amino acid derivatives (10), indole, N-methylindole, and tryptophan (17).

Figure 1 shows plots of calculations using Eq. 2 for the OPA/ β ME-Ala and OPA/ β ME-Asn derivatives, which represent two chromophores that have different photodestruction quantum yields but identical fluorescence quantum yields (Table 1). Figure 1 also shows the effect of increasing the transit time for the Ala derivative. Figure 2 shows the laser irradiance dependence for the same two derivatives in a CE experiment in which the analytes (same concentration corresponding to equal optical density at $\lambda_{abs}=325$ nm) are detected under identical conditions, that is identical excitation irradiance and transit time. Qualitatively, the results agree well with the calculations shown in Figure 1, which suggest that (1) the rate of photodestruction is the major difference between these two chromophores and (2) that the photophysical constants are similar. The Φ_f/Φ_D value obtained for the Ala derivative in this experiment was 1.99 ± 0.05 (mean \pm s.d.) times higher than that for the Asn derivative, which is close to the expected value of 1.74 ± 0.12 (mean \pm s.d.). More experiments are shown below that demonstrate how Φ_D values can be obtained in CE-LIF detection experiments for analytes that migrate at different velocities.

In experiments where the laser power dependence was investigated for Asn and Asp labeled with OPA/ethanethiol (OPA/EtSH), a similar result as shown in Figure 2 was obtained (data not shown). The only difference was that the EtSH-containing chromophores yielded slightly lower fluorescence intensities at the highest excitation irradiances. This result is consistent with lower fluorescence quantum yields of the EtSH-labeled analogs (8) and suggests that the photochemical properties of β ME- and EtSH-labeled chromophores are similar.

In CE, separated analytes travel through the separation column at different velocities and are therefore interrogated in an on-line LIF detection scheme by the laser beam for different periods of time. With a delta-function detector, this spread in analyte velocities

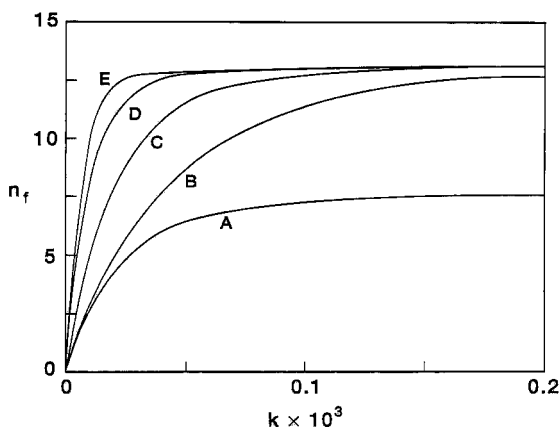


Figure 1.

Fluorescence intensity (n_f) for a single chromophore as a function of normalized excitation intensity k for the OPA/ β ME-Asn (A) and OPA/ β ME-Ala derivatives (B). The graphs were constructed using Eq. 2 and the Φ_f and Φ_D values listed in Table 1, a transit time of 23.7 ms, and the photodestruction lifetimes ($1/k_d$, see Table 1) for the respective derivatives. Also shown is the effect of varying the transit time for the Ala derivative (C, $\tau_t=47.4$ ms; D, $\tau_t=94.8$ ms; E, $\tau_t=142.2$ ms).

results in increased temporal widths of the analyte bands in proportion to their migration time (6). Shear et al. (5) previously showed that detection conditions can be optimized for bands moving at different velocities by adjusting the excitation irradiance and the data-digitization rate.

Here we will show quantitatively how this spread in analyte velocities and differences in photochemistry affects the signal output using low- and high-excitation irradiances. At low-excitation irradiances, the fluorescence intensity (I_f) increases linearly according to:

$$I_f \approx K \Phi_f I_0 \tau_t A \quad (I_0 < I_{SAT}) \quad (3)$$

where K is a constant, I_0 the excitation intensity, and A the absorbance [which equals $\epsilon c b$, where ϵ is the molar absorptivity ($M^{-1} \text{ cm}^{-1}$), c the concentration (M), and b the optical pathlength (cm) in the detection zone]. We define I_{SAT} to be the level at which $I_f = \Phi_f/2\Phi_D$. In our experiments, the product $K I_0 A$ is kept constant and hence:

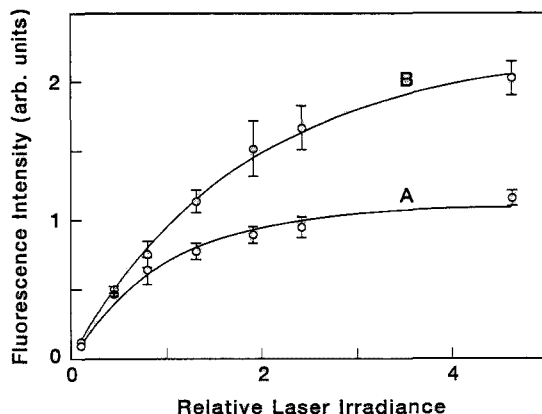


Figure 2.

Fluorescence intensity as a function of relative laser excitation irradiance for the OPA/ β ME-Asn (A) and OPA/ β ME-Ala (B) derivatives in CE-LIF detection experiments. Each data point represents the mean \pm s.d. ($n=3$). The solid lines show scaled best-curve-fits to Eq. 2.

$$I_f \propto \Phi_f \tau_t \quad (I_0 \ll I_{SAT}) \quad (4)$$

This linear relationship is demonstrated in Figure 3, which shows the results of electrophoresis of the Trp derivative at different velocities and excitation using a low-excitation irradiance ($I_0 \ll I_{SAT}$). This relationship is also shown in the electropherograms in Figure 4a-c, which represent results of four amino acid derivatives (having equal optical density at $\lambda_{abs}=325$ nm) traveling at different velocities and excited using low laser irradiance. As presented in Table 2, a good correlation exists between experimentally obtained peak areas in these CE experiments and peak areas calculated using Eq. 4. Figure 4d shows a computer simulation constructed to create gaussian peaks with areas proportional to $\Phi_f \tau_t$ for each derivative. The simulated peaks were centered at the experimentally found migration times for each analyte with a $\pm 3.5 \sigma$ basewidth based on the analyte's respective temporal width.

At high laser-excitation irradiance, at which point the fluorescence is saturated,

$$I_f \propto \Phi_f / \Phi_D \quad (I_0 >> I_{SAT}) \quad (5)$$

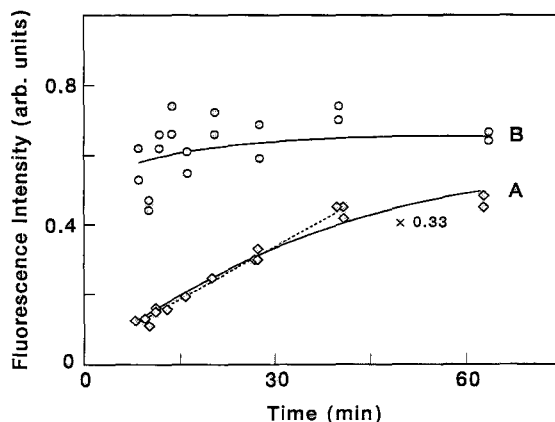


Figure 3.

Fluorescence intensity (peak area measurements) as a function of migration time for the Trp derivative at low (A) and high (B) laser-excitation irradiance. The desired migration times were obtained by adjusting the separation voltage. The dotted line shows a linear curve fit ($r=0.9938$) to all except the two last data points.

TABLE 2

Comparison between peak areas obtained using capillary electrophoresis with laser-induced fluorescence detection and the calculated product $\Phi_f \tau_t$ for each amino acid derivative at low-excitation irradiance.

Amine	Peak Area (mean \pm s.d.; n=3)	^a (Peak Area) _i /(Peak Area) _{Asp} (mean \pm s.d.)	^b ($\Phi_f \tau_t$) _i /($\Phi_f \tau_t$) _{Asp} (mean \pm s.d.)
Trp	6.53 \pm 0.55	0.60 \pm 0.06	0.50 \pm 0.05
Asn	7.43 \pm 0.55	0.69 \pm 0.07	0.62 \pm 0.06
Ala	7.30 \pm 0.75	0.67 \pm 0.08	0.64 \pm 0.06
Asp	10.83 \pm 0.66	1.00 \pm 0.09	1.00 \pm 0.10

^aPeak area for each derivative is normalized to that of the Asp derivative.

^bThe product $\Phi_f \tau_t$ for each derivative is normalized to that of the Asp derivative. The Φ_f values used are listed in Table 1 and are assumed to be correct within $\pm 5\%$ (no estimate of the error was given in ref. 8). τ_t was calculated as $\sqrt{\pi}r/v$, where r is the radius of the laser beam at focus and v the analyte velocity, and was calculated from distributions of retention times to be correct within $\pm 5\%$.

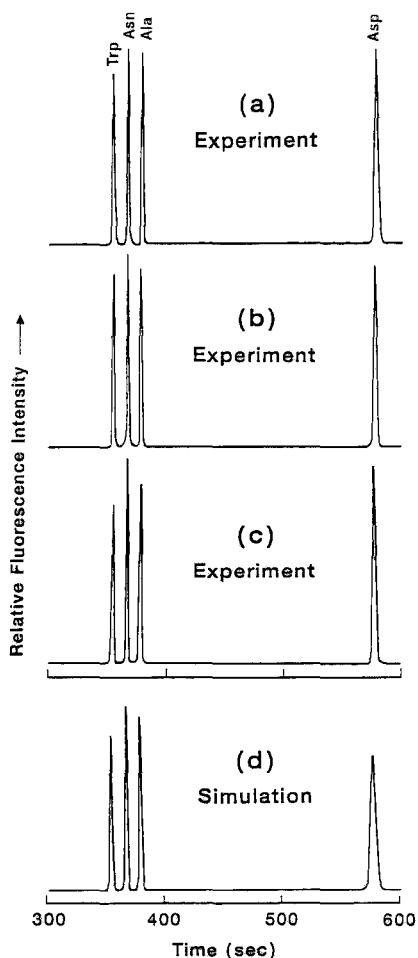


Figure 4.

a-c. Separation of an amino acid standard (Trp, Asn, Ala, and Asp) derivatized with OPA/ β ME. The concentrations of the amino acid derivatives were adjusted to give the same optical densities at $\lambda_{\text{abs}}=325$ nm. The derivatives were excited using low-excitation irradiance ($I_0 \ll I_{\text{SAT}}$). The baseline noise obtained in the CE experiments was subtracted using a linear fit.

d. A computer simulation constructed to create gaussian peaks with areas $\propto \Phi_f \tau_f$ for each derivative. The simulated peaks were centered at the experimentally found migration times for each analyte with a $\pm 3.5 \sigma$ basewidth based on the analyte's respective temporal width.

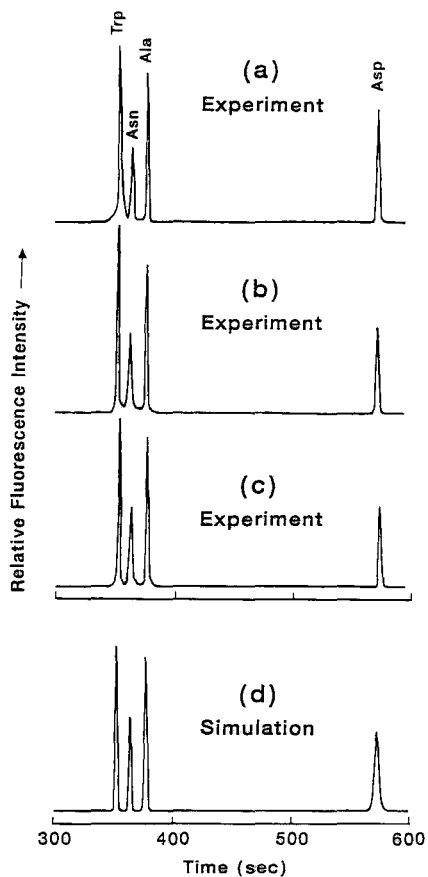


Figure 5

a-c. Same experimental conditions as in Figure 4a-c, except that high-excitation irradiance ($I_0 \gg I_{SAT}$) was employed.

d. A computer simulation performed as in Figure 4d, except that it was constructed to create gaussian peaks with areas $\propto \Phi_f/\Phi_D$ for each derivative.

TABLE 3

Comparison between peak areas obtained using capillary electrophoresis with laser-induced fluorescence detection and the calculated ratio Φ_f/Φ_D for each amino acid derivative at high-excitation irradiance.

Amine	Peak Area (mean \pm s.d.; n=3)	^a (Peak Area) _i /(Peak Area) _{Asp} (mean \pm s.d.)	^b (Φ_f/Φ_D) _i / (Φ_f/Φ_D) _{Asp} (mean \pm s.d.)
Trp	250 \pm 46	1.03 \pm 0.20	0.92 \pm 0.09
Asn	106 \pm 12	0.44 \pm 0.06	0.56 \pm 0.06
Ala	243 \pm 5.7	1.00 \pm 0.06	0.98 \pm 0.10
Asp	243 \pm 15	1.00 \pm 0.09	1.00 \pm 0.10

^aPeak area for each derivative is normalized to that of the Asp derivative.

^bThe ratio Φ_f/Φ_D for each derivative is normalized to that of the Asp derivative. The Φ_f and Φ_D values used are listed in Table 1. The errors in Φ_f and Φ_D are both estimated to be $\pm 5\%$.

is predicted from Eq. 2. This relationship was verified experimentally by using high-irradiance excitation in the CE runs presented in Figure 3, which shows the results of electrophoresis of the Trp derivative at different velocities, and in Figure 5a-c, which show separations of the same four derivatives as in Figure 4a-c. Table 3 presents a comparison of the relative peak areas obtained experimentally for each of these derivatives together with the relative peak areas calculated from Eq. 5. By using the Asp derivative as an internal standard with known Φ_f/Φ_D ratio it is straightforward to calculate the Φ_D values for the other three derivatives from the CE-LIF detection experiments from:

$$a_i/a_j = \Phi_{f_i}\Phi_{D_j}/\Phi_{f_j}\Phi_{D_i} \quad (6)$$

where a_i and a_j are the peak areas, Φ_{f_i} and Φ_{f_j} the fluorescence quantum yields, and Φ_{D_i} and Φ_{D_j} the photodestruction quantum yields of the analyte and the internal standard, respectively. The Φ_D values obtained in this way are 2.4%, 6.9%, and 3.0% for the Trp, Asn, and Ala derivatives, respectively, which generally is in good agreement with the Φ_D values obtained using *trans*-azobenzene actinometry (Table 1). The computer simulation (Fig. 5d) was performed as for Figure 4d, except that it was constructed to create gaussian peaks with areas proportional to Φ_f/Φ_D for each derivative.

The results demonstrate that if Φ_f and Φ_D values of the chromophores are known, peak characterization may be simply determined by performing detection at low excitation irradiance (where I_f increases linearly) and at high excitation irradiance (region where the fluorescence is saturated). Also, Φ_D values may be obtained using CE-LIF detection and the analysis provided by Eq. 2 if a suitable standard with known Φ_f/Φ_D ratio exist. The only requirement is that the Φ_f values of the analytes are known. The advantage of this procedure over that of bulk solution actinometry is that (1) it measures the photodestruction quantum yield of a separated pure product, (2) it is applicable for simultaneous multi-species determination, and (3) it requires only trace quantities of material.

ACKNOWLEDGMENTS

O. Orwar is supported by the Swedish Natural Science Research Council (No. K-PD 10481-301). H. A. Fishman is a W. R. Grace fellow. The authors gratefully acknowledge the help of Dr. Robert Guettler. Supported by grants from the National Institute of Mental Health (MH45423-03 and MH45324-05) and Beckman Instruments, Inc.

REFERENCES

1. S. Hjertén *J. Chrom.*, **270**: 1 (1983)
2. J. W. Jorgenson, K. D. Lukacs *Anal. Chem.*, **53**: 1298 (1981)
3. E. Gassmann, J. E. Kuo, R. N. Zare, *Science*, **230**: 813 (1985)
4. R. A. Mathies, K. Peck, L. Stryer *Anal. Chem.*, **62**: 1786 (1990)
5. J. B. Shear, R. Dadoo, H. A. Fishman, R. H. Scheller, R. N. Zare *Anal. Chem.*, **65**: 2977 (1993)
6. X. Huang, W. F. Coleman, R. N. Zare *J. Chrom.*, **480**: 95 (1989)
7. M. Albin, R. Weinberger, E. Sapp, S. Moring *Anal. Chem.*, **63**: 417 (1991)
8. R. F. Chen, C. Scott, E. Trepman *Biochim. Biophys. Acta*, **574**: 440 (1979)
9. T. Hirschfeld *Applied Optics* **15**: 3135 (1976)
10. O. Orwar, M. Sundahl, M. Sandberg, I. Jacobson, S. Folestad *Anal. Chem.*, **66**: 4471 (1994)
11. G. Gauglitz, S. Hubig *J. Photochem.* **30**: 121 (1985)
12. C. G. Hatchard, C. A. Parker *Proc. R. Soc. London A*, **235**: 518 (1956)
13. E. V. Khoroshilova, Y. A. Repyev, D. N. Nikogosyan *J. Photochem. and Photobiol. B.*, **7**: 159 (1990)
14. O. Orwar, S. G. Weber, M. Sandberg, S. Folestad, A. Tivesten, M. Sundahl *J. Chrom.* **696**: 139 (1995)
15. S. A. Soper, H. L. Nutter, R. A. Keller, L. M. Davis, E. B. Shera *Photochem. and Photobiol.*, **57**: 972 (1993)

16. R.A Mathies, L. Stryer Single-Molecule Fluorescence Detection: A Feasibility Study with β -Phycoerythrin in Applications of Fluorescence in the Biomedical Sciences. Allan R. Liss, New York, 1986, pp. 129-140
17. Y. Hirata, N. Murata, Y. Tanioka, N. Mataga J. Phys. Chem., 93: 4527 (1989)

Received: July 10, 1995

Accepted: August 6, 1995

SEPARATION OF SULFISOXAZOLE, PHENAZOPYRIDINE, AND THEIR RELATED IMPURITIES BY MICELLAR ELECTRO- KINETIC CHROMATOGRAPHY

BEVERLY NICKERSON^{1*}, STEPHEN SCYPINSKI¹,
HELEN SOKOLOFF², AND SWROOP SAHOTA²

¹*Analytical Research and Development*

²*Pharmaceutical Quality Control and Quality Assurance*

Hoffmann-La Roche Inc.

340 Kingsland Street

Nutley, New Jersey 07110-1199

ABSTRACT

A micellar electrokinetic chromatographic method for the analysis of sulfisoxazole, phenazopyridine and their related known impurities in a tablet dosage form has been developed and validated. Current methods employed for this dosage form involve the use of two separate ultraviolet spectrophotometric or titrimetric assay procedures for the determination of the actives. Traditional reversed-phase high performance liquid chromatographic separations of sulfisoxazole and its major degradation products, sulfanilamide and sulfanilic acid, result in the elution of the latter two components at or near the void volume, causing problems with their identification and quantitation. The micellar electrokinetic chromatographic method described here employs sodium dodecyl sulfate as the surfactant and effectively separates sulfisoxazole, phenazopyridine and all but two of their related impurities within thirty minutes. The method was found to be valid with respect to specificity, linearity and limits of detection. System precision, however, was relatively poor. Application of the method to the quantitation of these components in a tablet dosage form is presented.

INTRODUCTION

Azo Gantrisin^R is a tablet dosage form used for the treatment of uncomplicated urinary tract infections. It is composed of the antibacterial compound sulfisoxazole and the urinary analgesic phenazopyridine. Figures 1 and 2 show the structures of sulfisoxazole, phenazopyridine and their related impurities. Current testing methodologies for quantitating sulfisoxazole and phenazopyridine involve the use of separate ultraviolet (UV) spectrophotometric or titrimetric assay methods [1-4]. It was desired to develop a single chromatographic method to simultaneously quantitate these two substances. Efforts to develop a reversed-phase high performance liquid chromatographic (HPLC) method to separate sulfisoxazole, phenazopyridine and their related impurities were unsuccessful. Reversed-phase HPLC separations developed in our laboratory for the separation of sulfisoxazole and its two degradation products, sulfanilamide and sulfanilic acid, resulted in the elution of the latter two components at or near the void volume, causing problems with their identification and quantitation. The use of a basic ion-pairing reagent caused sulfanilamide and sulfanilic acid to be retained; however, other components in the sample matrix exhibited either a lack of retention or excessive retention [5]. The use of alternate separation techniques from reversed-phase HPLC were therefore explored for this dosage form.

Azo Gantrisin^R, which contains a combination of two active substances, was deemed a good model for testing the utility of micellar electrokinetic chromatography (MEKC), also referred to as micellar electrokinetic capillary chromatography (MECC), for practical pharmaceutical analysis. There are numerous examples in the literature

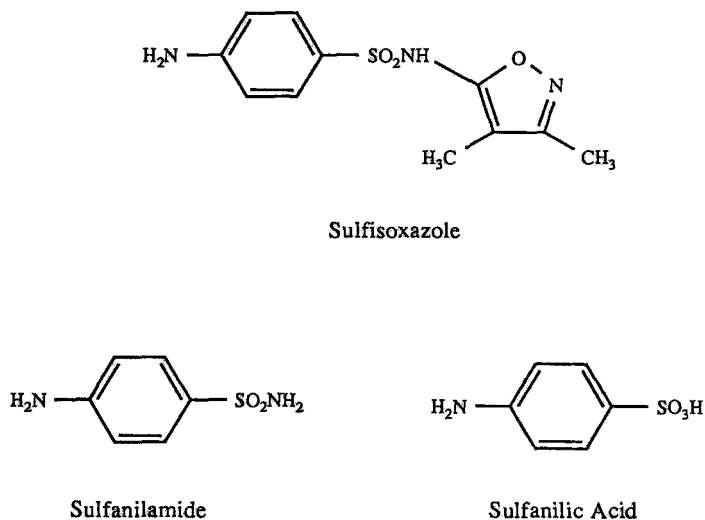
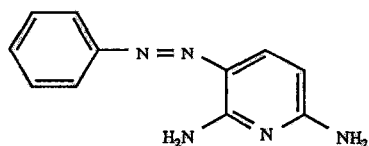


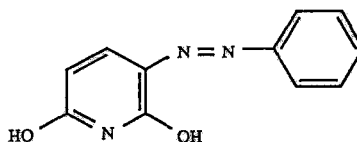
Figure 1

Chemical structures for sulfisoxazole and two of its potential degradation products, sulfanilamide and sulfanilic acid.

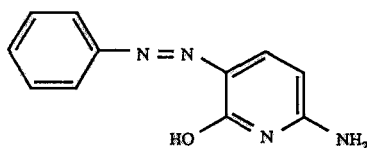
where capillary zone electrophoresis (CZE) [6-10] and MEKC [6, 11-14] have been employed as an alternative or complementary technique to HPLC in the analysis of "small-molecule" pharmaceuticals. MEKC is a variation of the increasingly popular technique of CZE [15-19]. In MEKC, surfactant molecules present at a sufficient concentration to form micelles are used to differentially solubilize analyte molecules based on their degree of hydrophobicity. The charged micelles are subject to electrophoretic effects and therefore migrate at a different rate than the surrounding aqueous phase. These micelles then behave as a moving chromatographic stationary phase and effectively separate molecules which have little or no differences in their electrophoretic mobilities but which do have different hydrophobicities [20-22].



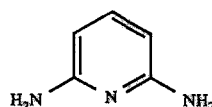
Phenazopyridine



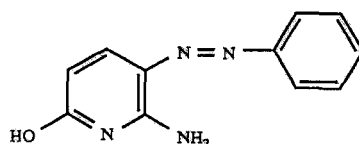
3-(Phenylazo)-2,6-pyridinediol



6-Amino-3-(phenylazo)-2-pyridinol



2,6-Diaminopyridine



6-Amino-5-(phenylazo)-2-pyridinol

Figure 2

Chemical structures for phenazopyridine and four of its possible synthetic by-products and degradation products.

MEKC was evaluated as a possible means of separating and quantitating sulfoxazole, phenazopyridine and their associated known impurities. Using a phosphate buffer system and sodium dodecyl sulfate as the micelle carrier, it was possible to separate all the analytes of interest except for the geometrically isomeric 3-

and 5-(phenylazo) pyridinols from each other within a run time of thirty minutes. This technique was demonstrated to be feasible for the complete separation of both active components and their related impurities in the tablet dosage form. The method is fairly rapid, simple and has been validated with respect to specificity, precision, linearity and detection limits.

MATERIALS

Sulfisoxazole and phenazopyridine were obtained from Hoffmann-La Roche Inc. (Nutley, NJ). 6-Amino-3-(phenylazo)-2-pyridinol, 6-amino-5-(phenylazo)-2-pyridinol, 2,6-diaminopyridine and 3-(phenylazo)-2,6-pyridinediol were obtained from F. Hoffmann-La Roche AG (Basel, Switzerland). Sulfanilamide was obtained from Eastman Kodak Company (Rochester, NY) and sulfanilic acid was purchased from MC&B (Cincinnati, OH). Sodium phosphate monobasic, sodium phosphate dibasic and sodium dodecyl sulfate were purchased from Fisher Scientific (Fair Lawn, NJ). All reagents and chemicals were used as received. Water was distilled and deionized using a NANOpure analytical grade system (Barnstead/Thermolyne Corporation, Dubuque, IA).

PROCEDURES

Preparation of Buffer

The buffer used to perform micellar electrokinetic chromatography consisted of 5 mM sodium phosphate monobasic, 5 mM sodium phosphate dibasic and 50 mM

sodium dodecyl sulfate. The pH of the buffer was adjusted to 7.0 using sodium hydroxide. This buffer was also used to dissolve and dilute samples.

Preparation of Solutions for Linearity, Limits of Detection and System Precision Studies

A solution containing 1 mg/mL sulfisoxazole and 0.1 mg/mL phenazopyridine was prepared by weighing 500 mg sulfisoxazole and 50 mg phenazopyridine into a 500 mL volumetric flask. Approximately 400 mL of buffer was added and the solution was sonicated for 30 minutes to completely dissolve the active components. The solution was then cooled and diluted to volume with buffer. Dilutions of this stock solution to perform the linearity and sensitivity studies for sulfisoxazole and phenazopyridine were made with buffer to the desired concentration.

Several stock solutions of the impurities were prepared as follows. A sulfisoxazole impurities stock solution containing 0.2 mg/mL each of sulfanilamide and sulfanilic acid was made by dissolving 5 mg of each of these compounds in 25 mL of sulfisoxazole/phenazopyridine stock solution using sonication as needed. A phenazopyridine impurities stock solution containing 0.04 mg/mL each 6-amino-5-(phenylazo)-2-pyridinol, 2,6-diaminopyridine and 3-(phenylazo)-2,6-pyridinediol was made by dissolving 1 mg of each of these standards in 25 mL of sulfisoxazole/phenazopyridine stock solution using sonication as needed. A stock solution containing 0.04 mg/mL 6-amino-3-(phenylazo)-2-pyridinol, another phenazopyridine impurity, was made by dissolving 1 mg of this compound in 25 mL of sulfisoxazole/phenazopyridine stock solution using sonication as needed.

One mL of the sulfisoxazole impurities stock solution, 0.5 mL of the phenazopyridine impurities stock solution and 0.5 mL of the stock solution containing 6-amino-3-(phenylazo)-2-pyridinol were diluted to 10 mL with sulfisoxazole/phenazopyridine stock solution. This resulting solution contained 1 mg/mL sulfisoxazole, 0.1 mg/mL phenazopyridine, 0.02 mg/mL or 2% each of sulfanilamide and sulfanilic acid with respect to sulfisoxazole and 0.002 mg/mL or 2% each of 6-amino-3-(phenylazo)-2-pyridinol, 6-amino-5-(phenylazo)-2-pyridinol, 2,6-diaminopyridine and 3-(phenylazo)-2,6-pyridinediol with respect to phenazopyridine. This solution, containing 1 mg/mL sulfisoxazole, 0.02 mg/mL of the two sulfisoxazole impurities, 0.1 mg/mL phenazopyridine and 0.002 mg/mL of the four phenazopyridine impurities, was used for method development purposes and to test the separation of the components with the MEKC method.

The above solution was prepared without 6-amino-3-(phenylazo)-2-pyridinol and was used to test the precision of the method. Dilutions of this mixture with sulfisoxazole/phenazopyridine stock solution were used to perform the linearity and sensitivity studies for these impurities.

Preparation of Standard Solution for Assay

Fifty mg of sulfisoxazole and 5 mg of phenazopyridine were accurately weighed into a 50-mL volumetric flask. Approximately 40 mL of buffer was added and the solution was sonicated for 30 minutes to completely dissolve the sulfisoxazole and phenazopyridine. The solution was then cooled and diluted to volume with buffer

to yield a standard containing 1 mg/mL sulfisoxazole and 0.1 mg/mL phenazopyridine.

This solution was diluted 1:25 with buffer to yield a solution containing 0.04 mg/mL sulfisoxazole and 0.004 mg/mL phenazopyridine for use in the assay of these components.

Preparation of Tablet Sample Solutions

Ten Azo Gantrisin^R tablets, each containing 500 mg sulfisoxazole and 50 mg phenazopyridine were ground in a mortar to form a composite mixture. A quantity of this composite equivalent to 50 mg sulfisoxazole and 5 mg phenazopyridine was accurately weighed into a 50 mL volumetric flask and approximately 40 mL of buffer was added. The solution was sonicated for 30 minutes to dissolve the sulfisoxazole and phenazopyridine. The solution was then diluted to volume with buffer and filtered through an HV filter (Millipore, Bedford, MA), 0.45 μm , to provide a solution for the determination of the impurities. A 1:25 dilution of this solution was made with buffer to provide a solution for the assay of sulfisoxazole and phenazopyridine.

Micellar Electrokinetic Chromatography

A Model CES I capillary electrophoresis system (Dionex Corporation, Sunnyvale, CA) was used to perform micellar electrokinetic chromatography. The fused-silica capillary was 75 μm x 70 cm and the detection window was formed as described in the CES I manual [23]. Hydrodynamic injections were performed at a height of 50 mm for 10 seconds. Electrophoresis was performed using a 15 kV (34

mA) potential across the electrodes. After each run, the buffer reservoirs were drained and refilled with fresh buffer (6 second rinse time at 7 psi) and the capillary was rinsed with fresh buffer (180 second rinse time at 7 psi). Detection was performed by measurement of the UV absorbance at 240 nm. Data were collected and analyzed using a Beckman PeakPro chromatographic data system (Beckman Instruments, Fullerton, CA).

RESULTS

Although CZE has been gaining popularity as a technique for the separation of small molecules, MEKC rather than CZE was chosen as the separation technique for this work due to the physico-chemical properties of two impurities of phenazopyridine, 6-amino-3-(phenylazo)-2-pyridinol and 6-amino-5-(phenylazo)-2-pyridinol. These two compounds possess the same mass-to-charge ratio and would therefore not be expected to separate by CZE. By using MEKC, it was hoped that the different locations of the hydroxyl groups would cause different degrees of repulsion of these groups with the negatively charged sodium dodecyl sulfate micelles and hence lead to separation. Unfortunately, this did not prove to be the case. The 3- and 5-(phenylazo) pyridinols could not be resolved by MEKC. All other components were successfully resolved. Figure 3 shows the separation obtained for sulfisoxazole, phenazopyridine and their related impurities. The buffer used to obtain this separation had a pH of 7.0. At buffer pH values of 7.5 to 8.6, 6-amino-5-(phenylazo)-2-pyridinol, 6-amino-5-(phenylazo)-2-pyridinol and phenazopyridine coeluted. By lowering the pH of the

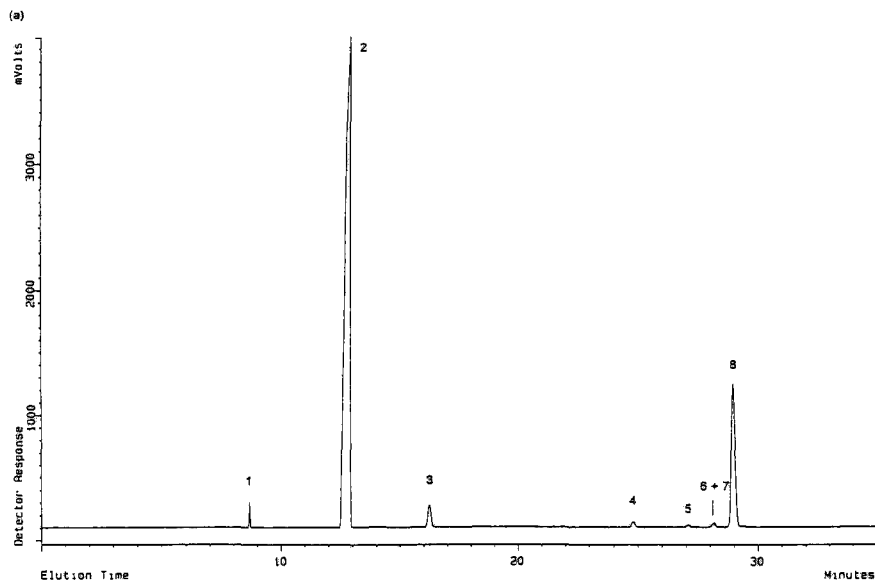


Figure 3

a) Full scale and b) expanded electropherograms showing 2% each of sulfanilamide and sulfanilic acid relative to sulfisoxazole and 2% each of 2,6-diaminopyridine, 3-(phenylazo)-2,6-pyridinediol, 6-amino-5-(phenylazo)-2-pyridinol and 6-amino-3-(phenylazo)-2-pyridinol relative to phenazopyridine. Components: 1 = sulfanilamide; 2 = sulfisoxazole; 3 = sulfanilic acid; 4 = 2,6-diaminopyridine; 5 = 3-(phenylazo)-2,6-pyridinediol; 6 = 6-amino-5-(phenylazo)-2-pyridinol; 7 = 6-amino-3-(phenylazo)-2-pyridinol; and 8 = phenazopyridine.

buffer and increasing the degree of protonation of the amino groups, two amino groups for phenazopyridine and one for the pyridinols, a good separation of phenazopyridine from these two impurities was achieved. The positively charged amine groups interacted with the negatively charged micelles, leading to later elution times. The 3- and 5-(phenylazo) pyridinols, however, eluted as a single well-shaped peak under the

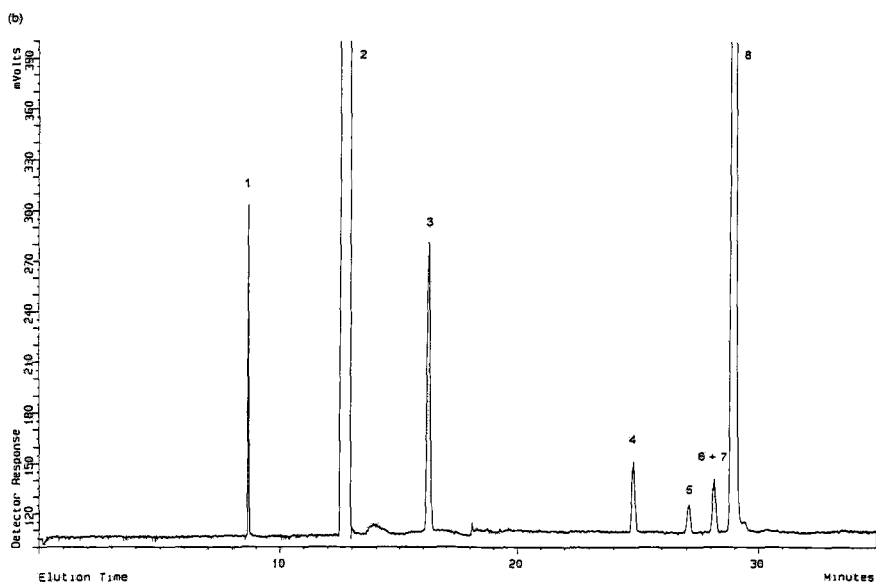


Figure 3 (continued)

conditions of this method. Subsequent work was therefore performed using all the impurities except 6-amino-5-(phenylazo)-2-pyridinol. Once a satisfactory separation had been obtained, the method was validated with respect to several key parameters which provided an indication of its performance. This was done to investigate the possible future utility of this technique for routine analysis.

System Precision

System precision provides a measure of system performance that is independent of the error introduced by sample handling and preparation. Six replicate

TABLE 1

System precision for the retention times (in minutes), t_r , and peak areas (in arbitrary units) for replicate injections of a standard solution containing 0.04 mg/mL sulfisoxazole and 0.004 mg/mL phenazopyridine.

Injection Number	Sulfisoxazole		Phenazopyridine	
	t_r	Peak Area	t_r	Peak Area
1	13.9	3101	36.4	773.4
2	14.0	3650	37.2	898.6
3	14.3	3028	39.0	804.3
4	14.5	3307	40.0	870.7
5	14.6	3023	40.2	754.8
6	14.8	3049	41.4	811.5
Mean	14.4	3193	39.0	818.9
%RSD	2.8	7.8	4.9	6.8

injections of a standard solution containing 0.04 mg/mL sulfisoxazole and 0.004 mg/mL phenazopyridine were made. These are the concentrations used to assay sulfisoxazole and phenazopyridine in Azo Gantrisin^R tablets. The retention times and peak area for sulfisoxazole and phenazopyridine for these six runs are listed in Table 1.

The percent relative standard deviation (%RSD) obtained for the retention times was 2.8% and 4.9% for sulfisoxazole and phenazopyridine, respectively. The percent relative standard deviation (%RSD) obtained for the peak areas was found to be 7.8% and 6.8%, for sulfisoxazole and phenazopyridine, respectively.

In this work approximately 6.8 nL of sample are injected onto the capillary. This corresponds to injecting approximately 0.27 ng sulfisoxazole and 0.027 ng phenazopyridine onto the capillary in this system precision study. Considering that the concentrations of both components are in the sub-nanogram range, the system precision obtained is reasonable. It is however, higher than those values typically obtained with HPLC methods. Currently, however, there is no HPLC method for the determination of these two compounds and their impurities.

System precision was also evaluated by performing replicate injections of a standard solution containing 1.0 mg/mL sulfisoxazole, 0.1 mg/mL phenazopyridine, 2% sulfanilamide and sulfanilic acid relative to sulfisoxazole and 2% 6-amino-5-(phenylazo)-2-pyridinol, 3-(phenylazo)-2,6-pyridinediol and 2,6-diaminopyridine relative to phenazopyridine. This mixture was analyzed to provide precision information on the levels of these samples used to quantitate the impurities. A set of ten replicate injections was performed on two different days. These results are summarized in Table 2. It should be noted that the sulfisoxazole peak at this level is non-Gaussian in shape. This is the reason that sulfisoxazole is quantitated at a lower concentration, 0.04 mg/mL. As shown in Table 2, the percent relative standard deviation for the peak areas ranged from 5.8% to 14.8% for day 1 and from 4.5% to 13.4% for day 2. Although values less than 2% RSD for peak areas have been obtained with CZE and MEKC methods, some groups [24-27] have reported higher values which are comparable to those obtained in this work. The %RSD values for peak retention time ranged from 0.77% to 2.5% on day 1 and from 1.2% to 2.6% on

TABLE 2

System precision for retention times (in minutes), t_r , and peak areas (in arbitrary units) for a solution containing the listed components as measured on two different days. The mean values and percent relative standard deviations (%RSD) are calculated for six runs.

Component	Mean t_r (%RSD)		Mean Peak Area (%RSD)	
	Day 1	Day 2	Day 1	Day 2
Sulfanilamide	8.7 (0.77)	9.6 (1.2)	750 (8.0)	750 (5.2)
Sulfisoxazole	13.0 (1.2)	14.6 (1.4)	67000 (5.8)	69600 (4.5)
Sulfanilic Acid	16.4 (1.5)	19.0 (1.6)	1950 (7.2)	2100 (5.7)
2,6-Diamino- pyridine	25.1 (2.4)	31.6 (2.6)	480 (6.9)	540 (8.4)
3-(Phenylazo)-2,6- pyridinediol	27.5 (2.3)	34.9 (2.5)	210 (14.8)	240 (13.4)
6-Amino-5-(phenylazo)-2- pyridinol	28.5 (2.5)	36.5 (2.5)	390 (8.0)	460 (8.9)
Phenazopyridine	29.3 (2.5)	37.8 (2.6)	15000 (6.0)	17000 (5.7)

day 2. In general, the %RSD increased as the retention time increased. This variation in retention times might cause a problem in peak identification for the later eluting peaks. In this work the capillary was rinsed with buffer between runs and the capillary was stored overnight filled with water. It may be possible that a different conditioning regime of the capillary may improve the reproducibility of the retention times. Lauer

and McManigill [28] showed that storing the capillary overnight filled with potassium hydroxide gave a standard deviation of less than 1% on a given day for the migration times of 10 runs and less than 4% from day-to-day for a nonmicellar capillary electrophoresis method. In addition, for an MEKC method for theophylline, Linhares and Kissinger [25] showed that capillary washes with sodium hydroxide gave retention times with 1.3% RSD for 31 runs, and that without these rinses between runs the retention times would increase with time. Different capillary conditioning regimes, however, were not explored in our work.

The percent relative standard deviation for peak area ranged from 5.8% to 14.8% for day 1 and from 4.5% to 13.4% for day 2. Again, these values are high compared to HPLC methods. In general, the percent relative standard deviation increased as the peak area decreased. This trend was also observed in the linearity study, where the impurities were injected in triplicate at concentrations of 0.025% to 2.0% of sulfisoxazole and phenazopyridine. A possible source of error is difficulty in integrating the smaller peaks due to the presence of baseline noise. Since the Dionex CES instrument uses uncapped Eppendorf centrifuge tubes to hold the sample, a second possible source of error is sample evaporation and concentration during the experiment, leading to injection of increasing quantities of solutes. On day 1 of the system precision study, the 10 system precision samples were analyzed immediately after preparation. On day 2, the 10 system precision samples were loaded onto the sample carousel after 22 other samples used for the linearity study. The run time was

30 minutes per sample with an additional 4 or 5 minutes to perform rinses between runs. The 10 system precision samples remained in the sample carousel for over 11 hours before analysis of the first of these samples began. As can be seen in Table 2, the mean peak areas for each component on day 2 is larger than on day 1, possibly due to sample evaporation and concentration. This phenomena may possibly effect the %RSD as well.

Linearity

The linearity of the method with respect to the response of sulfisoxazole, phenazopyridine and their impurities was evaluated. The observed linear ranges for these compounds and the correlation coefficient for the linear least-squares fit lines are listed in Table 3. Measurement of peak area for sulfisoxazole was found to be linear from 0.32 $\mu\text{g/mL}$ to 1000 $\mu\text{g/mL}$ with a correlation coefficient of 1.000. For a 6.8 nL injection volume this range corresponds to 2.2 pg to 6.8 ng injected. In addition, this range represents 1% to 2500% of the expected working concentration for the quantitation of sulfisoxazole. The peak shape for sulfisoxazole at concentrations greater than 40 $\mu\text{g/mL}$ was non-Gaussian due to capillary overloading as would be expected. The phenazopyridine peak area was found to be linear from 0.16 $\mu\text{g/mL}$ to 100 $\mu\text{g/mL}$ with a correlation coefficient of 0.9996. This range corresponds to 1.1 pg to 0.68 ng injected and represents 4% to 2500% of the expected working concentration for the determination of phenazopyridine. These peaks were Gaussian in shape. Concentrations greater than 100 $\mu\text{g/mL}$ phenazopyridine were not examined.

TABLE 3

Linear ranges for the components of interest. The mass linear ranges are calculated based on a 6.8 nL injection volume. The correlation coefficient is for the linear least-squares fit line of the data.

Component	Linear Range		Correlation Coefficient (R)
	Concentration ($\mu\text{g/mL}$)	Mass (pg)	
Sulfisoxazole	0.32 - 1000	2.2 - 6800	1.000
Phenazopyridine	0.16 - 100	1.1 - 680	0.9996
Sulfanilamide	0.5 - 20	3.4 - 140	0.9997
Sulfanilic Acid	0.5 - 20	3.4 - 140	0.9997
2,6-Diaminopyridine	0.1 - 2	0.68 - 13.6	0.9995
3-(Phenylazo)-2,6-pyridinediol	0.25 - 2	1.7 - 13.6	0.9995
6-Amino-5-(phenylazo)-2-pyridinol	0.25 - 2	1.7 - 13.6	0.9952

The responses for sulfanilamide and sulfanilic acid were found to be linear from 0.25 $\mu\text{g/mL}$ to 20 $\mu\text{g/mL}$ (3.4 pg to 0.14 ng injected) each with a correlation coefficient value of 0.9998. The 2,6-diaminopyridine response was found to linear from 0.1 $\mu\text{g/mL}$ to 2 $\mu\text{g/mL}$ (0.68 pg to 13.6 pg injected) with a correlation coefficient of 0.9995. The responses for 3-(phenylazo)-2,6-pyridinediol and 6-amino-5-(phenylazo)-2-pyridinol were found to be linear from 0.25 $\mu\text{g/mL}$ to 2 $\mu\text{g/mL}$ (1.7 pg to 13.6 pg) with correlation coefficient values of 0.9995 and 0.9952, respectively. Higher concentrations for the impurities were not examined.

TABLE 4

Limits of detection for the components of interest. The mass limits of detection are calculation based on a 6.8 nL injection volume.

Component	Limits of Detection	
	Concentration ($\mu\text{g/mL}$)	Mass (pg)
Sulfisoxazole	0.32	2.2
Phenazopyridine	0.16	1.1
Sulfanilamide	0.25	1.7
Sulfanilic Acid	0.25	1.7
2,6-Diaminopyridine	0.10	0.68
3-(Phenylazo)-2,6-pyridinediol	0.25	1.7
6-Amino-5-(phenylazo)-2-pyridinol	0.10	0.68

As demonstrated, the MEKC method provides excellent linearity for the active ingredients, sulfisoxazole and phenazopyridine, as well as for their impurities.

Limits of Detection

The limits of detection for sulfisoxazole, phenazopyridine and their related impurities are listed in Table 4. The limit of detection is defined as the concentration yielding a signal-to-noise ratio of approximately 2. The limit of detection for sulfisoxazole and phenazopyridine was found to be approximately 0.32 $\mu\text{g/mL}$ and

0.16 $\mu\text{g/mL}$, respectively. These limits represent 0.8% of the 0.04 mg/mL sulfisoxazole and 4.0% of the 0.004 mg/mL phenazopyridine injected in this work for the assay of these components in tablets. For the 6.8 nL injection volume used in this work, these detection limits represent 2.2 pg sulfisoxazole and 1.1 pg phenazopyridine injected onto the capillary. Electropherograms for sulfisoxazole and phenazopyridine at their limits of detection are shown in Figure 4.

The limit of detection for sulfanilamide and sulfanilic acid is 0.25 $\mu\text{g/mL}$ (1.7 pg injected) or 0.025% with respect to the 1.0 mg/mL sulfisoxazole concentration used in this work to quantitate impurities. The limit of detection for 2,6-diaminopyridine and 6-amino-5-(phenylazo)-2-pyridinol is 0.10 mg/mL (0.68 pg) and for 3-(phenylazo)-2,6-pyridinediol it is 0.25 $\mu\text{g/mL}$ (1.7 pg injected). These concentrations correspond to 0.1% and 0.25% of the 0.1 mg/mL phenazopyridine concentration used to quantitate impurities.

The limits of detection of the MEKC method for sulfisoxazole and phenazopyridine, as well as for their impurities, are acceptable for the application presented here.

Assay and Determination of Impurities in Tablets

Two samples of a tablet composite (sample taken from 10 ground tablets) were assayed for sulfisoxazole and phenazopyridine using standards containing 0.04 mg/mL sulfisoxazole and 0.004 mg/mL phenazopyridine and diluting the sample to this concentration based upon label claim. The results of this analysis are listed in Table 5.

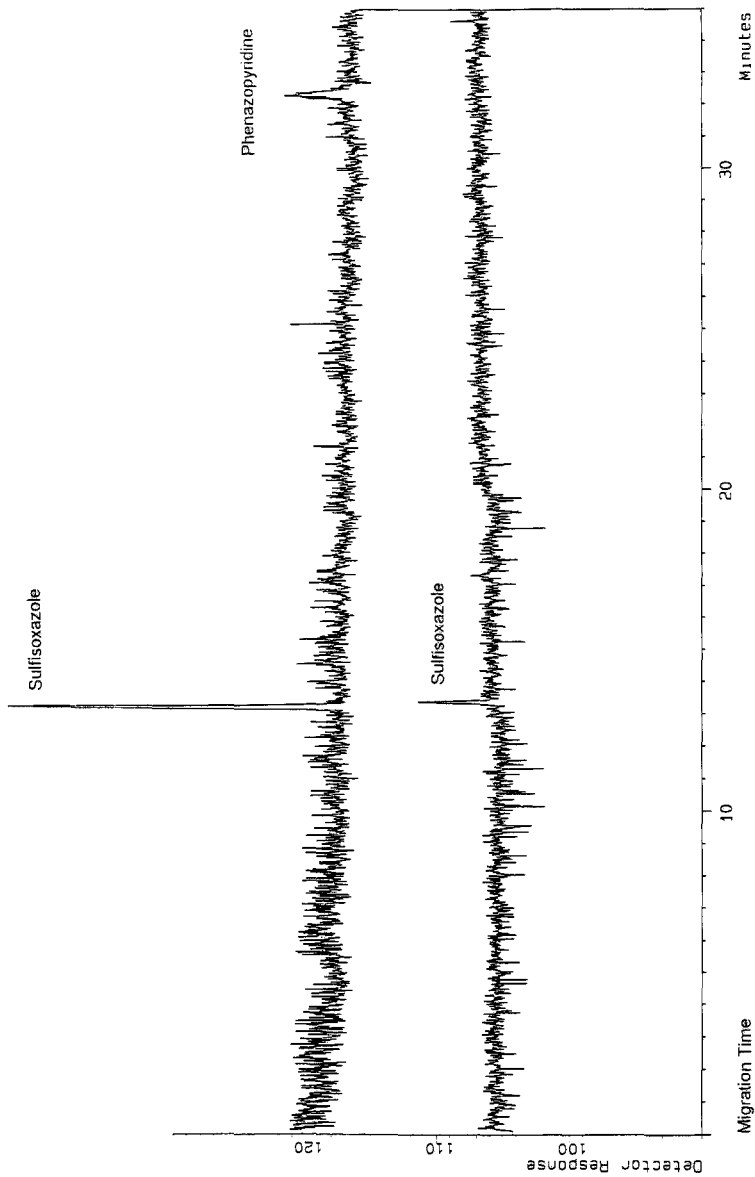


Figure 4

Electropherograms of sulfisoxazole (1.6 $\mu\text{g/mL}$ and 0.32 $\mu\text{g/mL}$) and phenazopyridine (0.16 $\mu\text{g/mL}$) at their limits of detection.

TABLE 5

Assay of composite samples of Azo Gantrisin^R tablets containing sulfisoxazole (500 mg) and phenazopyridine (50 mg).

Injection Number	Sample 1		Sample 2	
	Sulfisoxazole (mg)	Phenazopyridine (mg)	Sulfisoxazole (mg)	Phenazopyridine (mg)
1	518.7	55.35	468.8	53.90
2	447.5	49.95	477.8	56.87
3	481.0	50.93	466.8	47.90
Mean	482.4	52.08	471.1	52.89
% RSD	7.4	5.5	1.2	8.6
% of claim	96.5	104.2	94.2	105.8

Sulfisoxazole was found at 96.5% and 94.2% of claim, while phenazopyridine was found at 104.2% and 105.8% of claim. Figure 5 shows electropherograms of a blank, a standard and one injection for each sample preparation.

Analysis of a composite sample of this lot of tablets for sulfisoxazole and phenazopyridine by UV spectrophotometric methods found 104.4% sulfisoxazole and 103.8% phenazopyridine. The Uniformity of Dosage Units testing (assay of ten individual tablets) by UV spectrophotometric detection found from 92.6% to 104.8% (3.7% RSD) sulfisoxazole and from 105.4% to 107.4% (0.7% RSD) phenazopyridine.

A summary of the assay results for these tablets by MEKC and UV spectrophotometric methods is shown in Table 6. There is good agreement between

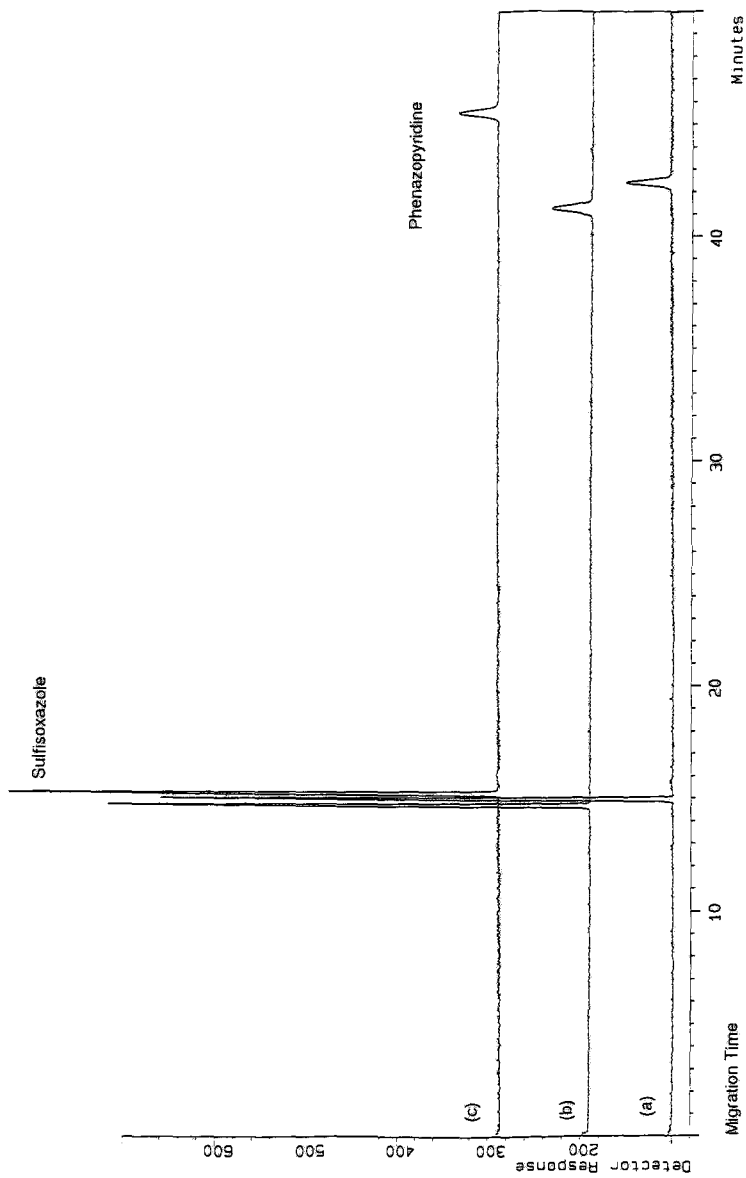


Figure 5

Electropherograms of (a) standard (0.04 mg/mL sulfisoxazole, 0.004 mg/mL phenazopyridine), (b) sample 1 and (c) sample 2 used for the composite assay of Azo Gantrisin[®] tablets.

TABLE 6

Assay results for Azo Gantrisin^R tablets using MEKC and UV spectrophotometry. UV spectrophotometry results are from an assay of a composite and from the uniformity of dosage units (UDU) which involves assaying 10 individual tablets.

Method of Analysis	% Label Claim	
	Sulfisoxazole	Phenazopyridine
MEKC	95.4	105.0
UV - Assay	104.4	103.8
UV - UDU	92.6 - 104.8 (3.7%RSD)	105.4 - 107.4 (0.7%RSD)

the determinations of sulfisoxazole and phenazopyridine obtained by MEKC and by the UV spectrophotometric methods.

Composite tablet sample preparations were also prepared at a concentration of 1.0 mg/mL sulfisoxazole and 0.1 mg/mL phenazopyridine to detect the presence of any of the known impurities in the samples. A solution containing 0.04% (0.40 $\mu\text{g/mL}$) each sulfanilamide and sulfisoxazole was also analyzed and used to quantitate these two impurities in the tablet composite samples. Samples 1 and 2 were found to contain 0.06% and 0.05% sulfanilamide and 0.03% and 0.04% sulfanilic acid, respectively. None of the known impurities of phenazopyridine (2,6-diaminopyridine, 3-(phenylazo)-2,6-pyridinediol or 6-amino-3-(phenylazo)-2-pyridinol/6-amino-5-(phenylazo)-2-pyridinol) were detected. Analysis of this lot of tablets by TLC found 0.1% sulfanilamide and no sulfanilic acid. These results are summarized in Table 7.

TABLE 7

Impurity results for Azo Gantrisin^R tablets using MEKC and TLC. 2,6-diaminopyridine, 3-(phenylazo)2,6-pyridinediol and 6-amino-3-(phenylazo)-2-pyridinol/6-amino-5-(phenylazo)-2-pyridinol were not detected.

	MEKC		TLC
	Sample 1	Sample 2	
Sulfanilamide	0.06%	0.05%	0.1%
Sulfanilic Acid	0.03%	0.04%	None Detected

There is general agreement between the results obtained for the impurities by MEKC and the TLC method. Due to the lower limits of detection for MEKC than TLC, sulfanilic acid was detected by MEKC and not TLC.

DISCUSSION

An MEKC method was evaluated for the analysis of sulfisoxazole, phenazopyridine and their related known impurities in a tablet dosage form. Two impurities of phenazopyridine, 6-amino-5-(phenylazo)-2-pyridinediol and 6-amino-3-(phenylazo)-2-pyridinediol, were not resolved by this method. System precision, limit of detection and linearity studies were therefore performed with sulfisoxazole, phenazopyridine and all their impurities except 6-amino-3-(phenylazo)-2-pyridinediol.

In this work samples of a tablet composite were analyzed at a relatively high concentration, 1.0 mg/mL sulfisoxazole and 0.1 mg/mL phenazopyridine, to allow

optimal detection of impurities. Higher concentrations could not be used due to the solubility limitations of sulfisoxazole. Results obtained for the impurities by MEKC and TLC were comparable. The limits of detection for both sulfanilamide and sulfanilic acid were found to be 0.32 $\mu\text{g}/\text{mL}$ (0.03% of the sulfisoxazole concentration) or 2.2 pg injected onto the capillary. The limits of detection for the other impurities were determined to be 0.10 $\mu\text{g}/\text{mL}$ (0.1% of the phenazopyridine concentration; 0.68 pg injected) for 2,6-diaminopyridine and 6-amino-5-(phenylazo)-2-pyridinol, and 0.25 $\mu\text{g}/\text{mL}$ (0.25% of the phenazopyridine concentration; 1.7 pg injected) for 3-(phenylazo)-2,6-pyridinediol. These detection limits are acceptable and represent an improvement to the limits of detection obtainable by TLC. The TLC method currently used to quantitate sulfanilic acid and sulfanilamide has an approximate detection limit of 0.05% of a 10 mg/mL standard solution or 0.05 μg applied to the TLC plate.

Lower concentrations of sulfisoxazole and phenazopyridine, 0.04 mg/mL and 0.004 mg/mL, respectively, were used to assay these components in samples of a tablet composite due to the non-Gaussian peak shape of sulfisoxazole at higher concentrations. The samples of tablet composite were found to contain 96.5% and 94.2% of claim for sulfisoxazole and 104.2% and 105.8% of claim for phenazopyridine. Sulfanilamide and sulfanilic acid were also found in these samples. Results obtained for the quantitation of sulfisoxazole and phenazopyridine by MEKC and the UV spectrophotometric methods were comparable. Since this work was undertaken to assess the feasibility of the use of MEKC to analyze a pharmaceutical dosage form, extensive method validation of drug recovery from the dosage form was

not undertaken. If this method were to be pursued in the future for routine use in testing this dosage form, then more extensive validation of drug recovery would need to be performed in order to meet regulatory requirements.

Current testing methodologies for quantitating sulfisoxazole and phenazopyridine involve the use of separate ultraviolet (UV) spectrophotometric or titrimetric assay methods with the use of TLC to monitor the impurities [1-4]. At least three techniques are therefore required to determine sulfisoxazole, phenazopyridine and their known impurities. The micellar electrokinetic chromatographic method described in this paper is a single method which can quantitate both sulfisoxazole and phenazopyridine, as well as their potential known impurities. The MEKC method, however, does have several disadvantages. Two of the phenazopyridine impurities, 6-amino-5-(phenylazo)-2-pyridinol and 6-amino-5-(phenylazo)-2-pyridinol, coelute as a single peak. In addition, the system precision as measured in terms of % RSD for the peak area is poor compared to what is typically obtained for HPLC methods.

CONCLUSIONS

An MEKC method was developed for the analysis of two active ingredients, sulfisoxazole and phenazopyridine, and their known impurities in a tablet dosage form. Two of the known impurities of phenazopyridine were not resolved from each other with this method. There is, however, no method currently available which resolves these two impurities of phenazopyridine. A disadvantage of the method is that samples

need to be analyzed twice, once for the known impurities and a second time for the main components, sulfisoxazole and phenazopyridine. The sample for the analysis of the main components is prepared by diluting the sample used for analysis of the known impurities. Another disadvantage of the method is that the retention times for the peaks tend to increase with time. This trend could pose a problem in identification of closely eluting peaks if numerous samples are run. In addition, the reproducibility of the peak areas is less than that typically obtained with HPLC methods. There is, however, no HPLC method currently available for the analysis of sulfisoxazole, phenazopyridine and their known impurities.

Despite the disadvantages, MEKC offers a chromatographic alternative to the separate, non-selective UV spectrophotometric and titrimetric assays currently employed for sulfisoxazole and phenazopyridine. In addition to the time savings afforded in the determination of the actives, the impurities can be quantitated without the use of a second method such as TLC. The method also offers additional convenience with the use of a commercial instrument which performs sample injections and sample runs automatically.

REFERENCES

1. "Phenazopyridine Hydrochloride," in The United States Pharmacopeia, 23rd ed., United States Pharmacopeial Convention, Inc., Rockville, MD 1994, 1197.
2. "Sulfisoxazole," in The United States Pharmacopeia, 23rd ed., United States Pharmacopeial Convention, Inc., Rockville, MD 1994, 1468.

3. K. W. Bleszel, B. C. Rudy, B. Z. Senkowski, "Phenazopyridine Hydrochloride," in *Analytical Profiles of Drug Substances*, v. 3, K. Florey, Ed., Academic Press, New York 1974, 465-482.
4. B. C. Rudy and B. Z. Senkowski, "Sulfisoxazole," in *Analytical Profiles of Drug Substances*, v. 2, K. Florey, Ed., Academic Press, New York 1973, 487-506.
5. Tom Perilli, Hoffmann-La Roche Inc., personal communication, 1993.
6. K.D. Altria, N.W. Smith, *J. Chromatogr.*, 538: 506-509 (1991).
7. K.D. Altria, *J. Chromatogr.*, 634: 323-328 (1993).
8. R. Hupoalahti, J. Sunell, *J. Chromatogr.*, 636: 125-132 (1993).
9. M. Korman, J. Vindevogel, P. Sandra, *J. Chromatogr.*, 645: 366-370 (1993).
10. K.D. Altria, Y. L. Chanter, *J. Chromatogr. A*, 652: 459-463 (1993).
11. Q. X. Dang, L. X. Yan, Z. P. Sun, K. K. Ling, *J. Chromatogr.*, 630: 363-370 (1993).
12. C. Bjerregaard, S. Michaelsen, K. Mortensen, H. Sorensen, *J. Chromatogr.*, 652: 477-485 (1993).
13. H. Nishi, S. Terabe, *J. Pharm. Biomed. Anal.*, 11: 1277-1287 (1993).
14. P. Sun, G. J. Mariano, G. Barker, R. A. Hartwick, *Anal. Lett.*, 27: 927-938 (1994).
15. J. W. Jorgenson, K. D. Lukacs, *Science*, 222: 266-272 (1983).
16. M. J. Gordon, X. Huang, S. L. Pentoney, Jr., R. N. Zare, *Science*, 242: 224-228 (1988).
17. A. G. Ewing, R. A. Wallingford, T. M. Olefirowicz, *Anal. Chem.*, 61: 292A-303A (1989).
18. P. D. Grossman, J. C. Colburn, Capillary Electrophoresis Theory & Practice, Academic Press, Inc., New York, 1992.
19. R. Weinberger, Practical Capillary Electrophoresis, Academic Press, Inc., New York, 1993.

20. S. Terabe, K. Otsuka, K. Ichikawa, A. Tsuchiya, T. Ando, *Anal. Chem.*, 56: 113-116 (1984).
21. S. Terabe, K. Otsuka, T. Ando, *Anal. Chem.*, 57: 834-841 (1985).
22. S. Terabe, Y. Miyashita, O. Shibata, E. R. Barnhardt, L. R. Alexander, D. G. Patterson, B. L. Karger, K. Hosoya, N. Tanaka, *J. Chromatogr.*, 516, 23-31 (1990).
23. Dionex Capillary Electrophoresis System I Operator's Manual, Dionex Corporation, Document No. 034196, Revision 01, May 1990.
24. B.R. Thomas, S. Ghodbane, *J. Liq. Chromatogr.*, 16, 1982-2006 (1993).
25. M.C. Linhares, P.T. Kissinger, *J. Chromatogr.*, 615, 327-333 (1993).
26. N. Nguyen, R. Siegler, W. Vincek, "A Capillary Electrophoresis (CE) Method for the Analysis of SK&F 108566 in Pharmaceutical Dosage Forms," presented at the Fourth Annual Frederick Conference on Capillary Electrophoresis, October 19-20, 1993.
27. H.K. Jones, M. Laskovics, "Chiral Electrophoresis versus HPLC for the Screening of Chiral Precursors of a Serotonin 5-HT² Antagonist," presented at the Fourth Annual Frederick Conference on Capillary Electrophoresis, October 19-20, 1993.
28. H. H. Lauer, D. McManigill, *Anal. Chem.*, 58, 168-170 (1986).

Received: July 9, 1995

Accepted: August 2, 1995

CAPILLARY ELECTROPHORESIS AS AN ALTERNATIVE METHOD FOR THE DETERMINATION OF CEFOTAXIME

H. FABRE AND G. CASTANEDA PENALVO¹

*Faculté de Pharmacie
15 Avenue Charles Flahault
34060, Montpellier, France*

ABSTRACT

Capillary Zone Electrophoresis (CZE) was evaluated for the determination of cefotaxime in the presence of its major decomposition products. The relative standard deviation of the migration times and peak areas were 0.26 and 0.31%, respectively. These figures and those obtained in the assay of cefotaxime were comparable with results of an HPLC method and comply with the requirements for drug quality control.

INTRODUCTION

This work is part of a study involving the investigation of new methods for the determination of cephalosporins in pharmaceutical formulations and biological samples (1-3), or following their degradation kinetics in aqueous solutions (4-6). Since capillary electrophoresis has proved to be a valuable

¹Permanent address: Universidad de Castilla-La Mancha, Facultad de Químicas, Departamento de Química Analítica, Campus Universitario, 13071 Ciudad Real (Spain).

method in the quality control of drug substances (7-8), its performance in the determination of cefotaxime sodium was evaluated in this study. This paper investigates the possibilities offered by capillary zone electrophoresis (CZE) for the routine analysis of this drug. The results were compared with those obtained by HPLC -UV which is the official method (9) for the assay of cefotaxime.

MATERIALS, REAGENTS AND SOLUTIONS

Milli-Q water and analytical grade chemicals were used throughout and all solutions were freshly prepared before use.

Cefotaxime sodium (C) and related compounds, deacetylcefotaxime lactone (L), desacetoxycefotaxime (DO), desacetylcefotaxime (DA), thiazoximic acid (TH), N-formyl cefotaxime (F), cefotaxime *anti*-isomer (AN), cefotaxime dimer (DIM) (Table I) were kindly donated by Roussel UCLAF laboratories (Romainville, France) and were used as received.

Aqueous solutions of the working standard and samples (both at 100 mg l⁻¹) were used for the cefotaxime assay in CZE. For HPLC, solutions of working standard and cefotaxime were 50 mg l⁻¹.

The electrolyte for separation in CZE was 40 mM potassium dihydrogen phosphate, pH 8.0 prepared daily by diluting a 100 mM stock solution of KH₂PO₄. The stock solution was stored at 4°C and used within fifteen days of preparation.

The mobile phase for HPLC was a phosphate buffer-methanol mixture (80 : 20, v/v). The buffer was prepared by dissolving 3.5 g of potassium dihydrogenophosphate and 11.6 g of disodium hydrogenophosphate. 12 H₂O in 1000 ml water.

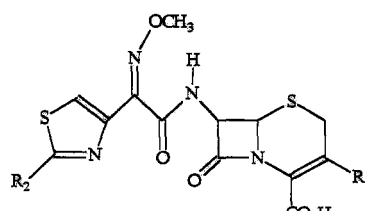
INSTRUMENTATION AND OPERATING CONDITIONS

CE

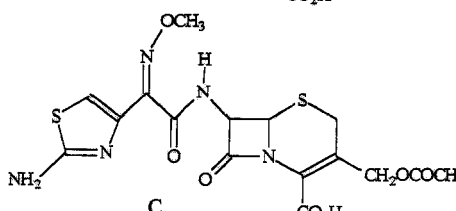
A Beckman P/ACE 5500 (Palo Alto, CA, USA) capillary electrophoresis system equipped with a UV filter detector at 254 nm was used. A diode array

TABLE 1. Structure of cefotaxime and related impurities.

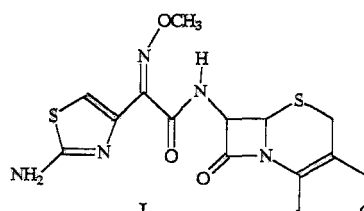
Name	R ₁	R ₂
DA	CH ₂ OH	NH ₂
DO	CH ₃	NH ₂
F	CH ₂ OCOCH ₃	NHCHO



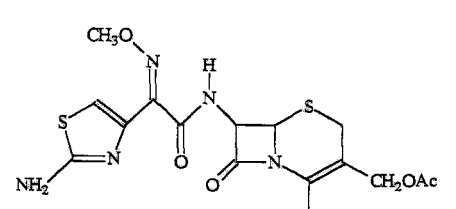
General structure of cefotaxime with substituents R₁ and R₂.



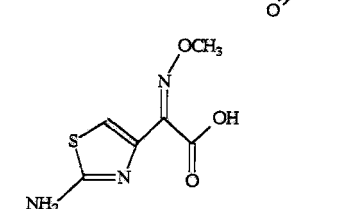
Structure C: Cefotaxime with R₁ = CH₂OCOCH₃ and R₂ = NH₂.



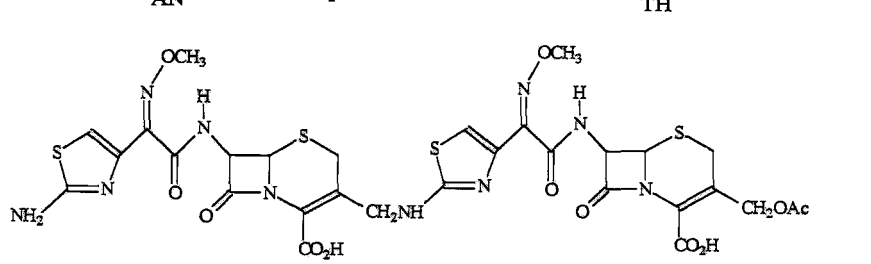
Structure L: Cefotaxime with R₁ = CH₂OH and R₂ = NH₂.



Structure AN: Cefotaxime with R₁ = CH₂OAc and R₂ = NH₂.



Structure TH: Cefotaxime with R₁ = CH₂OH and R₂ = NHCHO.



Structure DIM: Dimer of cefotaxime with R₁ = CH₂OAc and R₂ = NH₂.

DIM

detector was employed for peak purity assessment of cefotaxime. The system was controlled by a Dell Optiplex 466/L with Gold® and Array view® software. Separation was carried out on a 75 μm i.d. x 57 cm (50 cm to detector) fused silica capillary (Beckman) maintained in a cartridge with a detection window of 100 x 800 μm .

The capillary was conditioned prior to its first use by rinsing with 0.25 M NaOH for 30 min and with water for 10 min. Before commencing a sequence, the capillary was washed with 0.25 M sodium hydroxide and then water both for 5 min. The capillary was filled with the separation buffer for 2 min, then a 5 s injection of the sample was performed, immediately followed by a 1 s injection of the separation buffer. The capillary was filled from separate vials of buffer for rinsing operations in order to keep the level of buffer constant in the anodic separation vial. The separation was performed at + 15 kV for 15 min, with a ramp voltage of 37.5 kV min^{-1} at 25°C.

Average peak areas (PA) were used for quantitation without correction with respect to the migration times, unless otherwise stated. The data generated from first two injections in a sequence were not used on account of the requirement for system equilibration.

HPLC

A Waters (Bedford, MA, USA) Model 510 pump was used to deliver the mobile phase. Sample introduction was via a Rheodyne, (Cotati, CA, USA) Model 7125 injection valve fitted with a 20- μl loop. Detection was by UV absorbance at 254 nm using Waters 920 diode array detector. This was connected to a Nec Powermate SX Plus with Waters PAD software. Separation was carried out on a 250 x 4 mm i.d. Lichrospher (Merck, Darmstadt, Germany) 100 C₁₈ column (5 μm). A disposable guard column (4 mm x 4 mm i.d.) packed with the same material was fitted in advance of the analytical column. The mobile phase was delivered at a flow rate of 1 ml min^{-1} .

RESULTS AND DISCUSSION

Preliminary Studies.

On account of the structure of the analytes (with the exception the lactone compound) basic or acidic buffers could be used to promote the ionisation of the carboxylic or amino functions, respectively. A basic buffer of pH 8.0 was chosen to avoid adsorption on the capillary wall, since both the analytes and the wall are negatively charged at this pH. In addition, since the capillary wall can be considered at this pH to be totally ionised at pH 8, the electroosmotic flow (e.o.f) is stable (10). A 40 mM borate buffer pH, 9.2 was found to yield similar resolution between the compounds, but the pH 8 buffer was chosen in preference to avoid artefacts arising from degradation of cefotaxime in the capillary during the separation; cefotaxime hydrolysis has been shown to be dramatically increased above pH 9.0 (4). A systematic study of the buffer ionic strength, voltage and temperature was conducted to optimise the electrophoretic separation. Under the selected conditions, the current was about 85 μ A. Of the wavelengths available on the UV filter detector (200, 214, 254 and 280 nm) 254 nm was selected based on the UV absorption spectrum of cefotaxime.

Cefotaxime Assay Validation.

Specificity.

Fig. 1 shows the electropherogram of a cefotaxime sample at 500 mg l⁻¹ and 100 mg l⁻¹. Cefotaxime is separated from its main decomposition products or synthesis intermediates, which were identified by co-injection of standard solutions (50 mg l⁻¹). The lactone, which is uncharged migrates with the e.o.f. ; all other compounds have a similar charge at the separation pH and migrate according to their size. DA + DO and F almost coelute (as they have a similar size) and migrate after C which has a higher molecular mass; TH has the longest migration time due to its small size. The dimeric compound was not available for this study, but based on the charge-to-size ratio it should migrate after

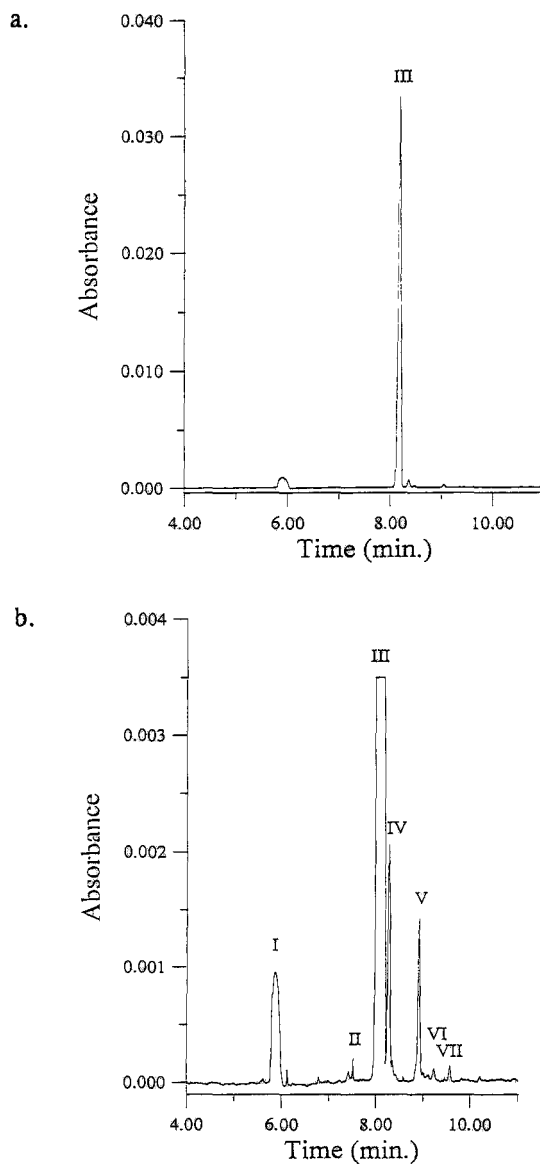


Figure 1: CZE separation of cefotaxime from its related impurities. I: e.f.o.+L; III: C; IV: DA+DO+F; V: DIM; II, VI and VII: Unknown.

a. Electropherogram with cefotaxime (100 mg l^{-1}) on scale.

b. Electropherogram with cefotaxime (500 mg l^{-1}) off scale

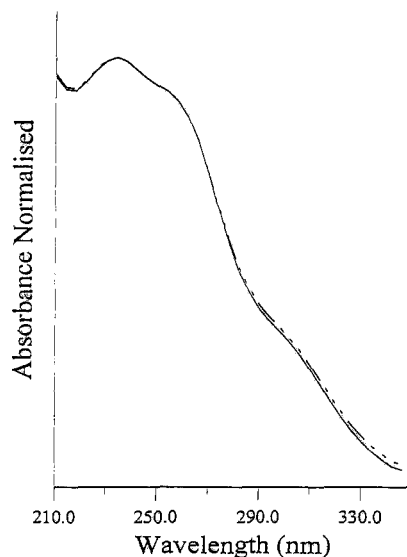


Figure 2: Spectral overlay (apex, upslope, downslope) for a 500 mg l⁻¹ solution of cefotaxime.

cefotaxime. AN coelutes with C but this is not of major concern as it is not often present in the drug substance or, if so, only at trace levels. The critical resolution between C and the co-eluted DA + DO + F showed a high degree of repeatability throughout this study using different capillaries from the same supplier.

Peak purity was assessed for both the working standard and samples of cefotaxime. A typical overlay of the spectra captured at the apex, upslope and downslope is presented in Fig. 2.

Linearity

Linearity was assessed both by injecting solutions of C in the concentration range 50-150 mg l⁻¹ (n = 5) at a constant injection time (5 s), and by injecting a C solution (100 mg l⁻¹) with variable injection times (from 1 to 10 s, n = 5). The regression equations were :

Area = -0.042 (± 0.178) + 0.021 (± 0.002) conc.(mg l⁻¹); r = 0.998 (constant injection time)

TABLE 2. Repeatability (RSD, %, n = 8 injections), for the migration times (MT), peak areas (PA) and PA corrected from the MT (CPA).

	M.T.	P.A.	C.P.A
	8.125	1.95336	0.240414
	8.135	1.95471	0.240284
	8.135	1.95015	0.239723
	8.131	1.94998	0.23982
	8.146	1.94257	0.238469
	8.152	1.95031	0.239243
	8.159	1.95393	0.239482
	8.173	1.9496	0.23854
Average	8.145	1.95057	0.239497
S.D.	0.016	0.00381	0.000722
R.S.D. %	0.198	0.19545	0.301474

Area = 0.132 (\pm 0.010) + 0.445 (\pm 0.002) time (s) ; r = 0.999 (constant volume)

The correlation coefficient values are satisfactory for both methods. The graph obtained with different concentrations passed through the origin, whereas that obtained with different injection times ($p = 0.05$) showed a slight bias. This may be related to the "spontaneous injection" which takes place even when no injection is carried out (11). However the bias was only 2 % of the response at the targeted concentration, which may be considered to be satisfactory for validation in pharmaceutical analysis (12). For routine use, it is possible to use one calibration point in addition.

Precision.

Repeatability was assessed under the following conditions, which have been shown to optimise the precision in quantitative assays (13): the capillary was rinsed with separation buffer held in a separate vial; an aliquot of buffer was introduced after the sample was injected; the sample and buffer vials were

TABLE 3. Comparison of CZE and HPLC results for the determination of cefotaxime content (% , m/m)

SAMPLE	RECOVERY (%)	
	HPLC	CZE
Batch 2G	99.3	98.9
Batch 3G	99.6	99.3

maintained at the same level at all times; a high sample concentration was used and water was used as a dissolution solvent; a constant injection of 5 seconds was used and the buffer was selected to have a high buffer capacity; the operating voltage was ramped and a constant temperature was maintained. Table II shows the migration times (MT), peak areas (PA) and PA corrected from the MT (CPA) resulting from 8 replicate injections of C using the same set of buffer vials. These results show that it is unnecessary to use corrected PA since the repeatability of migration times is more than acceptable. Comparable MTs (8.23 and 8.15 min) were also obtained on two different capillaries with RSD values of 0.21 and 0.20 % (n = 8 injections).

Accuracy.

Two different batches of cefotaxime were analyzed against a reference standard of cefotaxime both by the proposed CE method and a HPLC method with UV detection at 254 nm. The results given in table III, obtained from duplicate preparations of standard and sample solutions, demonstrate a good agreement between the two methods.

CONCLUSION

The results obtained show that CZE is a valuable method for the determination of cefotaxime. Assay and repeatability results are comparable to

those obtained with an HPLC method and comply with the requirements of drug quality control. CZE is suitable for routine use and offers advantages of simplicity of operation, flexibility and low cost. The proposed method may allow a total evaluation of the related impurities present in the drug substance but individual quantitation of each compound is not possible in CZE because DA, DO and F co-elute. A MEKC method is presently under investigation in our laboratory for the individual determination of the related substances.

ACKNOWLEDGEMENTS

The authors wish to acknowledge the financial assistance of the European Community in supporting the work of this project.

REFERENCES

1. H. Fabre, W. Th. Kok, *Anal. Chem.*, 60: 136-141 (1988)
2. H. Fabre, M. D. Blanchin, W. Th. Kok, *Analyst*, 113: 651-655 (1988)
3. M. D. Blanchin, H. Fabre, M. L. Rondot-Dudragne, B. Mandrou, *Analyst*, 113: 899-902 (1988)
4. H. Fabre, N. Hussam Eddine, G. Berge, *J. Pharm. Sci.*, 73: 611-618 (1984)
5. D. Lerner, G. Bonnefond, H. Fabre, B. Mandrou, M. Simeon de Buochberg, *J. Pharm. Sci.*, 77: 699-703 (1988)
6. H. Fabre, H. Ibork, D. A. Lerner, *J. Pharm. Sci.*, 83: 553-558 (1994)
7. K. D. Altria, *J. Chromatogr.*, 646: 245-257 (1993)
8. B. R. Thomas, X. G. Fang, X. Chen, R. J. Tyrell, S. Ghodbane, *J. Chromatogr.*, 657: 383-394 (1994)
9. The United States Pharmacopeia XXIII rev., Cefotaxime Monograph, United States Pharmacopeial Convention, Inc., Rockville, MD, 1995, pp. 299-300

10. K. D. Lukacs, J. W. Jorgenson, *J. High Res. Chromatogr.*, 8: 407-411 (1985)
11. E. V. Dose, G. Guiochon, *Anal. Chem.*, 64: 123-128 (1992)
12. G. P. Carr, J. C. Wahlich, *J. Pharm. Biomed. Anal.*, 8: 613-618 (1990)
13. K. D. Altria, H. Fabre, *Chromatographia*, 40: 313-320 (1995)

Received: July 19, 1995

Accepted: July 31, 1995

**AN IMPROVEMENT FOR THE SYNTHESIS OF
A STYRENE-DIVINYLBENZENE, COPOLYMER
BASED, 6-AMINOQUINOLINE CARBAMATE
REAGENT. APPLICATIONS FOR DERIVATIZATION
OF AMINO ACIDS, PEPTIDES, AND PROTEINS**

G. LI¹⁺, J. YU¹, I. S. KRULL^{1*},
AND S. COHEN²

*¹Department of Chemistry
102 Hurtig Building
Northeastern University
360 Huntington Avenue
Boston, Massachusetts 02115*

*²Waters Corporation
34 Maple Street
Milford, Massachusetts 01757*

Abstract

An improved method for the synthesis of a styrene-divinylbenzene based 6-aminoquinoline carbamate (6-AQC) reagent with a benzotriazole linkage is reported in this paper. By using 6-aminoquinoline (6-AQ) and triphosgene as the starting materials, the synthesis of the intermediate quinoline-6-isocyanate became much simpler. Directly from quinolyl-6-isocyanate, instead of from the rearrangement of quinolyl acyl azide, a polymeric reagent with high loading and few adsorbed impurities was obtained. This was then used for the derivatization of amino acids (AAs) and peptides. High efficiencies and reproducibilities of the derivatizations make this reagent attractive for the analysis of AAs and small peptides. The reagent was also used for a derivatization study of proteins. This was the first time that any polymeric reagent has been described for the successful, more selective tagging of larger proteins. The effect of surfactants on the reaction was also studied.

*Visiting Scientist from Nanjing Normal University, Nanjing, China

Derivatizations with the solid polymeric reagent and a 6-AQC solution reagent were compared. With the solid phase reagent, fewer tagged products were usually obtained, conditions dependent. Derivatization with the solution reagent can yield a single product, again conditions dependent, corresponding, it is believed, to all amino groups tagged. This precolumn reaction now makes it possible to detect subpicomoles of proteins in reverse phase high performance liquid chromatography (HPLC).

Introduction

Solid phase reagents have been developed for performing derivatizations of numerous organic analytes in various HPLC modes [1]. Such reagents utilize ionic or covalent attachments of various labile tags that possess specific detector enhancement properties; UV, EC, FL, and so forth. The covalently attached moiety has better stability and other desirable properties. Many kinds of polystyrene based covalent reagents have been developed and applied for reaction detection [2]. An immobilized anhydride was prepared on a microporous polystyrene (PS) crosslinked with small amounts of divinylbenzene (DVB) (STY-DVB) support for the analysis of primary and secondary amines [3]. This reagent was based on a 1% crosslinked, DVB chloromethylated polystyrene. The anhydride was capable of rapid conversion of amines in aqueous/organic environments to stable amides, which were chromatographically stable and possessed excellent UV and EC detection properties.

Gao et al. also prepared an active ester based on a 1-hydroxybenzotriazole leash [4]. The benzotriazole activated ester on a macroporous support proved to be a powerful acylating reagent when labeled with 9-fluorenylmethoxycarbonyl chloroformate (9-FMOC). Urinary polyamines were analyzed successfully using this reagent. The chemical leash, *o*-nitro-*p*-carbonyl benzophenol, was prepared on a 4% crosslinked microporous STY/DVB polymer. The polymer, labelled with a 9-FMOC tag proved to be stable for on-line precolumn conversions [5]. Amphetamine spiked in urine has been derivatized and detected via HPLC-UV/FL with this particular reagent.

Although many polystyrene based reagents, with different underlying supports and final analytical tags, have been reported within the last decade, few of them dealt with the derivatization of amino acids (AAs) and peptides. Zhou et al. developed a polymeric reagent containing a 9-fluorenylacetyl (9-FA) tag [6], which was successfully used for the derivatization of AAs and peptides. However, the derivatization efficiencies were not sufficient to perform quantitative determinations of AAs, especially with the less hydrophobic species.

Recently, a polymer tagged 6-AQ, activated carbamate reagent was prepared for derivatization of amines and AAs in HPLC or HPCE [7]. The major advantage of this reagent has been that the hydrolysate(s) of the tag (6-AQ or its urea dimer) usually show(s) little interference(s) with the 6-AQC derivatives by FL detection [8]. The derivatization yields of AAs; however, were still not optimal, due to the low loading of the 6-AQC tag [7]. In the current paper, the method for preparing this polystyrene based 6-AQC reagent has been improved. A reagent with a higher loading of the final tag and less adsorbed impurities was finally obtained. Reasonable derivatization efficiencies of AAs and small peptides have been obtained.

In the case of proteins, in general, solution derivatization reactions tend to be random, indiscriminate, and nonselective, often leading to multiple products [9-10]. Almost all solution reactions tag multiple sites on a protein's surface, and usually cannot select one in particular to form a single derivatized product. The formation of multiple protein products, each having different sites and number of tags present, leads to confusion and complexity in HPLC or HPCE, as well as increased detection limits (DLs) and questionable identification of the original protein or a specific derivative. This is not a trivial problem, and it has become more important in the case of precolumn tagging in HPLC or HPCE, wherein a single, highly tagged single product is the ultimate goal (11-12). Because of this, most work for enhancing the detection of proteins has focused on postcolumn derivatization [13-15], and few articles deal with precolumn derivatizations [16], especially in reverse phase HPLC [17].

There exists a real need in the field of protein reaction chemistry to develop reactions that will form fewer and more selective or controlled products [9-10]. At times, a single, well defined product should be the goal for improved (lowered) HPLC/HPCE applications. Improved DLs will result from fewer products formed in the precolumn derivatization mode. Careful control of the conformations present, and limiting the protein reactions to terminal and/or exposed lysine (Lys) groups should result in improved reproducibility and fewer products for all protein tagging. Aside from HPLC/HPCE purposes, there is a general, long-standing need to be able to modify proteins in more specific and selective ways, such as when adding polyethylene glycol (PEG) side chains, carbohydrate side chains, protecting groups, and other chemical (tagging) modifications at specific amino acid sites [9-10]. Almost all prior and current work has involved solution chemical reactions on proteins.

Solution reactions can be affected by the nature and concentration of surfactants added along with the reagent and buffers, though this has not been studied very

extensively. Altering the mixture and/or nature of products formed, such as by the addition of surfactants in solution chemistry, presents an alternative control in protein reactions to the use of polymeric reagents. Similarly, the use of surfactants to affect altered products derived from proteins has not been studied with any polymeric reagents.

We have investigated here the solution and solid phase reagent reactions of some typical proteins, partly to demonstrate the differences that result from immobilizing the same tag on a polymeric support. Thus, it is the solution reagent that has become immobilized on the polymeric support, while the protein is free in solution, at times with pH control, surfactant additives, organic solvents, and so forth. We anticipate that these studies will lead to a general approach to improve and make more selective and specific future protein reaction chemistries. A wide variety of polymeric reagents already exist that could then be applied to novel protein tagging, for several reasons, such as enhanced detector response in HPLC/HPCE modes. An entirely separate issue relates to recovering bioactive (biorecognition), tagged proteins from any of these solution/polymeric reactions, in addition to limiting the sites of tagging and total number of tagged protein products. In part, we address that question as well, demonstrating in initial results, that tagged proteins can be recovered from some of these reactions that still recognize their antibodies in the form of immunoaffinity chromatography purification.

Experimental

Materials

Styrene-divinylbenzene copolymer (12% cross-linked, 102 Å templated, 16-20 μm) was obtained from Supelco Corporation (Bellefonte, PA, USA). 6-aminoquinoline (6-AQ), triethylamine (TEA), cetyltrimethylammonium bromide (CTAB), sodium dodecyl sulfate (SDS), and sodium tetraborate were obtained from Aldrich Chemical Company (Milwaukee, WI, USA). AAs, peptides, proteins, and trypsin-TPCK were all purchased from Sigma Chemical Company (St. Louis, MO, USA). Bovine growth hormone releasing factor (GHRF) was donated by The Upjohn Company (Kalamazoo, MI, USA). Sodium acetate, phosphoric acid, sodium phosphate (monobasic and dibasic), sodium hydroxide, and hydrochloric acid were obtained from Fisher Chemical Company (Fair Lawn, NJ, USA). HPLC grade solvents were generously donated by EM Science, Inc. (Gibbstown, NJ, USA) as their Omnisolv[®] grade. 6-Aminoquinolyl-N-hydroxysuccinimidyl carbamate (6-AQC) (Waters AccQ.Fluor[™] Reagent) and borate buffer (pH 8.8) were obtained as a kit from Waters Corporation (Milford, MA, USA).

Solutions and HPLC Mobile Phases.

AAs, peptides and proteins were dissolved in water, except insulin, which was dissolved in 50 mM HCl. CTAB, SDS, and Brij 35 were dissolved in water to a concentration of 20%. Mobile phase A consisted of 140 mM sodium acetate and 17 mM TEA, titrated to pH 5.05 using phosphoric acid; mobile phase B consisted of 60% acetonitrile in water (v/v), mobile phase C consisted of 20 mM sodium phosphate (monobasic) titrated to pH 3.0 with phosphoric acid; and mobile phase D consisted of 80% acetonitrile in water (v/v).

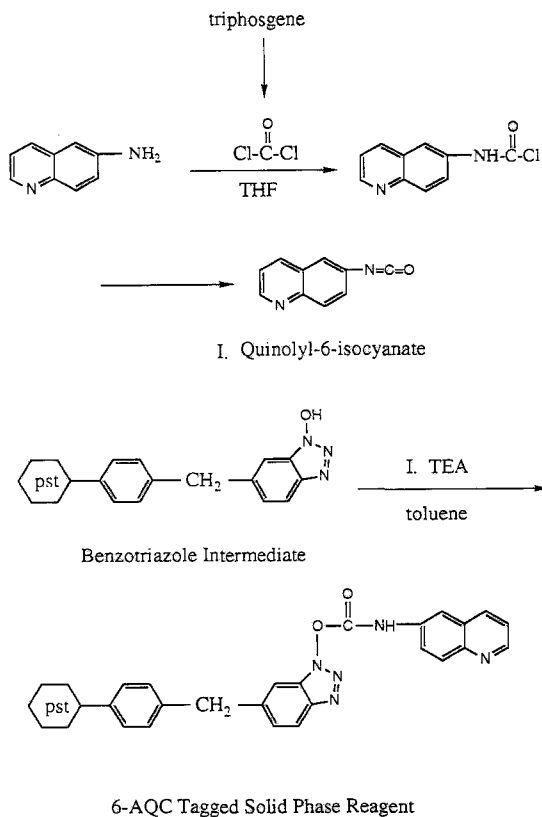
Preparation and Characterization of the 6-AQC Polymeric Reagent.

The synthesis of the polymeric benzotriazole intermediate followed a literature procedure [18-20]. The attachment of the analytical label, 6-AQ, to the polymeric intermediate involved the synthesis of quinoly-6-isocyanate (Scheme I). This was first prepared by adding 1 ml TEA and 0.3 g 6-AQ in 10 ml dried THF dropwise to an ice-cooled flask containing a solution of 0.6 g triphosgene in 10 ml dry THF with stirring. The mixture was stirred for 30 min at 0⁰ C, and then rotoevaporated to remove the solvent at 50⁰ C. The solid residue showed an absorbance at 2250 cm⁻¹ in its IR spectrum (mineral oil), which suggested the existence of an isocyanate group. The IR spectrum was obtained on a Perkin-Elmer Model 1310 infrared spectrophotometer (Perkin-Elmer Corporation, Norwalk, CT). To this solid, 20 ml toluene and 1 g of polymeric benzotriazole intermediate were added. The slurry was stirred and heated until the temperature gradually increased to 65⁰ C, and then held there for a further 1.5 h. The reaction slurry was filtered over a sintered glass funnel. The solid polymeric reagent was washed with 10 ml toluene, 2 x 10 ml THF, 7 x 10 ml DCM, and then dried in vacuo at room temperature, overnight. 1.09 g of the polymeric reagent was obtained, Scheme I.

The amount of 6-AQC attached to the polymeric intermediate was determined by a base promoted hydrolysis of the final polymeric reagent. The procedure used for characterization was performed as described elsewhere [6-7]. An authentic sample of 6-AQ was used together with its calibration plot in HPLC-UV to determine the final loading.

Off-line Derivatizations of AAs and Small Peptides with the Polymeric Reagent.

Off-line derivatizations of AAs and peptides were performed as described elsewhere [6-7]. An aliquot of 25 μ l of the analyte solution, 25 μ l of ACN, 25 μ l of saturated



Scheme I. Synthesis of quinolyl-6-isocyanate, and its attachment to the polymeric benzotriazole substrate.

sodium borate solution, and 25 μ l of 20 mM CTAB solution were added in a disposable pipet packed with the 6-AQ tagged reagent (10-20 mg). The pipet was kept at 70⁰ C for 10 min. After derivatization, the solid reagent was washed with 1.0 ml of 70% ACN-H₂O, and an aliquot of the solution was injected into the HPLC system.

Trypsin Digestion of Cytochrome c.

A solution of 2 mg/ml cytochrome c (cyt c) (horse heart) was prepared in 100 mM, pH 8, ammonium bicarbonate buffer. Trypsin-TPCK was dissolved in the same buffer at a concentration of 0.1 mg/ml. An aliquot of 0.5 ml of the trypsin solution was added to a

digestion vial which contained 0.5 ml of the cyt c solution. After vortexing, the vial was incubated at 37⁰ C for 24 h, and the digestion was terminated by heating the solution at 100⁰ C for 5 min [6]. The digested solution was lyophilized and reconstituted with 1.0 ml H₂O, and 50 μl of this solution was derivatized with 20 mg of the polymeric reagent.

Derivatization of Proteins With Solution and Solid Phase Reagents.

A 2 mg/ml GHRF solution was prepared by dissolving 1 mg GHRF in 0.5 ml H₂O. In order to prevent precipitation of GHRF derivatives, a surfactant such as SDS, CTAB, or Brij 35 was used in the derivatization. For solution reagent derivatizations, 60 μl borate buffer (0.2 M, pH 8.8), 20 μl surfactant solution (20%), and 10 μl or 20 μl GHRF solution were first mixed in a 55 x 6 mm glass tube. A portion of different volumes of 6-AQC solutions (3 mg/ml or 0.3 mg/ml) were added and vortexed quickly. The reaction solution was kept at room temperature (r.t.) before being injected into the HPLC system. When necessary, the solutions were incubated in a water bath at 50⁰ C for 10 min to hydrolyze the phenolic esters of 6-AQ derived from Tyr. The derivatizing procedure for insulin and glucagon was nearly the same as for GHRF, except surfactants were sometimes omitted.

For derivatizations with the immobilized reagent, 25 μl borate buffer, 25 μl surfactant solution, 25 μl ACN, and 25 μl protein solution were mixed, then put into a disposable reaction cartridge containing the polymeric reagent. The mixture was vortexed at r.t. After the reaction, the slurry was filtered through a glass wool cartridge and washed with 200 μl ACN/H₂O, 70/30, v/v. A portion of the solution was injected into the HPLC system. When desired, the solution was incubated at 50⁰ C for 10 min before injection.

Chromatographic Separations.

The HPLC gradient system consisted of a Waters Model 6000 pump, a Waters Model 501 pump, a Waters Model 660 Solvent Programmer, a Waters Model 420 Fluorescence detector (254 nm/395 nm, ex/em) (Waters Corporation, Milford, MA, USA), a Rheodyne Model 7125 injector (Rheodyne Corporation, Cotati, CA, USA), and a Spectra Model 100 UV detector (Thermo Separation Products, Fremont, CA, USA). Data were collected by a Linear recorder (Linear Laboratories, Fremont, CA, USA), a HP 3394A integrator (Hewlett Packed Corporation, Palo Alto, CA, USA), and a Macintosh SE 20 computer (Apple Corporation, Cupertino, CA). For the separation of AA and small peptide derivatives, a YMC ODS column (5μm, 300 Å, 250 x 4.6 mm i.d.) (YMC, Inc., Wilmington, NC, USA) was used. Gradient elution conditions for the

AA derivatives involved: initial mobile phase at 100% A, and B was linearly increased to 30 % over 30 min. For the elution of small peptide derivatives, B was linearly increased to 40% over 30 min. In the separation of protein derivatives, a Delta Pak C4 column (5 μ m, 300 Å, 150 x 3.9 mm) (Waters Corporation) was used. Gradient elution conditions for tagged proteins involved: initial mobile phase at 30% C, and D was linearly increased to 80% over 40 min. All separations were performed at r.t. Specific detection conditions are indicated in the figure legends.

Preparation and Usage of an Immobilized Antibody (Ab) HPIAC Column for Recovery of Tagged, Bioactive GHRF.

a. Development of GHRF Ab HPIAC Column (Streptavidin-Biotin Linkage)

We have chosen a streptavidin-biotin type linkage of the Ab to support for the HPIAC Ab purification columns. This was prepared by taking 10 mg streptavidin (Prozyme, Inc., El Cerrito, CA, USA) and dissolving this in 2 ml phosphate buffered saline (PBS), pH 9.0 (100 mM sodium phosphate, 150 mM NaCl, pH 9.0). To this solution, 0.5 g POROS epoxide support (PerSeptive Biosystems, Inc., Framingham, MA, USA) was added. The slurry was well mixed, and 2.5 ml of 2 M Na₂SO₄ in PBS (pH 9.0) was then added. The mixture was shaken gently at r.t. for 22 hrs. After this time, the support was washed in a Buchner funnel with 5 x 100 ml PBS (pH 7.4) (10 mM sodium phosphate, 150 mM NaCl, pH 7.4), and resuspended in 2.5 ml PBS (pH 7.4) with 0.1% NaN₃. A portion of this support was packed into an ID cartridge (PEEK, 2.1 mm i.d. x 30 mm) (PerSeptive Biosystems).

For the biotinylation of the purified Ab, 0.5 mg NHS-LC-Biotin II (Pierce Catalog and Handbook, NHS-LC-Biotin II Technical Literature, Pierce Chemical Company, Rockford, IL, USA) was dissolved in 0.5 ml DMF. Of this solution, 10 μ l was added to a centrifuge tube that contained 150 μ g of the purified GHRF monoclonal Ab (mAb) in 300 μ l 50 mM NaHCO₃ buffer, pH 8.5. The mixture was incubated at ice temperatures for 2 hr. The unreacted biotinylation reagent was removed by centrifuging the product using a Centricon-30 Microcon (Amicon Corporation, Danvers, MA, USA). After centrifugation, the sample was diluted in PBS (pH 7.4) buffer and again centrifuged. After this process was repeated a total of three times, the biotinylated Ab was immobilized onto the packed ID cartridge prepared above.

b. HPIAC of Derivatized GHRF Products.

An HPLC system was used for the HPIAC studies of previously tagged proteins. Derivatized GHRF was injected onto the Ab column, which was first equilibrated with a loading buffer (PBS, pH 7.4). After immobilization, the column was washed with

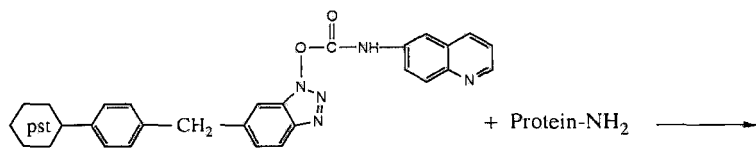
loading buffer until a stable baseline was obtained. An eluting buffer was then passed through the HPIAC column (150 mM NaCl, titrated to pH 2.0 with HCl), and the elution buffer was continued until the GHRF derivatives were fully eluted (as evidenced by UV/FL detection). The eluted derivatives were collected and then analyzed separately by reverse phase HPLC. The gradient elution HPLC conditions used a mobile phase A of PBS, pH 7.0, a mobile phase B of ACN/H₂O, 80/20 (v/v), and initial conditions of 30% B. B was linearly increased to 80% over 30 mins for gradient elution, and FL detection utilized 254nm/395nm, excitation/emission wavelengths (ex/em).

Results and Discussion

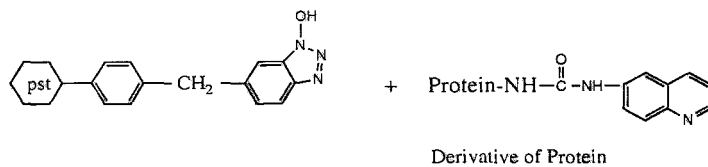
The solution, 6-AQC reagent is known to be very effective for derivatization of AAs, providing very high FL sensitivity in HPLC [8]. Based on the literature, we have synthesized and evaluated a polymer based reagent with a benzotriazole linkage containing the same 6-AQ tag with a carbamate linkage to the polymer. This has been used for derivatization of amines and AAs (Scheme II) [7]. However, for practical applications, our prior results were not adequate, because of a low loading capacity on that first synthesized reagent. That original material, though identical in structure to that prepared in this work, involved a slightly different synthetic scheme [7]. We have previously discussed, as have others, the various synthetic approaches possible to prepare polymeric, carbamate reagents involving various tags [19-20].

In part, this work was designed to develop a better approach for the synthesis of this same polymeric reagent, Scheme I. By using 6-AQ and triphosgene as the starting materials, this newer procedure for the synthesis of the intermediate quinolyl-6-isocyanate became much simpler than that previously described [7], and fewer side reactions or products were present. A peak at 2225 cm⁻¹ in the IR spectrum (Experimental) clearly showed the existence of an isocyanate (-NCO) type structure, Figure 1. Using the actual quinolyl-6-isocyanate reagent, instead of that from rearrangement of the quinolyl acyl azide [7], to react with the solid phase benzotriazole intermediate, a final polymeric reagent was obtained with high loading of tag and few adsorbed impurities, Scheme I.

The method for the determination of loading capacity involved HPLC-UV quantification, as described elsewhere [6-7]. When using such a base promoted hydrolysis method, authentic 6-AQ was used as the external standard. The loading capacity of the 6-AQ tag for this reagent was found to be 0.45 mmol/g, which was sufficient for most polymeric derivatization reactions [5-7, 19-20]. This loading was



6-AQC Tagged Solid Phase Reagent



Scheme II. Derivatization of proteins with the polymeric reagent.

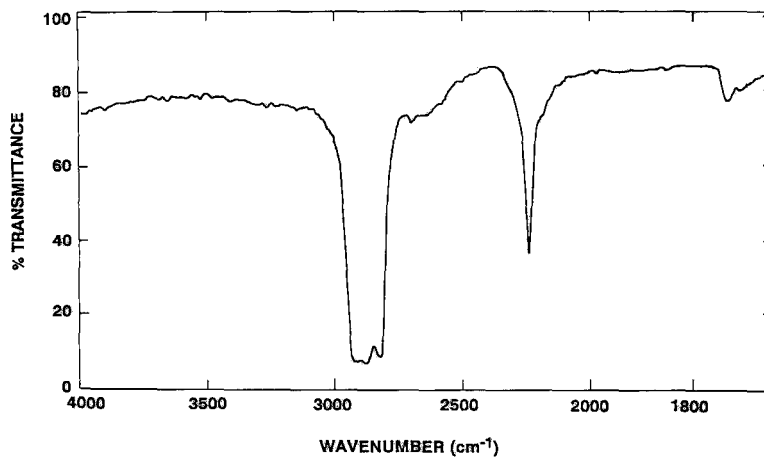


Figure 1. IR spectrum of quinolyl-6-isocyanate.

also higher than what we previously reported for the first synthetic approach (viz., 0.18 mmol/g) [7].

As has been reported [6-7], this reagent can be stored for a relatively long period of time without affecting its reactivity. The previous work showed that a >1 month stored reagent, without any special protection, had almost the same derivatization yields as a freshly prepared material [7]. However, several decomposition peaks were observed in those chromatograms, when using a stored reagent for off-line derivatizations. As these can interfere with analyte derivative peak(s), it was desirable to both increase the loading of the 6-AQC tag on this newly prepared polymeric reagent, and also to reduce the number and amounts of physically adsorbed impurities that could lead to chromatographic interferences. With the current synthesis protocol, these desirable goals have now been realized.

Reactivity of AAs and Peptides with the Solid Polymeric 6-AQC Reagent.

The off-line derivatizations of AAs and peptides with the 6-AQC tagged polymeric reagent were performed under the same optimized conditions used for the 9-FA tagged polymeric reagent [6]. For quantification of the derivatization efficiency, a calibration curve of the authentic standard derivative of phenylalanine, viz., 6-AQC-L-Phe, was used. The preparation and characterization of this authentic, external standard have been reported elsewhere [21].

The derivatization efficiency was largely affected by the amount of polymeric reagent (mass) used in the derivatization reaction. When 10 mg of reagent was used for the derivatizations, percent derivatizations for Ala, Met, Leu, and Phe were 19.7, 42.9, 54.7, and 74.6%, respectively. When 20 mg of reagent was used, reaction yields of these AAs were: 63.0 (13), 64.8 (9.3), 87.9 (5.5), and 94.3 (5.1), respectively. The data represent the average value and, in parentheses, percent relative standard deviation (%RSD, n=3). These results were obtained using gradient elution HPLC with UV detection, Figure 2. Figure 2 also compares the same derivatized mixture of AAs by both UV and FL modes. If even more of the reagent were used, one might obtain higher derivatization efficiencies, but this was not attempted. The more hydrophobic AAs, such as Phe, not only provided higher derivatization efficiency, but also better reproducibility in their reactions with polymeric reagent, as previously observed [6-7]. Though we have previously reported reactions of typical AAs with the earlier prepared polymeric 6-AQC reagent, the current results represent a substantial improvement in terms of conversion efficiencies and overall chromatographic performance, Figure 2 [7].

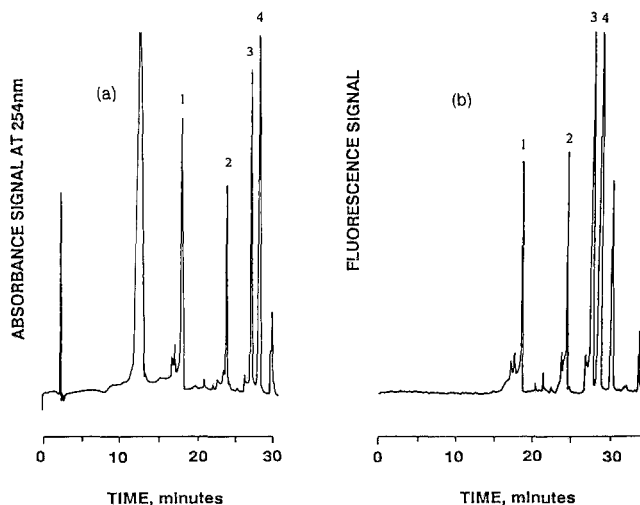


Figure 2. Chromatograms of the polymeric reagent derivatization of an amino acid mixture of Ala, Met, Leu, and Phe (1-4). HPLC conditions as indicated in Experimental. (a) UV detection at 254 nm; (b) FL detection at 254/395 nm, ex/em.

The derivatization of small peptides containing different numbers of AAs was also performed with this polymeric reagent. The yields of derivatization were all >60%, except for Gly-Ala, a highly hydrophilic dipeptide. Chromatograms for mixtures of these peptides are not described here [21]. Its percent derivatization was only [average (%RSD), $n=3$] 47.3 (2.3), while others were: Gly-Val: 65.4 (3.6), Ala-Phe: 73.8 (4.0), Phe-Gly: 60.5 (2.4), Leu-Phe: 72.3 (6.6), Phe-Gly-Gly-Phe amide: 71.6 (1.9), Trp-Ala-Trp-Phe: 79.4 (7.5). Again, the more hydrophobic the peptide, the higher the derivatization yield obtained.

Derivatization of Enzymatically Digested Protein.

Trypsin digested cyt C was chosen as an illustrative example of a peptide digest mixture. After derivatization, the derivatives of these peptides were separated on a gradient elution HPLC system (Experimental). There were several major peptide derivatives, Figure 3a-b. Resolution of the 6-AQC tagged peptides was not fully optimized. These initial, qualitative results again demonstrated that peptides from a digested protein can be derivatized with polymeric reagents [6]. We did not previously

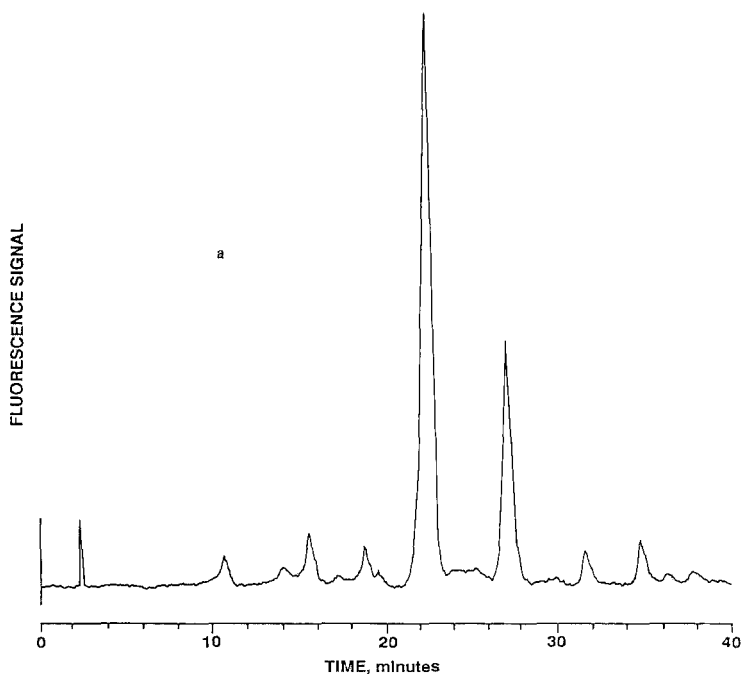


Figure 3. Chromatograms of the polymeric reagent derivatization of a peptide digest derived from cyt C. HPLC conditions as indicated in Experimental. Detection: Fluorescence 254/395 nm, ex/em. (a) blank; (b) enzyme digested cyt c derivatives.

(continued)

demonstrate peptide tagging with any polymeric 6-AQC reagent [7]. Each peptide from the current digest may not have been 100% derivatized. Based on the above results with standard, known peptides, it appears these peptide digests may show different percent conversions. These results may be of a more qualitative use for peptide mapping, as opposed to the quantitative conversion of AAs and peptides when using a solution 6-AQC reagent [8, 22-23]. This is a general disadvantage when using a hydrophobic, immobilized reagent for tagging peptides [1].

Derivatization of Proteins with Solution and Solid Polymeric Reagents.

Generally, derivatization with an electrophilic reagent may result in the attachment of

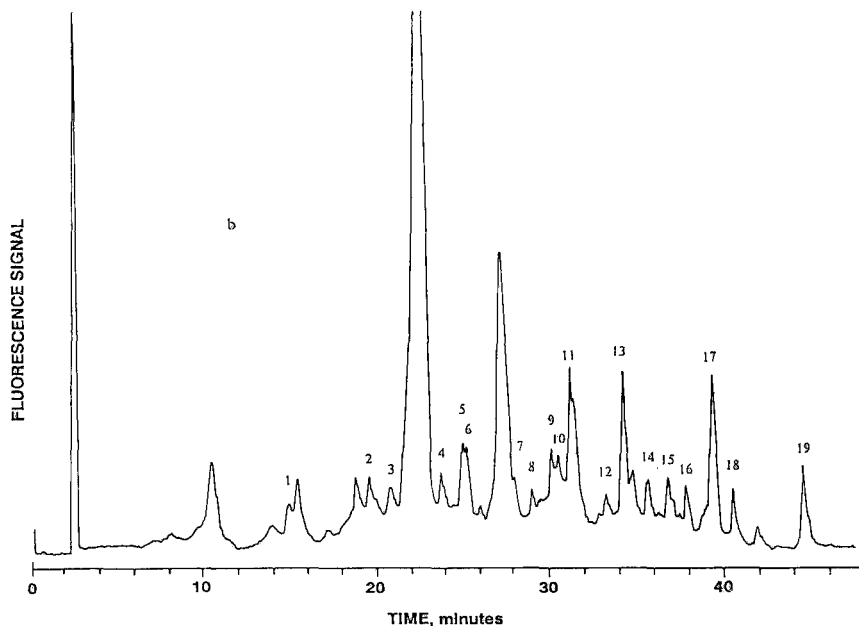
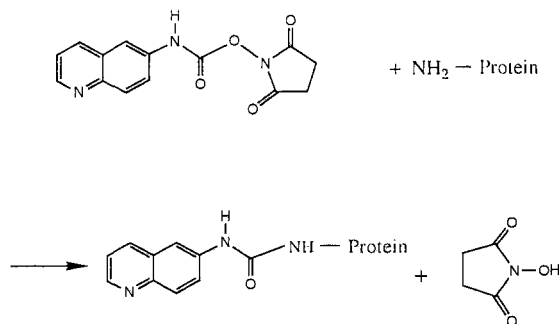


Figure 3 (continued)

the tagging groups to all amino, thiol, and hydroxyl groups on proteins, such as amino terminus and Lys side chains, phenol on Tyr, thiol on Cys and hydroxyl on Ser and Thr [8-10]. However, the chemical reactivities and final stabilities of these functional groups differ. Most reagents neither discriminate between these groups to get selective tagging, nor completely derivatize each and every possible site/group. There are some SH selective reagents, as well as some that will be selective towards Ser and Thr [9-10].

In addition, the derivatives formed from certain functional groups are unstable; they may hydrolyze simultaneously with formation or slowly thereafter [8]. Usually, the derivatization of proteins yields multiple products, which may lead to questionable identification of the original protein(s) and increased (elevated) DLs. Such results detract from the application of precolumn, solution derivatization of proteins for the purpose of enhancing detection, in any separation method (HPLC, HPCE).



Scheme III. Derivatization of proteins with the 6-AQC solution reagent.

Solution 6-AQC can react with several nucleophilic centers, such as amino and phenolic groups in proteins, Scheme III. The urea products derived from amine derivatizations are quite stable, which makes the derivatization of amino groups highly efficient and reproducible [8-10]. However, the derivatization of phenolic group on Tyr is often incomplete, and the carbamate structure derived from phenol derivatization is usually unstable [8-10]. This structure slowly hydrolyzes at r.t. As shown in Figure 4, multiple products were observed at r.t from the derivatization of insulin, glucagon, and bovine GHRF. This was the case even when these reactions were performed under conditions of high molar ratio of reagent to protein. The products formed could be simplified if the derivatization was performed at a higher temperature, or if the r.t. reaction products were subsequently heated to the same higher temperature (50⁰ C), since hydrolysis of the phenolic carbamates present was then accelerated.

A single tagged product (one HPLC peak) was obtained for each of these standard proteins by incubating the reaction mixture at 50⁰ C for 10 min, Figure 5. Further studies (see below), using different stoichiometric ratios of reagent to protein, have shown that this single peak (product) probably corresponded to a derivative in which all of the free amino groups (terminal and Lys side chains) were completely derivatized but no phenolic group remained tagged. We do not currently believe that reactions at the higher temperature inhibit the Tyr reaction, but rather that any adduct once formed will rapidly hydrolyze under these conditions ($t_{1/2}$ Tyr <6 min. at 50⁰ C) [24].

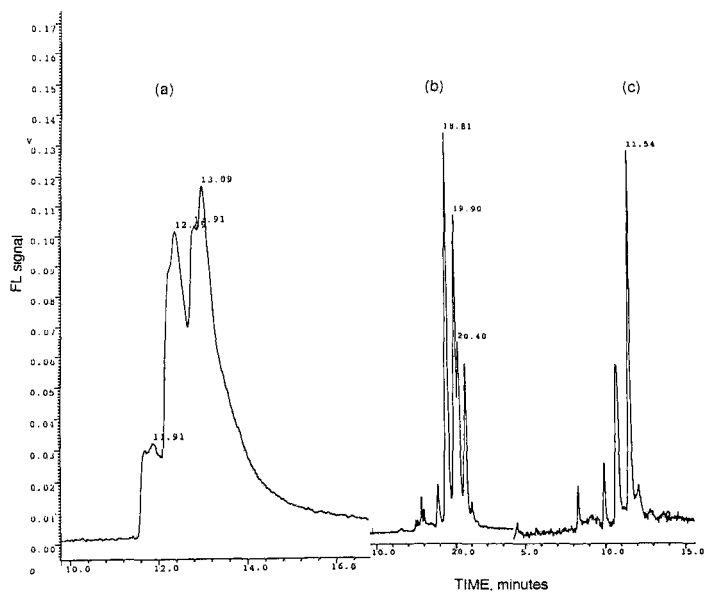


Figure 4. Chromatograms of protein derivatives. Reaction conditions: 10 μ l of protein (1 mg/ml), 70 μ l borate buffer (0.2 M, pH 8.8), and 20 μ l 6-AQC solution reagent (3 mg/ml), mixed at room temperature and incubated for 10 min. For GHRF, another 20 μ l CTAB (20% in water) was added. HPLC conditions are indicated in Experimental. Detection: FL 254/395 nm, ex/em. (a) insulin, (b) glucagon, (c) bovine growth hormone releasing factor (GHRF).

Mass spectrometric (MS) analysis of these protein products (Figures 4-5) has not, as yet, been attempted, in order to confirm the AA sites of tagging. Under the above reaction conditions, detection of proteins could be enhanced in HPLC and HPCE by precolumn derivatization with the solution 6-AQC reagent, Figure 5. This has been further demonstrated by the elevated temperature derivatization of insulin and GHRF. Picomole amounts of these proteins could be detected with FL, Figure 6. These particular HPLC-FL conditions were not fully optimized in terms of pH [8]. Ideal FL responses occur at neutral or slightly basic pH values, whereas the optimal HPLC conditions we have used were acidic, pH 5.0. It is likely that by operating at a more basic pH, perhaps by postcolumn pH adjustment, these minimum DLs could be further lowered [8].

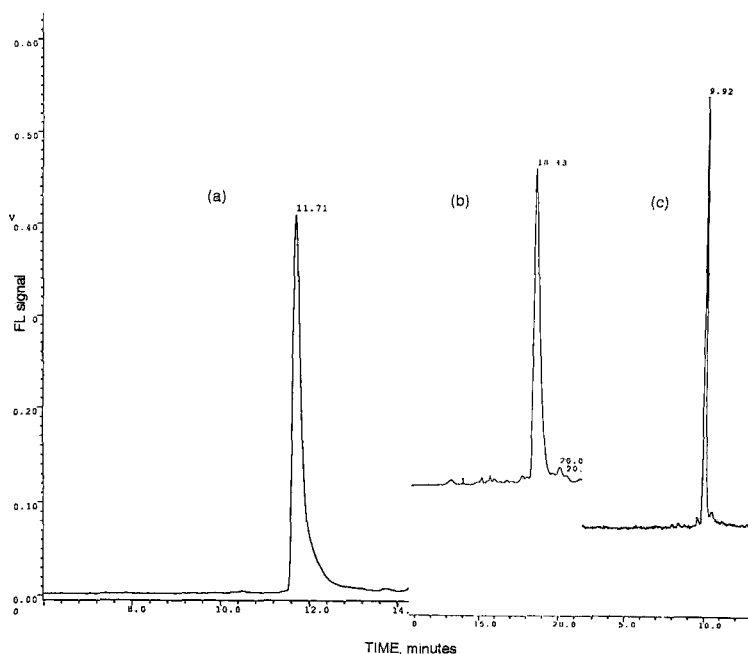


Figure 5. Chromatograms of protein derivatizations at elevated temperature. Reaction conditions are the same as in Figure 4, except the reaction solutions were incubated at 50⁰ C over 10 min. (a) insulin, (b) glucagon, (c) GHRF. HPLC and detection conditions as in Figure 4.

Further experiments have shown that phenolic groups on Tyr can only be derivatized when the solution reagent is present in high excess. If the amount of the reagent was controlled at low levels, e.g., less than a 1/1 equivalence of free amino groups in the proteins, then the phenolic groups were not readily derivatized. Free amino groups are better nucleophiles than phenols, and thus should react more rapidly with the same, perhaps limited reagent. If there is a large excess of reagent, e.g., Figure 4, then most likely all amines and perhaps phenols are derivatized by the end of 10 mins. At a low molar ratio of reagent to protein, reactions at r.t and at 50⁰ C yielded the same chromatograms (same number and types of products). This again suggested that no phenolic groups were being derivatized, and also that the derivatization of phenolic groups is much slower than amino, compatible with the literature [9-10].

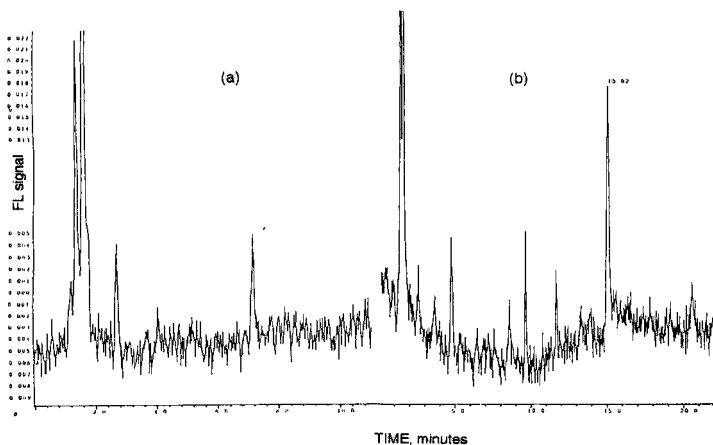


Figure 6. Determination of the detection limits of protein 6-AQC derivatives. (a) 10 ng ($10\ \mu\text{l} \times 1\ \text{ng}/\mu\text{l}$), about 1 picomole of insulin, (b) 20 ng ($20\ \mu\text{l} \times 1\ \text{ng}/\mu\text{l}$), about 3 picomoles of bovine growth hormone releasing factor (GHRF). HPLC conditions: Experimental and mobile phase A consisted of 20 mM sodium acetate titrated to pH 5.0 with phosphoric acid, mobile phase B consisted of ACN/ H_2O , 80/20, v/v. Gradient elution: B was linearly increased from 30% to 80% over 30 min. Detection: FL 254/395 nm, ex/em.

The possible product differences became even clearer when comparing derivatizations between the solution 6-AQC (excess reagent/protein) and the 6-AQC tagged polymeric reagent. The reaction with the 6-AQC polymeric reagent often yielded fewer tags on the protein (compare Figures 4 vs. 7). These products were very similar to those obtained from the solution reagent derivatization when using a molar ratio of 1/1 (reagent to protein), Figures 7-9. These Figures 7-9 make direct comparisons of both the solution and polymeric reagent reaction products for three different proteins (insulin, GHRF, glucagon). These chromatograms represent both UV and FL responses to the tagged proteins present, and almost identical chromatograms were obtained by simultaneous UV/FL detection, other than for the presence (at times) of unreacted starting protein by UV (214 nm), as below. Untagged, starting proteins (except glucagon) showed no FL responses under these same HPLC-FL conditions. We chose 214 nm detection in the UV to ensure detection of all proteins and peptides, as well as any unreacted species.

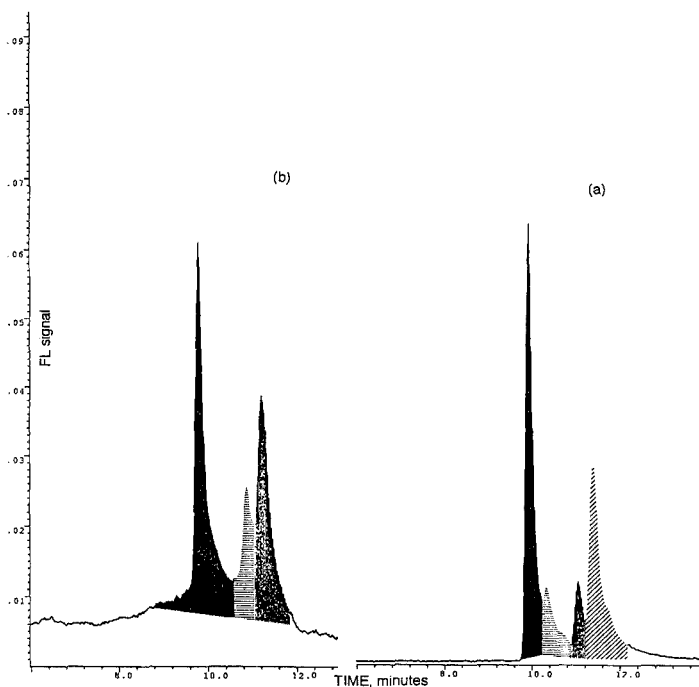


Figure 7A. Chromatograms of polymeric reagent vs. solution reagent derivatized insulin with FL detection. Reactions were performed at room temperature: (a) derivatized with 6-AQC solution reagent at a molar ratio of reagent to insulin of 1:1. (b) derivatized with polymeric reagent. HPLC conditions as in Figure 4. Peak shadings do not attempt to identify individual proteins.

In the case of insulin, Figures 7A-B, the shaded peaks represent those products derived just from tagging of the protein, after subtraction of the blank chromatograms (reagent blanks). Figure 7A (FL) shows no residual starting insulin, which does appear at a retention time of about 9.2 mins in Figure 7B (UV). Otherwise, the peak profiles are identical, which means that we are indeed seeing all of the tagged proteins formed by HPLC-UV/FL. These results should be directly compared with Figure 4, which represents products formed when the solution 6-AQC reagent was in large excess (Experimental). When the molar ratio of solution reagent/protein was

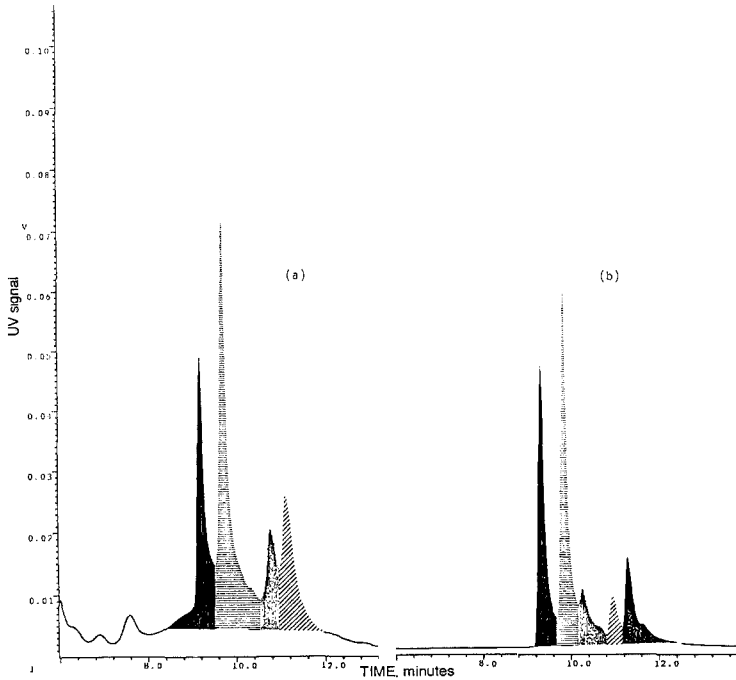


Figure 7B. Chromatograms of polymeric vs. solution reagent derivatized insulin with UV detection at 214 nm. Reaction conditions are the same as in Figure 7A. (a) derivatized with the 6-AQC solution reagent at a molar ratio of reagent to insulin of 1:1; (b) derivatized with polymeric reagent. HPLC conditions as in Figure 4. Peak shadings do not attempt to identify individual proteins.

closer to 1/1, the number of products observed was reduced in every case, Figures 7-9, to varying extents. Even though the polymeric reagent contained a large excess of available tags to protein present, far fewer products were formed than from the analogous, solution situation, Figure 4. This again suggested that not all of the potentially taggable sites on the proteins can reach the immobilized tags to be reacted, for example, phenolic groups on Tyr. Perhaps only those more active, exposed amino groups (N-terminal and Lys) were reacted by the polymeric, immobilized reagent. When the solution reagent was present in a limited amount (1/1),

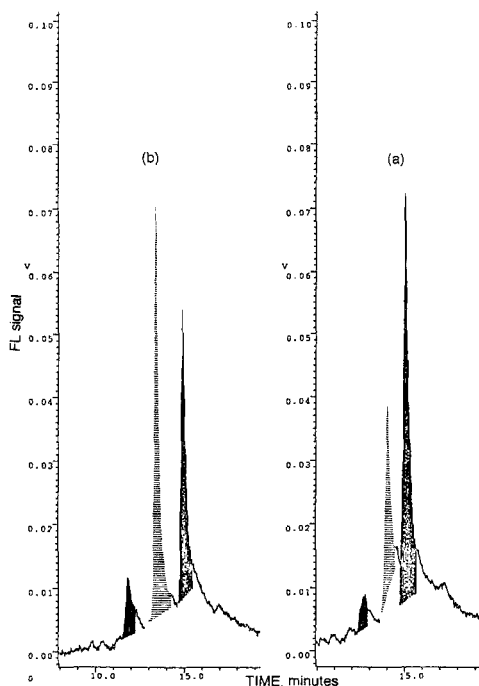


Figure 8A. Chromatograms of polymeric vs. solution reagent derivatized GHRF with FL detection. Reactions were performed at room temperature. (a) derivatized with polymeric reagent; (b) derivatized with the 6-AQC solution reagent at a molar ratio of reagent to GHRF of 1:1. HPLC conditions are the same as in Figure 4. Peak shadings do not attempt to identify individual proteins.

fewer products were formed (Figures 7-9) than in Figure 4, and those were most likely derived from N-terminal and Lys groups, for the above reasons.

In comparing, Figures 7A-B, solution vs. polymeric reagent for insulin tagging, though the products appeared to be the same, they were not formed in the exact same relative ratios (peak area comparisons). There were subtle, but seemingly real differences in the relative (not absolute) ratios of tagged products formed in going from solution to polymeric reagent. This may have been due to steric hindrance in the case of the polymeric reagent, obviously absent for the solution case.

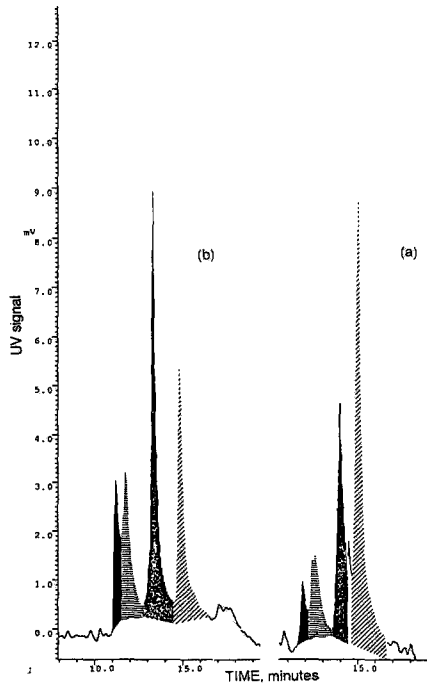


Figure 8B Chromatograms of polymeric vs. solution reagent derivatized GHRF with UV detection at 214 nm. Reaction conditions are the same as in Figure 8A. (a) derivatized with polymeric reagent, (b) derivatized with the 6-AQC solution reagent at a molar ratio of reagent to GHRF of 1:1. HPLC conditions are the same as in Figure 4. Peak shadings do not attempt to identify individual proteins.

There is a reversal of the relative ratios of formation of the two products coming from GHRF, Figures 8A-B. Again, Figure 8A (FL) does not show the presence of unreacted GHRF, but Figure 8B (UV) clearly shows this additional peak at a retention time of about 10.4 mins, just before the first tagged GHRF peak, also present (reduced) in Figure 8A (FL). As expected, all of these hydrophobically tagged peptide/protein peaks elute later than underivatized starting proteins.

In the case of glucagon, Figures 9A-B, there is again a difference in the relative ratios of products. This still suggests some degree of site selectivity, which could/should vary

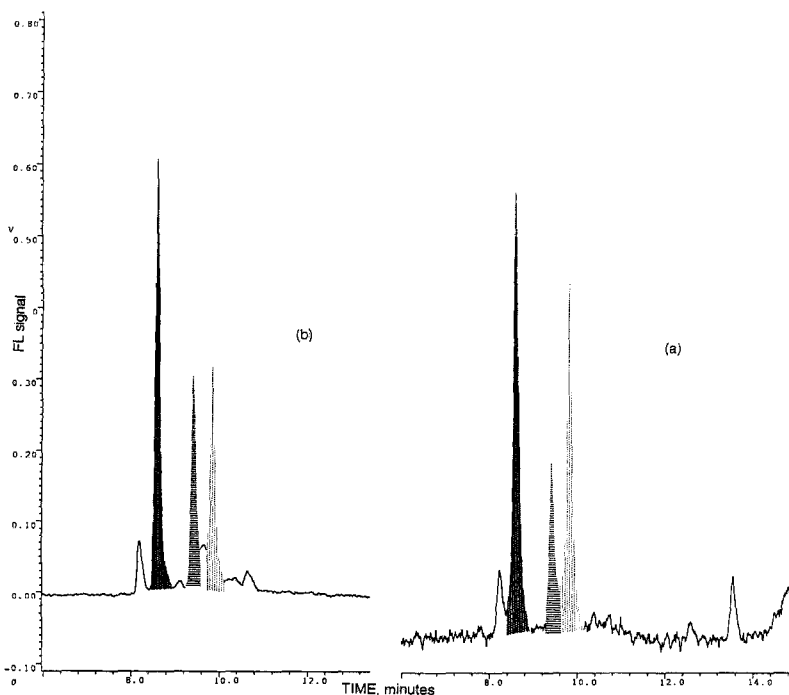


Figure 9A. Chromatograms of polymeric vs. solution reagent derivatized glucagon with FL detection. Reactions were performed at room temperature. (a) derivatized with polymeric reagent; (b) derivatized with the 6-AQC solution reagent at a molar ratio of reagent to GHRF of 1:1. HPLC conditions are the same as in Figure 4. Peak shadings do not attempt to identify individual proteins.

from protein to protein, and may also be reaction conditions dependent. Figure 9A (FL) illustrates the presence of three tagged products, with unreacted glucagon eluting at about 8.0 mins in both Figures 9A and 9B. Separate injections of unreacted, starting protein were injected for all proteins under these very HPLC-UV/FL conditions to ensure identification of the untagged protein peak. There is a small FL response for what appears to be the untagged glucagon peak in Figure 9A, which is considerably larger relative to the tagged products by UV in Figure 9B. This may be due to the presence of Trp in the individual, respective proteins.

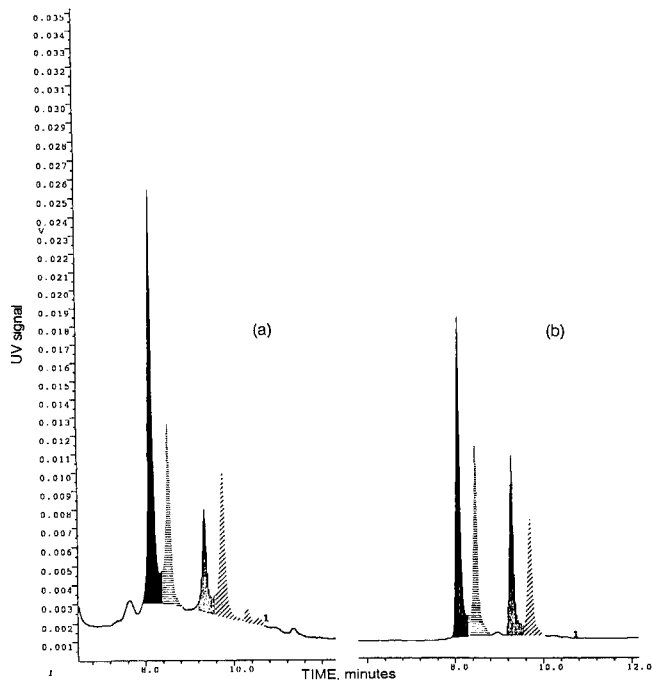


Figure 9B Chromatograms of polymeric vs. solution reagent derivatized glucagon with UV detection at 214 nm. Reaction conditions are the same as in Figure 9A. (a) derivatized with polymeric reagent, (b) derivatized with the 6-AQC solution reagent at a molar ratio of reagent to GHRF of 1:1. HPLC conditions are the same as in Figure 4. Peak shadings do not attempt to identify individual proteins.

Polymeric Reagents With Outer Tags First Removed; Possible Selective Tagging of Specific Sites on Proteins.

These particular polymeric reagents had tags on their outer surface and within the more restricted pores [20, 25]. Because the polymer support used for preparation of these reagents was made from a controlled pore silica substrate using a template polymerization method, the final reagents contained a narrow, fixed pore size, which was reaction solvent dependent [25-26]. We have now shown that the size of these pores changes with the reaction solvent, and that a size selectivity occurs with

different sized amine type analytes [26]. It is entirely possible that if the outer surface tags were first removed with a large, bulky amine, leaving a polymeric reagent with tags only on the inner pore surfaces, reaction selectivity towards proteins will be more pronounced and obvious. These studies are now in progress [26].

The incomplete reaction of amino groups, with the current polymeric reagent, may be due to steric hindrance restricting access to functional groups within the protein's interior. This may only allow the functional groups on the outer surface of the proteins to be tagged. This could be useful for keeping the protein derivatives bioactive. Such studies are now in progress, as below.

The 6-AQC tagged polymeric reagent seems to be less chemically reactive than the solution reagent, since the same products were obtained from reactions first performed at room temperature or then filtered and heated to 50⁰ C. We may conclude that the phenolic groups in these proteins cannot be readily derivatized with the immobilized reagent. This result is reasonable given the reagent's structure and perhaps accessibility of Tyr sites in the proteins. The bond (carbamate) holding the 6-AQ tag in the polymeric reagent is perhaps less reactive than that in the analogous solution reagent, because the activating groups [benzotriazole (polymeric) vs. N-hydroxysuccinimide (solution)] are different. There are basic differences in the overall, solution reactivities of these functional groups, combined with the fact that one reaction is in a homogeneous solution and the other on a heterogeneous support. In general, solution reactions using the same labile linkage are kinetically faster than the analogous, immobilized reaction, just because of the number of effective collisions per unit time with the same analyte [15]. Also, carbamate linkages in solution reagents tend to be less labile or reactive than activated esters (NHS) [19-20].

It is therefore more difficult for this tagging group on the polymeric reagent to react with weaker nucleophilic centers, such as phenolic groups. There is also the further issue of accessibility of the reactive sites on the polymeric vs. solution reagents to perhaps buried phenolic sites in the protein.

Effects of Surfactants on Derivatizations of Proteins, Bioactive vs. Bioinactive, Tagged Protein Products.

We have also undertaken preliminary studies with surfactants to assess their effect on product distribution and reactivity with both solution and polymeric reagents. Surfactants have some effect on protein derivatizations with the polymeric reagent. This effect was compared by using GHRF as a standard protein example. The neutral

surfactant Brij 35, cationic surfactant CTAB, and anionic surfactant SDS, were tested with the polymeric reagent. The reaction with Brij 35 had the lowest yield of products, SDS was better than Brij 35, and the reaction with CTAB had the highest yield of tagged products. These results agreed with those obtained for typical AAs using an analogous polymeric 9-FA reagent [6]. Since the reaction was performed in a basic buffer, where most proteins were negatively charged, cationic surfactants could form ion pairs with proteins, and enable them to penetrate the hydrophobic surface of the polymeric reagent for subsequent reaction. SDS could not form ion pairs with proteins under the same conditions. Brij 35 is a hydrophilic surfactant, and it would protect proteins from approach to the surface of the polymeric reagent to some extent.

The presence of such surfactants with solution reactions has also been initially investigated. At a high molar ratio of reagent to protein, no significant differences were observed with or without surfactants present. All the amino groups in the protein must have been fully derivatized, though in the one case studied, the final products were not recognized by their antibody (Ab) (GHRF) (not bioactive). At a lower ratio of solution reagent to protein, the products were still not bioactive if SDS and CTAB were present in the reaction solution. When the derivatization of GHRF was done at a molar ratio of about 1/1 with 0.5% Brij present, the final tagged products were now bioactive. They could now be recognized and captured by their N- or C-terminal Ab high performance immunoaffinity column (HPIAC)(Experimental). Figure 10 illustrates the RPC chromatograms of those solution tagged proteins first captured (b, c) on an immobilized Ab column, as indicated. Figure 10a illustrates, again by RPC, the total mixture of tagged products, only some of which are recognized on the two different immunoaffinity columns (N- and C-terminal Abs to GHRF). Apparently, there are but three tagged GHRF products formed under these particular, solution reagent, Brij conditions, Figure 10a. Only one of these is being recognized by the C-terminal Ab column, Figure 10b. All three tagged proteins; however, are recognized to differing degrees by the N-terminal Ab column, Figure 10c, when compared with Figure 10a.

There remains a significant problem in tagging of proteins by solution reactions, perhaps exemplified by the recent works of Schultz and Kennedy, and Banks and Paquette [11-12]. In such studies, using conventional solution reagents for preparing tagged, bioactive proteins, multiple products are formed, as a function of the reaction conditions (concentration, stoichiometric ratios, temperature, time, etc.). These products can have several tags per protein molecule, making such species problematic as part of an immunoassay or HPLC/HPCE-detection schemes. Still

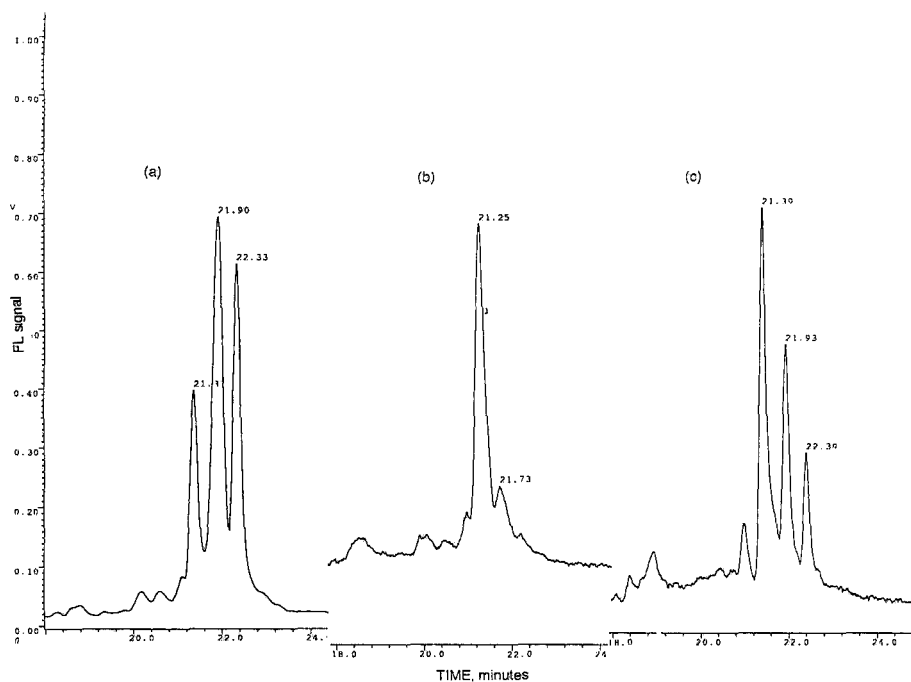


Figure 10. RPC chromatograms of solution tagged 6-AQC derivatives. Reaction conditions used a small amount of Brij present, leading to bioactive, tagged GHRF products. a) total reaction products without initial affinity isolation; b) products first captured by C-terminal Ab column to GHRF, then assayed by RPC; c) products first captured by N-terminal Ab column to GHRF, then assayed by RPC. HPLC conditions: mobile phase A was PBS 7, mobile phase B consisted of ACN/H₂O, 80/20, v/v. Initial at 30% B, and B was linearly increased to 80% over 30 min in gradient elution. Fluorescence detection: 254 nm/ 395 nm, ex/em.

today, there are no simple approaches for the preparation of a single, controlled tagged, bioactive protein, except in certain cases where one deals with small peptides or polypeptides. The above approaches address these issues and hopefully will permit us to eventually control reaction conditions leading to a single, tagged, and bioactive protein suitable for analytical applications and determinations.

Identification of 6-AQ Tagged Proteins by HPLC-UV/FL.

A need exists to discuss the differences in retention (elution) times for the variously tagged proteins, for example GHRF, Figures 4-5, 8, 10. In not knowing specific conformations for these tagged species, nor the exact number of sites of tagging in the products, it is impossible to correlate HPLC retention or elution times. It is not clear that we are indeed looking at the exact same tagged species in comparing, for example, Figures 4-5 and 8-10. These may very well be quite different species, which would explain their somewhat different elution times in HPLC. It is possible that we are also dealing with different conformations for these tagged species, concomitant with differences in tagging levels and/or sites. Hence, to correlate their chromatographic properties, at the moment, without knowing more about specific conformations and levels/sites of tagging is problematic. It is clear that further understanding of the exact nature of these tagged species will require extensive MS analyses, work contemplated for the future.

Conclusions

An improved method for the synthesis of a styrene-divinylbenzene based polymeric 6-AQC reagent has been developed. The obtained polymeric reagent was successfully used for the derivatization of AAs and peptides. The efficiency of derivatization and improved HPLC detectability (UV/FL) of these derivatives makes this reagent attractive for the qualitative analysis of AAs and small peptides. Such newer derivatization methods may be applied for quantitative analysis, in view of their high reproducibility.

The derivatization of proteins with the polymeric reagent usually yielded fewer or altered ratios of tagged products in comparison with the analogous solution reagent. Some bioaffinity sites may be blocked in this way, affecting biorecognition. In general, forming a single, tagged product with bioactivity is useful for enhancing detection of proteins in affinity chromatography (HPIAC). The derivatization of proteins at elevated temperatures yielded a single product when using the 6-AQC solution reagent, but such products were usually bioinactive towards their antibodies (data not shown). These reaction approaches can now be used for precolumn derivatization in reverse

phase HPLC or HPCE, in order to improve the general detection of proteins. Under optimized conditions, picomoles of proteins could be detected with FL, depending on the final number of 6-AQ tags present per protein molecule.

Acknowledgements

We gratefully acknowledge Waters Corporation (Milford, MA) and EM Science, Inc. (Gibbstown, NJ) for their donations of HPLC columns, solvents, and reagents. The Upjohn Company provided partial financial support and all of the GHRF and its antibodies used in these studies. Guodong Li wishes to express his appreciation to the State Education Commission (PRC), for financial support while a Visiting Scientist at Northeastern University (1993-94). Additional financial support was provided by the Analytical Research Department of Pfizer, Inc., Groton, CT.

References

1. I.S. Krull, F.-X. Zhou, A.J. Bourque, M. Szulc, J. Yu, and R. Strong. *J. Chromatogr.*, B, 659(1/2), 19 (1994).
2. C.-X. Gao and I.S. Krull. *BioChromatography*, 4(4), 222 (1989).
3. T.-Y. Chou, I.S. Krull, S.T. Colgan, D.M. Kao, C. Dorschel, C. Stacey, and B. Bidlingmeyer. *J. Chromatogr.*, 367(2), 335 (1986).
4. C.-X. Gao, T.-Y. Chou, S.T. Colgan, I.S. Krull, C. Dorschel, and B. Bidlingmeyer. *J. Chromatogr. Sci.*, 26, 449 (1988).
5. C.-X. Gao, T.-Y. Chou, and I.S. Krull. *Anal. Chem.*, 61(14), 1538 (1989).
6. F.-X. Zhou, I.S. Krull, and B. Feibush. *J. Chromatogr.*, 648, 357 (1993).
7. J. Yu, G. Li, I.S. Krull, and S. Cohen. *J. Chromatogr.*, 658, 249 (1994).
8. S. A. Cohen and D. P. Michaud. *Anal. Biochem.*, 211, 279 (1993).
9. R.L. Lundblad. Chemical Reagents for Protein Modifications, Second Edition, CRC Press, Boca Raton, FL, 1991.
10. Protein Immobilization, Fundamentals and Applications, Ed. by R.F. Taylor, Marcel Dekker, NY, 1991.
11. N.M. Schultz and R.T. Kennedy. *Anal. Chem.*, 65, 3161 (1993).
12. P.R. Banks and D.M. Paquette. *J. Chromatogr.*, A, 693, 145 (1995).
13. W. Ding, S. Xu, and R. Zhang. *Fenxi Huaxue*, 15, 17 (1987).
14. T. Yakoyama and T. Kinoshita. *J. Chromatogr.* 518, 141 (1990).
15. H. Miyano, T. Toyooka, and K. Imai. *Anal. Chim. Acta.*, 170, 81 (1985).
16. V. A. Fried, M. E. Ando, and A.J. Bell. *Anal. Biochem.*, 146, 271 (1985).
17. V. J. Lenz, H. G. Gattner, M. Leithauser, D. Brandenburg, A. Wollmer, and H. Hocker. *Anal. Biochem.*, 221, 85 (1994).

18. R. Kalir, A. Warshawsky, M. Fridkin, and A. Patchornik. *Eur. J. Biochem.*, 59, 55 (1975).
19. A.J. Bourque and I.S. Krull. *J. Pharm. Biomed. Anal.*, 11(6), 495 (1993).
20. A.J. Bourque. Ph.D. Thesis, Northeastern University, 1993.
21. G. Li, I.S. Krull, and S. Cohen. *J. Chromatogr.*, submitted for publication (1995).
22. K.M. De Antonis, P.R. Brown, and S.A. Cohen. *Anal. Biochem.*, 223, 191 (1994).
23. K. M. De Antonis, P.R. Brown, Y.-F. Cheng, and S.A. Cohen. *J. Chromatogr., A*, 661, 279 (1994).
24. S.A. Cohen. Unpublished results (1994).
25. A.J. Bourque, I.S. Krull, and B. Feibush. *Anal. Chem.*, 65(21), 2983 (1993).
26. M.E. Szulc, P. Swett, F.-X. Zhou, and I.S. Krull. *J. Chromatogr.*, in preparation (1995).

Received: July 26, 1995

Accepted: August 6, 1995

**A COMPARATIVE STUDY ON THE EFFECT
OF HYDROCHLORIC, PHOSPHORIC, AND
TRIFLUOROACETIC ACID IN THE REVERSED
PHASE CHROMATOGRAPHY OF ANGIOTENSINS
AND RELATED PEPTIDES**

DANILO CORRADINI* AND GIANFRANCO CANNARSA

Istituto di Cromatografia del CNR

Area delle Ricerche di Roma

P.O. Box 10

I-00016 Monterotondo Stazione, Rome, Italy

ABSTRACT

This paper examines the effect of hydrochloric acid as an alternative mobile phase additive in reversed phase chromatography of closely related peptides, such as the analogs of human angiotensin I and III, in comparison to the retention behavior and selectivity obtained with the two most popular additives TFA and phosphoric acid. The effect of the concentration of the additive and of the apparent pH of the mobile phase was investigated by isocratic elution of the selected peptides on a totally porous butyl-silica column with water-acetonitrile eluents containing either additive at various concentrations, corresponding to different values of the apparent pH of the mobile phase within the range 1.23 to 2.28. Differences in retention behavior and selectivity observed with the three mobile phase additives were discussed in terms of differences in the ion-pair associations between the ionized peptides and the counterions in the mobile phase.

INTRODUCTION

Reversed-phase chromatography (RPC) is the predominant mode of high-performance liquid chromatography (HPLC) for both analytical and preparative scale separations of peptides (1). Its excellent resolving power and flexibility is mainly due to the wide possibility of manipulation of mobile phase composition, which include the type and the concentration of organic modifier, pH, choice of buffering agent, and use of hydrophilic or hydrophobic ion-pairing reagents (2).

Peptides are charged molecules at most pH values and the presence of different counterions in the mobile phase influences their charge and hydrophobicity to different extent, depending on the nature of both the counterion and peptide. Mobile phases in the range of pH 2-3 are usually selected in order to ensure protonation of hydrophilic acidic groups of peptides and to suppress the ionization of the surface silanols of the silica-based sorbents which are the dominant reversed-phase columns used in peptide RPC. Ionization of peptide carboxyl groups increases the analyte polarity and hence reduce its retention, whereas silanols dissociation is believed to be the main source of the dual functionalities (polar and hydrophobic) exhibited by silica-based reversed-phase sorbents (3-4).

The most commonly used additive for acidic mobile phases employed in RPC of peptides is trifluoroacetic acid (TFA), due to its anionic ion-pairing properties, excellent solubilization characteristics for most peptides, low UV transparency, capability to minimize the ionic effects of free silanols of the sorbent, and volatility, which renders this additive particularly suitable for preparative scale separations (5-6). Acetate, formate and dihydrogen phosphate are also popular alternative choices (2, 7-8). Furthermore, a variety of alkylsulfonates and alkyl sulfates offer a range of anionic ion-pairing reagents with varying degree of hydrophobicity. Cationic ion-pairing additives have also been employed including tertiary alkyl amines (e.g. triethylamine) and quaternary ammonium salts (e.g., tetrabutylammonium phosphate) (9-12). However, using these hydrophobic ion-pairing reagents as mobile phase additives induces an increase in peptide retention time thus requiring the use of higher organic modifier concentrations.

The purpose of this study is to examine the effect of hydrochloric acid in reversed phase chromatography of small peptides, in comparison to the retention behavior and selectivity obtained with the two most popular additives TFA and phosphoric acid. While TFA and to a lesser extent phosphoric and hydrochloric acid were exploited in HPLC of peptides (7-8, 13-14), a systematic study involving the use and examination of the effect of hydrochloric acid in peptide RPC is sorely needed .

This report summarizes the results obtained by comparing the chromatographic behavior of a set of angiotensin analogs, selected as typical models of closely related peptides, on a totally porous 5- μ m butyl-silica column which were eluted under isocratic conditions with water-acetonitrile mobile phases containing either TFA or hydrochloric or phosphoric acid at concentration corresponding to various values of the apparent pH of the hydro-organic eluents, ranging from 1.23 to 2.28.

EXPERIMENTAL

Instrument and column

The experiments were carried out with an HPLC unit assembled from two Model 114 solvent delivery pumps, a Model 420 system controller, both from Beckman (Fullerton, CA, USA), a Varian (Walnut Creek, CA, USA) Model Star 9050 variable wavelength UV-vis detector, and a Rheodyne (Cotati, CA, USA) Model 7125 injection valve with a 5- μ l sample loop. Chromatograms were obtained with a Spectra-Physics (San Jose, CA, USA) Model SP 4400 integrator. HPLC was performed on a Vydac (The Separations Group, Hesperia, CA, USA) Protein C-4 column (150 x 4.6 mm, I.D.) containing 5- μ m butyl-silica.

Materials

The following synthetic bioactive peptides were obtained from Sigma (Milan, Italy): Angiotensin I from human, bullfrog, and salmon, human angiotensin III, human angiotensin III analogs and des-Arg¹-bradykinin. The sequence of these peptides are in Table 1. Reagent-grade phosphoric acid and TFA were purchased from Fluka (Milan, Italy).

TABLE 1

Sequence of Peptides Used in This Study.

Peptides	Amino-acid residues	Sequence
Human Angiotensin I	10	Asp-Arg-Val-Tyr-Ile-His-Pro-Phe-His-Leu
Bullfrog Angiotensin I	10	Asp-Arg-Val-Tyr-Val-His-Pro-Phe-Asn-Leu
Salmon Angiotensin I	10	Asn-Arg-Val-Tyr-Val-His-Pro-Phe-Asn-Leu
Human Angiotensin III	7	Arg-Val-Tyr-Ile-His-Pro-Phe
[Val ⁴]-Angiotensin III	7	Arg-Val-Tyr-Val-His-Pro-Phe
[Val ⁴ -Ile ⁷]-Angiotensin III	7	Arg-Val-Tyr-Val-His-Pro-Ile
des-Arg ¹ -Bradykinin	8	Pro-Pro-Gly-Phe-Ser-Pro-Phe-Arg

Reagent-grade hydrochloric acid as well as HPLC-grade water and acetonitrile (ACN) were obtained from Carlo Erba (Milan, Italy).

Preparation of eluents

The eluents were prepared by mixing in a volumetric flask the required volumes of acetonitrile and additive for the concentration stated. The apparent pH was measured with a glass electrode model HI 1131 and Model HI 9017 Microprocessor pH-Meter, both from Hanna Instruments (Woonsocket, RI, USA), and was taken as the pH of the solution. All solutions were filtered through a Millipore (Milan, Italy) type FH 0.5- μ m membrane filter and degassed by sparging with helium before use.

Chromatographic measurements

Acetonitrile-water mixtures having ACN concentration of 19.95% (v/v) and containing either TFA or phosphoric acid or hydrochloric acid at a given concentration were used for isocratic elution at room temperature. The column was allowed to equilibrate for a period of 1-h after each change

of mobile phase composition. The peak obtained by injecting pure acetonitrile was used to evaluate the hold-up time at each mobile phase composition. All measurements of retention data were made in triplicate.

RESULTS AND DISCUSSION

Angiotensin I from three different biological sources (human, salmon, bullfrog), human angiotensin III and two analogs of this peptide, [Val⁴]-angiotensin III and [Val⁴-Ile⁷]-angiotensin III, were selected as typical models of closely related peptides. The dependence of the retention factors, k' , of these bioactive peptides on the concentration of TFA in the mobile phase containing acetonitrile as the organic modifier was examined on a Vydac Protein C-4 column and the results are shown in Fig. 1. The peptides were eluted at room temperature under isocratic conditions at a flow rate of 1.0 ml/min with hydro-organic mobile phases containing the same percentage of acetonitrile, 19.95 % (v/v), and TFA at concentration ranging from 5 to 40 mM. The concentration of acetonitrile in the mobile phase was selected so as to obtain accurately measurable retention factors and peptide separation.

As seen in Fig. 1, all of the peptides exhibited increasing retention factors with increasing the TFA concentration in the eluent. The measurement of the apparent pH of the hydro-organic mobile phases revealed that as the concentration of TFA increased from 5 to 40 mM the apparent pH of the hydro-organic eluent decreased from 2.28 to 1.41. Since the pH of the mobile phase can affect the net charge of the peptide, resulting in a variation of the analyte polarity, we decided to examine the effect of the apparent pH of the mobile phase on the retention behavior of the various peptides under investigation. This study was performed by eluting the selected angiotensins with mobile phases containing acetonitrile at the same concentration as in the previous experiments and phosphoric acid at concentrations needed to bring the apparent pH of the hydro-organic mobile phases to the values of 2.28, 2.00, 1.66, and 1.41, which were the values of the apparent pH measured with TFA at concentrations of 5, 13.5, 25, and 40 mM, respectively. Further experiments were carried out using

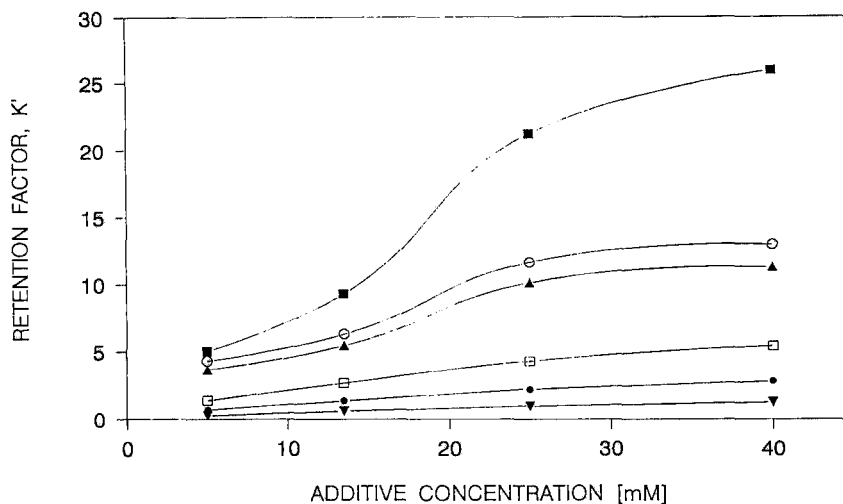


FIGURE 1. Dependence of retention factor on the concentration of TFA in the hydro-organic mobile phase containing 19.95% (v/v) acetonitrile. Column, Vydac Protein C-4 (150 x 4.6 mm I.D.); flow rate, 1.0 ml/min; detection, 214 nm, 0.05 a.u.f.s.; peptides: [Val⁴-Ile⁷]-angiotensin III (wedge), [Val⁴]-angiotensin III (dot), human angiotensin III (square), angiotensin I from human (filled square), bullfrog (circle) and salmon (triangle).

hydro-organic mobile phases with the same content of acetonitrile as above and hydrochloric acid as the acidic additive at concentration ranging from 4.4 to 36.5 mM, the apparent pH of which ranged from 1.23 to 2.0.

The retention factors obtained with the mobile phases containing the three acids are plotted in Fig. 2 against the value of the apparent pH measured by the pH-meter with the glass electrode. It is shown that with either hydrochloric or phosphoric acid the retention factors are only slightly affected by the variations in the apparent pH of the mobile phase. It should be noted that the concentration of the acid in the mobile phase corresponding to a given value of the apparent pH varied with the strength of the acid. For example, the concentration of TFA, hydrochloric, and phosphoric acid corresponding to the apparent pH 2.0 was 13.5, 4.5, and 31 mM, respectively. Consequently, plots of Figure 2 express also the

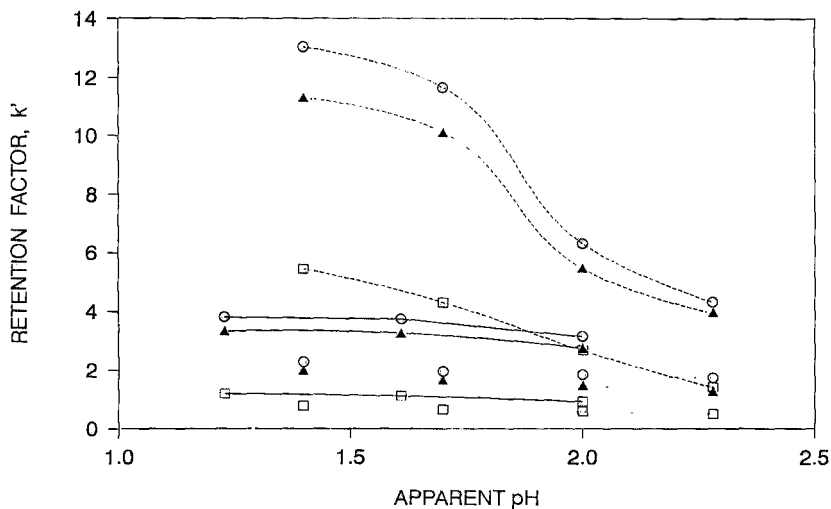


FIGURE 2. Dependence of retention factor on the value of the apparent pH of the mobile phase containing 19.95% (v/v) acetonitrile and either TFA (dashed lines) or phosphoric acid (dotted lines) or hydrochloric acid (solid lines). Symbols and experimental conditions as in Fig. 1.

variations of the retention factors within the different concentration ranges of the three acids in the mobile phase, which varied from 5 to 40, 4.4 to 36.5, and 9.4 to 203 mM for TFA, hydrochloric and phosphoric acid, respectively. Plots of Fig. 2 indicate that for the peptides investigated in this study the apparent pH of the mobile phase, at least within the range from 1.23 to 2.28, may not be a critical parameter in the case of the two inorganic acids (i.e. phosphoric and hydrochloric acid). On the other hand, the increasing retention of peptides observed with TFA is related to the effect of increasing the concentration of this organic acid to lowering the value of the apparent pH of the mobile phase and reflects the more hydrophobic character of TFA than that of phosphoric and hydrochloric acid.

Besides lowering the pH and thus suppressing the ionization of the residual silanol groups at the chromatographic surface, acidic additives are

believed to interact with the amino functions of the peptides via ion-pair formation (2). Furthermore, TFA and phosphoric acid possess high hydrogen-bonding capability (15) which is believed to affect both surface and solute polarity (16). TFA is a proton acceptor via its fluoro atoms and the carboxyl group and is less polar than phosphoric and hydrochloric acid. Extensive hydrogen-bonding of the trifluoroacetate ion to the silica surface and the peptide molecules led to enhancing the hydrophobicity of both the sorbent and the peptide, so that the retention of peptides is greater with TFA than with hydrochloric or phosphoric acid as the additive under otherwise identical conditions.

The peak capacity measured in the presence of the different mobile phase additives was used to compare their effect on the separation of a peptide test mixture, which included des-Arg¹-bradykinin and angiotensin I from three different biological sources: human, salmon and bullfrog. The peak capacity is calculated by dividing the net retention time of the last peak in the chromatogram by the average peak width. It expresses the maximum number of peaks that can theoretically be resolved in the chromatogram (17).

In order to facilitate the comparison, peak capacities were measured with the same mobile phases used to study the effect of the apparent pH on the retention behavior of peptides and the results are reported in Table 2. It is observed that peak capacity increases with the concentration of the additive up to a limiting value which is greater with mobile phases containing TFA. The increased value of peak capacity with increasing the additive concentration is related to both the improved peak efficiency, due to a better masking effect of the free silanol groups on the surface of the chromatographic sorbent and the greater separation distance obtained with increasing the additive concentration, which was larger with TFA due to the longer retention times obtained with this mobile phase additive.

Figure 3 and 4 report the chromatograms of the above peptide test mixture obtained with hydrochloric and phosphoric acid as the additives of the hydro-organic mobile phases. With mobile phases containing hydrochloric acid (see Fig. 3), angiotensin I from salmon elutes after des-Arg¹-bradykinin, which elutes first, followed by the peptide from bullfrog and then that from human, which elutes last. It is observed that the chromatographic resolution of the three angiotensins improves as the

TABLE 2

Peak Capacity of the Vydac Protein C-4 Column as Determined by Isocratic Elution of a Peptide Mixture with Hydro-organic Mobile Phases Containing 19.95% (v/v) Acetonitrile and Either Hydrochloric or Phosphoric or Trifluoroacetic Acid at Different Concentrations.

HCl		H ₃ PO ₄		TFA	
Concentration [mM]	Peak Capacity	Concentration [mM]	Peak Capacity	Concentration [mM]	Peak Capacity
4.4	10	9.4	6	5.0	14
8.3	14	31.0	7	13.5	21
19.4	14	90.0	8	25.0	27
36.5	15	203.0	8	40.0	32

concentration of the additive increases. Similar results (not shown) were also obtained with TFA. However, with this additive the retention times were noticeably longer than those obtained with either hydrochloric or phosphoric acid (see Fig. 2). In contrast, dramatic selectivity changes were obtained with the use of phosphoric acid as the mobile phase additive. This is illustrated in Fig. 4 which displays the chromatograms obtained with the hydro-organic mobile phases containing phosphoric acid at concentration ranging from 9.4 to 203 mM. It is of interest to note the reversal of elution order for angiotensin I from bullfrog and from human and the co-elution of this angiotensin with the peptide from salmon observed with the lower concentration of phosphoric acid in the eluent. Furthermore, the chromatographic resolution of these peptides decreases as the concentration of phosphoric acid increases.

The differences in selectivity and resolution observed with hydrochloric and phosphoric acid as the additives can be attributed to differences in the ion-pair associations between the ionized peptides and the counterions in the mobile phase. We have already mentioned that

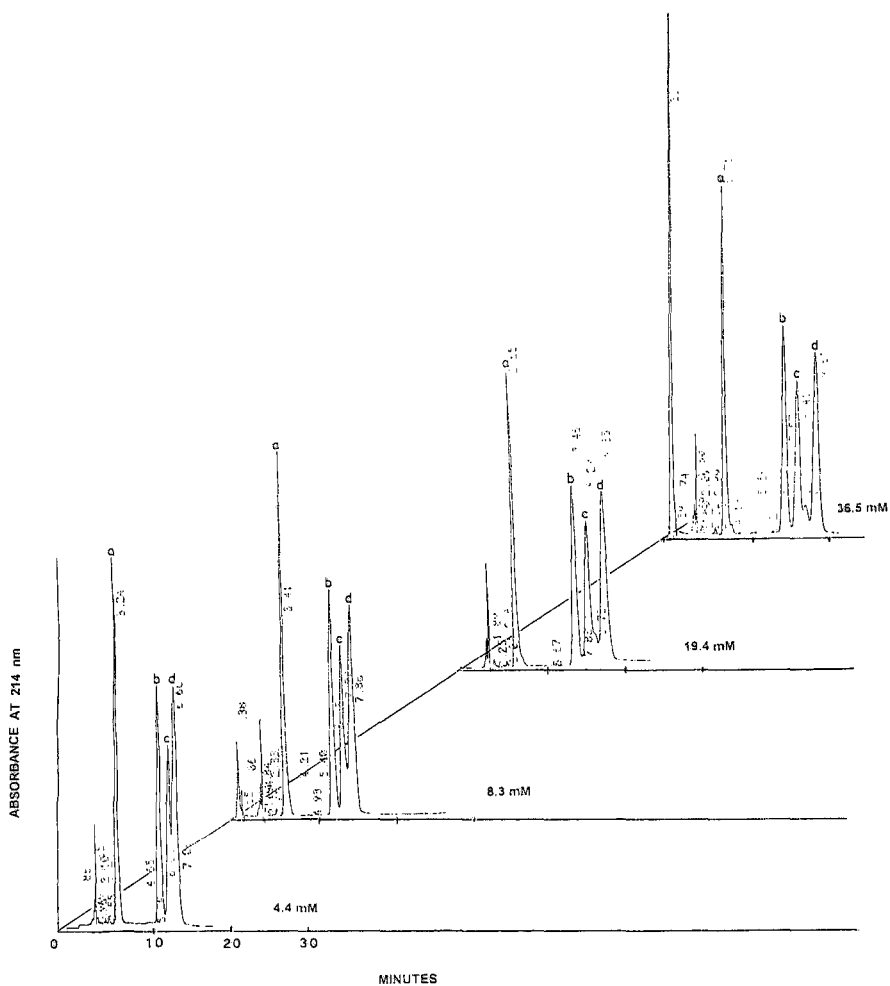


FIGURE 3. Chromatographic separation of des-Arg¹-bradykinin (a) and angiotensin I from salmon (b), bullfrog (c) and human (d) with mobile phases containing 19.95% (v/v) acetonitrile and hydrochloric acid at various concentrations as indicated on the chromatogram. Other conditions as in Fig. 1.

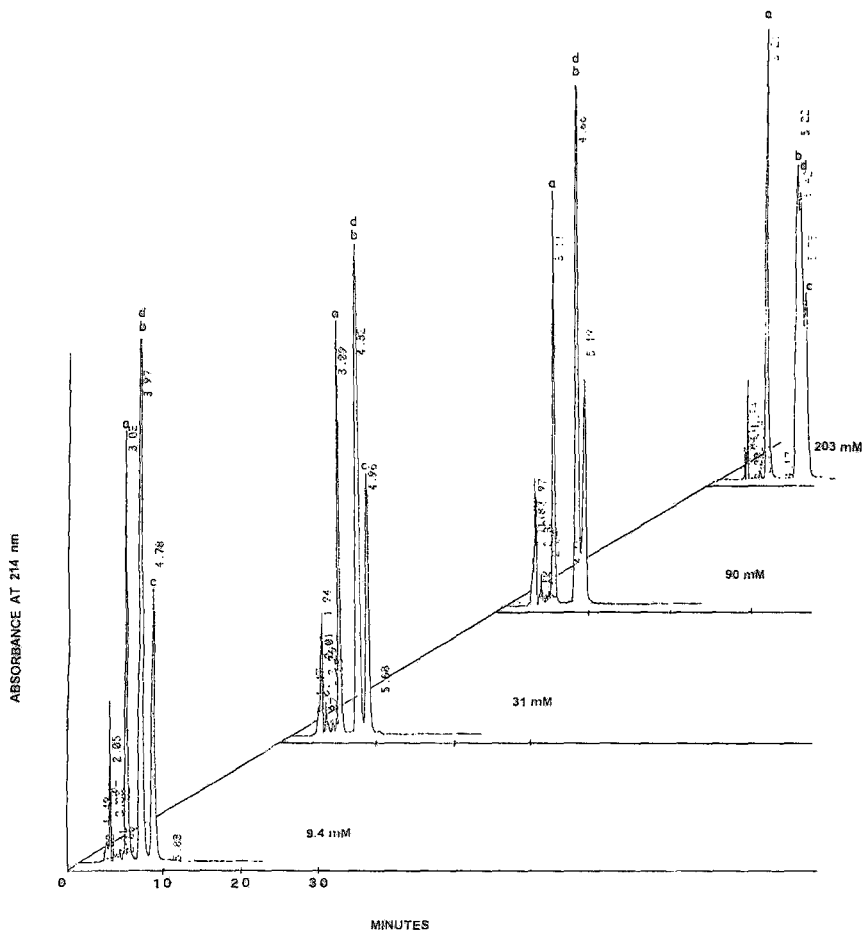


FIGURE 4. Chromatographic separation of des-Arg¹-bradykinin (a) and angiotensin I from salmon (b), bullfrog (c) and human (d) with mobile phases containing 19.95% (v/v) acetonitrile and phosphoric acid at various concentrations as indicated on the chromatogram. Other conditions as in Fig. 1.

phosphoric acid exhibit strong hydrogen-bonding properties, acting both as the donor and the acceptor. In most cases, each oxygen of phosphate ions can enter into more than one hydrogen bond owing to its tetrahedral symmetry (18). Extensive hydrogen-bonding of the phosphate ions to the molecules of the three angiotensins may enhance the virtual polarity of the ion-pair complexes of these closely related peptides to an extent that may level off the selectivity of the hydrophobic stationary phase towards these molecules. In contrast, hydrochloric acid is expected to suppress the ionization of the peptide carboxyl groups without the ion-pairing effect seen with phosphoric acid. Therefore, it can be inferred that the variations of the chromatographic behavior of the selected peptides observed with increasing the concentration of hydrochloric acid is mainly due to the effect of lowering the value of the apparent pH of the hydro-organic mobile phase.

ACKNOWLEDGEMENTS

G. C. was the recipient of a postdoctoral fellowship from CNR (National Research Council).

REFERENCES

1. C.T. Mant, R.S. Hodges, "HPLC of Peptides" in HPLC of Biological Macromolecules, Methods and Applications, K.M. Gooding, F.E. Regnier, eds., Marcel Dekker, Inc., New York, 1990, pp. 301-332.
2. M.T.W. Hearn, "High Performance Liquid Chromatography of Peptides" in High Performance Liquid Chromatography - Advances and Perspectives, Cs. Horváth, ed., Academic Press, New York, 1983, pp. 87-155.
3. A. Nahum, Cs. Horváth, J. Chromatogr., 203: 53-63 (1981)
4. K. E. Bij, Cs. Horváth, W.R. Melander, A. Nahum, J. Chromatogr., 203: 65-84 (1981)
5. H. Hagestam Freiser, K.M. Gooding, BioChromatogr., 2: 186-189 (1987)

6. D. Guo, C.T. Mant, R.S. Hodges, *J. Chromatogr.*, **386**: 205-222 (1987)
7. W.S. Hancock, C.A. Bishop, R.L. Prestidge, D.R.K. Harding, M.T.W. Hearn, *Science*, **200**: 1168-1170 (1978)
8. W.S. Hancock, C.A. Bishop, R.L. Prestidge, D.R.K. Harding, M.T.W. Hearn, *J. Chromatogr.*, **153**: 391-398 (1978)
9. W.S. Hancock, C.A. Bishop, L.J. Meyer, D.R.K. Harding, M.T.W. Hearn, *J. Chromatogr.*, **161**: 291-298 (1978)
10. W.S. Hancock, C.A. Bishop, J.E. Battersby, D.R.K. Harding, M.T.W. Hearn, *J. Chromatogr.*, **168**: 377-384 (1979)
11. W.M.M. Schaaper, D. Voskamp, C. Olieman, *J. Chromatogr.*, **195**: 181-186 (1980)
12. C.T. Mant, R.S. Hodges, "The Effect of Anionic Reagents on Peptide Retention in Reversed Phase Chromatography", in HPLC of Peptides and Proteins: Separation, Analysis and Conformation, C.T. Mant, R.S. Hodges, eds., CRC Press, Boca Raton, 1990, pp. 327-341.
13. M. J. O'Hare, E. Nice, *J. Chromatogr.*, **171**: 209-226 (1979)
14. P.M. Young, T.E. Wheat, *J. Chromatogr.*, **512**: 273-281 (1990)
15. G. Zundel, "Easily Polarizable Hydrogen Bonds", in The Hydrogen Bond, P. Schuster, G. Zundel, C. Sandorfy, eds., North-Holland Publishing Company, Amsterdam, 1976, pp. 750-753
16. B. Grego, F. Lambrou, M.T.W. Hearn, *J. Chromatogr.*, **266**: 89-103 (1983)
17. A.J. Banes, G. W. Link, L.R. Snyder, *J. Chromatogr.*, **326**: 419-431 (1985)
18. D.E.C. Corbridge "Phosphorous: An Outline of its Chemistry, Biochemistry and Technology", Elsevier, Amsterdam, 1990, pp. 959-971

Received: July 27, 1995

Accepted: August 6, 1995

THE BOOK CORNER

PROCESS SCALE LIQUID CHROMATOGRAPHY, Edited by G. Subramanian, VCH Publishers, Weinheim, Germany, 1995. xvi + 225 pp., DM178.00; ISBN: 3-527-28672-1.

This book discusses preparative and process scale liquid chromatography which are rapidly becoming important techniques in research and development. This modality offers more advantages over the traditional purification techniques.

The book consists of 9 chapters and discusses a theoretical basis and practical application of large-scale liquid chromatography. Chapter 1 discusses chromatography systems, designs and control systems for process scale chromatography. Chapter 2 discusses the practical application of theory in preparative liquid chromatography with two useful appendices dealing with calculation of column saturation capacity and mathematical models for preparative chromatography.

Alternative modes of operation of chromatography columns in the process situation are presented in Chapter 3. In this chapter, elution chromatography, displacement chromatography, frontal chromatography, among other operating modes, are discussed. The application of size-exclusion chromatography in process-scale purification of proteins is discussed in Chapter 4. Chapters 5 and 6 give an account of the application of polymeric media in preparative separation and non-exchange liquid chromatography in the biochemical field.

Supercritical-fluid chromatography and its application in industrial scaling up, including instrument design, are described in Chapters 7 and 8.

Finally, Chapter 9 deals with affinity chromatography and its application in large-scale separations.

The book is well illustrated and each chapter ends with list of references as recent as 1993.

The book is highly recommended to scientists and technical staff in pharmaceuticals, agrochemicals, industrial chemicals and the biochemical industry.

Reviewed by

Hassan Y. Aboul-Enein, PhD, FRSC
Bioanalytical and Drug Development Laboratory
Biological and Medical Research Department (MBC-03)
King Faisal Specialist Hospital & Research Centre
P.O. Box 3354, Riyadh 11211 Saudi Arabia

THIN-LAYER CHROMATOGRAPHY. TECHNIQUES AND APPLICATIONS, Chromatographic Science Series, Volume 66, 3rd Edition, Revised & Expanded, B. Fried and J. Sherma publ. by Marcel Dekker, Inc., New York, 1994, viii + 451 pages, US\$165.00; ISBN: 0-8247-9171-1

This book represents volume 66 in the Chromatographic Science Series published by Marcel Dekker. It is the third and expanded edition of this book on thin-layer chromatography (TLC); the second edition was published in 1986.

The book gives an detailed overview of current TLC techniques and equipment and also is well illustrated. The text comprises two sections. The first section discusses the general practices of TLC and consists of the following topics:

- Introduction and History
- Mechanism and Theory
- Sorbents, Layers, and Precoated Plates
- Obtaining Material for TLC and Sample Preparation
- Application of Samples
- Solvent Systems
- Development Techniques

Detection and Visualization
Qualitative Evaluation and Documentation
Quantification
Reproducibility of Results
Preparative Layer Chromatography
Radiochemical Techniques

The second section discusses the applications of TLC to different classes of compounds including lipids, amino acids, carbohydrates, natural pigments, vitamins, nucleic acids, steroids and terpenoids, pharmaceuticals and miscellaneous compounds. I believe that the chapter on pharmaceuticals needs more expansion, as the examples cited in this edition are limited. Also, certain topics were not adequately covered, e.g., discussion of multi-modal TLC, and the section on chiral phases. Each chapter ends with a list of references up to 1993. The book includes a directory of manufacturers and sources of standards, sample preparation supplies and TLC instruments, plates and reagents which is useful as well as a glossary. The book is highly recommended for analytical, pharmaceutical chemists, biologists and both graduate and undergraduate students applying this technique.

The book is a valuable reference as it presents up-to-date developments in modern instrumental TLC, along with the conventional techniques of planar chromatography.

Reviewed by

Hassan Y. Aboul-Enein, PhD, FRSC
Bioanalytical and Drug Development Lab.
Biological & Medical Research Department (MBC-03)
King Faisal Specialist Hospital & Research Centre
P.O. Box 3354, Riyadh 11211 Saudi Arabia

CAPILLARY ELECTROPHORESIS TECHNOLOGY, Chromatographic Science Series Volume 64, Edited by N. A. Guzman, publ. by Marcel Dekker Inc., New York, 1993, xv + 857 pages US\$165.00, ISBN: 0-8247-9042-1

This book represents volume 64 in the Chromatographic Science Series which is edited by Dr. Jack Cazes and published by Marcel Dekker. It is

a quite useful source for analytical and clinical chemists, biochemists, scientists and technical staff who are involved in this new separation modality, Capillary Electrophoresis, which is a rapidly expanding technique of separation science.

The book is written by over 50 experts widely recognized for their contributions to this area. The book consists of 5 separate parts.

- Part I: Overview includes 3 chapters
- Part II: Buffer system includes 4 chapters
- Part III: Capillary Column includes 5 chapters
- Part IV: Instrumentation includes 7 chapters
- Part V: Applications includes 11 chapters

Each chapter ends with a list of references up to 1992. However, it is of interest to mention that there is some information and even some figures being reproduced in two or three different chapters, but this does not represent a significant drawback.

The book is a welcome addition to academic, industrial and research centers libraries and is highly recommended for its up-to-date discussion of several topics of capillary electrophoresis. Finally, congratulations are extended for Dr. Guzman as an Editor for this volume and a job well done for being able to compile 30 chapters written by this impressive list of scientists.

Reviewed by

Hassan Y. Aboul-Enein, PhD, FRSC
Biological & Medical Research Department (MBC-03)
King Faisal Specialist Hospital & Research Centre
P.O. Box 3354, Riyadh 11211
Saudi Arabia

ANNOUNCEMENT

BASIC PRINCIPLES OF HPLC and HPLC SYSTEM TROUBLESHOOTING

One-Day & Two-Day In-House Training Courses

The courses, which are offered for presentation at corporate laboratories, are aimed at chemists and technicians who work with HPLC. They cover HPLC fundamentals and method development, as well as systematic diagnosis and solution of HPLC module and system problems.

The following topics are covered in depth:

- Introduction to HPLC Theory
 - Modes of HPLC Separation
 - Developing and Controlling Resolution
 - Mobile Phase Selection & Optimization
 - Ion-Pairing Principles
 - Gradient Elution Techniques
 - Calibration & Quantitation
 - Logical HPLC Troubleshooting

The instructor for the courses, Dr. Jack Cazes, is Editor-in-Chief of the Journal of Liquid Chromatography, of Instrumentation Science & Technology journal, and of the Chromatographic Science Book Series. He has been intimately involved with liquid chromatography for more than 30 years; he pioneered the development of modern HPLC technology. Dr. Cazes was also Professor-in-Charge of the ACS short course and the ACS audio course on Gel Permeation Chromatography for many years.

Details of these in-house courses may be obtained from Dr. Jack Cazes, Post Office Box 2180, Cherry Hill, NJ 08034-0162, USA; Tel: (609) 424-3505; FAX: (609) 751-8724.

LIQUID CHROMATOGRAPHY CALENDAR

1995

NOVEMBER 1 - 3: 30th Midwestern Regional ACS Meeting, Joplin, Missouri. Contact: J. H. Adams, 1519 Washington Dr., Miami, OK 74354-3854, USA.

NOVEMBER 1 - 4: 31st Western Regional ACS Meeting, San Diego, California. Contact: T. Lobl, Tanabe Research Labs, 4450 Town Center Ct., San Diego, CA 92121, USA.

NOVEMBER 2: Anachem Symposium, Dearborn, Michigan. Contact: Prof. C. Evans, University of Michigan, Chem Dept, 4807 Chemistry Bldg, Ann Arbor, MI 48109-1055, USA.

NOVEMBER 5 - 7: Midwestern Regional Meeting, ACS, Joplin, Missouri. Contact: J. H. Adams, 1519 Washington Dr, Miami, OK 74354, USA.

NOVEMBER 12 - 17: AIChE Annual Meeting, Fontainbleu Hotel, Miami Beach, Florida. Contact: AIChE, 345 East 47th Street, New York, NY 10017-2395, USA.

NOVEMBER 14 - 16: Kemia'95: Finnish Chemical Congress, Helsinki Fair Center, Helsinki, Finland. Contact: The Association of Finnish Chemical Societies, Hietaniemenkatu 2, FIN-00100 Helsinki, Finland.

NOVEMBER 29 - DECEMBER 1: Joint 51st Southwestern/47th Southeastern Regional Meeting, ACS, Peabody Hotel, Memphis, Tenn. Contact: P.K. Bridson, Chem Dept, Memphis State Univ, Memphis, TN 38152, USA.

DECEMBER 17 - 22: 1995 International Chemical Congress of Pacific Basin Societies, Honolulu, Hawaii. Contact: ACS Meetings, 1155 16th Street, NW, Washington, DC 20036-4899, USA.

1996

FEBRUARY 5 - 7: PrepTech'96, Sheraton Meadowlands Hotel, East Rutherford, New Jersey. Contact: Dr. R. Stevenson, 3338 Carlyle Terrace, Lafayette, CA 94549, USA.

FEBRUARY 25 - 29: AIChE Spring National Meeting, Sheraton Hotel, New Orleans, Louisiana. Contact: AIChE, 345 East 47th Street, New York, NY 10017-2395, USA.

MARCH 3 - 8: PittCon'96: Pittsburgh Conference on Analytical Chemistry & Applied Spectroscopy, Chicago, Illinois. Contact: Pittsburgh Conference, Suite 332, 300 Penn Center Blvd., Pittsburgh, PA 15235-9962, USA.

MARCH 24 - 29: 211th ACS National Meeting, New Orleans, LA. Contact: ACS Meetings, ACS, 1155 16th Street, NW, Washington, DC 20036-4899, USA.

MARCH 31 - APRIL 4: 7th International Symposium on Supercritical Fluid Chromatography and Extraction, Indianapolis, Indiana. Contact: Janet Cunningham, Barr Enterprises, P. O. Box 279, Walkersville, MD 21793, USA.

MARCH 31 - APRIL 4: 7th International Symposium on Supercritical Fluid Chromatography & Extraction, Indianapolis, Indiana. Contact: Janet Cunningham, Barr Enterprises, P. O. Box 279, Walkersville, MD 21793, USA.

APRIL 17 - 19: VIITH International Symposium on Luminescence Spectrometry in Biomedical Analysis - Detection Techniques and Applications in Chromatography and Capillary Electrophoresis, Université de Nice, France. Contact: Prof. W. R. G. Baeyens, University of Ghent Pharmaceutical Institute, Lab or Drug Quality Control, Harelbekestraat 72, Ghent, Belgium. Email: willy.baeyens@rug.ac.be.

MAY 7 - 9: VIIth International Symposium on Luminescence Spectrometry in Biomedical Analysis - Detection Techniques and Applications in Chromatography and Capillary Electrophoresis, Monte Carlo, Monaco. Contact: Prof. Willy R. G. Baeyens, University of Ghent, Pharmaceutical Institute, Harelbekestraat 72, B-9000 Ghent, Belgium.

JUNE 16 - 21: "HPLC '96: Twentieth International Symposium on High Performance Liquid Chromatography," San Francisco Marriott Hotel, San Francisco, California. Contact: Mrs. Janet Cunningham, Barr Enterprises, P. O. Box 279, Walkersville, MD 21793, USA.

JULY 14 - 18: 5th World Congress of Chemical Engineering, Marriott Hotel, San Diego, California. Contact: AIChE, 345 East 47th Street, New York, NY 10017-2395, USA.

AUGUST 9 - 14: 31st Intersociety Energy Conversion Engineering Conference (co-sponsored with IEEE), Omni Shoreham Hotel, Washington, DC. Contact: AIChE, 345 East 47th Street, New York, NY 10017-2395, USA.

AUGUST 17 - 20: 31st National Heat Transfer Conference, Westin Galleria, Houston, Texas. Contact: AIChE, 345 East 47th Street, New York, NY 10017-2395, USA.

AUGUST 18 - 23: 212th ACS National Meeting, Boston, Mass. Contact: ACS Meetings, 1155 16th Street, NW, Washington, DC 20036-4899, USA.

SEPTEMBER 1 - 6: 11th Symposium on Quantitative Structure-Activity Relationships: Computer-Assisted Lead Finding and Optimization," Lausanne, Switzerland. Contact: Dr. Han van de Waterbeemd, F. Hoffmann-La Roche Ltd., Dept PRPC 65/314, CH-4002 Basle, Switzerland.

SEPTEMBER 9 - 12: Safety in Ammonia Plants & Related Facilities, Westin at Copley Place, Boston, Massachusetts. Contact: AIChE, 345 East 47th Street, New York, NY 10017-2395, USA.

OCTOBER 16 - 19: 52nd Southwest Regional ACS Meeting, Houston, Texas. Contact: J. W. Hightower, Dept. Chem. Eng., Rice University, Houston, TX 77251, USA.

OCTOBER 24 - 26: 52nd Southwestern Regional Meeting, ACS, Houston, Texas. Contact: J. W. Hightower, Chem Eng Dept, Rice Univ, Houston, TX 77251, USA.

NOVEMBER 6 - 8: 31st Midwestern Regional Meeting, ACS, Sioux Falls, South Dakota. Contact: J. Rice, Chem Dept, S. Dakota State Univ, Shepard Hall Box 2202, Brookings, SD 57007-2202, USA.

NOVEMBER 9 - 12: 48th Southeast Regional ACS Meeting, Greenville, South Carolina. Contact: H. C. Ramsey, BASF Corp., P. O. Drawer 3025, Anderson, SC 29624-3025, USA.

NOVEMBER 10 - 15: AIChE Annual Meeting, Palmer House, Chicago, Illinois. Contact: AIChE, 345 East 47th Street, New York, NY 10017-2395, USA.

1997

APRIL 6 - 11: 213th ACS National Meeting, San Antonio, Texas. Contact: ACS Meetings, ACS, 1155 16th Street, NW, Washington, DC 20036-4899, USA.

APRIL 14 - 19: Genes and Gen Families in Medical, Agricultural and Biological Research: 9th International Congress on Isozymes, sponsored by the Southwest Foundation for Biomedical Research, Hilton Palacio del Rio, San Antonio, Texas. Contact: Mrs. Janet Cunningham, Barr Enterprises, P. O. Box 279, Walkersville, MD 21793, USA.

SEPTEMBER 7 - 12: 214th ACS National Meeting, Las Vegas, Nevada. Contact: ACS Meetings, 1155 16th Street, NW, Washington, DC 20036-4899, USA.

1998

MARCH 29 - APRIL 3: 215th ACS National Meeting, St. Louis, Missouri. Contact: ACS Meetings, 1155 16th Street, NW, Washington, DC 20036-4899, USA.

AUGUST 23 - 28: 216th ACS National Meeting, Orlando, Florida. Contact: ACS Meetings, 1155 16th Street, NW, Washington, DC 20036-4899, USA.

1999

MARCH 21 - 26: 217th ACS National Meeting, Anaheim, Calif. Contact: ACS Meetings, 1155 16th Street, NW, Washington, DC 20036-4899, USA.

AUGUST 22 - 27: 218th ACS National Meeting, New Orleans, Louisiana. Contact: ACS Meetings, 1155 16th Street, NW, Washington, DC 20036-4899, USA.

2000

MARCH 26 - 31: 219th ACS National Meeting, Las Vegas, Nevada. Contact: ACS Meetings, 1155 16th Street, NW, Washington, DC 20036-4899, USA.

AUGUST 20 - 25: 220th ACS National Meeting, Washington, DC. Contact: ACS Meetings, 1155 16th Street, NW, Washington, DC 20036-4899, USA.

2001

APRIL 1 - 6: 221st ACS National Meeting, San Francisco, Calif. Contact: ACS Meetings, 1155 16th Street, NW, Washington, DC 20036-4899, USA.

AUGUST 19 - 24: 222nd ACS National Meeting, Chicago, Illinois. Contact: ACS Meetings, 1155 16th Street, NW, Washington, DC 20036-4899, USA.

2002

APRIL 7 - 12: 223rd ACS National Meeting, Orlando, Florida. Contact: ACS Meetings, 1155 16th Street, NW, Washington, DC 20036-4899, USA.

SEPTEMBER 8 - 13: 224th ACS National Meeting, Boston, Mass. Contact: ACS Meetings, 1155 16th Street, NW, Washington, DC 20036-4899, USA.

The **Journal of Liquid Chromatography** will publish, at no charge, announcements of interest to scientists in every issue of the journal. To be listed in Meetings & Symposia, we will need to know:

- a) Name of the meeting or symposium,
- b) Sponsoring organization,
- c) When and where it will be held, and
- d) Whom to contact for additional details.

Incomplete information will not be published. You are invited to send announcements to **Dr. Jack Cazes, Editor, Journal of Liquid Chromatography, P.O. Box 2180, Cherry Hill, NJ 08034-0162, USA.**

**GET MORE FROM OUR JOURNALS
TAKE ADVANTAGE OF OUR SPECIAL REPRINT OFFERS**

Order high quality reprints of any article in our journals and see the difference it will make for you.

REPRINTS SERVE AS AN EXCELLENT MARKETING TOOL BY...

- ♦ supplementing your training materials
- ♦ educating and informing your staff
- ♦ promoting your company and its products *cost effectively*

DON'T DELAY
order your reprints today!!

Contact Ms. Delores Bradshaw at (212) 696-9000 x420
or
For bulk quantities (over 500 copies) contact Ms. Tara DePalma at x226

MARCEL DEKKER, INC.
270 MADISON AVENUE, NEW YORK, NY 10016

Explore the latest
advances in the
field of...

Ion Exchange and Solvent Extraction 12

VOLUME

Offers easy access to
Russian and Chinese
source material previ-
ously unavailable
to Western researchers!

edited by

JACOB A. MARINSKY

State University of New York at Buffalo

YIZHAK MARCUS

Hebrew University of Jerusalem, Israel

March, 1995

456 pages, illustrated

\$195.00

Volume 12 of this unique series continues in the tradition of its widely received predecessors, presenting **current** developments in the theory and practice of ion exchange.

This authoritative reference provides interdisciplinary coverage of contemporary topics, including

- the nature of metal-ion interaction with oppositely charged sites of ion exchangers
- high-pressure ion-exchange separation of rare earth elements
- the commercial recovery of valuable minerals from seawater and brines by ion exchange and sorption
- the kinetics of ion exchange in heterogeneous systems
- the ion-exchange equilibria of amino acids
- and much more!

The ***Ion Exchange and Solvent Extraction Series*** treats ion exchange and solvent extraction both as discrete topics and as a unified, multi-disciplinary study—presenting new insights for researchers in many chemical and related fields. The volumes in this now classic series are of major importance to analytical, coordination, process, separation, surface, organic, inorganic, physical, and environmental chemists; geochemists; electrochemists; radiochemists; biochemists; biophysicists; hydrometallurgists; membrane researchers; and chemical engineers.

Contents

High-Pressure Ion-Exchange
Separation of Rare Earths

*Liquan Chen, Wenda Xin,
Changfa Dong, Wangsuo Wu,
and Sujun Yue*

Ion Exchange in Countercurrent
Columns

Vladimir I. Gorshkov

Recovery of Valuable Mineral Com-
ponents from Seawater by Ion-Exchange
and Sorption Methods

*Ruslan Khamizov, Dmitri N. Muraviev,
and Abraham Warshawsky*

Investigation of Intraparticle Ion-
Exchange Kinetics in Selective
Systems

A. I. Kalinitchev

Equilibrium Analysis of Complexation
in Ion-Exchangers Using Spectro-
scopic and Distribution Methods

Hirohiko Waki

Ion Exchange Kinetics in Hetero-
geneous Systems

K. Bunzl

Evaluation of the Electrostatic Effect
on Metal Ion-Binding Equilibria in
Negatively Charged Polyion Systems

Tohru Miyajima

Ion-Exchange Equilibria of Amino Acids

Zuyi Tao

Ion Exchange Selectivities of Inorganic
Ion Exchangers

Mitsuo Abe

ISBN: 0-8247-9382-X

This book is printed on acid-free paper.

Marcel Dekker, Inc.

270 Madison Avenue
New York, NY 10016
(212) 696-9000

Hutgasse 4, Postfach 812
CH-4001 Basel, Switzerland
Tel. 061-261-8482

Gain insight into novel, highly reliable countercurrent chromatographic techniques and apply them in your work with...

Centrifugal Partition Chromatography

(Chromatographic Science Series/68)

edited by

ALAIN P. FOUCAULT

Centre National de la Recherche Scientifique, Paris, France

September, 1994

432 pages, illustrated

\$150.00

This outstanding guide introduces centrifugal partition chromatography (CPC) for any biphasic system—offering in-depth coverage of instrumentation, theory, liquid-liquid partition coefficients, and CPC in organic and inorganic chemistry.

Contains over 80 diagrams for three-solvent systems that can be applied to virtually all partitioning, separation, and purification situations!

Written by international experts from North America, Europe, and Japan, *Centrifugal Partition Chromatography*

- examines chromatographic properties, illustrates practical operations, and gives examples of CPC solutions to real experimental problems
- highlights the distinction between CPC and high-performance liquid chromatography
- explains hydrostatic, hydrodynamic, and overall pressure drops
- discusses solvent systems, strategies for solvent selection, and the elution mode in CPC
- shows how to design solvent systems for CPC of complex organic mixtures
- describes carrier-aided CPC for preparative-scale separations and the use of CPC as a multistage liquid-membrane transport system
- and much more!

With nearly 800 references, tables, equations, and figures, *Centrifugal Partition Chromatography* is an incomparable resource for analytical and pharmaceutical chemists and biochemists, separation scientists, pharmacologists, and upper-level undergraduate and graduate students in these disciplines.

Contents

- Operating the Centrifugal Partition Chromatograph, *Alain Bertbod, Chau-Dung Chang, and Daniel W. Armstrong*
- Theory of Centrifugal Partition Chromatography, *Alain P. Foucault*
- Pressure Drop in Centrifugal Partition Chromatography, *M. J. van Buel, L. A. M. van der Wielen, and K. Ch. A. M. Luyben*
- Solvent Systems in Centrifugal Partition Chromatography, *Alain P. Foucault*
- Fractionation of Plant Polyphenols, *Takuo Okuda, Takasbi Yoshida, and Tsutomu Hatano*
- Centrifugal Partition Chromatography in Assay-Guided Isolation of Natural Products: A Case Study of Immunosuppressive Components of *Tripterygium wilfordii*, *Jan A. Glinski and Gary O. Caviness*
- Liquid-Liquid Partition Coefficients: The Particular Case of Octanol-Water Coefficients, *Alain Bertbod*
- Centrifugal Partition Chromatography for the Determination of Octanol-Water Partition Coefficients, *Steven J. Gluck, Eric Martin, and Marguerite Healy Benko*
- Mutual Separation of Lanthanoid Elements by Centrifugal Partition Chromatography, *Kenichi Akiba*
- Separator-Aided Centrifugal Partition Chromatography, *Takeo Araki*
- Centrifugal Partition Chromatographic Separations of Metal Ions, *S. Muralidharan and H. Freiser*
- Preparative Centrifugal Partition Chromatography, *Rodolphe Margraff*
- Appendix I: Various Ways to Fill a CPC
- Appendix II: CPC Instrumentation
- Appendix III: Ternary Diagrams
- ISBN: 0-8247-9257-2

This book is printed on acid-free paper

Marcel Dekker, Inc.

270 Madison Avenue, New York, NY 10016
(212) 696-9000

Hutgasse 4, Postfach 812, CH-4001 Basel, Switzerland
Tel. 061-261-8482

Apply the latest advances in analysis techniques to both drugs of abuse and athletically banned substances with...

ANALYSIS OF ADDICTIVE AND MISUSED DRUGS

Furnishes important
contributions by international
authorities representing
North America, South
America, and Europe!

edited by
JOHN A. ADAMOVIĆ
Cytogen Corporation, Princeton, New Jersey

October, 1994
800 pages, illustrated
\$195.00

This **state-of-the-art** resource examines the chromatographic and nonchromatographic methods available to identify, measure, and screen for nonmedical drug use—highlighting the **latest technologies** in immunochemical analysis, biosensors, thin-layer gas chromatography, high-performance liquid chromatography, and capillary electrophoresis.

Provides a comprehensive alphabetic listing of over 400 controlled-use drugs, including the drug name, sample matrix, handling procedure, and mode of detection.

Uniquely integrating the testing for drugs of abuse with the testing for banned substances in athletes, ***Analysis of Addictive and Misused Drugs***

- ◆ discusses a paper chromatographic technique employed extensively to screen for drugs in biological matrices
- ◆ addresses the use of underivatized silica gel with polar solvents
- ◆ presents a simple and sensitive identification system for the detection of a broad spectrum of drugs
- ◆ evaluates the applicability of capillary electrophoresis for the separation of illicit drugs
- ◆ describes the most up-to-date robotics technology
- ◆ delineates an extensive sports drug testing program
- ◆ suggests approaches to solving forensic problems in developing countries with limited resources
- ◆ and more!

Containing over **1700** bibliographic citations and some **200** tables, figures, and equations, ***Analysis of Addictive and Misused Drugs*** is a practical *day-to-day* guide for analytical, clinical, forensic, and pharmaceutical chemists and biochemists; pharmacologists; chemical engineers; biotechnologists; clinical toxicologists; and upper-level undergraduate and graduate students in these disciplines.

CONTENTS

- Enzyme Immunoassays
Thomas Foley
- Biosensors
Jean-Michel Kauffmann and George G. Guilbault
- Thin-Layer Chromatography Using the Toxi-Lab System
Sheldon D. Brunk
- Reversed-Phase High-Performance Liquid Chromatography Analysis of Drugs of Forensic Interest
Ira S. Lurie
- High-Performance Liquid Chromatography Using Unmodified Silica with Polar Solvents
Steven R. Binder
- Analysis of Seized Drugs by Capillary Electrophoresis
Ira S. Lurie
- Thin-Layer Chromatographic Screening and Gas Chromatographic/Mass Spectrometric Confirmation in the Analysis of Abused Drugs
Pirjo Lillsunde and Taimi Korte
- Robotics and the Analysis of Drugs of Abuse
John de Kanel and Tim Karbar
- Drug Testing of Athletes
Sui C. Chan and Jitka Petruzelka
- Drug Analysis in South America
Juan Carlos Garcia Fernández
- Appendix: Supplementary Applications and Information
- ISBN: 0-8247-9238-6

This book is printed on acid-free paper

Marcel Dekker, Inc.

270 Madison Avenue, New York, NY 10016
■ (212) 696-9000
Hutgasse 4, Postfach 812, CH-4001 Basel, Switzerland
■ Tel. 061-261-8482

Employ the latest analytical techniques in the solute partitioning between immiscible aqueous phases with...

Aqueous Two-Phase Partitioning

BORIS Y. ZASLAVSKY

*KV Pharmaceutical Company
St. Louis, Missouri*

November, 1994 / 688 pages, illustrated / \$195.00

Provides over **150** phase diagrams for a variety of aqueous polymer systems—more than **70** of which have never before been published!

Physical Chemistry and Bioanalytical Applications

This useful reference offers **in-depth coverage** of the fundamental principles of solute partitioning in aqueous two-phase systems, explains their important practical features, **and** furnishes methods of characterization.

Examines—for the first time in a book of this kind—the information provided by the partition behavior of a solute in an aqueous two-phase system!

Integrating experimental results and theoretical concepts from a wide range of fields such as drug design, bioseparation, physical organic chemistry, and water soluble polymers, *Aqueous Two-Phase Partitioning*

- describes the phase separation of two polymers in an aqueous medium and the role of the solvent in this phenomenon
- compares the physicochemical properties of the aqueous polymer phases governing solute partitioning with those of water-organic systems
- supplies a definitive model for the partitioning of solutes in aqueous two-phase systems that accounts for **all** experimental data available
- demonstrates the advantages of the partition technique over other methods for studying the hydrophobicity of synthetic and biological substances
- delineates the role of hydrophobicity as a general structure descriptor in quantitative structure-activity relationship analyses for drugs and biopharmaceuticals
- gives hands-on recommendations for the development of timesaving analytical and separation procedures using aqueous two-phase systems
- illustrates **new technical applications** of the partition technique as a bioanalytical tool for quality control in recombinant products, medical diagnostics, toxicology, and other areas
- and much more!

With over **1000** literature citations, figures, and equations, *Aqueous Two-Phase Partitioning* is an incomparable resource for biochemists; biophysicists; chemical and biochemical engineers; physical, biophysical, analytical, medicinal, and clinical chemists; bioprocess technologists; pharmacologists and biopharmacologists; soil scientists; microbiologists and virologists; pathologists; toxicologists; and graduate-level students in these disciplines.

Contents

Aqueous Polymer Systems and Phase Separation

Water in the Presence of Additives
Aqueous Polymer Solutions
Phase Separation in Aqueous Polymer Systems:
Experimental Facts and Theoretical Models

Partitioning of Solutes in Aqueous Two-Phase Systems

Physicochemical Properties of Phases in Aqueous Polymer Systems
General Trends in Solute Partition Behavior

Analytical Applications of the Partition Technique

Hydrophobicity of Biological Solutes
Measurements of the Relative Hydrophobicity of Biological Solutes by the Aqueous Two-Phase Partition Technique
Analysis of Individual Biopolymers and Their Mixtures
Separation of Biomolecules
Phase Diagrams

ISBN: 0-8247-9461-3

This book is printed on acid-free paper

Marcel Dekker, Inc.

270 Madison Avenue, New York, NY 10016
(212) 696-9000

Hutgasse 4, Postfach 812, CH-4001 Basel, Switzerland
Tel. 061-261-8482

Gain insight into the fundamental concepts
and numerous applications of neural networks with...

Neural Networks and Simulation Methods

(Electrical Engineering and Electronics Series/87)

JIAN-KANG WU

National University of Singapore and the University of
Science and Technology of China, Hefei, People's Republic of China

December, 1993
456 pages, illustrated
\$155.00
\$ 55.00 ◀ on orders of five or more copies,
for classroom use only

Introduces for the first time a
novel neural network model—
Learning based on Experiences
and Perspectives (LEP)!

Covering all essential aspects of neural networks, this outstanding **reference/text** explains network dynamics, learning paradigms, and computational capabilities of feedforward, self-organization, and feedback neural network models—addressing specific problems such as data fusion and data modeling.

Describes a neural network simulation software package—USTCNET—and gives some segments of the program, providing basic tools for users to explore neural network simulation and write their own programs.

Emphasizing concepts and techniques throughout rather than their mathematical derivations, *Neural Networks and Simulation Methods*

- highlights spatial and dynamic self-organization of self-organization networks, the functional approximation of feedforward networks, and the optimization of feedback networks
- supplies source codes and explanations for various **state-of-the-art** neural network model simulations
- details a wide array of applications for neural networks ranging from data coding, character, and 3-D object recognition to image database indexing
- discusses various learning algorithms
- investigates high-level knowledge bases and object recognition systems
- examines applications for nonlinear dynamic systems
- and much more!

Furnishing more than 675 up-to-date references, useful equations, and insightful tables, drawings, and photographs, *Neural Networks and Simulation Methods* is a vital **reference** for computer scientists and electrical and electronics, artificial intelligence, computer, robotics, systems control, and mechanical engineers; and a valuable **text** for upper-level undergraduate and graduate students taking neural network courses in computer science or electrical engineering and electronics departments.

Contents

Introduction
General Concepts of Pattern Recognition
Feedforward Neural Networks
Feedforward Neural Networks for Functional Approximation
Applications of Feedforward Neural Networks
Fuzzy Neural Networks
Competitive Learning and Self-Organization
Adaptive Self-Organization
Associative Memory
Optimization Through Neural Networks

ISBN: 0-8247-9181-9

This book is printed on acid-free paper.

Marcel Dekker, Inc.

270 Madison Avenue
New York, NY 10016
(212) 696-9000

Hutgasse 4, Postfach 812
CH-4001 Basel, Switzerland
Tel. 061-261-8482

Keep state-of-the-art theoretical and applied research developments at your fingertips with...

Advances in Chromatography

Volume 36

edited by

PHYLLIS R. BROWN

University of Rhode Island, Kingston

ELI GRUSHKA

Hebrew University of Jerusalem, Israel

October, 1995 / 464 pages, illustrated / \$175.00

Reviewer praise for previous editions...

"...reflects the high standards expected from this respected series."

—*Clinical Chemistry*

"...the articles [are] of high scientific standard, up to date, very well written, and interesting to read...well presented and edited."

—*Journal of Chromatography*

"...a valuable contribution to the chromatography literature... belongs in every library used by chromatographers."

—*Liquid Chromatography*

"...maintains the high quality that chromatographers have come to expect from this invaluable series."

—*Journal of Pharmaceutical Sciences*

The rapidly expanding growth of the literature on chromatography, capillary electrophoresis, field flow fractionation, and other separation techniques makes it difficult for any individual to maintain a coherent view of progress in the field. Rather than attempt to read the avalanche of original research papers, investigators trying to preserve even a modest awareness of advances must rely upon **authoritative surveys**.

Featuring reliable, **up-to-the-minute reviews** of major developments in separations, this critically praised series separates the most important advances from an overabundance of supplementary materials.

Internationally acclaimed experts analyze the most current innovations in their areas of specialization!

Providing more than **850** bibliographic citations, allowing for further, in-depth study of recent trends in research, **Volume 36** examines timely subjects such as

- multilinear regression, canonical correlation, and factor and principal component methods of analysis in the evaluation of retention data matrices
- molecular recognition mechanisms in the liquid chromatographic separation of fullerenes
- the **latest techniques** in the use of capillary electrophoresis and mass spectrometry for sequencing antisense oligonucleotides
- analytical tools and separation methods for the analysis of drugs of abuse in biological fluids
- the applications of high-performance liquid chromatography coupled with nuclear magnetic resonance spectroscopy
- and much more!

Advances in Chromatography is an indispensable resource for all researchers who need to use separation methods effectively—especially analytical, organic, inorganic, clinical, and physical chemists; chromatographers; biochemists and biological chemists; agrochemists; chemical, materials, pollution, and quality control engineers; biotechnologists; toxicologists; pharmacologists; pharmacists; physiologists; zoologists; botanists; food, cosmetic, polymer, and environmental scientists; microbiologists; virologists; oceanographers; research and quality control scientists in academia, government, hospitals, and industry; and upper-level undergraduate and graduate students in these disciplines.

CONTENTS

Use of Multivariate Mathematical Methods for the Evaluation of Retention Data Matrices, *Tibor Cserbáti and Esther Forgács*

Separation of Fullerenes by Liquid Chromatography: Molecular Recognition Mechanism in Liquid Chromatographic Separation, *Kiyokatsu Jinno and Yoshihiro Saito*

Emerging Technologies for Sequencing Antisense Oligonucleotides: Capillary Electrophoresis and Mass Spectrometry, *Abaron S. Cohen, David L. Smisek, and Bing H. Wang*

Capillary Electrophoretic Analysis of Glycoproteins and Glycoprotein-Derived Oligosaccharides, *Robert P. Oda, Benjamin J. Madden, and James P. Landers*

Analysis of Drugs of Abuse in Biological Fluids by Liquid Chromatography, *Steven R. Binder*

Electrochemical Detection of Biomolecules in Liquid Chromatography and Capillary Electrophoresis, *Jian-Ge Chen, Steven J. Woltman, and Steven G. Weber*

The Development and Application of Coupled HPLC-NMR Spectroscopy, *John C. Lindon, Jeremy K. Nicholson, and Ian D. Wilson*

Microdialysis Sampling for Pharmacological Studies: HPLC and CE Analysis, *Susan M. Lunte and Craig E. Lunte*

ISBN: 0-8247-9551-2

This book is printed on acid-free paper

MARCEL DEKKER, INC.

270 Madison Avenue, New York, NY 10016 • (212) 696-9000
Hutgasse 4, Postfach 812, CH-4001 Basel, Switzerland • Tel. 061-261-8482

INSTRUCTIONS TO AUTHORS

The *Journal of Liquid Chromatography* is published in the English language for the rapid communication of research in liquid chromatography and its related sciences and technologies.

Directions for Submission

One complete original manuscript, and two (2) clear copies, with figures, must be submitted for peer review. After all required revisions have been completed, and the final manuscript has been accepted, the author will be asked to provide, if possible, a 3½" or 5¼" PC-compatible computer diskette containing the complete manuscript. Microsoft Word, Word for Windows, WordPerfect, WordPerfect for Windows and ASCII are preferred formats. Text (including tables), and figures (if in electronic format) should be saved in separate files on the diskette. Label the diskette with the corresponding author's last name, the title of the manuscript and the file number assigned to the manuscript.

Submission of a manuscript on diskette, in a suitable format, will significantly expedite its publication.

Manuscripts and computer diskettes should be mailed to the Editor:

Dr. Jack Cazes
Journal of Liquid Chromatography
P. O. Box 2180
Cherry Hill, NJ 08034-0162

Reprints

Due to the short production time for papers in this journal, it is essential to order reprints immediately upon receiving notification of acceptance of the manuscript. A reprint order form will be sent to the corresponding author with the letter of acceptance for the manuscript. Reprints are available in quantities of 100 and multiples thereof. Twenty (20) free reprints will be included only with orders of 100 or more reprints.

Format of the Manuscript

NOTE: Failure to adhere to the following guidelines will delay publication of a manuscript.

1. The preferred dimensions of the printed area of a page are 6" (15.2 cm) width by 8.5" (21.6 cm) height. Use Times Roman 12 point font, if possible.

The general organization of the manuscript should be:

Title
Author(s)' names and full address(es)
Abstract
Text Discussion
Acknowledgements
References

2. **Title & Authors:** The entire title should be in boldface capital letters and centered within the width of the printed area, located 2" (5.1 cm) from the top of the page. This should be followed by 2 lines of space, then by the names and addresses of the authors, also centered, in the following manner:

A SEMI-AUTOMATIC TECHNIQUE FOR THE SEPARATION AND DETERMINATION OF BARIUM AND STRONTIUM IN WATER BY ION EXCHANGE CHROMATOGRAPHY AND ATOMIC EMISSION SPECTROMETRY

F. D. Pierce, H. R. Brown
Utah Biomedical Test Laboratory
520 Wakara Way
Salt Lake City, Utah 84108

3. **Abstract:** The heading, **ABSTRACT**, should be typed capitalized and centered, 2 lines below the addresses. This should be followed by a single line space, then a concise abstract. Allow 2 lines of space below the abstract before beginning the text of the manuscript.

4. **Text Discussion:** Text should be typed with full (left & right) justification. Whenever possible, the text discussion should be divided into major sections such as

INTRODUCTION
MATERIALS
METHODS
RESULTS
DISCUSSION
ACKNOWLEDGEMENTS
REFERENCES

These major headings should be separated from text by two lines of space above and one line of space below the headings. Each major heading should be typed centered in capital letters.

Secondary headings, if any, should be placed flush with the left margin, bold face, and have the first letter of main words capitalized. Leave two lines of space above and one line of space below secondary headings.

5. The first word of each paragraph within the body of the text should be indented five spaces.

6. **Acknowledgements**, sources of research funds and address changes for authors should be listed in a separate section at the end of the manuscript, immediately preceding the references.

7. **References** should be numbered consecutively, with Arabic numerals, and placed at the end of the manuscript. They should be typed single-spaced. Each reference should contain names of all authors (with initials of their first and middle names placed before their last names); do not use *et al.* for a list of authors. Abbreviations of journal titles should follow the American Chemical Society's Chemical Abstracts List of Periodicals. The word **REFERENCES** should be capitalized and centered above the reference list.

Following are acceptable reference formats:

Journal.

1. D. K. Morgan, N. D. Danielson, J. E. Katon, *Anal. Lett.*, **18**, 1979-1988 (1985).

2. N. H. Foda, "Quantitative Analysis of Fluvoxamine Maleate in Tablet Formulations by HPLC," *J. Liquid Chrom.*, **18**, 1591-1601 (1995)

Book

1. L. R. Snyder, J. J. Kirkland, *Introduction to Modern Liquid Chromatography*, John Wiley & Sons, Inc., New York, 1979

Chapter in a Book:

1. C. T. Mant, R. S. Hodges, "HPLC of Peptides," in *HPLC of Biological Macromolecules*, K. M. Gooding, F. E. Regnier, eds., Marcel Dekker, Inc., New York, 1990, pp. 301-332

8. Each page of the printed manuscript should be numbered lightly, with a light blue pencil, at the bottom of the page.

9. Only standard symbols and nomenclature, approved by the International Union of Pure and Applied Chemistry (IUPAC) should be used. Hand-drawn characters are not acceptable

Additional Typing Instructions

1. The manuscript must be prepared on good quality US Letter size or international A4 size white bond paper. The typing area of each page, including the title and authors, should be 6" (15.2 cm) width by 8.5" (21.6 cm) height

2. All text should be typed single-spaced.

3. It is essential to use dark black typewriter or printer ribbon, or a laser printer so that clean, clear, solid characters are produced. Characters produced with a dot/matrix printer are not acceptable, even if they are "near letter quality" or "letter quality." Erasure marks, smudges, hand-drawn corrections and creases are not acceptable

4. Tables should be typed within the body of the text, but in such a way as to separate them from the text by a two-line space above and below the table. Tables should be inserted into the text as close to the point of reference as possible. A table may not be longer than one page. If a table is larger than one page, it should be divided into more than one table

The word TABLE, on a line by itself, (typed bold-face, capitalized and followed by an Arabic number) should precede the table and should be centered above the table. The title of the table, on the next line, should have the first letters of all main words in capitals. Table titles should be typed single line spaced, bold-face across the full width of the table

5. Figures (drawings, graphs, etc.) should be professionally drawn in black India ink (or computer-generated) on separate sheets of white paper and should be placed at the end of the text. Figures should not be inserted into the body of the text. They should not be reduced to a small size. Preferred size for figures is from 5" x 7" (12.7 cm x 17.8 cm) to 8½" by 11" (21.6 cm x 27.9 cm). Photographs should be professionally-prepared glossy prints. A typewriter or lettering set should be used for all labels on the figures or photographs, they may not be hand drawn

Captions for figures should be typed single-spaced on a separate sheet of white paper, along the full width of the type page, and should be preceded with the word Figure and an Arabic number. All figures and lettering must be of a size that will remain legible after a 20-30% reduction from the original size. Figure numbers, name of senior author and an arrow indicating "top" should be written with a light blue pencil on the back of the figure. Indicate the approximate placement for each figure in the text with a note written with a light blue pencil in the margin of the manuscript page.

6. The reference list should be typed single-spaced. The format for references should be as given above.

Contributors, particularly those unfamiliar with English usage, are encouraged to seek the assistance of colleagues who are well versed in English language usage prior to submission.

For the latest developments in all areas
of analytical chemistry turn to...

ANALYTICAL LETTERS

Editor

GEORGE G. GUILBAULT

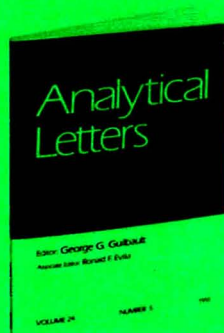
Department of Chemistry, University of New Orleans
New Orleans, Louisiana 70148

This rapid communication journal provides the fastest, most efficient transmittal of recent advances in the areas of analytical chemistry, analytical biochemistry, clinical chemistry, forensic and toxicological analyses, environmental analyses, separations, electrochemistry, and spectroscopy.

Presenting short papers, original ideas, observations, and important analytical discoveries, *Analytical Letters* fulfills a critical need by furnishing scientists with new results to apply in their own research in the briefest time possible.

CALL FOR PAPERS

Analytical Letters, published in English, welcomes manuscript contributions. Those accepted will be published promptly. For complete details regarding manuscript preparation and submission, please contact the Editor directly.



1995 Volume 28, 15 Numbers
Institutional rate: \$1550.00
Individual rate: \$ 775.00
ISSN: 0003-2719

To subscribe to *Analytical Letters* or to receive a complimentary copy, please contact the Promotion Department at:

Marcel Dekker, Inc.
270 Madison Avenue
New York, N.Y. 10016
(212) 696-9000

MARCEL DEKKER, INC.